NGF/p75^{NTR} or HSPB1-mediated regulation of cell survival under stress

---

A thesis submitted to the National University of Ireland Galway in fulfillment of the requirement for the degree of

Doctor of Philosophy

by

Reka Chakravarthy

Discipline of Biochemistry, School of Natural Sciences,

National University of Ireland, Galway

Thesis Supervisors: Dr. Adrienne Gorman

Co-supervised by: Dr. Eva Szegezdi

September, 2015

Table of contents

Acknowledgements

Abbreviations

ABSTRACT

Acknowledgements

First and foremost I would like to thank my supervisor Dr. Adrienne Gorman for her unwavering support, guidance and encouragement at all times of my PhD. I thank her sincerely for seeing in me the passion I had for science and giving me this opportunity to work on many exciting projects. I cannot thank her enough for the kind of support she extended especially during the last month of my PhD. Thank you Adrienne for transforming me from a Research assistant to a Research Scientist and making me a capable and competent researcher. It has been an absolute pleasure working with you.

I would like to thank Prof. Afshin Samali and Dr. Eva Szegezdi for their valuable feedback and experimental suggestions/ideas in the lab meetings.

A big thanks to the entire NGF, ER stress and TRAIL group for supporting me at the earlier stages of my PhD and bringing me into the comfort zone without having to go out for wine! ☺

I would like to thank Laura Carleton, Jennifer Hillis, Rola Jaafar and Sarah Conmy for all their help during my PhD. A special thanks to Jennifer and Trish for being with me during my hardships and helping me get over them. Thank you so much to all my junior colleagues and post- docs especially Kasia for supporting me throughout and being there to discuss science at all times. Amazingly, I only had to go out very few times for lunch or hot chocolate to make such lovely bunch of friends here in Ireland ☺

Last but not the least; I would like to express my sincere thanks and gratitude to my parents, my sister and my brother-in-law for having the belief in me and sending me miles away to pursue my passion. I cannot thank my mother and father enough for all the sacrifices they have made, for me to get what I desired. Thanks for all the support and understanding Appa and Amma!!

A final thanks to all my relatives and cousins scattered around the globe for their constant motivation and for all their love.

List of abbreviations

ACD	Alpha-crystallin domain
AD	Alzheimer's disease
AIF	Apoptosis inducing factor
ALS	Amyotrophic Lateral Sclerosis
AMC	Aminomethylcoumarin
APAF-1	Apoptosis protease activating factor-1
APP	Amyloid precursor protein
ASK1	Apoptosis signal-regulation kinase 1
ATCC	American Type Culture Collection
ATP	Adenosine triphosphate
Aβ	β-amyloid
BAD	BCL-2 antagonist of cell death
BAK	BCL-2 homologous antagonist/killer
BAX	BCL-2 associated protein X
BCL-2	B-cell lymphoma 2
BCL-XL	BCL-2 extra large
BDNF	Brain derived neurotrophic factor
BEX2	Brain expressed X–linked 2 gene
BFCN	Basal forebrain cholinergic neurons
BH	Bcl-2 homology
BID	BH3-interacting domain death agonist
BIM	BCL-2 interacting mediator of cell death
BIR	Baculoviral IAP repeats
BOK	BCL-2 related ovarian killer
BOP	BH3 only protein
BSA	Bovine serum albumin
BZip	Basic-leucine zipper

CAD	Caspase-activated DNase
CARD	Caspase recruitment domain
CASPASES	Cysteine-dependent aspartate directed proteases
c-FLIP	Cellular FLIP
cIAP	Cellular inhibitor of apoptosis protein
CMT	Charcot Marie Tooth disease
CNS	Central nervous system
CRD	Cysteine rich domains
CSR	Cellular stress response
CTF	C-terminal fragment of $p75^{NTR}$
DD	Death domain
DED	Death effector domain
DISC	Death inducing signaling complex
DMEM	Dulbecco's modified Eagle medium
DMN	Distal motor neuropathy
DR	Death receptor
ECACC	European Collection of Cell Cultures
ELISA	Enzyme linked immunosorbent assay
EndoG	Endonuclease G
Er	Estrogen receptor
ER	Endoplasmic reticulum
ERAD	ER-associated degradation
ERK	Extracellular signal-regulated kinase
FADD	Fas-associated death domain containing protein
FBS	Fetal bovine serum
HEPES	2-hydroxyethyl-piperazine-N-2-ethanesulphonic acid
Her-2	Human epidermal growth factor receptor-2
HRP	Horseradish peroxidase
HRK	Harakiri BCL-2 interacting protein

HS	Horse serum
HSE	Heat shock sequence element
HSF	Heat shock factor
HSP	Heat shock protein
sHSPs	Small heat shock proteins
HSPA5/GRP78	Heat shock protein A5
HSPA1	Heat shock protein 72
HSPB1	Heat shock protein 27
HSR	Heat shock response
IAPs	Inhibitor of apoptosis proteins
ICAD	Inhibitor of caspase-activated DNase
IDP	Intrinsically disordered protein
Ig	Immunoglobulin-like
I-κK	Inhibitor of NF-κB kinase
JNK	c-Jun N-terminal kinase
KEAP1	Kelch-like ECH associated protein
LRR	Leucine-rich repeats
MAPK	Mitogen activated protein kinase
MCL-1	Myeloid cell leukemia sequence 1
MEF	Mouse embryonic fibroblast
MMP7	Matrix metalloprotease 7
MND	Motor neuron disease
MOMP	Mitochondrial outer membrane permeabilization
MTT	3-(4, 5-dimethylthiazol-, 2-yl)-2,5-diphenyl tetrazolium bromide solution
NADE	$p75^{NTR}$-associated cell death executor
NBEC	Normal breast epithelial cells
NF-κB	Nuclear factor-κB
NGF	Nerve growth factor

NRAGE	neurotrophin receptor-interacting MAGE homolog
NRIF	Neurotrophin receptor interacting factor
NSAIDs	Non-steroidal anti-inflammatory drugs
NTs	Neurotrophins
$P75^{NTR}$	75 kDa neurotrophin receptor
PARP	Poly (ADP-ribose) polymerase
PBS	Phosphate buffered saline
PBST	Phosphate buffered saline containing Tween
PC	Proconvertase
PCR	Polymerase chain reaction
PI3K	Phosphatidylinositol 3-kinase
PKC	Protein kinase C
PLC-γ	Phospholipase C-γ
PLL	Poly-L-lysine
PMSF	Phenylmethylsulfonyl fluoride
Pr	Progesterone receptor
PS	Phosphatidylserine
PUMA	p53 up-regulated modulator of apoptosis
PYD	Pyrin domain
RIP	Receptor interacting protein
RNA	Ribonucleic acid
ROS	Reactive oxygen species
RPMI	Roswell Park Memorial Institute medium
SERCA	Sarco/Endoplasmic reticulum Ca^{2+} ATPase
SDS-PAGE	Sodium dodecyl sulphate polyacrylamide gel electrophoresis
siRNA	Small interfering RNA
Smac/DIABLO	Second mitochondria-derived activator of caspases/direct IAP binding protein with low pI
TAE	Tris-acetate-EDTA

TAK1	Transforming factor-β-activated kinase 1
TG	Thapsigargin
TM	Tunicamycin
TMB	3,3’,5,5’-Tetramethylbenzidine
TMRE	Tetramethylrhodamine, Ethyl Ester, Perchlorate
TNBC	triple negative breast cancer
TNF	Tumor necrosis factor
TNFR	TNF receptor
TNFR1	TNF receptor 1
TP	Thermal preconditioning
TNFRsf	TNFR superfamily
TRADD	TNF-receptor associated death domain
TRAF2	TNFR-associated factor 2
TRAILR1	TNF-related apoptosis-inducing ligand receptor 1
TrkA	Tropomyosin related kinase A
UPR	Unfolded protein response
UPR^{ER}	Endoplasmic reticulum UPR
UPR^{MT}	Mitochondrial UPR
XBP1	X-box binding protein 1
XBP1s	Spliced X-box binding protein 1
XIAP	X-linked IAP
ΔΨm	Mitochondrial membrane potential

Abstract

Triple negative breast cancers (TNBC) lack estrogen, progesterone and HER-2 receptors rendering them insensitive to current hormone targeted therapies. However, TNBC have been reported to express and secrete an additional growth factor, Nerve Growth Factor (NGF). They also express the two cognate receptors, the 75 kDa neurotrophin receptor ($p75^{NTR}$) and the tropomyosin related kinase A receptor (TrkA) to which NGF can bind. Identifying NGF -mediated $p75^{NTR}$signaling is a potential therapeutic target for TNBC.

Using MDA-MB-231 cells, a representative of TNBC I confirmed a role for NGF-mediated pro-survival signaling through $p75^{NTR}$. It is well known that NGF signaling through TrkA mediates cancer cell proliferation, while its signaling through $p75^{NTR}$ protects breast cancer cells from apoptosis. Therefore, targeting NGF/$p75^{NTR}$ signaling could potentially sensitize cells to chemotherapeutics. In this study, shRNA targeted to $p75^{NTR}$ to knock down the receptor or inhibitors designed to disrupt the NGF/$p75^{NTR}$ signaling were used and it was found that disrupting NGF/$p75^{NTR}$ signaling sensitized TNBC cells to apoptosis. The findings also illustrate that NGF regulates the levels of $p75^{NTR}$ through two distinct mechanisms, post-translational and transcriptional. Firstly, using Western blotting it was found that exogenous NGF inhibits the endogenous processing of $p75^{NTR}$. Secondly, it was shown that exogenous NGF increased $p75^{NTR}$ mRNA transcription as determined by RT-PCR. A differential sensitivity of the cells to apoptosis induction was observed with and without induction of $p75^{NTR}$ by NGF. This regulation of $p75^{NTR}$ by NGF is linked to increased resistance of these cells to chemotherapeutic drugs. Alteration in NGF signaling is not only implicated in resistance of breast cancer to chemotherapeutic reagents but it is also associated with a number of other disease states.

Previous work in our group involved the design and generation of NGF variants with a view to using them to selectively target Trk or $p75^{NTR}$ receptors. Here these variants were produced in HEK293T cells and their biological signaling was examined. Eight NGF variants were chosen and expressed into the media of HEK293T cells. The concentration of the variants was determined using an NGF ELISA followed by the analysis of TrkA-induced pro-survival signaling. The I31R and R69D NGF variants displayed no TrkA pro-survival activity as they were unable to protect PC12 cells from TG induced cell death. Interestingly I31R displayed no TrkA activity but retained binding affinity to

$p75^{NTR}$. I31 residue on NGF was identified as a target to disrupt TrkA signaling in disease conditions.

The second part of the thesis focused on the pro-survival signaling mediated by the intracellular ER chaperone protein HSPB1 in response to ER stress. HSPB1 that belongs to the family of small heat shock proteins is a potent regulator of apoptosis. However, the role of HSPB1 in ER-stress induced apoptosis has not been delineated. Previous work in the lab has shown that thermal pre-conditioning can protect cells from ER stress induced cell death through its ability to regulate BH3 only protein, BIM. Here it is shown that overexpression of HSPB1 protected PC12 cells from ER stress induced apoptosis through ERK-mediated phosphorylation of BH3 only protein, BIM leading to proteasomal degradation of BIM. It is also shown that HSPB1 interacts with phospho-ERK 1/2 and BIM to mediate a cytoprotective effect against thapsigargin-induced ER stress. I also characterized the effect of mutations in HSPB1 in response to ER stress in PC12 cells. PC12 cells that stably expressed mutations in HSPB1 showed an inability to confer protection in response to ER stress and were unable to mediate degradation of BIM as they did in their wild type counterpart.

1 Chapter 1: Introduction

1. General Introduction

Cells continually encounter various environmental insults causing mild to severe stress. As such they have evolved defense mechanisms to adapt to the adverse conditions and activate various extracellular and intracellular molecules to repair the damage caused by stress. If the cellular stress is particularly acute, or if the accumulation of damaged proteins is beyond repair, then the cells commit themselves to die. This thesis highlights (a) the role of ligand induced pro-survival signaling in the context of cancers, where resistance to cell death or sustaining proliferative signals through growth factors are hallmarks of cancer (Hanahan and Weinberg, 2011), and how specifically targeting the sites of ligand-receptor interaction can prove to be a therapeutic target in disease models, and (b) the pro-survival role of molecular chaperones (specifically, small heat shock proteins) that are activated in response to cellular stress.

The two parts of the thesis thus examine extracellular (NGF/$p75^{NTR}$) and intracellular (HSPB1) pro-survival molecules that negatively regulate cell death depending on cellular context. Although HSPB1, a molecular chaperone, has recently been reported to be secreted by macrophages (Salari et al., 2013), in our context HSPB1 is an example of intracellular negative regulator of apoptosis.

The introduction to the thesis will be divided into three discrete sections, i.e. (a) Apoptosis, (b) Neurotrophin signaling, (c) Heat shock proteins and the background to each of these sections will be described.

Cell death is a natural process that takes place continually in our body when cells can no longer divide and are replaced by new cells. It may also occur as a result of factors such as disease, localized injury or stress to mention a few. Cell death is classified according to the following guidelines: the morphological features (apoptosis, necrotic, autophagic); functional aspects (programmed cell death or accidental); the enzymes involved (with or without involvement of nucleases such as caspase-activated deoxyribonuclease (CAD) or proteases, such as caspases, calpains, cathepsins); and finally through immunogenic characteristics (immunogenic or non-immunogenic) (Kroemer et al., 2009). To date there are at least 13 different accepted biochemical forms of programmed cell death (PCD) characterized including apoptosis, necroptosis, autophagic cell death, ferroptosis, and

pyroptosis to mention some (Dixon et al., 2012, Galluzzi et al., 2012). This thesis will focus on the apoptotic mode of cell death.

1.1 APOPTOSIS

The term apoptosis was coined by Kerr, Wyllie and Currie in 1972 (Kerr et al., 1972). This is a process which is inherently programmed and has been shown to be initiated or inhibited by variety of stimuli including physiological and pathological stimuli (Kerr et al., 1972). During the formation of an adult animal from a fertilized embryo, there are several events of cell genesis and cell death. In fact, many cells are produced during development with the ultimate fate of early cell death, and this is required for the normal physiological process to carry on. In this context, programmed cell death is a term indicating apoptosis. When defects in apoptosis occur, it can lead to developmental abnormalities and several disorders like cancers and autoimmunity (Baehrecke, 2002). Many signals such as neurotrophic factor deprivation, or metabolic stress or environmental toxins can activate neuronal cell death by triggering the apoptotic machinery in several neurodegenerative diseases such as Alzheimer's disease or Huntington's and Parkinson's disease (Mattson, 2000). Therefore, investigation into the apoptotic machinery could reveal novel therapeutic targets.

1.1.1 Morphological and biochemical characterization of apoptosis

Apoptosis, which is defined as genetically programmed method of elimination of cells, is characterized by rounding-up of the cell, retraction of pseudopods, reduction of cellular volume (pyknosis), chromatin condensation, nuclear condensation and fragmentation (karyorrhexis), plasma membrane blebbing and formation of apoptotic bodies (Elmore, 2007). The biochemical characterization of apoptosis include loss of plasma membrane integrity, exposure of phosphatidylserine (PS) residues from the inner to the outer plasma membrane, mitochondrial outer membrane permeabilization (MOMP), loss of mitochondrial membrane potential ($\Delta\Psi m$), release of intra-mitochondrial space proteins, respiratory chain inhibition, caspase activation and DNA laddering (Kroemer et al., 2009).

Apoptosis has been observed in *Caenorhabditis elegans* (C. *elegans*) where 131 cells of 1090 undergo apoptosis during somatic development. (Ellis and Horvitz, 1986) This machinery was genetically controlled by key genes: *CED-3, CED-4, CED-9* and *EGL1* (Lettre and Hengartner, 2006). Key members of the mammalian cell death machinery were identified based on their similarity to the C. *elegans* orthologue. For example, *CED-3* is related to the cysteine protease interleukin-1β converting enzyme (ICE, caspase-1) in mammals (Ellis et al., 1991). Interestingly, all vertebrate species studied thus far demonstrated evolutionarily conserved apoptotic machinery (Degterev et al., 2003).

1.1.2 Caspases in the execution of apoptosis

Caspases belong to the family of cysteine-dependent aspartate specific proteases and are characteristically activated during apoptosis (Alnemri et al., 1996). A family of at least 10 related cysteine proteases have been identified (Cohen, 1997). They play an important role in maintaining cellular homeostasis through regulating inflammation and cell death (Wang and Lenardo, 2000) . Depending on the initiator caspases involved in regulating apoptosis, the apoptotic pathways can be distinguished between extrinsic or intrinsic apoptotic pathways (McIlwain et al., 2013)

1.1.2.1 Classification of caspases

Caspases can be classified based on (a) functions, (b) structure of caspases and (c) substrate specificity (Thornberry et al., 1997). To date, 11 human caspases have been identified: caspases-1-10 and caspase-14 (Alnemri et al., 1996, Pistritto et al., 2002). Caspase-13, was later found not to be a human but bovine (Koenig et al., 2001) and caspase-11 and -12 are murine enzymes that are most likely homologues of caspase-4 and -5 (Degterev et al., 2003).

Functionally, there are two different families of caspases, the inflammatory caspases and apoptotic caspases. Inflammatory caspases include caspase-1, -4, -5, -11, -12 and -14. The apoptotic caspases can further be classified as initiator caspases and executioner caspases. These caspases act at different stages in the apoptotic cascade. Therefore, members of caspases that act to initiate the apoptotic cascade are called “initiator” caspases (including caspases-2, -8, -9,-10 and -15) and the members that execute apoptosis following signals from initiators of apoptosis are called “executioners or effector caspases” (including caspases- 3, -6 and -7) (Thornberry et al., 1997).

Structurally, caspases are classified based on their long or short pro-domains. All caspases are synthesized as inactive zymogens called pro-caspases that contain a pro-domain followed by large p20 and small p17 subunits. The activation of the zymogen precursor occurs after a series of cleavage events leads to the separation of the large and small subunits, followed by removal of the pro-domain (Ramage et al., 1995, Yamin et al., 1996). The initiator and inflammatory caspases contain a long pro-domain that mediates the interaction of caspases with adaptor proteins (Chang and Yang, 2000). These domains include the death effector domain (DED), the caspases recruitment domain (CARD) or the pyrin domain (PYD). In apoptosis, initiator caspases get activated, and signal to the effector caspases. Effector caspases can activate each other or get activated by initiator caspases. Following this, the caspase activation signal is amplified and if the activation of caspases is high, then the cells commit to undergoing apoptosis. This effect is not reversible (Budihardjo et al., 1999). The effector caspases are characterized by the presence of a short pro-domain (Degterev et al., 2003).

Caspases have high specificity for cleavage after the C-terminal aspartic acid residue and the three amino acids before the aspartic acid residue provide the substrate specificity for particular caspases (Thornberry et al., 1997). The substrate specificity for all caspases along with classification of caspases based on function and structure is shown in Table 1.1.

Table 1.1 Mammalian caspases classified based on their function, structure and substrate specificity

Functions	Caspases	Substrate specificity	Structure
Inflammatory caspases	1	YVAD	
	4	LEHD	
	5	WEHD	
	11	VEHD	
	12	ATAD	
	14	-	
Apoptosis initiator caspases	2	VDVAD	
	8	IETD	
	9	LEHD	
	10	AEVD	
	15	IETD	
Apoptosis effector (executioner) caspases	3	DEVD	
	6	VEID	
	7	DEVD	

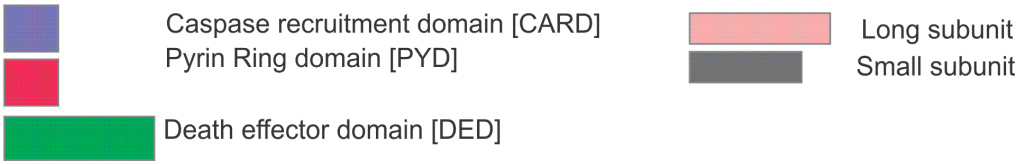

The table above shows classification of caspases based on their function, structure and substrate specificity.

1.1.2.2 Activation of caspases

Initiator caspases are present as monomers with their dimerization resulting in inter-chain autocatalytic cleavage and activation (Shi, 2004). This dimerization is facilitated by protein platforms or activating complexes which provide a focal point to concentrate caspases leading to proximity-induced activation and auto-cleavage (Shi, 2004). Proximity-induced activation of caspase is seen in caspase-9 activation and the complex is called the "apoptosome". The caspase- 8/10 activating complex is called the Death Inducing Signaling Complex (DISC) (Sessler et al., 2013). Formation of the PIDDosome

is required for caspase-2 activation or the inflammasome for caspase-1,-4 and-5 activation (Tinel and Tschopp, 2004, Martinon et al., 2002).

Executioner caspases are present as dimers in the cell. The proteolytic cleavage and activation of initiator caspases leads to re-organization of the enzyme favoring formation of an active catalytic site. This mode of activation prevents inappropriate activation of executioner caspases (Shi, 2004, Taylor et al., 2008, Pop and Salvesen, 2009).

1.1.3 Apoptosis pathways

Apoptosis can be initiated either at the plasma membrane upon ligation of a death receptor (extrinsic receptor pathway), or at the mitochondria (mitochondrial intrinsic pathway) (Hengartner, 2000). There is also evidence that the two pathways are linked together and that molecules involved in one pathway can participate and influence the other pathway (Igney and Krammer, 2002). Other than these two major pathways, there is a third pathway which involves T-cell mediated cytotoxicity and perforin-granzyme-dependent killing of the cell (Barry and Bleackley, 2002). This pathway engages granzyme B and all the three pathways converge at the mitochondrial intrinsic pathway and activate the executioner caspases (Martinvalet et al., 2005).

1.1.3.1 The extrinsic apoptosis pathway

One of the best characterized extrinsic apoptotic pathways is the binding of the death inducing ligand Fas (FasL) to the death receptor or Tumor Necrosis Factor (TNF)-α (ligand) binding to Tumor Necrosis Factor Receptor 1 (TNFR1) (Ashkenazi and Dixit, 1998) as shown in Fig. 1.1. Upon binding of the ligand to its corresponding receptor at the plasma membrane, clustering of receptors takes place (Hsu et al., 1995). This then causes recruitment of the cytoplasmic adaptor proteins to the death domain (DD) (region on the receptor that is responsible for mediating apoptotic signaling by interaction with downstream effector molecules) of the respective receptors, i.e. binding of FasL to FasR causes binding of Fas-associated death domain (FADD) and similarly, binding of TNFα to TNFR results in the binding of the adaptor protein TNF receptor associated death domain (TRADD) with recruitment of FADD and receptor-interacting protein (RIP) (Hsu et al., 1995, Wajant, 2002). FADD then associates with procaspase-8 through dimerization of the death effector domain (DED). This leads to the formation of the Death-inducing signaling complex (DISC), resulting in activation of pro-caspase-8

(Kischkel et al., 1995). The extrinsic apoptotic pathway is inhibited by cellular FLICE-inhibitory protein (c-FLIP) that binds to FADD and caspase-8 inactivating them (Kataoka et al., 1998). The activated caspase-8 now dissociates from the complex and either directly activates other caspases (Movassagh and Foo, 2008) or cleaves the BCL-2 pro-apoptotic protein BID to its truncated form (tBID) that then translocates to the mitochondria (Li et al., 1998), resulting in the activation of the mitochondrial intrinsic pathway described below.

1.1.3.2 The intrinsic apoptosis pathway

The intrinsic apoptosis pathway is triggered by a wide range of stimuli such as endoplasmic reticulum (ER) stress, growth factor withdrawal, DNA damage, and radiation (Hotchkiss et al., 2009). These stressors cause oligomerization of the BAX/BAK which then causes pores in the mitochondrial membrane. This process is called mitochondrial outer membrane permeabilization (MOMP) (Tait and Green, 2010). MOMP allows release of pro-apoptotic proteins like cytochrome *c*, Smac/DIABLO, endonuclease G (EndoG), and apoptosis inducing factor (AIF) into the cytoplasm of the cell (Martinou and Green, 2001). Upon release, cytochrome *c* binds to APAF-1 (apoptotic protease activating factor-1) activating it and causing its oligomerization in the presence of dATP. Pro-caspase-9 binds to the APAF-1 and cytochrome *c* complex which is called the apoptosome. The apoptosome is a heptamer and causes proximity-induced activation of caspase-9. Active caspase-9 causes the cleavage and activation of the effector caspases-3 and -7 (Acehan et al., 2002, Cain et al., 2002) leading to the classical morphology associated with apoptotic cells.

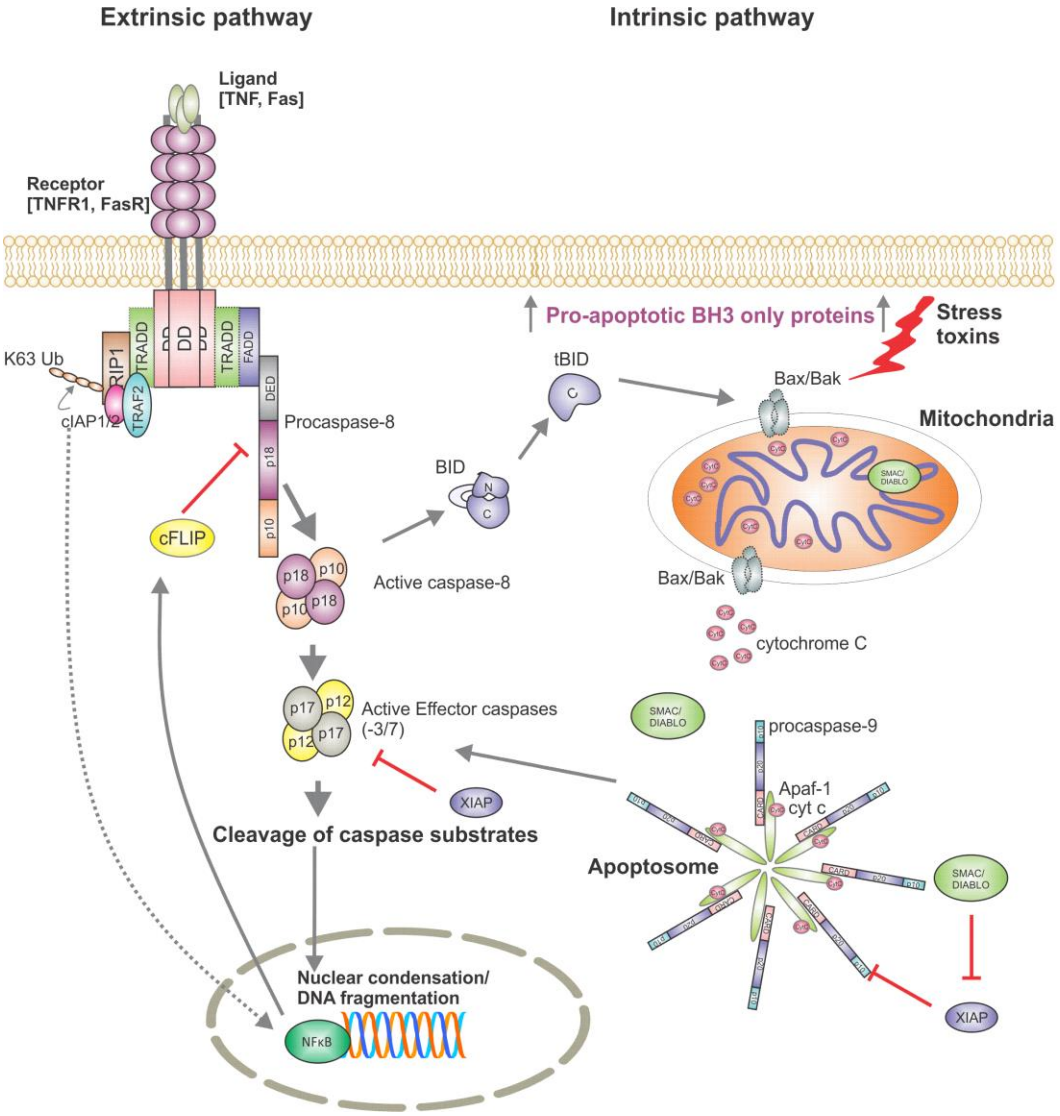

Fig. 1.1 The extrinsic and intrinsic apoptotic pathways

Apoptosis can be mediated either through extrinsic pathway (receptor-mediated) or intrinsic pathway (mitochondria-mediated). During the extrinsic apoptosis pathway, receptors mediate the activation of the initiator caspases. The active initiator caspases either directly activate the effector caspases or causes the cleavage of BID to tBID. tBID translocates to the mitochondria and causes heteromerization of Bax/Bak pro-apoptotic molecules in the mitochondrial membrane, causing a pore leading to MOMP. Cyt c is released from the mitochondria inner membrane into the cytosol and is incorporated into a complex with procaspase- 9 and Apaf-1 leading to the formation of the apoptosome. The apoptosome activates the effector caspases leading to the activation of effector caspases. At this point both the pathways converge on activating the effector caspases-3 or -7 that cleave various other caspase substrates causing nuclear condensation, fragmentation of DNA and finally the death of the cell. Apoptosis can be inhibited by inhibitors of apoptosis proteins (IAPs)

like cIAP1/2 or XIAP (X-linked inhibitor of apoptosis). Smac (Second mitochondria-derived activator of caspases) inhibits the activity of XIAP.

1.1.4 Regulation of apoptosis by the BCL-2 family of proteins

Apoptosis is regulated by pro-apoptotic and anti-apoptotic members of the B-cell lymphoma-2 (BCL-2) family of proteins. They are related to each other by their conserved regions called BCL-2 homology (BH) domains (van Delft and Huang, 2006). Proteins belonging to this family have the ability to form homodimers or heterodimers, suggesting a competition between these proteins to elicit apoptosis (Gross et al., 1999).

BCL-2 family members possess up to four conserved BCL-2 homology (BH) domains which are designated BH1, BH2, BH3 and BH4 as shown in Fig. 1.2. These correspond to α-helical segments (Adams and Cory, 1998). The anti-apoptotic members of this family such as BCL-2, BCL-X_L, BCL-W, A1 and MCL-1 display sequence conservation in all four domains, whereas the pro-apoptotic proteins display less sequence conservation of BH4. On deletion or mutagenesis of BH4, the amphipathic α-helical BH3 domain has been reported to serve as a critical death domain in the pro-apoptotic members. Pro-apoptotic members BAX and BAK lack a BH4 domain while they have BH1, BH2 and BH3 domains to mediate cell death. Other pro-apoptotic BCL-2 family members such as BIM, BID, BIK, BAD, HRK, NOXA, PUMA and BMF have sequence homology to one another but only within their BH3 domain (Gross et al., 1999). Many BCL-2 members contain a carboxy-terminal hydrophobic signal sequence and, in the case of BCL-2, this is essential for its targeting to membranes such as the mitochondrial outer membrane (Nguyen et al., 1993).

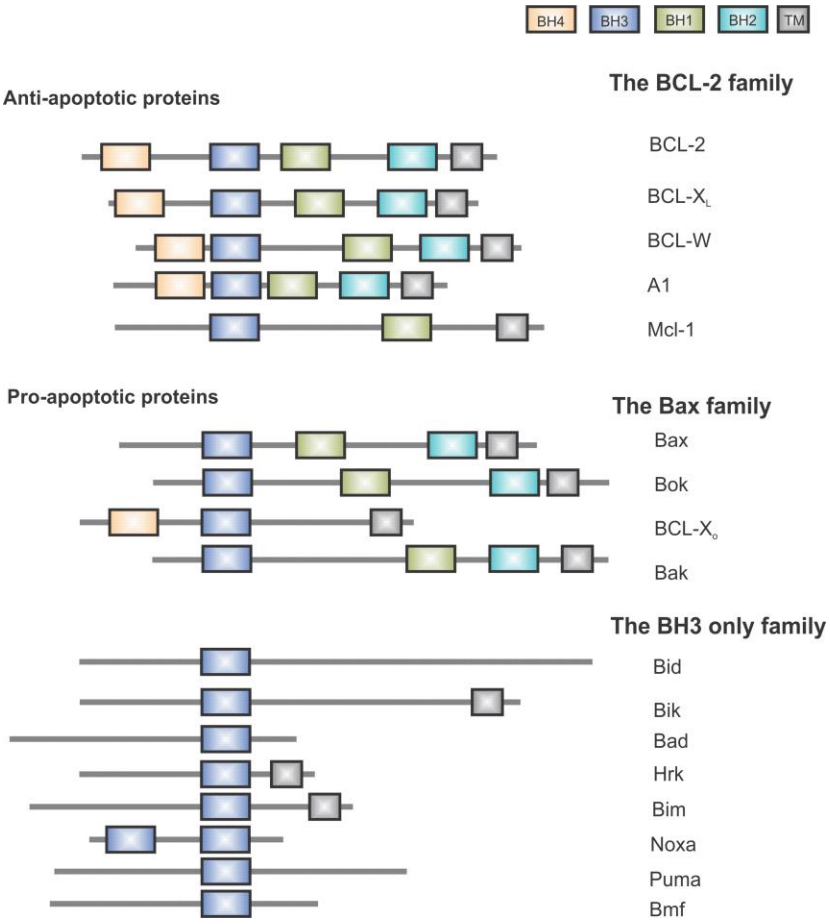

Fig. 1.2 Structure of the BCL-2 family members

The BCL-2 family members are subdivided into anti-apoptotic and pro-apoptotic members and the structure of each member of the BCL-2 family is shown above. The members are further divided into ***(A)*** The BCL-2 family, ***(B)*** The Bax family or ***(C)*** The BH3 only family members.

The BCL-2 family of proteins act upstream of irreversible cellular damage and act at the mitochondrion (Brunelle and Letai, 2009). The proteins belonging to the BCL-2 family have diverse modes of action. The BH3-only proteins (BID, BIK, BAD, HRK, BIM, BMF, NOXA and PUMA) are essential initiators of apoptosis (Huang and Strasser, 2000). They can bind to the pro-survival members of the BCL-2 family such as BCL-2 and BCL-X_L with high affinity and induce apoptosis upon stress. The other pro-apoptotic BCL-2 proteins, BCL-2 associated X protein (BAX) and BCL-2 antagonist/killer-1 (BAK) have an essential role downstream of loss of MOMP resulting in induction of caspase activation. The BH3-only proteins can also bind to BAX and BAK to mediate their pro-apoptotic effect (van Delft and Huang, 2006). The anti-apoptotic proteins in this

family, such as BCL-2 protein, block cell death by preventing the activation of BAX and BAK and inhibiting their oligomerization (van Delft and Huang, 2006). The anti-apoptotic proteins function by sequestering BH3-only proteins and monomeric activated BAX and BAK. Certain cancer cells have been shown to depend on BCL-2 for their survival and a BCL-2 antagonist like ABT-737 in this scenario has therapeutic potential. However, these compounds are not effective in cells that express high levels of MCL-1 or A1, other members of anti-apoptotic family of proteins (Oltersdorf et al., 2005). The anti-apoptotic and pro-apoptotic BCL-2 family members interact with one another. So, it is thought that the ratio of the pro- and anti-apoptotic genes determines the fate of the cell in response to cytotoxic stimuli (Oltvai et al., 1993). For instance, BIM has been shown to be induced in response to ER stress (Szegezdi et al., 2008, Puthalakath et al., 2007). The anti-apoptotic BCL-2 proteins function by inhibiting adaptors needed for activation of the caspases, and the pro-apoptotic BCL-2 proteins induce cell death by displacing this inhibition (Adams and Cory, 1998). Depending on the cellular context and specific death signals, certain pro-apoptotic members of the BCL-2 family can be induced. Of particular interest to this thesis is BIM, which is induced in response to many apoptosis stimuli, and undergoes transcriptional, post-transcriptional and post-translational modifications that lead to MOMP (Bouillet and Strasser, 2002, Szegezdi et al., 2008, Puthalakath et al., 2007).

BIM protein is an important member of the pro-apoptotic BCL-2 proteins; its expression is induced in response to various cellular stressors like ER stress and is directly involved in cell death (Puthalakath et al., 2007, Szegezdi et al., 2008).

Bim mRNA undergoes alternative splicing, generating several isoforms of BIM. The known isoforms of BIM are BIM_{EL}, BIM_{L} and BIM_{S} (O'Reilly et al., 2000). The isoforms of BIM vary in their expression and exhibit tissue- specific transcriptional regulation in humans (U et al., 2001). In response to ER stress, it is usually BIM_{EL} that is expressed at the protein level (Puthalakath et al., 2007). BIM_{S} potently induces apoptosis and is only transiently expressed during apoptosis. BIM_{L} and $BIME_{L}$ are expressed in unstressed cells, but the apoptotic activity of these isoforms is suppressed by their binding to microtubule-associated dynein motor complex via a dynein light chain binding domain (DLC domain) (Puthalakath et al., 1999).

The activity of BIM is tightly regulated by transcriptional, post-transcriptional and post-translational modifications. *Bim* is transcriptionally regulated by X-box Binding Protein 1 (XBP1) (Kurata et al., 2011), and by CHOP in response to ER stress (Puthalakath et al., 2007). Another study shows that the *Bim* promoter has a binding site for Fork head box class O, (FOXO) which induces expression of *Bim* in response to growth factor withdrawal (Gilley et al., 2003).

BIM is also regulated post-transcriptionally via the control of microRNAs. These microRNAs are a class of non-coding RNAs that bind to the 3' UTR of the target gene and repress its translation from mRNA to protein (Ambros, 2004). Some examples of microRNA clusters that have been reported to post-transcriptionally regulate the expression of BIM are: miR-24, where repression of BIM inhibits apoptosis in mouse cardiomyocytes (Qian et al., 2011); miR 17-92 cluster, where this cluster is oncogenic and the repression of this cluster contributes to the induction of BIM and therefore initiation of apoptosis (Molitoris et al., 2011); and miR-106B-25, where PERK-dependent repression of this cluster contributes to the induction of ER stress-induced apoptosis via BIM (Gupta et al., 2012).

BIM can also be post-translationally modified by phosphorylation under cellular stress conditions. BIM_{EL} can be phosphorylated by various stress-activated kinases such as ERK1/2, JNK, p38 MAPK, and AKT (Ley et al., 2003, Luciano et al., 2003, Lei and Davis, 2003, Qi et al., 2006). This modification can alter the stability of protein and it can also alter its interaction with proteins in the BCL-2 family. For example, mutation in the Thr-112 site of BIM_{EL} and BIM_{L} decreases its interaction with the pro-survival BCL-2 gene, thereby causing increased cell survival (Hubner et al., 2008), whereas phosphorylation of BIM_{L} by JNK results in BAX-dependent induction of apoptosis (Lei and Davis, 2003).

1.2 NEUROTROPHIN SIGNALING

Pro-survival signaling can be mediated by extracellular growth factors. Dysregulated growth factor signaling is one of the hallmarks of cancer (Hanahan and Weinberg, 2000). This section will elaborate on neurotrophin signaling with particular emphasis on nerve growth factor (NGF) signaling.

Neurotrophins are critical for the development and maintenance of the peripheral and central nervous system. They play a crucial role in controlling cell survival, differentiation, growth arrest and apoptosis of sensory neurons (Wiesmann and de Vos, 2001). The family of neurotrophins comprises of NGF, brain-derived neurotrophic factor (BDNF), neurotrophin-3 or -4/5 (NT-3/4/5). All the neurotrophins bind to $p75^{NTR}$ with low affinity and with high specificity to the Trk family of receptor tyrosine kinases. The four mammalian neurotrophins can bind and activate one or more of the Trk receptors (Patapoutian and Reichardt, 2001).

1.2.1 Neurotrophin family

Neurotrophins are polypeptides that regulate the proliferation, survival, migration and differentiation of cells in the nervous system (Huang and Reichardt, 2003). Rita Levi-Montalcini and Cohen identified the first member of this family in the 1950s. They discovered a target-derived soluble factor that induced neuronal cell survival and named it "Nerve growth factor (NGF)" (Levi-Montalcini and Angeletti, 1968). In 1982, Barde *et al*. discovered the second member of the neurotrophin family and named it BDNF. They purified BDNF from the porcine brain and found that this factor supported survival and neurite outgrowth of embryonic chick sensory neurons (Barde et al., 1982). NT-3, another neurotrophic factor related to NGF and BDNF was discovered by Maisonpierre (Maisonpierre et al., 1990). These three members of the neurotrophin family (NGF, BDNF and NT-3) are highly conserved from fish to mammals. A fourth member of the family, NT-4, was originally isolated in *Xenopus* and in viper venom. It displays 50%-60% amino acid identity to NGF, BDNF, and NT-3 and has been shown to interact with the low-affinity NGF receptor and to induce neurite outgrowth from explanted dorsal root ganglia (Hallbook et al., 1991). The fifth member of this family, neurotrophin-5 (NT-5) was identified in 1991 (Berkemeier et al., 1991). This was structurally related to NGF and is expressed in embryonic as well as adult tissues.

1.2.2 Structure of neurotrophins

The structure of all the members of neurotrophin family is highly conserved except NT-4/5 (Shooter, 2001). The structure of neurotrophins will be detailed below with NGF as the primary neurotrophin of interest.

1.2.2.1 ProNGF and NGF

NGF is a well characterized prototype member of a larger family of neurotrophins. It is a 28 kDa protein consisting of two covalently linked 14 kDa monomers. It has a tertiary structure based on a cluster of 3 cysteine disulfides and 2 very extended, but distorted β-hairpins. NGF interacts as a dimer, which is stabilized by interactions between aromatic residues (Bradshaw et al., 1994). The NGF dimer binds to the two distinct neurotrophin receptors TrkA and $p75^{NTR}$ in neuronal and non-neuronal cells. They bind to the receptors through specific lysine residues (Bradshaw et al., 1994).

Each mature NGF monomer contains a cysteine knot that is essential for the structure of the protein. Cys58-108 and Cys63-110 form a ring structure through which the third disulphide bond, Cys15-80 penetrates (McDonald, 1991). NGF is expressed as a pre-pro-protein. The 18 amino acid N-terminal signal sequence targets the pre-pro-protein to the ER (Kliemannel et al., 2004). The 241 amino acid proNGF is necessary for protein expression, secretion and folding of the mature NGF (Suter et al., 1991, Rattenholl et al., 2001, Lessmann et al., 2003, Kliemannel et al., 2004, Kliemannel et al., 2007). All neurotrophins generated from 31-35 kDa precursors can be intracellularly cleaved by several mammalian pro-protein convertases (PC) like furin, PC1, PC2, PACE4, PC5 and the PC5 isoform PC5/6-B (Seidah et al., 1996) and extracellularly by matrix metalloprotease 7 (MMP7) as well as plasmin (Lee et al., 2001b) to generate mature, secreted ligands.

As illustrated in Fig. 1.3, proNGF has two N-linked glycosylation sites (at residues -52 and -7) and five proteolytic cleavage sites. The first site is the pre-pro-domain region that is cleaved when the protein is targeted to the ER. The second and third sites of cleavage are at amino acid sites 193 and 162. These are the sites where proconvertases act to generate proNGF. The exact proconvertase is not known. The fourth site of cleavage is 7 amino acids from the furin cleavage site. This site can be cleaved extracellularly by MMP7. The intracellular cleavage of proNGF by furin generates the mature NGF, which, alternatively can be cleaved extracellularly by plasmin (Lee et al., 2001b).

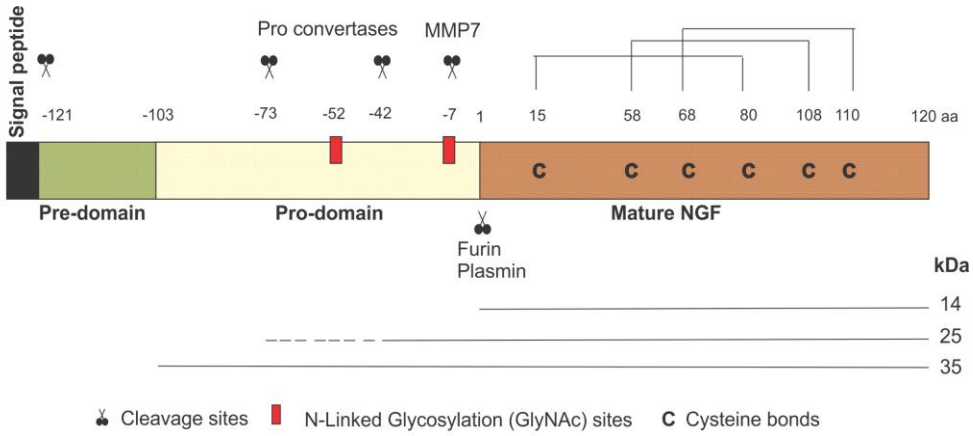

Fig. 1.3 Structure of ProNGF and mature NGF

ProNGF is a 241 aa long protein with two post-translational modification sites (N-linked Glycosylation sites; GlyNAc) highlighted in red and 5 cleavage sites as indicated above. The first cleavage site is the signal peptide or pre domain that gets cleaved during protein trafficking in the Golgi. The second and third sites of cleavage are mediated by pro-convertases. The fourth site of cleavage is 7 amino acids upstream of the furin cleavage site. This site is cleaved extracellularly by matrix metallo-protease 7 (MMP7). The final cleavage site generates the mature NGF and can be targeted intracellularly by furin and extracellularly by plasmin. The cysteine residues within the mature NGF are essential for protein structure. The molecular sizes of the different domains of NGF are also indicated.

1.2.2.2 Crystal structure of NGF

The crystal structure of NGF has been resolved (McDonald et al., 1991). NGF is a 27 kDa symmetrical homodimer which is generated by hydrophobic forces between a core of β-stranded sheets joined by three cysteine bonds. The NGF molecule contains a clustering of ten charged residues around the β-hairpin loop incorporating Asp30-Lys34. This feature creates a dimer surface with a continuous positive charge that has been suggested to be involved in NGF/ $p75^{NTR}$ interaction (He and Garcia, 2004). The crystal structure of NGF determined on co-crystallization with the TrkA, high affinity NGF receptor displayed structural features absent in the unbound NGF crystal structure. Importantly in the NGF/TrkA co-crystallization structure the N-terminal domain was resolved from residue serine 2; this region was unresolved on other structures but forms an important interface in the NGF/TrkA interaction (Wiesmann et al., 1999, Wehrman et al., 2007). The second difference was in the 10 amino acid loop from Ala40 - Arg50 of

the NGF when it interacts with the TrkA receptor (Wehrman et al., 2007). This region has a secondary structure resembling a beta hairpin. This difference suggests that the N-terminal region and the Ala40-Arg50 are essential for NGF-TrkA interaction. When the crystal structure between unbound NGF and NGF bound to $p75^{NTR}$ was compared, it was found that NGF binds to $p75^{NTR}$ in the opposite orientation to TrkA. The NGF bound to $p75^{NTR}$ is similar to the unbound ligand (Wehrman et al., 2007, He and Garcia, 2004).

It has been proposed that NGF interacts with its receptors through two different sites creating a "high-affinity" NGF binding site through formation of a ternary TrkA/NGF/$p75^{NTR}$ complex. It has been shown that the affinity of NGF for TrkA increases when $p75^{NTR}$ is co-expressed (Hempstead et al., 1991). However, a recent study has shown that there is no evidence of a direct interaction between TrkA and $p75^{NTR}$. It has been suggested that the increased affinity observed when TrkA and $p75^{NTR}$ are co-expressed may be through convergence of downstream signaling pathways and/or adaptor molecules that participate in both signaling pathways, rather than by physical interaction of the two receptors at the extracellular level (Wehrman et al., 2007). Shown in Fig. 1.4 is a schematic of the NGF in complex with TrkA and $p75^{NTR}$.

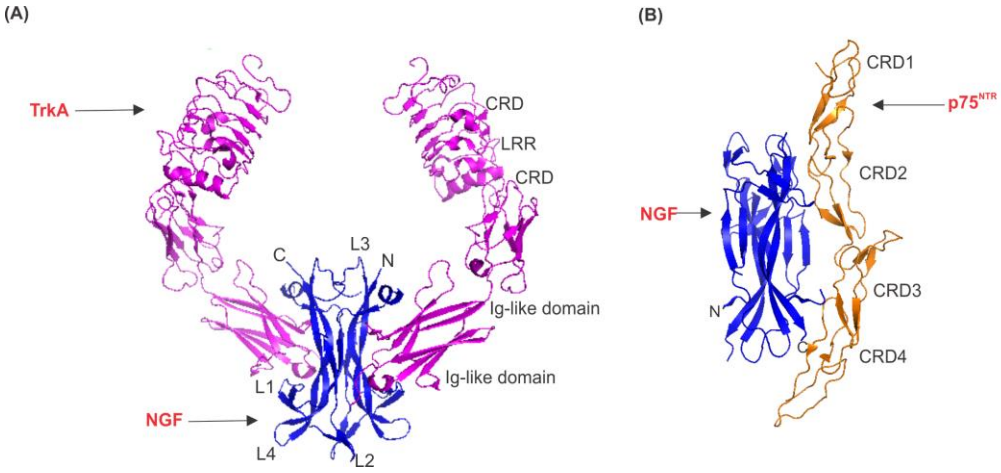

Fig. 1.4 Schematic of the NGF in complex with TrkA and $p75^{NTR}$

(A) The TrkA receptor (pink) consists of a leucine rich repeat (LRR) between two cysteine rich domains (CRD) that is followed by two large immunoglobulin like domains (Ig-like domains). The Ig-like domain that is proximal to the membrane interacts with the NGF dimer (blue). This domain is also called domain 5. **(B)** $p75^{NTR}$ (orange). $P75^{NTR}$ consists of 4 CRD, labelled

consecutively from the amino terminal of the receptor. The NGF interacts with the receptor at two sites. Site I is the interaction of CRD2 with the NGF and site II is where the C-terminal and N-terminal domain of the NGF interacts with CRD3 and CRD4. The NGF (blue) is in opposite orientation in the complexes.

1.2.3 Structure of neurotrophin receptors

1.2.3.1 Tropomyosin–related kinase receptors (Trk receptors)

Trk receptors are a family of three receptor tyrosine kinases, which bind to the family of neurotrophins with different affinities. The TrkA proto-oncogene was the first NGF receptor identified (Kaplan et al., 1991, Klein et al., 1991). Neurotrophin signaling mediated by Trk receptors regulates cell survival, proliferation, the fate of neural precursors, and axon and dendrite growth and in the adult nervous system the Trk receptors regulate synaptic strength and plasticity (Huang and Reichardt, 2003). The Trk receptors have highly conserved intracellular domains and unconserved extracellular domains that confer ligand specificity to the Trk family (Klein et al., 1990).

As illustrated in Fig. 1.5, the Trk extracellular domain consists of two cysteine-rich domains (CRD) flanking three leucine-rich motifs (LRR), followed by two C2-type immunoglobulin-like (Ig-1 and Ig-2) domains (Huang and Reichardt, 2003). There is a linker region composed of 30-50 residues which links the extracellular domain to the transmembrane domain (Schneider and Schweiger, 1991). NGF binds to the Ig-2 domain that is proximal to the transmembrane region of TrkA (Wehrman et al., 2007, Wiesmann et al., 1999). These Ig-like domains have been reported to inhibit ligand independent dimerization of the receptor. This suggests that the conformation of Ig-like domains are altered upon NGF binding, leading to dimerization of the receptors and its phosphorylation and the activation of signaling pathway (Arevalo et al., 2000).

The intracellular domain of TrkA contains 5 tyrosine residues that are critical for receptor function. These are: Y490 in the juxtamembrane domain; Y670, Y674, Y675 in the activation loop of the tyrosine kinase domain; and Y785 in the C-terminal domain. NGF binding to TrkA causes the phosphorylation of the tyrosine kinase domain leading to a downstream signaling cascade (Bibel and Barde, 2000).

1.2.3.2 p75^{NTR}

p75^{NTR} is a cell surface receptor glycoprotein that belongs to the Tumor Necrosis Factor receptor super family (TNFRsf). The alternative names for p75^{NTR} are LNGFR, CD271, TNFRsf16, and NGFR. It is classified as part of this family due to the structural homology and sequence homology of this protein with other members of TNFRsf (Chao, 1994, Chapman, 1995). p75^{NTR} can bind to all neurotrophins with equal affinity. It can either form a complex with the Trk family of receptors or it can act by independent mechanisms to mediate its biological effect (Chao, 1994).

p75^{NTR} has an N-terminal extracellular ligand binding domain, a short transmembrane domain and an intracellular death domain (Vroegop et al., 1992). It is 427 amino acids in length and its actual molecular weight is 55 kDa. N-linked and O-linked glycosylation in the extracellular domain of p75^{NTR} give it a molecular weight of 75 kDa. p75^{NTR} has a single N-glycosylation site, located within the first cysteine-rich repeat (Johnson et al., 1986). The removal of N-linked glycan does not affect the protein folding and its efficient exit from the ER (Baldwin and Shooter, 1995, Grob et al., 1985). The proximal stalk region contains several O-linked glycosylation sites that are essential for the apical sorting of the receptor (Yeaman et al., 1997). The extracellular domain of p75^{NTR} contains 4 cysteine rich domains (CRD). Two different models of NGF binding to p75^{NTR} have been reported: a 2:1 stoichiometry where an NGF dimer binds to a p75^{NTR} monomer; and a 2:2 stoichiometry where an NGF dimer binds to two p75^{NTR}. The 2:1 stoichiometry could potentially engage a Trk receptor to form a tri-molecular NGF signaling complex (He and Garcia, 2004). The transmembrane region of p75^{NTR} contains a conserved Cys (257). p75^{NTR} forms dimers through disulphide linkage independent of ligand binding via this Cys (257) residue (Vilar et al., 2009).

p75^{NTR} has been widely reported to be induced in response to stress (Roux et al., 1999). Several transcription factors have been shown to the involved in the regulation of expression of p75^{NTR} under stress (Ramos et al., 2007). p75^{NTR} has also been reported in several cell types to undergo constitutive proteolytic cleavage that is required for its signaling (Ceni et al., 2010).

1.2.3.3 Sortilin

Mature NGF has been reported to bind to TrkA and have a pro-survival effect, whereas proNGF selectively binds to $p75^{NTR}$ and induces apoptosis (Lee et al., 2001b). However, not all $p75^{NTR}$ expressing cells respond to proNGF suggesting an involvement of additional membrane proteins. Sortilin, a ~95 kDa molecular weight protein belonging to the family of vacuolar protein sorting-associated protein 10 domain receptors (Vps-10p domain receptors) was found to act as a co-receptor, which on binding to $p75^{NTR}$ and proNGF can induce apoptotic signalling in neuronal cells (Nykjaer et al., 2004).

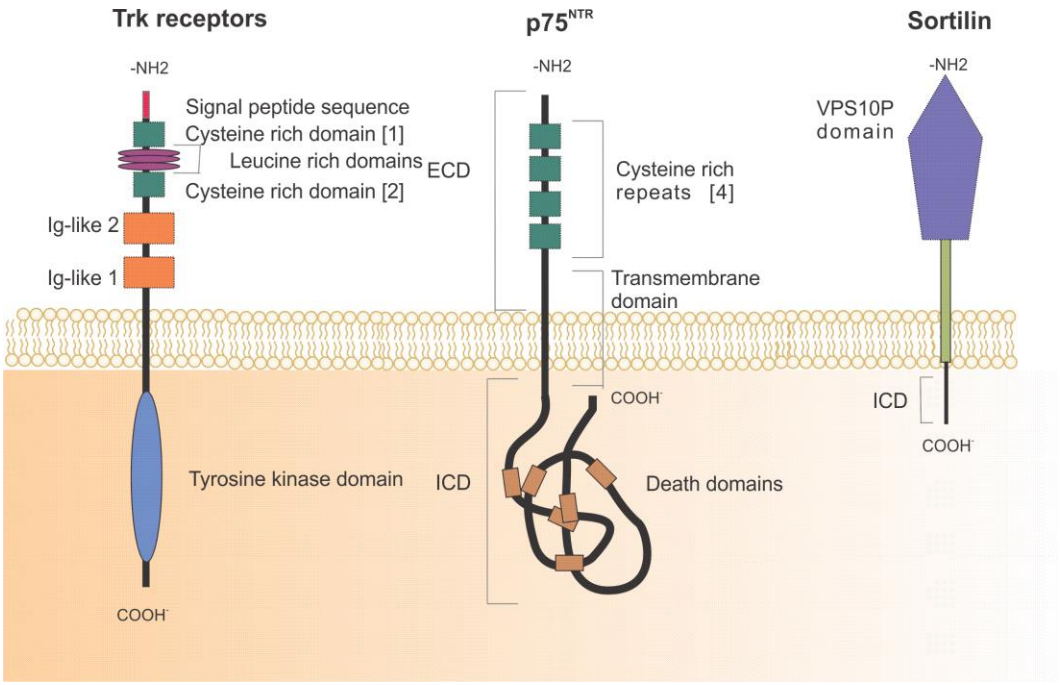

Fig. 1.5 Structure of neurotrophin receptors

Neurotrophins can bind to $p75^{NTR}$, Tropomyosin related kinase (Trk) receptors and Sortilin (SORT) receptor. Sortilin is a member of vacuolar protein sorting -associated protein 10-domain receptors. This figure was adapted from (Hondermarck, 2012).

1.2.4 NGF signaling

Other than their neurite outgrowth-inducing function or survival-promoting function on neuronal cells, the family of neurotrophins has varied biological effects depending on the cellular context. The role of NGF and its receptors have been reported in various cancers

outside of the nervous system (Kruttgen et al., 2006). The following section will elaborate on NGF signaling through TrkA and $p75^{NTR}$ on neuronal cells and cancers.

1.2.4.1 NGF/TrkA signaling

The binding of NGF to TrkA results in the phosphorylation of the receptor tyrosine kinase domain of TrkA. Ligand-induced dimerization of the Trk receptor causes phosphorylation of specific tyrosine residues in the activation loop of the tyrosine kinase domain (Cunningham and Greene, 1998). This phosphorylation leads to an open conformation of the receptor kinase domain which allows the access of substrates to the kinases (Bibel and Barde, 2000). The two specific phosphorylated tyrosine residues Y490 and Y785 serve as docking sites for binding of adaptor molecules to mediate signaling (Friedman and Greene, 1999).

In neuronal cells, NGF/TrkA signaling can activate three signaling pathways: the Ras/Raf/MEK/MAPK pathway; the PI3K/AKT pathway; and the phospholipase C- γ (PLC-γ) pathway. Firstly, phosphorylation of TrkA upon NGF binding leads to the formation of variety of complexes of adaptor molecules. This leads to the activation of Ras/Raf/MEK/MAPK pathway. This pathway was identified in developing neurons and has been shown to mediate neuronal differentiation (Bibel and Barde, 2000). Secondly, NGF/TrkA signaling can activate phosphoinositide 3 kinase (PI3K), one of whose substrates is AKT. This plays an important role in neuronal survival (Franke et al., 1997). Activation of PI3K directly by Ras is an important pathway by which NGF activates AKT through TrkA as PI3K do not directly interact with the Trk receptors (Franke et al., 1997).. Thirdly phosphorylation of TrkA induces phosphorylation of PLC-γ, which through activation of intermediate proteins results in the activation of Protein Kinase C (PKC). It has been reported that one of the PKC isoforms, PKCδ is required for NGF-induced neurite outgrowth (Corbit et al., 1999).

In cancer cells, NGF /TrkA signaling has been reported to mediate their proliferation survival, invasion, migration, angiogenesis and metastasis (Descamps et al., 2001c, Dolle et al., 2005, Romon et al., 2010, Lagadec et al., 2009, Zhang et al., 2015). It has been reported that TrkA overexpression in breast cancer cells enhanced tumor cell growth, angiogenesis and metastasis (Lagadec et al., 2009). This was attributed to the constitutive activation of tyrosine kinase activity, and hyper-activation of PI3K-Akt and ERK/p38MAP kinases in breast cancer cells (Lagadec et al., 2009). Studies in the past

suggest that NGF activation of TrkA promotes a proliferative signal via the MAPK pathway in breast cancer cells and that this effect was independent of $p75^{NTR}$ (Descamps et al., 2001c). This effect through TrkA was inhibited with the use of K252a (Descamps et al., 2001c), a pharmacological inhibitor of Trk receptors that inhibits the phosphorylation of the tyrosine kinase domain of Trks (Kase et al., 1986)

1.2.4.2 NGF/$p75^{NTR}$ signaling

NGF signaling through $p75^{NTR}$ can mediate a pro-apoptotic or pro-survival effect depending on the form of NGF that binds to $p75^{NTR}$. The effect of NGF/$p75^{NTR}$ is highly dependent on cellular context. For example, although $p75^{NTR}$ signaling was originally studied in neuronal cells and it was identified to be a member of death receptor family, several studies have investigated NGF/$p75^{NTR}$ signaling in non-neuronal cells and in several cancer models where they mediate different signaling pathways conferring pro-survival effects. Constitutive processing of $p75^{NTR}$ has been reported in several cell types and this has been shown to be important in NGF signaling through $p75^{NTR}$ (Skeldal et al., 2011).

In the following section, proNGF/Aβ-mediated cell death through $p75^{NTR}$ signaling in neuronal cells and NGF-mediated pro-survival signaling in cancers will be elaborated.

1.2.4.2.1 $p75^{NTR}$ mediated pro-death signaling

Several studies have shown that proneurotrophins, including proNGF, can induce cell death in neuronal cells via $p75^{NTR}$ (Nykjaer et al., 2004). However, not all cells that express $p75^{NTR}$ can induce apoptosis as they require the co-expression of the sortilin receptor. Sortilin acts as a molecular switch governing the $p75^{NTR}$ mediated pro-apoptotic signaling induced by proNGF (Nykjaer et al., 2004). The same observation is true for proBDNF-induced pro-apoptotic signaling in sympathetic neurons where co-expression of $p75^{NTR}$ and sortilin are required for cell death (Teng et al., 2005). The mechanism of proNGF induced cell death is thought to be the same as the mechanism by which mature NGF binds to $p75^{NTR}$ and induces neuronal apoptosis, occurring through activation of JNK and caspases (Harrington et al., 2002, Diarra et al., 2009). Another well –known example of $p75^{NTR}$-mediated cell death in neuronal cells is through the binding of amyloid β (Aβ) peptide (Rabizadeh et al., 1994). Aβ peptides are the soluble fragment generated by cleavage of amyloid precursor protein (APP). Large Aβ peptide deposits are

found in the brain of patients suffering with Alzheimer's disease (AD) (Selkoe, 2001). Aβ has been reported to directly interact with $p75^{NTR}$ leading to c-Jun mediated apoptosis in hippocampal neurons (Diarra et al., 2009, Yaar et al., 1997).

1.2.4.2.2 $p75^{NTR}$- mediated pro-survival signaling

NGF/$p75^{NTR}$ signaling has been reported in several cancers such as breast cancer, prostate cancer and in melanomas. Reports show that primary and metastatic melanoma cell lines express and secrete all neurotrophins and that they also express $p75^{NTR}$, Trk receptors and the $p75^{NTR}$ co-receptor sortilin. NT-3, NT-4 and NGF have been reported to induce migration in the more metastatic melanoma cell lines and this effect is inhibited by the use of $p75^{NTR}$ siRNA (Truzzi et al., 2008). In prostate cancers, $p75^{NTR}$ has been proposed to be a tumor suppressor, where the loss of $p75^{NTR}$ expression facilitates survival, proliferation and metastasis of tumor cells (Krygier and Djakiew, 2002, Krygier and Djakiew, 2001).

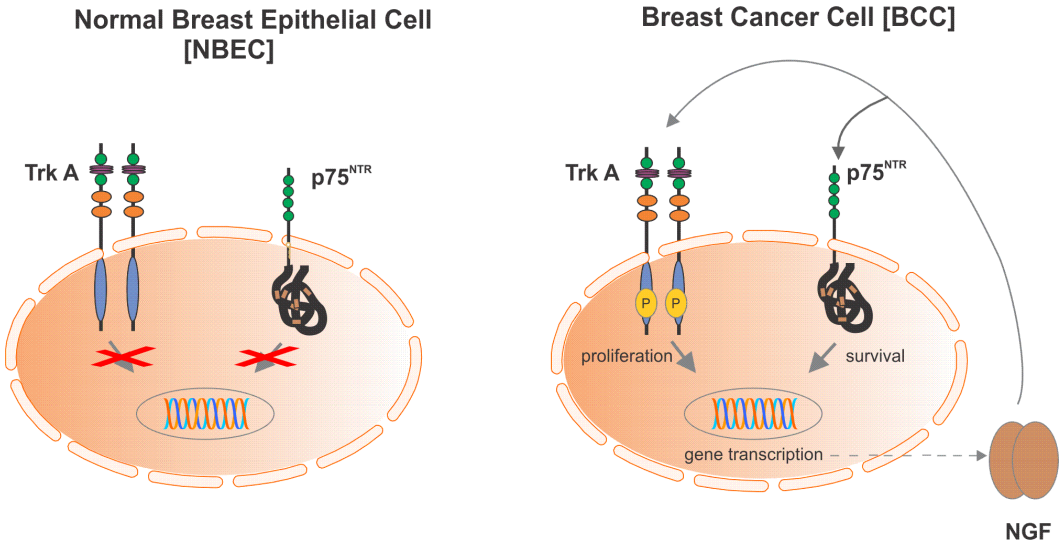

Fig. 1.6 Autocrine signaling between NGF and its receptors in Breast cancer cells

NGF receptors are expressed in both NBEC and BCC, but NGF is only produced by BCC which can activate its receptors through an autocrine signaling loop. NGF activates TrkA, mediating proliferative effects and it activates $p75^{NTR}$, mediating pro-survival effects in BCC.

NGF expression has been reported to contribute to breast cancer progression and pathogenesis (Adriaenssens et al., 2008, Descamps et al., 2001c). As shown in Fig. 1.6 NGF receptors are expressed in both breast cancer cells (BCC) and NBEC, but the latter

do not express NGF, which highlights the potential use of anti-NGF in the treatment of breast cancers (Descamps et al., 1998). NGF mediates a pro-survival effect through autocrine signaling via $p75^{NTR}$ in breast cancers (Descamps et al., 2001c). It has been shown to protect MCF-7, MDA-MB-231, T47-D, BT-20 cell lines from C2-ceramide induced cell death (Descamps et al., 2001c). It has been reported that NGF exerts its anti-apoptotic effects through $p75^{NTR}$ by activation of NF-κB (Descamps et al., 2001c). The expression of $p75^{NTR}$ is high in basal-like breast cancer cells and this can be used as a marker to predict a group of basal-like breast cancers with good prognosis (Reis-Filho et al., 2006). The activation of $p75^{NTR}$ results in recruitment of adaptor proteins to the death domain of $p75^{NTR}$ that then lead to pro-survival signaling through NF-κB in breast cancers, but the adaptor molecules that link NGF/$p75^{NTR}$ activation and the NF-κB mediated pro-survival effect remain unknown (El Yazidi-Belkoura et al., 2003). This is illustrated in Fig. 1.7. There is only one report so far that shows the interaction of Tumor necrosis factor receptor associated death domain (TRADD) with the death domain of $p75^{NTR}$ upon NGF binding to $p75^{NTR}$ and its involvement in mediating the anti-apoptotic effect on MCF-7 cells by activating NF-κB pathway (El Yazidi-Belkoura et al., 2003). This report shows that the death domain of TRADD is required for its binding to the death domain of $p75^{NTR}$ to mediate this effect. Other members of the TNFRSF like TNF-R1 or TRAIL recruit TRADD to their death domains and use that as a platform to recruit other adaptor molecules, including Receptor-interacting protein 1 (RIP-1), TNF-R associated factor 2 (TRAF-2) and Fas-associated death domain (FADD), to promote cell survival or cell death (Muppidi et al., 2004). So far, there is no evidence showing the recruitment of other adaptor proteins to TRADD in breast cancer cells. In Schwann cells, RIP2 has been shown to bind to the death domain of $p75^{NTR}$ and mediate a pro-survival effect by activating NF-κB (Khursigara et al., 2001). There are reports that show the interaction of other members of the TRAF family (TRAF2, 4, 6) directly with the $p75^{NTR}$ intracellular domain in 293T cells expressing $p75^{NTR}$ (Ye et al., 1999, Zampieri and Chao, 2006, Khursigara et al., 1999, Kanning et al., 2003). Involvement of RIP2 or other TRAFs in NGF-mediated $p75^{NTR}$ signaling in breast cancers is not known.

Brain expressed X-linked 2 (BEX2) has been reported to be overexpressed in a subset of primary breast cancers, mainly in Er positive subtypes of breast cancers, and is reported to be regulated by estrogen (Naderi et al., 2007). In this cellular context, BEX2 has been shown to be required for NGF/$p75^{NTR}$ dependent NF-κB activation and pro-survival

effects (Naderi et al., 2010b). There is no evidence so far of a direct interaction with $p75^{NTR}$, but it is reported to be sufficient to bring about the anti-apoptotic effect of NGF in breast cancer (Naderi et al., 2007, Naderi et al., 2010a, Naderi et al., 2010b). BEX2 has also been shown to protect breast cancer cells from the intrinsic apoptotic pathway through modulation of Bcl-2 family members, including up-regulation of the anti-apoptotic protein Bcl-2 and down-regulation of pro-apoptotic members Bad, Bak and PUMA (Naderi et al., 2010a). The homologues BEX1 and BEX3 have also been shown to interact with $p75^{NTR}$. In neural tissues BEX1 inhibits NF-κB, links neurotrophin signaling to the cell cycle and may sensitize cells to apoptosis (Vilar et al., 2006, Ding et al., 2009). BEX2 has been shown to be required for progression of MCF-7 breast cancer cells through the G1 phase of the cell cycle via its regulation of cyclin D and p21 (Naderi et al., 2010b, Naderi et al., 2010a).

Overexpression of $p75^{NTR}$ in breast cancer cells has been shown to increase their survival through $p21^{waf1}$ (Verbeke et al., 2010). This effect was associated with inhibition of apoptosis. The anti-proliferative effect was due to accumulation of cells in the G0/G1 phase associated with decreased Rb phosphorylation and increased $p21^{waf1}$. Inhibition of $p21^{waf1}$ not only restored proliferation but also abolished the pro-survival effect of $p75^{NTR}$ (Verbeke et al., 2010).

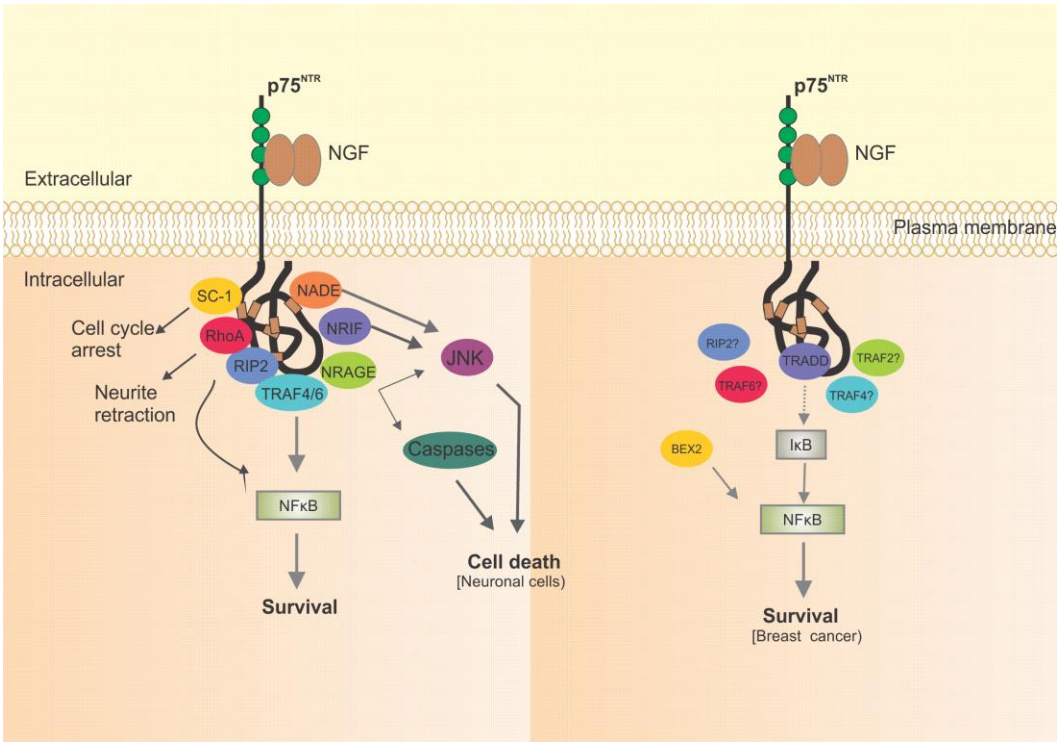

Fig. 1.7 NGF-p75^{NTR} signaling pathway

NGF binds to p75^{NTR} and mediates cell survival through activation of NF-κB (Descamps et al., 2001c) or cell death signal through activation of JNK (Gentry et al., 2000). In addition to these, NGF/p75^{NTR} signaling can also lead to cell cycle arrest (Chittka et al., 2004) or neurite retraction (Yamashita and Tohyama, 2003b).

1.2.4.2.3 Regulated intramembrane proteolysis of p75^{NTR}

Several studies have shown that p75^{NTR} undergoes constitutive proteolytic cleavage in many cellular contexts (Kanning et al., 2003, Skeldal et al., 2011, Verbeke et al., 2013). p75^{NTR} undergoes regulated intramembrane proteolytic cleavage as shown in Fig. 1.8 that involves cleavage at the extracellular domain by phorbol myristate acetate (PMA)-inducible membrane metalloproteinase (α-secretases) resulting in shedding of the ectodomain (Kanning et al., 2003). The resulting fragment is called the carboxy-terminal fragment (CTF) as shown in Fig.1.7. This is next cleaved by gamma-secretases around or within the transmembrane region to generate the intracellular domain fragment (ICD). The ICD is released into the cytoplasm with signaling capability (Kanning et al., 2003). This fragment has been shown to function in concert with TRAF-6 to activate the NF-κB pathway (Kanning et al., 2003). Several proteins including matrix metalloproteinases

(MMPs), a disintegrin and metalloproteases (ADAMs) have been reported to be implicated in glioma invasion (Nakada et al., 2007). The processing of $p75^{NTR}$ was found to be required for the highly invasive behavior of $p75^{NTR}$ positive malignant glioma (Wang et al., 2008). γ-secretase inhibitors have proven promising in the treatment of invasive glioma mediated by $p75^{NTR}$ (Wang et al., 2008).

A recent study showed that $p75^{NTR}$ undergoes constitutive regulated proteolysis in TNBC cells (Verbeke et al., 2013). In this study, the CTF was shown to be important for the survival of breast cancer cells and the ICD had no effect (Verbeke et al., 2013), while the generation of the ICD by γ-secretase mediated cleavage of $p75^{NTR}$ was important in glioma cell survival (Wang et al., 2008). Interestingly this CTF-mediated cell survival was independent of PI3K, NF-κB or MAPK signaling pathways. Which pathway contributes to the breast cancer cell survival is unknown (Verbeke et al., 2013) . The mechanism of neurotrophin mediated processing of $p75^{NTR}$ is highly cell type dependent (Carter and Lewin, 1997). In PC12 cells, NGF has been shown to induce the processing of $p75^{NTR}$ and this mechanism requires activated TrkA (Ceni et al., 2010). There are currently no reports that have investigated the mechanism of $p75^{NTR}$ processing in breast cancers.

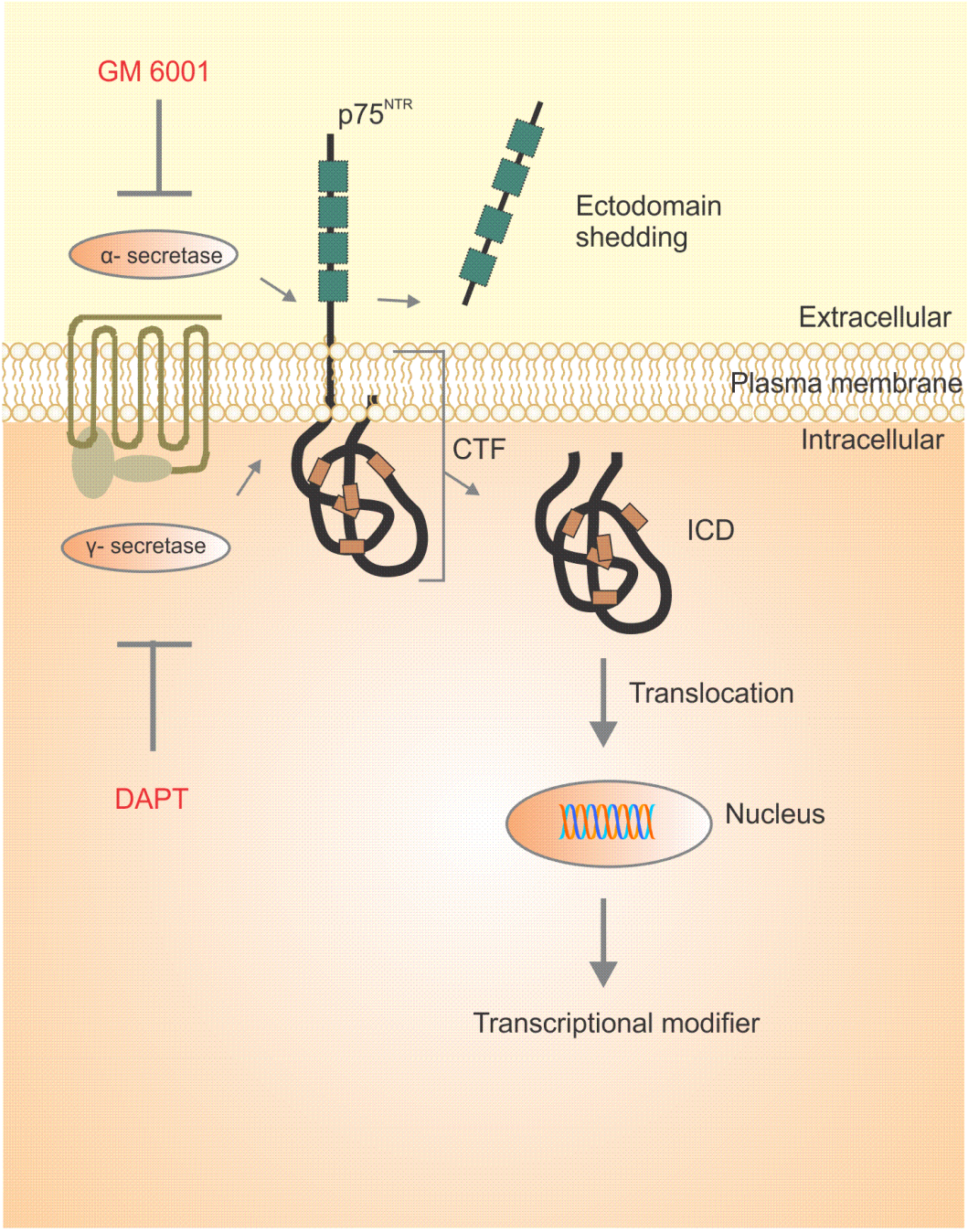

Fig. 1.8 Regulated intramembrane proteolysis of $p75^{NTR}$

$p75^{NTR}$ undergoes sequential cleavage by PMA-inducible activation of secretases. The first cleavage by α-secretases leads to shedding of the extracellular domain of $p75^{NTR}$. This generates carboxy- terminal fragment (CTF). This is subjected to sequential cleavage by γ-secretases which leads to generation of intracellular domain fragment (ICD) which translocates to the nucleus to

activate various transcription factors. GM 6001 and DAPT are the inhibitors of activators of α- and γ- secretases, respectively.

1.2.5 Regulation of $p75^{NTR}$ expression

$p75^{NTR}$ expression and signaling has been implicated in mediating neuronal apoptosis after injury to the CNS (Roux et al., 1999), but very little is known about the mechanisms that regulate its expression. For example, $p75^{NTR}$ expression is induced in apoptotic neurons after seizures (Roux et al., 1999) and via nitric oxide in conditions of osmotic swelling following brain injuries (Peterson and Bogenmann, 2003). Basal levels of $p75^{NTR}$ are also rapidly induced after focal cerebral ischemia (Irmady et al., 2014). A few transcription factors are reported to regulate expression of $p75^{NTR}$ under stress conditions. Hypo-osmolar stress induces $p75^{NTR}$ expression by activating Sp1-dependent transcription in neurons (Ramos et al., 2007). Early growth response (Egr1 and Egr3) transcription regulators have been shown to directly activate $p75^{NTR}$ gene expression and signaling in vivo (Gao et al., 2007). Induction of $p75^{NTR}$ expression by NSAIDs (non-steroidal anti-inflammatory drugs) decreases the $p75^{NTR}$-dependent survival of prostate tumor cells (Quann et al., 2007). Reports also suggest that NGF is involved in the induction of $p75^{NTR}$ expression in prostate cancer which is accompanied by a reduction in prostate cancer cell malignancy (Sigala et al., 2008). The regulation of $p75^{NTR}$ expression by NGF has only been studied in prostate cancer.

1.3 HEAT SHOCK PROTEINS [HSPS]

Intracellular pro-survival signaling can be mediated by various factors such as molecular chaperones. The following section will elaborate on the role of molecular chaperones with heat shock protein as an example in mediating pro-survival signaling in response to stressors.

Cells are subjected to various internal and external stimuli, which in some cases may induce stress. The induction of stress may lead to an altered cellular response to subsequent environmental signals. Prolonged exposure of the cells to such insults may result in accumulation of damaged DNA, proteins and lipids. To maintain homeostasis, cellular stress response (CSR) is initiated (Kultz, 2003). If the intensity of stress is mild, then it can lead to protective mechanisms by activation of heat shock proteins (HSPs)

(Samali et al., 2010), the endoplasmic reticulum unfolded protein response (UPR^{ER}), or autophagy (Fulda et al., 2010).

The heat shock response (HSR) is one of the most ancient and evolutionarily conserved cyto-protective mechanisms found in nature (Ritossa, 1996). It is an essential defense mechanism used by cells to protect themselves from a varied range of stimuli like heat shock, alcohols, inhibitors of energy metabolism, heavy metals, oxidative stress, slight alterations in the optimum temperature, inflammation and proteasomal inhibition (Lindquist, 1986, Morimoto, 1993, Bush et al., 1997). The redox state of the cells is affected by stress inducing agents and this in turn, causes an increase and accumulation in the levels of misfolded proteins which may be deleterious by virtue of their altered biologic activities (Jolly and Morimoto, 2000). HSPs induced in response to cellular stress serve as molecular chaperones that function by transiently interacting with other proteins undergoing synthesis, aiding in their protein folding, translocation and refolding. The proteins that cannot be refolded or are damaged beyond repair are targeted for degradation (Ellis, 1993, Georgopoulos and Welch, 1993). Stress induced transcription of HSPs requires activation of Heat shock factor 1 (HSF 1), the master regulator of HSP genes in vertebrates (Akerfelt et al., 2010). The increased expression and accumulation of the stress proteins provides the cell with an added degree of protection (Welch, 1993). The induction of HSPs in response to a cellular stress can protect the cells against a subsequent stressor with this phenomenon termed as "cross protection" (Lindquist, 1986, Richter et al., 2010, Morimoto, 1998).

1.3.1 Families of Heat shock proteins [HSPs]

HSPs are classified into five major groups/families based on their molecular size: HSPH (HSP100), HSPC (HSP90), HSPA (HSP70), DNAJ (HSP40) and HSPB (the small heat shock proteins [sHSPs]) (Vos et al., 2008). The HSPB is a family of molecular chaperones consisting of at least 10 members in mammals (Taylor and Benjamin, 2005). Within each family are members that are expressed either constitutively or transiently or are inducibly regulated and/or shuttled or targeted to different cellular compartments (Jolly and Morimoto, 2000). Along with this classification are the human chaperonin families HSPD/E (HSP60/HSP10) and CCT (TRiC). These are class of proteins that play an important role in the proper folding of newly synthesized cytosolic proteins and prevent their aggregation (Kampinga et al., 2009).

1.3.1.1 Small heat shock proteins [HSPB]

Small heat shock proteins range from 12-43 kDa and they share significant sequence similarity within the "alpha-crystallin domain" (Taylor and Benjamin, 2005). They are defined by the conserved sequence of approximately 90 amino acid residues termed the alpha-crystallin domain which is flanked by variable amino- and carboxy-terminal extensions (MacRae, 2000). Although they share sequence similarity, they exhibit different patterns of gene expression, transcriptional regulation, localization within the cellular compartments and also functions (Taylor and Benjamin, 2005). The HSPB can be classified into two functional categories (Taylor and Benjamin, 2005). Class I sHSPs are ubiquitously expressed and include HSP27/HSPB1, CRYAB/HSPB5, HSP20/HSPB6, H11/HSPB8. Class II sHSPs display a tissue specific pattern of expression and include HSPB2, HSPB3, cvHSP/HSPB7, CRYAA/HSPB4, HSPB9 and ODF1/HSPB10. The expression of class II proteins is restricted to myogenic and testicular lineages (Taylor and Benjamin, 2005). Apart from containing a conserved α-crystallin domain, the family of sHSPs do share similarity in their ability to form large oligomers, a dynamic quaternary structure and mediate ATP independent chaperone activity (Haslbeck et al., 2005). Although HSPs confer a cytoprotective effect in response to stress, mutations in these chaperones have been reported to cause diseases and these are termed chaperonopathies (Vos et al., 2008). Distal peripheral neuropathy such as Charcot-Marie Tooth Syndrome is linked to mutations in HSPB1 and HSPB8 (Houlden et al., 2008)

The functions of small HSPs and αβ crystallin are to protect cells from cellular stress by acting as molecular chaperones (Horwitz, 1992). They mediate re-folding of unfolded proteins and mis-folded proteins (Horwitz, 1992). They also confer thermo-tolerance (Landry et al., 1989) through stabilization of microfilaments (Miron et al., 1991). Small HSPs, in particular HSPB1 protect cells against apoptosis by binding to Cu^{2+} thereby inhibiting generation of ROS, oxidative stress and amyloid aggregation of Aβ peptides (Asthana et al., 2014), (Bakthisaran et al., 2015), they also mediate protection to apoptosis by binding to several components in the apoptotic cascade mediate effect on pro-survival pathways. They also function in RNA stabilization (Nover et al., 2001). Circulating HSPs confer immune-modulatory anti- inflammatory functions. They play a role in differentiation, proteasomal degradation, autophagy and development (Bakthisaran et al., 2015).

1.3.1.1.1 Heat shock protein B1 [HSPB1]

Of all the sHSPs identified so far only a few of them, including HSPB1, are true heat shock proteins whose expression is enhanced in response to stress (Arrigo et al., 2007). As shown in Fig. 1.9, HSPB1 has a conserved C-terminal domain (the α-crystallin domain). This region is a highly structured β-pleated sheet with several contact points allowing oligomer formation and stabilization (Kim et al., 1998). HSPB1 also contains a WDPF domain in its N-terminal segment and a non-conserved flexible domain at the carboxy terminal which usually promotes solubility, chaperoning and oligomerization (Sun and MacRae, 2005). It is the property of sHSPs to form oligomers that controls the activity of these proteins. In contrast to other regions of the sHSPs, several mutations have been reported in the α-crystallin domain as shown in Fig. 1.8 (Baranova et al., 2011, Arrigo et al., 2007).

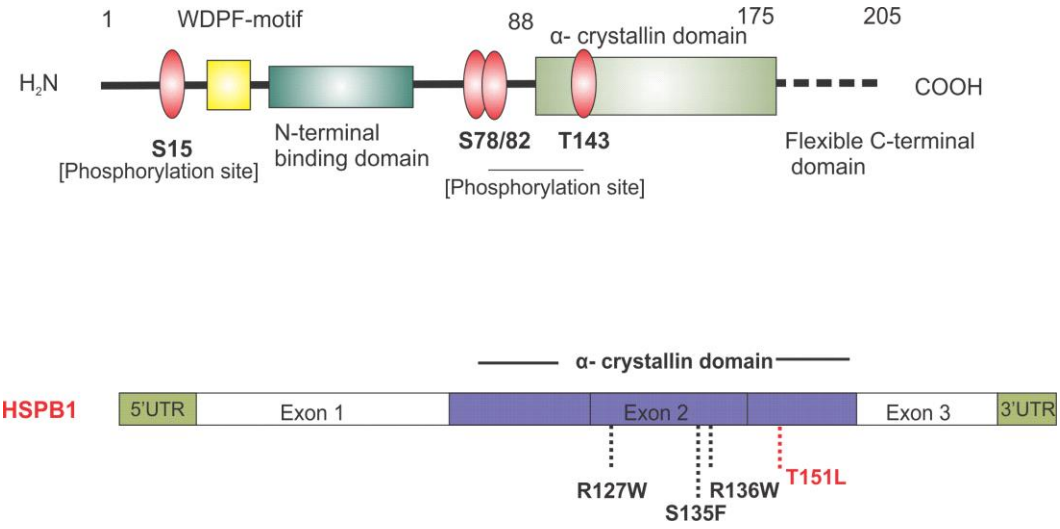

Fig. 1.9 Structure of HSPB1 and mutations in HSPB1

The illustration shows structure of HSPB1 with sites of phosphorylation of HSPB1. It also shows{} mutations of HSPB1 reported in Charcot Marie Tooth disease.

1.3.1.1.2 Functions of HSPB1

HSPB1 is a 27 kDa molecular chaperone with an ability to interact with other members of the family such as HSPB8 (Sun et al., 2004) These chaperones have been thought to mediate protection against apoptosis by interacting with key components; such as caspases, or cytochrome c of the apoptotic signaling pathway (Concannon et al., 2003).

HSPB1 can function as (a) an anti-apoptotic protein by exerting inhibition at various stages of the extrinsic and intrinsic apoptotic machinery, (b) a mediator of proteasomal degradation of target proteins. The following sections explain these two aspects in detail.

1.3.1.1.2.1 HSPB1, as an anti-apoptotic protein

HSPB1 can inhibit apoptosis at various stages in the apoptotic pathway, as shown in Fig. 1.9. In response to cellular stress like heat shock or oxidative stress, induced HSPB1 binds to and activates AKT, a pro-survival gene, thereby inhibiting apoptosis. Cells that express high levels of HSPB1 are most likely to be resistant to cell death in response to stressors (Konishi et al., 1997). As a molecular chaperone, HSPB1 has the ability to bind to various proteins and in this way HSPB1 can inhibit apoptosis by directly binding to effector procaspase and inhibiting caspase activation (Garrido et al., 1999, Samali et al., 2001). HSPB1 can exert its anti-apoptotic effect through many possible ways. (a) Overexpression of HSPB1 blocks ROS production and suppresses the loss of mitochondrial membrane potential ($\Delta\Psi m$) which mediates the release of cytochrome c. (b) It can directly interact with mitochondria and inhibit the release of cytochrome c. (c) It can bind to the components of the apoptosome complex and inhibit the activation of effector caspases (Samali et al., 2001). However a study by Pandey et al showed no association of HSPB1 with cytochrome c, Apaf-1 or procaspase- 9 and that HSPB1 exerts an inhibitory effect on apoptosis by binding to caspase-3 directly (Pandey et al., 2000). (d) HSPB1 has been shown to mediate cytoprotection in response to agents that damage the cytoskeleton of the mitochondria by negatively regulating the re-distribution of BID to the mitochondria, thereby preventing the release of cytochrome c and subsequent activation of the intrinsic apoptotic pathway (Paul et al., 2002). (e) Overexpression of HSPB1 in response to stress inhibited conformational BAX activation, oligomerization and translocation to the mitochondria, release of cytochrome c and apoptosis inducing factor (AIF) via a PI3-kinase dependent mechanism. HSPB1 prevented the inactivation of pro-survival kinase AKT by promoting PI3-kinase activity, an upstream activator of AKT and thereby increasing the interaction of AKT with BAX, an AKT substrate (Havasi et al., 2008). (f) HSPB1 and AKT are reported to co-exist in a signaling complex with p38MAPK, MAPK-activated protein kinase 2 (MK2) which phosphorylates AKT at Ser-473 (Rane et al., 2003). HSPB1 regulates AKT activation by scaffolding MK2 to the AKT signaling complex thereby mediating its pro-survival effect. (g) HSPB1 has been shown to bind to procaspase-3 which is in its inactive form and due to the sequestering of

procaspase-3 by HSPB1, the residues on procaspase-3 required for caspase-9 to cleave are masked and this results in inhibition of activation of caspase-3 (Concannon et al., 2001). (h) HSPB1 can also exert its inhibitory effect by binding the death ligands to cell surface receptors like Fas (Mehlen et al., 1996). HSPB1 can interact with Daxx, a mediator of Fas- induced apoptosis (Charette et al., 2000).

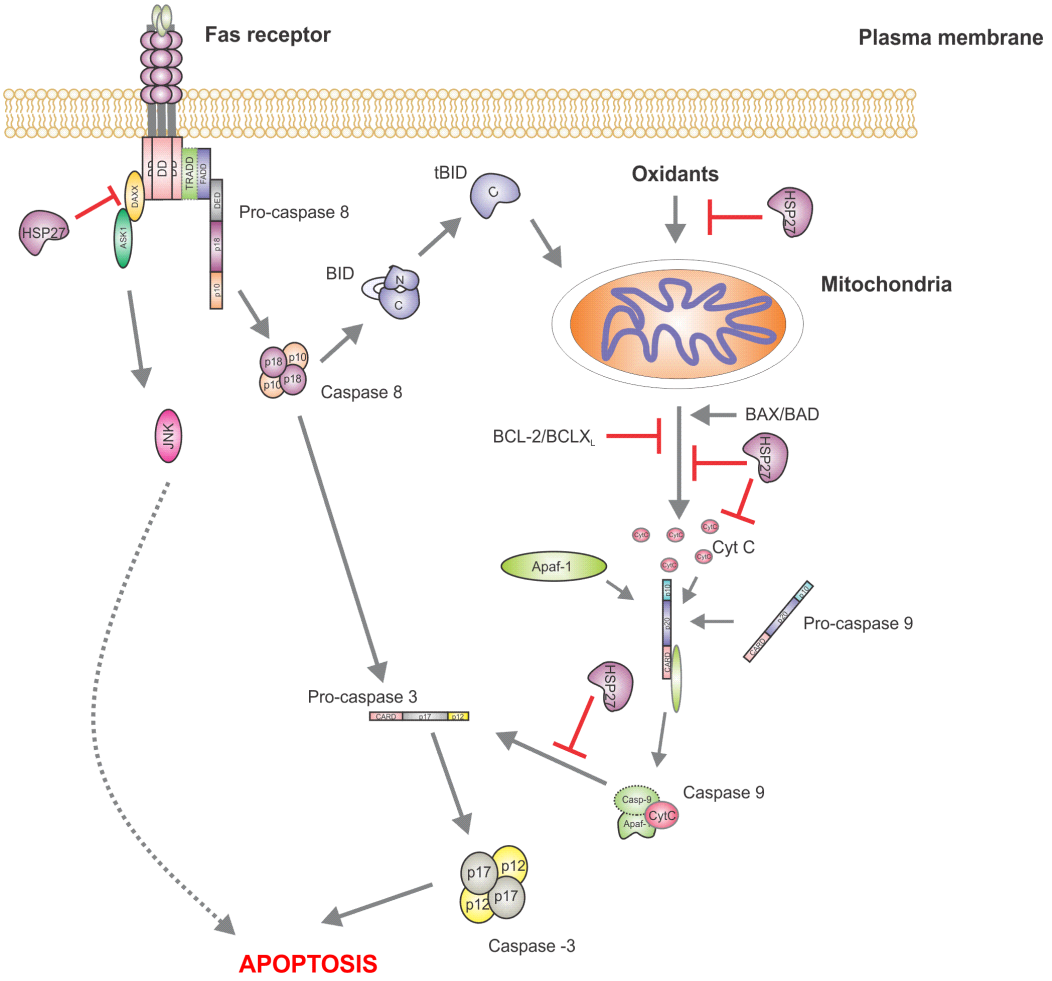

Fig. 1.9 Regulation of anti-apoptotic machinery by HSPB1

HSPB1 is able to inhibit apoptosis at various stages. It can inhibit at various stages within the mitochondria by indirectly binding to BAX; by inhibiting cytochrome c release; by binding directly to pro-caspase 3 and preventing its activation by caspase-9; by binding to one or more components of the apoptosome complex and it can bind to DAXX and prevent the activation of ASK-1 which in turn activates JNK, leading to apoptosis.

The cytoprotective function of HSPB1 has also in part been attributed to its post-translational modification. HSPB1 can be phosphorylated in response to cellular stress

such as ER stress (Ito et al., 2005). HSPB1 is phosphorylated at the serine residues in the N-terminal part of the polypeptide, in the WDPF domain and close to the α-crystallin domain as shown in Fig. 1.9. HSPB1 is phosphorylated at serine residues 15, 86 in rodents and serine 15, 78 and 82 in humans by mitogen-activated protein kinases associated protein kinases (MAPKAP kinases 2, 3) which are themselves activated by phosphorylation by MAP p38 protein kinase (Stokoe et al., 1992, Rouse et al., 1994). The phosphorylation of HSPB1 has been shown to decrease the size of the oligomers it forms (Kato et al., 1994). Phosphorylation at Ser-82 present in the region of dimerization results in dissociation of HSPB1 oligomers (Theriault et al., 2004). The conversion of HSPB1 oligomers to dimers has been reported in the past to be mediated through phosphorylation of HSPB1 at Ser-78/Ser-82 or 86, while phosphorylation at Ser-15 only seemed to induce a small effect on oligomerization (Lambert et al., 1999, Gusev et al., 2002). So far, HSPB1 has been shown to have a cytoprotective effect in response to stress induced apoptosis. Recently in a study by Sun *et al*. the expression of HSPB1, which is under the control of HSF1, has been shown to negatively regulate ferroptotic cell death, an iron-dependent form of non-apoptotic cell death. It has been shown that protein kinase C-mediated phosphorylation of HSPB1 at Ser 15 conferred protection against ferroptosis by reducing the iron mediated production of lipid reactive oxygen species (Sun et al., 2015). This points to the finding that phosphorylation of HSPB1 also plays a cytoprotective role in non-apoptotic cell death. The phosphorylation status and structural organization of sHSPs act as an intracellular stressor leading to initiation of adaptive strategies (Arrigo, 2013). The presence of mutations in HSPBs also alter their oligomeric size (Arrigo, 2013).

1.3.1.1.2.2 HSPB1 as a mediator of proteasomal degradation

As mentioned earlier, small heat shock proteins act as molecules that target proteins for proteasomal degradation. When the misfolded proteins are beyond repair, HSPB1 takes up the role of proteasomal degradation enhancer that targets the toxic misfolded protein for degradation (Georgopoulos and Welch, 1993). Ubiquitin is a highly expressed cytosolic protein which is classified as one of the smallest HSPs (8 kDa). It belongs to the family of HSPs because it contains a HSE in its promoter region and its primary function is to target misfolded proteins that are beyond repair to degradation via the ubiquitin-proteasome pathway. This process is of paramount importance in the cellular stress and

restoration of proteostasis because, with increased ubiquitin-dependent degradation, the requirement for HSP induction can be compromised (Friant et al., 2003).

The proteasome is a multisubunit enzyme complex that plays a central role in the regulation of proteins that control cell cycle progression and apoptosis (Adams, 2003). It is found both in the nucleus and in the cytoplasm. It consists of a 20S proteolytic core and two 19S regulatory complexes which are involved in the degradation of ubiquitin tagged and also in some cases non-ubiquitinated substrates (Jariel-Encontre et al., 2008).

HSPB1 has been shown to enhance proteasome activity in response to cellular stress (Parcellier et al., 2003). HSPB1 specifically binds to poly-ubiquitin chains and to the 26S proteasome in vitro and in vivo thereby enhancing their degradation of poly-ubiquitinated proteins under cellular stress (Parcellier et al., 2003). Some of the proteins that are degraded by the activity of HSPB1 are $p27^{KIP1}$ and IκBα (Parcellier et al., 2003). In contrast, HSPB1 can also protect eukaryotic initiation factor eIF4E from ubiquitination and inhibit their proteasomal degradation (Andrieu et al., 2010). Therefore HSPB1 appears to exert substrate specific effects on proteasomal degradation and protein stability.

1.3.1.1.3 Cancers associated with overexpression of HSPB1

Under cellular stress, HSPB1 is phosphorylated and this results in the formation of HSPB1 oligomers. These oligomers prevent aggregation and regulate activity and degradation of several client proteins (Garrido et al., 2002). HSPB1 has been reported to be overexpressed in a wide range of malignancies including breast (Love et al., 1994), ovarian (Langdon et al., 1995), gastric (Huang et al., 2010), prostate (Rocchi et al., 2005), bladder (Lebret et al., 2003) and pancreatic cancer (Melle et al., 2007). Over expression of HSPB1 in cancers is associated with poor prognosis and multi-drug resistance by protecting cells from therapeutic agent induced apoptosis. Hence, HSPB1 can be used as a potential therapeutic target in cancers (Acunzo et al., 2014). The overexpression of HSPB1 can be targeted by the use of antisense oligonucleotides (ASOs) such as OGX-427. OGX-427 is a modified antisense oligonucleotide that is complimentary to HSPB1, and it inhibits the expression of HSPB1 and also enhances drug efficacy in cancer xenograft models. Phase II clinical trials using OGX-427 in cancers of breast, lung, bladder, ovary and prostate are in progress. This approach in combination with chemotherapy can potentially enhance sensitivity of cancer cells to apoptosis (Baylot et

al., 2011). For instance, MiaPaCa-2 cells; a representative of pancreatic cancer cell line, grown both in vitro and xenografted in mice, showed enhanced gemcitabine sensitivity when used in combination with OGX-427 via mechanism involving eIF4E (Baylot et al., 2011).

1.3.1.1.4 Diseases associated with aberrant expressions of heat shock proteins

Aberrant expressions of HSPs have been reported widely across a range of tumors. Because a prominent characteristic feature of tumor cells is their resistance to cell death, and HSPs contribute to cytoprotection in response to stressors, several studies are ongoing to understand if the association of altered expression of HSPs is causal or correlative across tumors (Jolly and Morimoto, 2000). Neurodegenerative diseases are characterized usually by the accumulation or oligomerization of misfolded proteins which form aggregates, thereby inducing cytotoxicity. In such cases, enhancement of components that stabilize protein folding have been thought to suppress the aggregation and toxicity to allow restoration of cellular function (Westerheide and Morimoto, 2005). Therefore understanding the cellular signaling mechanisms and functioning of HSPs with respect to cellular context warrants further studies.

1.4 Aims of the work

1. To investigate the regulation of expression of $p75^{NTR}$ in TNBCs
2. To determine the biological relevance of the regulation of $p75^{NTR}$ expression in TNBCs
3. To determine the biological activity of NGF variants with altered receptor specificity
4. To investigate the mechanism of HSPB1-mediated regulation of ER stress-induced apoptosis

The central theme of this thesis is" ***investigating the role of extracellular and intracellular molecules in pro-survival signaling in response to varied stressors"***.

2 Chapter 2: Materials and methods

2.1 Suppliers

Alomone Labs, Jerusalem 91042, Israel.

BD Biosciences-Pharmingen, San Diego, CA 92121, USA.

Biomatik, Wilmington, Delaware, 19809, USA.

Biosciences, Dun Laoghaire, Co Dublin, Ireland.

Bio-Techne, Abingdon, OX14 3NB, United Kingdom.

Calbiochem, Nottingham, NG9 2JR.

Cell Signalling Technology (CST), Inc., Beverley, MA 01915, USA.

Enzo lifesciences, Exeter, EX2 4DG, United Kingdom.

Fisher Scientific Ireland, Dublin 15, Ireland.

Genecopoeia, Rockville, MD, USA.

Integrated DNA technologies, Leuven, B-3001, Belgium.

Invitrogen, Crofton Rd., Dun Laoghaire, Dublin, Ireland.

Medray Imaging systems, Dublin 22, Ireland.

Merck Millipore, Billerica, MA 01821, USA.

MyBio Ltd., Kilkenny, Ireland.

New England Biolabs (NEB), Ipswich, MA01938-2723, UK.

Pierce, Subsidiary of Thermo Scientific Ltd, Rockford, IL 61105 USA.

Promega, Mulhuddart, Dublin 15, Ireland.

R&D systems, Abingdon, OX14 3NB, UK.

Santa Cruz Biotechnologies (SantaCruz), Inc., Santa Cruz, CA 95060, USA.

Sigma-Aldrich Ireland, Dublin, Ireland. All chemicals were obtained from Sigma-Aldrich unless otherwise stated.

2.2 Methods

2.2.1 Cell culture

Breast cancer cell lines

A panel of breast cancer cell lines was used in this study. MDA-MB-231 and MCF-7 were brought from European Collection of Cell Cultures (ECACC), HCC1806 was obtained from American Type Culture Collection (ATCC) and T47D was available in the lab. The expression of Er, Pr, Her2, $p75^{NTR}$ in these cell lines are listed in Table 2.1.

Cell line	Er	Pr	Her-2	$P75^{NTR}$	Subtype
MDA-MB-231	-	-	-	+	Basal like
HCC1806	-	-	-	+	Basal like
MCF-7	+	+	-	-	Luminal A
T47D	+	+	-	-	Luminal A

Table 2.1: Expression of Er, Pr, Her2 and $p75^{NTR}$ across a panel of breast cancer cell lines.

The above table summarizes the expression of Er, Pr, Her2 and $p75^{NTR}$ across a panel of breast cancer cell lines with information on the subtype of breast cancer.

MDA-MB-231 and MCF-7 were maintained in Dulbecco's Modified Eagle Medium (DMEM) (Sigma, cat. no. D6429) which contains 4500 mg/L glucose, L-glutamine, sodium pyruvate, and sodium bicarbonate. Media were supplemented with 10% heat-inactivated fetal bovine serum (FBS) and the cells were maintained in a 5% CO_2 humidified incubator at 37 $^{\circ}$C. Once the cells reached confluence, cells were seeded at $3x10^4$ cells/cm^2 and were sub-cultured by trypsinization every 48 h.

HCC1806 and T47D were maintained in Roswell Park Memorial Institute Medium (RPMI 1640) (Sigma, cat. no. R0883) supplemented with heat-inactivated 10% FBS. The cells were maintained in a 5% CO_2 humidified incubator at 37 $^{\circ}$C. Once these cells reached confluence, cells were seeded at $3x10^4$ cells/cm^2 and the remaining cells were sub-cultured every 72 h.

PC12 cells

PC12 cells, a semi- adherent rat pheochromocytoma cell line, were obtained from ECACC and were maintained in DMEM supplemented with heat-inactivated 10% Horse serum (HS), 5% FBS. Since these cells are semi-adherent, to facilitate their attachment to the flask, the flasks were coated with poly L-lysine hydrobromide (Sigma, cat. no. P6282) at 0.001% for 2-3 h at 37 $^{\circ}$C. The flask was washed three times with 13 ml of sterile autoclaved distilled water. The cells were then seeded at $3x10^4$ cells/cm^2 or $4x10^4$ cells/cm^2 for experiments in chapter 4 and 5 respectively and the stock flasks were subcultured every 72 h. The cells were maintained in 5% CO_2 humidified incubator at 37 $^{\circ}$C

RN22 Schwannoma cells

RN22 Schwannoma cells were cultured in DMEM supplemented with heat-inactivated 10% FBS and maintained in a 5% CO_2 humidified incubator at 37 $^{\circ}$C. Once cells reached confluence they were seeded at a density of 3 x 10^4 cells/cm^2, and cells were sub cultured every 60 h.

Human embryonic kidney (HEK) cells

Human embryonic kidney cells (HEK293T) were obtained from ATCC and HEK293T cells stably transfected with $p75^{NTR}$ was made in the lab with HA-tagged $p75^{NTR}$ overexpressing plasmid kindly provided by Dr. Carlos Ibanez, Karolinska Institute, Stockholm, Sweden. The cells were cultured in DMEM supplemented with 10% FBS and maintained in a 5% CO_2 humidified incubator at 37 $^{\circ}$C. Once cells reached confluence they were seeded at a density of 2 x 10^4 cells/cm^2, and cell were sub-cultured every 60 h.

2.2.2 Splitting Cells

For regular passage of the cells, the culture medium was removed from the cells and the cells were washed in 7-8 ml of pre-warmed (37 $^{\circ}$C) Hank's Balanced Salt Solution (HBSS) (Sigma, cat. no. H9394). Attached cells were incubated with 2 ml of pre-warmed trypsin-ethylene diamine tetra acetic acid solution (0.05% trypsin-EDTA diluted in HBSS) for cells cultured in 75 cm^2 flasks and 3-4 ml of trypsin-EDTA for cells cultured in 175 cm^2 flasks. The flask was left for 2-3 min at 37 $^{\circ}$C and the flask was swirled until the cells detach from the flask. 8 ml of pre-warmed complete medium was added to de-activate the trypsin and the cells were centrifuged at 1200 rpm for 5 min. The medium

was decanted and the cell pellet was re-suspended in 10 ml complete medium, triturating few times to obtain a single-cell suspension. Cells were then counted using a hemocytometer under 10X magnification, and cells were seeded at the required density.

2.2.3 Drug preparation and storage

Drug	**Solvent**	**Stock concentration**	**Storage**
mNGF	Culture media	250 µg/ml	-80 ºC
hβNGFc	dH_2O	50 µg/ml	-80 ºC
N-acetyl sphingosine (C2-ceramide)	DMSO	10 mM	-20 ºC
Etoposide	DMSO	100 mM	-20 ºC
Thapsigargin	DMSO	4 mM	-20 ºC
Tunicamycin	DMSO	2 mg/ml	-20 ºC
Ro 08-2750	DMSO	20 mM	-20 ºC
TAT-Pep5	DMSO	25 mM	-20 ºC
Epoxomicin	DMSO	1 mM	-20 ºC
GM6001	DMSO	10 mM	4 ºC
DAPT	DMSO	10 mM	-20 ºC
Phorbol myristate acetate (PMA)	DMSO	1 mg/ml	-20 ºC
Cycloheximide	DMSO	10 mg/ml	-20 ºC
Actinomycin D	DMSO	10 mg/ml	-20 ºC
UO126	DMSO	10 mM	4 ºC

Table 2.2 summarizes the details of drug preparation.

The above table summarizes information on preparation of drug indicating the stock concentration and storage conditions of the drug.

2.2.4 Plasmids

shRNA for $p75^{NTR}$ and the scrambled control (Sc.eGFP) were obtained from Genecopoeia and these were used to transiently transfect MDA-MB-231 and HCC1806 cells. HA-tagged $p75^{NTR}$ was also used in the MDA-MB-231 cells to overexpress $p75^{NTR}$. EV (PCDNA 3.1), WT-NGF and number of NGF variants were developed by Dr. Laura Carleton and these plasmids were transiently transfected and expressed in HEK393T cells.

2.2.4.1 Transformation of plasmids into E.coli cells

For the generation of all plasmids, DH5α *E. coli* cells were used. Plasmid DNA (~10 ng) was combined with 25 µl of DH5α competent *E. coli* cells and incubated on ice for 30 min to aid in the permeabilization of cells allowing them to take up the foreign DNA. The mixture was then heat shocked at 42°C for 40 sec. Cells were placed on ice for 2 min and combined with 475 µl of Luria-Bertani (LB) Broth. Cells were allowed to recover and started to grow at 37 ° C for 1 h. The cells were spread on LB agar plate containing 50 µg/ml Ampicillin and grown overnight at 37 °C. Next day, bacteria from a single colonies were further inoculated into 5 ml of LB broth containing antibiotic. This starter culture was incubated overnight at 37 ° C with shaking. The resulting culture was centrifuged at 5000g for 30 min to pellet the bacterial cells containing the plasmid of interest. Plasmid extraction was carried out using a Qiagen maxi-prep kit as per manufacturer's guidelines (Qiagen, Cat. No. 12163)

2.2.4.2 Transient transfection of cells

2.2.4.2.1 DNA transfection

2.2.4.2.1.1 Transient transfection of triple negative breast cancer cells

At 24 h post seeding, cells were transfected with the desired plasmid using Turbofect transfection reagent (Fermentas). The transfection complex consists of 1:2 ratio of DNA: lipid in serum free media. The transfection mixture was gently pipetted to ensure mixing and was incubated at room temperature (RT) for 20 min. In the meantime, the wells were washed twice with DMEM containing 10% FBS, without antibiotic, alternatively, if the cells were cultured in antibiotic free media, then the media need not be changed prior to transfection; however, the media should be replaced 4 h post-transfection. After the

incubation the DNA: lipid complex was added slowly drop-wise on to the cells and the plate was swirled gently and incubated at 37 °C. At 4 h post transfection, media on the cells was changed to complete media and cells were treated as required. The typical transfection efficiency obtained was 90-95%.

2.2.4.2.1.2 Transient transfection of PC12 cells

At 24 h post seeding, cells were transfected with plasmid of interest using Lipofectamine 2000 (Invitrogen) in 1:2 ratio of DNA: lipid, i.e., 0.75 µg of DNA plus 1.5 µl of transfection reagent in a volume of 500 µl of serum free media. The complex was incubated for 20 min at RT and was added drop wise on the cells and incubated at 37 °C. At 5 h post transfection, the antibiotic- free, serum- containing medium was replaced with complete medium. The typical transfection efficiency obtained was 90%.

2.2.4.2.1.3 Transient transfection of HEK293T cells

At 24 h post seeding, HEK293T cells were transfected using JetPEI transfection reagent (Polyplus transfection reagents) with a DNA to lipid ration of 1:2. Briefly, for a 175 cm^2 flask containing 20 ml of antibiotic free media, 30 µg of DNA was diluted in 500 µl 150 mM NaCl buffer, and in a separate tube 60 µl of JetPEI transfection reagent was incubated in 500 µl of 150 mM NaCl. The tubes were vortexed and incubated for at room temperature for 5 min. The transfection reagent was added to the DNA, vortexed, incubated at room temperature for 30 min and then added dropwise onto the cells. The cells were placed back into the incubator for 6 h, after which the media containing the transfection reagent was removed and replaced with fresh serum free media. The typical transfection efficiency obtained was 90-95%.

2.2.4.2.2 siRNA transfection of PC12 cells

Dharmacon siGENOME siRNA against BIM or MEK and a non-targeting control were obtained from Fisher Scientific. siRNAs were re-suspended in Sigma water to a stock concentration of 40 µM and the non-targeting siRNA was re-suspended in Sigma water to a stock concentration of 20 µM. The stock tubes of siRNAwere stored at -80 ºC.

The cells were regularly sub-cultured in antibiotic free media. For siRNA transfection of PC12 cells Lipofectamine (Fermentas) was used. 200,000 cells/ml were seeded in PLL coated 12 well plate. 24 h later media was replaced with 450 µl of antibiotic free culturemedia and then transfected with siRNA of interest in a 1:2 ratio of DNA to

Lipofectamine or 1 µl of 10 µM siRNA plus 2 µl Lipofectamine in 47µl of serum free medium. The concentration of siRNA used was 20 nM. The DNA-Lipofectamine complex was mixed by gently pipetting and incubated at RT for 20 min. The complexes were added drop by drop to the cells and mixed gently by swirling the plate, and incubated for 5 h at 37 $^{\circ}$C. Media was changed and 24 h later cells were either used for experiments.

2.2.5 Determination of protein expression

Expression of proteins is determined using the Western Blotting technique. This technique makes use of Sodium dodecyl sulphate-polyacrylamide gel electrophoresis (SDS-PAGE) which separate proteins based on their molecular weight. The separated proteins are then transferred on to a nitrocellulose membrane which is then probed with antibodies against the protein of interest.

2.2.5.1 Preparation of whole cell extracts for western blotting

Cells were seeded at desired density and allowed to adhere to the culture dish overnight. Following treatments, cells were harvested by scraping them into culture medium. The remaining cells were washed with phosphate-buffered saline (PBS). Cells were then centrifuged at 2100 rpm for 5 min at 4 $^{\circ}$C. The supernatant was discarded and the cell pellet was washed twice in 1 ml of ice-cold PBS. The cells were centrifuged at maximum speed for 30 sec. The supernatant was discarded and the cell pellet was lysed in desired volume of whole cell lysis buffer. Whole cell lysis buffer (WCLB) contained 1 M N-2-hydroxyethyl-piperazine-N-2-ethanesulphonic acid (HEPES) pH 7.5, 350 mM NaCl, 1 mM $Mgcl_2$, 0.5 mM Ethylenediaminetetraacetic acid (EDTA), 0.1 mM Ethyleneglycoltetraacetic acid (EGTA) and 1% Nonidet-P40 (NP-40)). Reducing agent, 1, 4-dithio-DL-threitol (DTT) (0.5 mM), and protease inhibitors phenylmethylsulphonyl fluoride (PMSF) (0.1%), and 1% aprotinin were added to the lysis buffer at the time of lysing. The lysis buffer also contained phosphatase inhibitor sodium fluoride (NaF) (5 mM) and sodium orthovanadate (Na_3VO_4) (1 mM). For detection of phosphorylated proteins, addition of DTT was avoided as this could inhibit the activity of phosphatase inhibitors. The cell pellet lysed in WCLB was allowed to swell on ice for 25 min and centrifuged at 14000 rpm for 10 min at 4 $^{\circ}$C to remove genomic DNA and cell debris. The supernatant containing the cytosolic proteins was transferred to a new 1.5ml tube. The samples were prepared using this method unless otherwise specified. For harvest of cells

in Chapter 5, cells were centrifuged at 5000 g for 5 min at 4 $^{\circ}$C throughout the harvest. The pellet was lysed in 46 µl RIPA buffer on ice for 30 min. The RIPA buffer is made up of 50 mM Tris-HCL, pH 8.8, 150 mM NaCl, 0.5 % Sodium deoxycholate (NaDeox), 0.1 % SDS, and 1 % NP-40. To this lysis buffer, cocktail of protease inhibitors 1 µM, PMSF, 1 µg/ml, Pepstatin , 10 µM, Leupeptin, 2.5 µg/ml, Aprotinin and 250 µM, ALLN,) and phosphatase inhibitors (10 mM NaF, 1 mM Na_3VO_4) were added before lysing the samples.

2.2.5.2 Protein quantification of samples

The protein concentration of samples (in chapter 3 and 4), was determined using Bradford method with bovine serum albumin (BSA) as the standard. Samples were stored at -20°C until further analysis. The proteins in the lysed samples (in chapter 5) were then quantified using BCA assay (Pierce #23227). The constituents in the Bradford reagent react with the components of RIPA buffer and hence a different method of protein quantification was used. Samples were stored at -20°C until further analysis.

2.2.5.3 Sodium dodecyl sulphate-polyacrylamide gel electrophoresis (SDS-PAGE)

2.2.5.3.1 Preparation of samples

5X Laemmli's SDS-PAGE sample buffer (62.5 mM Tris-HCl, pH 6.8, 2% SDS, 5% β-mercaptoethanol, 1 mM PMSF, 0.05% bromophenol blue) was added to the protein samples until a concentration of 1X Laemmli's SDS-PAGE buffer was obtained. The samples were centrifuged briefly before boiling at 95 $^{\circ}$C for 5 min. 15 µg-30 µg protein was then resolved on to 8-15 % SDS-PAGE gels; the composition of gel is tabulated in Table 2.3.

Components (in ml)	**8% (Running gel)**	**12% (Running gel)**	**15% (Running gel)**	**Stacking gel**
H_2O	1.9	1.7	1.2	1.36
30% acrylamide	1.8	2	2.5	0.34
1.5 M Tris-HCl pH 8.8	1.3	1.3	1.3	-
1.5 M Tris-HCl pH 6.8	-	-	-	0.26
SDS	0.05	0.05	0.02	0.02
Ammonium Per Sulphate (APS)	0.05	0.05	0.05	0.02
Tetramethylethylenediamine (TEMED)	0.002	0.002	0.002	0.002
Total	**5**	**5**	**5**	**2**

Table 2.3: Composition of the SDS-PAGE gel

The above table describes the components of SDS-PAGE running and SDS-PAGE stacking gels

2.2.5.3.2 Running of the gel

A broad range protein marker (10-230 kDa) (NEB) was run alongside the protein samples. Gels were electrophoresed in running buffer (25 mM s pH 8.3, 2 M glycine, 3 mM SDS) at 80 V until the samples enter into the separating phase and then the voltage was increased to 100 V. The gel was stopped when the bromophenol blue dye present in the laemelli has reached the end of the gel.

2.2.5.3.3 Western Blotting: Transfer of proteins onto membrane

The proteins from SDS-PAGE gels were electrophoretically transferred onto nitrocellulose membrane (Whatman) for 90 min at 110 V in transfer buffer (25 mM Tris pH 8.3, 2 M glycine and 20% methanol)..

2.2.5.3.4 Probing membrane with antibody

The membranes were blocked for 2 h (for $p75^{NTR}$ determination) or 1 h for other proteins in blocking buffer (5% non-fat dried milk in 1X PBS containing 0.1% Tween-20 (PBS-T)). The membrane was then incubated with primary antibodies according to the conditions in Table 2.4. Following the overnight (O/N) incubation with primary antibody, the membranes were washed 3 times with 0.1% 1X PBS-T, 10 min each at room temperature (RT) to remove any non-specific binding of the primary antibody or any unbound antibody. Then, the membrane was incubated for 1 h at RT with the appropriate horse radish peroxidase (HRP)-conjugated IgG antibody diluted in 5% non-fat dried milk in 0.1% 1X PBS-T. After incubation with secondary antibody, the membrane was washed thrice with 0.1% 1X PBS-T for 10 min each at RT followed by a 10 min wash with 1X PBS without Tween.

2.2.5.3.5 Developing the membrane

The membrane was then incubated with 1 ml Western Chemiluminescent HRP substrate (Advansta or Pierce) for 2 min at RT and the protein bands were visualized by exposure to X-ray film (AGFA).

2.2.5.3.6 Stripping the membrane

Before re-probing the membrane for different protein, antibodies were stripped from the membrane. The membrane was washed twice with 10 ml of 1X PBST for 10 min at RT. The membrane was then incubated for 30 min at RT in 10 ml of the stripping buffer (2 M Tris HCl pH 6.8, 10% SDS, and 0.5 % Tween, 100 mM β-mercaptoethanol). β-mercaptoethanol is added fresh to the stripping buffer. The membrane was washed twice with 10 ml of 1X PBST for 10 min at room temperature. Membrane was then blocked with blocking buffer and incubated with desired primary antibody and developed as described in the previous section.

Table 2.4: Conditions for probing membranes with antibodies

Primary antibody (1° Ab)	Dilution of 1° Ab	Incubation	Secondary antibody (2° Ab)	Dilution of 2° Ab	ECL	Source	Cat. No.
α- actin	1:2000	1 h at RT	Rabbit	1:10000	Advansta	Sigma	A2066
α- BIM	1:1000	1 h at RT	Rabbit	1:10000	Advansta	Enzo	ADI-AAP-330-E
α- pBIM	1:1000	O/N at 4° C	Rabbit	1:10000	Advansta	CST	4581
α-caspase-3	1:1000	O/N at 4° C	Rabbit	1:10000	ECL-Plus	CST	9662
α-caspase-9	1:1000	O/N at 4° C	Rabbit	1:10000	ECL-Plus	CST	9058
α- Total ERK	1:1000	O/N at 4° C	Mouse	1:10000	Advansta	CST	4696
α- pERK	1:1000	O/N at 4° C	Rabbit	1:10000	Advansta	CST	9101
α-HSPB1	1:1000	1 h at RT	Rabbit	1:10000	Advansta	Enzo	ADI-SPA-803-F
α- pIκBα	1:1000	O/N at 4° C	Mouse	1:10000	Advansta	CST	9246
α- Total JNK	1:1000	O/N at 4° C	Rabbit	1:10000	Advansta	CST	9252
α- pJNK	1:1000	O/N at 4° C	Mouse	1:10000	Advansta	CST	9251
α- NGF	1:1000	O/N at 4° C	Rabbit	1:10000	Advansta	Santa Cruz	SC548
α- $p75^{NTR}$	1:5000	O/N at 4° C	Rabbit	1:10000	Advansta	Millipore	07-476
α- PARP	1:1000	O/N at 4° C	Rabbit	1:10000	Advansta	CST	9542

The above table details conditions for probing membrane with antibodies with details of the species antibodies were raised in, source of purchase of antibody and catalogue number.

2.2.6 mRNA expression analysis

2.2.6.1 Total RNA extraction

For experiments to characterize expression of $p75^{NTR}$ in MDA-MB-231, HCC1806, MCF-7 and T47D cells, cells were seeded at $3.5x10^4$ cells/cm^2 into 75 cm^2 flask. For the rest of the experiments, MDA-MB-231 and HCC1806 cells were used and were or not subjected to treatments in 25 cm^2 flask. Cells were harvested by scraping into medium and transferred to 15 ml falcon tubes. Flasks were washed with 1X PBS to ensure removal of all the cells. This was added to the falcon tube and centrifuged at 2100 rpm for 5 min at 4^{o}C. The supernatant was removed and the pellet was re-suspended in 1 ml of Trizol reagent (Sigma) and this was transferred to 1.5 ml Eppendorf tubes. Cells remained in Trizol for maximum time of 5 min and were vortexed for 1 min. The tubes were left at RT for 5 min and stored in -80 $^{\circ}$C for longer storage. On the day of continuation of RNA extraction, the samples were left to thaw on ice. 200 µl of chloroform/ml Trizol was added to the tubes and the suspension was mixed well by inversion for 15 seconds. The tubes were incubated for 15 min at RT and then spun at 13000 rpm for 15 min at 4 $^{\circ}$C. 400 µl of upper aqueous phase containing the RNA was transferred to new Eppendorf tube, while being careful not to touch the white interphase layer. 400 µl of isopropanol/ ml Trizol was added drop wise to the tube to precipitate the RNA. The tubes were inverted quickly 6-7 times and left at -20 $^{\circ}$C overnight. The following day, the samples were spun at 13000 rpm for 15 min at 4 $^{\circ}$C. Supernatant was removed avoiding the area of pellet. The supernatant at this point was retained until the yield of RNA was confirmed. 1 ml of 85% ethanol (diluted with the RNase inhibitor diethyl pyrocarbonate (DEPC)-treated water) was added to the pellet and vortexed gently to mix. The tubes were centrifuged at 13000 rpm for 15 min at 4 $^{\circ}$C. Supernatant was removed and the pellet was air-dried in a laminar hood for approximately 25 min. The pellet was re-suspended in 15 µl of RNase free water (Sigma) and heated on a 65 $^{\circ}$C heat block for 15 min to completely dissolve the RNA. RNA concentration was determined by measuring absorbance at 260 nm (A260 nm) using a spectrometer (Nanodrop). 40 µg/ml RNA has an A260 nm of 1.0. Purity of RNA was ascertained with respect to protein contamination using A260 nm/ A280 nm ratio. The ratio of nucleic acid to protein between 1.7 and 2.1 was considered acceptable. RNA was stored at -80 $^{\circ}$C.

2.2.6.2 cDNA synthesis (reverse transcription)

All reagents used in the cDNA synthesis were from Invitrogen. 2 µg RNA was used for each sample. To this 1 µl of 10X DNase I reaction buffer, 1 µl of 1 U/µl amplification grade DNase-I enzyme (to remove genomic DNA contamination) and sterile dH_2O were added to make up the reaction volume to 10 µl in sterile PCR Eppendorf. The tubes were incubated for 15 min at room temperature and then spun down. 1 µl of 25 mM EDTA was added and mixed gently with pipette. This step helps in deactivating the DNase thereby providing high quality and quantity of cDNA. The tubes were then incubated at 65 °C for 8 min in a 'Biometra T3' thermocycler. 1 µl of 0.5 µg/µl oligo (dT) 12-18 (the cDNA primer) was then added to the tubes and incubated at 65 °C for 2 min to reduce secondary structures (denaturation). This was followed by incubation at 42 °C for 2 min (allows annealing and cooling to catalytic temperature of superscript). While the samples were incubating at the deactivating of DNase step, 1X strand master mix was prepared. This mix contained: 4 µl 5X First strand buffer, 2 µl of 0.1 M DTT, 1 µl of 10 mM deoxynucleotide triphosphate (dNTPs). 2.6 µl of DEPC water was added to the mix. 0.4 µl of Superscript III was added just before the samples were incubated at 42 °C for 50 min. The samples were then incubated at 75 °C for 10 min to inactivate superscript reverse transcriptase. The samples could at this step be incubated at 4 °C indefinitely.

2.2.6.3 Reverse transcription Polymerase chain reaction (RT-PCR)

2 µl of cDNA was amplified using 10 mM forward and reverse primers corresponding to the gene of interest. Glyceraldehyde-3-phosphate dehydrogenase (GAPDH) was amplified in parallel to confirm whether equal quality and quantity of cDNA was used. The PCR was carried out in a total reaction volume of 25 µl, containing 2 µl cDNA, 3 µl of primers each, 12.5 µl of 2 X Go Taq PCR master mix (Promega) and the volume was made up to 25 µl with RNase and DNase free H_2O (DEPC water). Reactions were kept on ice during preparation and a master mix was made for multiple samples. The negative control used contained master mix and primers with water instead of cDNA. The PCR reagents were placed in the thermocycler and cDNA was amplified under the optimized conditions for corresponding genes as shown in Table 2.5 A. The PCR products were spun down and stored short-term at 4 °C or long-term (3-4 weeks) at -20 °C. The sequence of primers for each gene of interest is tabulated in Table 2.5 B.

Table 2.5 A: Optimized PCR conditions for amplification of respective genes

Steps	***P75^{NTR}***	***NGF***	***BDNF***	***GAPDH***
Hot start	95 °C /3 min	95 °C /3 min	95 °C /3 min	95 °C /3 min
Denaturation	95 °C /1 min (32 cycles)	95 °C /1 min (32 cycles)	95 °C /1 min (32 cycles)	94 °C / 30 sec (24 cycles)
Annealing	59.8 °C /1min	53 °C / 1 min	54 °C / 1 min	58 °C / 1 min
Extension	72 °C / 1 min	72 °C / 1 min	72 °C / 1 min	72 °C / 1 min
Final extension	72 °C /10 min	72 °C /10 min	72 °C /10 min	72 °C /10 min
Size	201 bp	313 bp	266 bp	452 bp

Table 2.5 B: Primer sequences for gene of interest

Gene of interest		Primer sequence
P75^{NTR}	*Forward primer*	5'-GTGGGACAGAGTCTGGGTGT-3'
	Reverse primer	AAGGAGGGGAGGTGATAGGA
NGF	*Forward primer*	ATACAGGCGGAACCACACTC
	Reverse primer	TGCTCCTGTGAGTCCTGTTG
BDNF	*Forward primer*	TACTTTGGTTGCATGAAGGCTGCC
	Reverse primer	ACTTGACTACTGAGCATCACCCTG
GAPDH	*Forward primer*	ACCACAGTCCATGCCATC
	Reverse primer	TCCACCACCCTGTTGCTG

2.2.7 Flow cytometry based assays

2.2.7.1 Sub G1 analysis

Cells were seeded into a 6 well plate at desired density and allowed to adhere overnight. Following the experimental treatment, cells were harvested by trypsinization. Following observable detachment of cells from the culture dish, trypsin was combined with media in the tube and centrifuged at 1200 rpm for 5 min. Supernatant was removed and the cell pellet was re-suspended in 500 µl of ice cold 1X PBS. Cells were centrifuged at 14000 rpm for 30 sec. Supernatant was removed and cell pellet was re-suspended in 150 µl of 1X PBS (ice cold) and 350 µl of 100 % ice cold ethanol was added drop wise while the cell suspension was gently vortexed. This avoids clumping of the cells. The cells were then stored at -20 $^{\circ}$C overnight. The samples can remain at this step for 2-4 weeks. On the day of analysis, samples were removed from -20 $^{\circ}$C and were centrifuged gently at 5000g for 5 min. Supernatant was removed and the cell pellet was re-suspended in 300 µl of Propidium Iodide (PI) stain (50 µg/ml PI and 100 µg/ml RNase A in 1X PBS) and incubated in the dark on ice for 30 min before analysis. 10000 events were recorded by flow cytometry on a BD FACSCanto on channel PE. The analysis was carried out using Cyflogic software.

2.2.7.2 Tetramethylrhodamine, Ethyl Ester, Perchlorate (TMRE) staining

Cells were seeded into a 24 well plate at desired density and allowed to adhere overnight. Following the experimental treatments, cells were harvested by trypsinization. Following detachment of cells, trypsinized cells were combined with media and the cells were allowed to recover for 15 min at 37 $^{\circ}$C.

2 mM of TMRE was diluted to 10 µM TMRE in HBSS and the cells were re-suspended gently in a final concentration of 100 nM in HBSS. The cells were then incubated in the dark for 30 min with occasional mixing of the tubes to avoid settling of the cells to the bottom of the tube. The samples were measured by flow cytometry using a BD FACSCanto on channel PerCP and PE. The analysis was carried out using Cyflogic software.

2.2.7.3 Annexin V staining

Cells were seeded into a 24 well plate at the desired seeding density and allowed to adhere overnight. The cells were treated as desired and harvested by trypsinization. The

trypsin was the inactivated by addition of media and the cell suspension was added to a 1.5 ml tube. The cells were then allowed to recover membrane integrity by incubation under normal culture conditions for 15 min.

After the recovery time the cells were placed on ice and centrifuged a 5000g at 4 $^{\circ}$C for 5 min with soft brake. The supernatant was then removed and the cells were gently re-suspended in 500 µl 1X PBS, the cells were centrifuged as before and the supernatant was removed. The cells were gently re-suspended in 50 µl calcium buffer (10 mM HEPES pH 7.5, 140 mM NaCl and 2.5 mM $CaCl_2$) containing 20 µg/ml of recombinantly expressed and purified Annexin V conjugated to Fluorescein isothiocyanate (FITC). The cells were then incubated in the dark for 15 min after which 300 µl of calcium buffer was added and the samples were analyzed immediately by flow cytometry using a BD FACSCanto on channel FITC. All analysis was carried out using Cyflogic software.

2.2.8 Plate reader- based assays

2.2.8.1 Detection of caspase-3 activity by DEVDase assay

Cells were seeded at desired densities in 25 cm^2 flasks and allowed to adhere overnight. Following experimental treatments, the activity of caspase-3 like enzymes (DEVDase activity) was determined fluorometrically using DEVDase assay. The cells were scraped into the medium and centrifuged at 2100 rpm for 5 min at 4 $^{\circ}$C. The supernatant was discarded and the cell pellet was re-suspended in 500 µl of ice cold 1X PBS. The cells were centrifuged at maximum speed for 30 sec. The cell pellet was re-suspended in 50 µl of ice cold 1X PBS, and 25 µl of the re-suspended pellet was added to microtitre plate and was flash-frozen in liquid nitrogen. The samples can be stored for weeks at -80 $^{\circ}$C. On the day of analysis, samples were thawed on ice and Wallac Victor x3 microplate reader (excitation 355 nm, emission 460 nm) was set to 37 $^{\circ}$C. 50 µM of DEVDase-substrate (DEVD-AMC) in reaction buffer (100 mM HEPES) pH 7.5, 10% sucrose, 0.1% 3-[(3-cholamidopropyl)-dimethylammonio]-1-propanesulphonate (CHAPS), 5 mM DTT, 0.01% NP-40) was added to the lysates. The release of free AMC was monitored at 37 $^{\circ}$C at 60 s intervals over a 30 min period. Fluorescence units were converted to nanomoles of AMC released per minute per mg of enzyme using a standard curve generated with free AMC and related to protein concentration.

2.2.8.2 MTT assay

Cells were seeded into a 96 well plate at the required seeding densities and allowed to adhere overnight. After desired treatments, cell viability was determined by adding 10 µl of 3-(4, 5-dimethylthiazol- 2-yl)-2, 5-diphenyl tetrazolium bromide solution (MTT) at 5 mg/ml in HBSS to each well. The cells were left in the incubator for 2-3 h and the reaction was stopped by the addition of 100 µl of stop solution (20% SDS, 50% dimethylformamide in dH_2O) to the wells. The plate was left rocking in dark for 3-18 h at RT to re-dissolve the resulting formazan precipitate. The absorbance was then determined at 550 nm using the Victor x3 plate reader.

2.2.9 Nuclear morphology assay

2.2.9.1 DAPI staining

Cells were seeded in a 24 well plate in 0.5 ml complete medium. The cells were treated according to the experimental protocol. After the treatment time the medium was removed and the cells were harvested by trypsinization. 200 µl of the cells were loaded on to the cytocentrifuge and the cells were cytocentrifuged on to the slides at 200 rpm for 5 min. The slides were allowed to air dry and 200 µl of 3.7% paraformaldehyde was added on to the cells and incubated for 20 min at RT. Following the fixation step, slides were washed three times in 1X PBS and the slides were allowed to dry. To mount the cells onto slides, 3 µl of DAPI in VECTASHIELD (Vector Laboratories Ltd) was placed on the slide which was overlaid with a cover slip and the edges sealed with varnish. The DAPI stained nuclei were then visualized using the Olympus IX51 fluorescence microscope (excitation 360 nm, emission 460 nm).

2.2.9.2 Haematoxylin and eosin stain

Cells were treated as desired and cells were harvested by trypsinization. The cells were cytocentrifuged on to the slides at 200xg for 5 min. Cells were then fixed in methanol for 5 min at room temperature and stained in Harris hematoxylin solution for 5 min. The slides were then washed in running tap water to get rid of excess stain. The cytosol was stained with Eosin Y for 30 sec. Excess eosin stain was removed by washing the slides in running tap water. The slides were allowed to air dry and were mounted with approximately 10 µl mounting medium and covered with a coverslip.

2.2.10 Expression of NGF and NGF variants in mammalian cells

Plasmids containing WT-NGF sequence or NGF variant sequence in a pcDNA3.1 backbone under the control of T7 promoter were previously made in the lab (L.Carleton, PhD thesis 2013). These NGF constructs generated contained a C-terminal His tag in order to help in purification. To express NGF protein, HEK293T cells were seeded into serum free and antibiotic-free medium at $10x10^6$ cells/T175 flask and allowed to adhere overnight. The cells were then transfected using 1:2 ratio of DNA: JetPEI reagent. At 5 h post-transfection the media on the cells were replaced with 20 ml of fresh serum free media. The cells were left in culture for 72 h to allow accumulation of secreted NGF in the media. The media from the cells were collected and spun down at 1200 rpm for 5 min to remove any cells from the collected media. This media was collected in a 50 ml falcon tube under sterile conditions and was stored at -80 ^{0}C until quantified. The transfected cells were then harvested for western blotting.

2.2.11 Determination of NGF concentration using enzyme linked immunosorbent assay (ELISA)

To detect and quantify secreted recombinant NGF, an ELISA was used. 100 µl of 1:1000 dilution of NGF antibody (sc-548, SantaCruz) (capture antibody) made up in 1X PBS was coated onto microplate immune maxisorp 96 well plates (Fisher Scientific) and the plate was incubated at room temperature overnight. Next, any unbound antibody was washed away from the plate and the plate was washed 3 times with 200 µl 1X PBST. The plate was then blocked with 100 µl of 1% BSA in 1X PBST. The plate was incubated for 1 h at room temperature. Following the incubation, plate was washed 3 times with 200 µl 1X PBST. 100 µl of NGF- containing sample was applied to the plate. hβNGF (Alomone) was used to generate a standard curve, with concentrations from 0.312 ng/ml to 10 ng/ml. The stock hβNGF (50 µg/ml) was first diluted in dH_20 to 500 ng/ml and the subsequent dilutions were made in 1XPBST containing 1% BSA. The samples were incubated at room temperature for 2 h. Any proteins that did not bind to the capture antibody were removed and washed 3 times with 200 µl 1X PBST. The bound NGF was then detected using a biotin-tagged anti-NGF antibody (detection antibody, R&D systems). 100 µl of 50 ng/ml antibody made up in 1% BSA-1XPBST was added to the wells and the plate was incubated at room temperature for 4 h. The unbound antibody was removed and the plate was washed 3 times with 200 µl 1X PBST. 100 µl of 1:400 dilution (made in 1% BSA- 1XPBST) of Streptavidin-Horse Raddish Peroxidase (Strep-

HRP) (R&D systems) was added to the wells and incubated in the dark at room temperature for 20-30 min. The plate was then washed 3 times with 200 µl 1X PBST to remove excess HRP. 100 µl of 3, 3', 5, 5'- Tetramethylbenzidine (TMB) was added to the plate and incubated in the dark for 20 min at room temperature. The reaction was stopped by addition of 50 µl of 2 M H_2SO_4 (Fisher Scientific) and the absorbance was read at 450 nm and 550 nm immediately using the Victor x3 microplate reader. The values from the two absorbance were then subtracted and this was used in calculating the amounts of NGF secreted.

2.2.12 Preparation of beta-amyloid ($A\beta_{1-42}$) peptide

Human beta amyloid peptide was custom synthesized by Biomatik based on the sequence (from N to C): Asp-Ala-Glu-Phe-Arg-His-Asp-Ser-Gly-Tyr-Glu-Val-His-His-Gln-Lys-Leu-Val-Phe-Phe-Ala-Glu-Asp-Val-Gly-Ser-Asn-Lys-Gly-Ala-Ile-Ile-Gly-Leu-Met-Val-Gly-Gly-Val-Val-Ile-Ala (42aa). This was obtained in the form of lyophilized powder. Human beta amyloid was re-suspended using two different protocols adapted from (Hu et al., 2013) and (Song et al., 2013).

$A\beta_{1-42}$ oligomers were prepared by dissolving the peptide in Hexafluoro-2-propanol (HFIP) and HFIP was removed by air-drying the tubes in fume hood O/N. The peptide was then dissolved at 2.5 mM in DMSO, and brought to 100 µM in ice-cold DMEM and incubated at 4 $^{\circ}$C for 24 h. This method of preparing $A\beta_{1-42}$ oligomers will be referred to as protocol 1 (Song et al., 2013). $A\beta_{1-42}$ fibrils were prepared by dissolving the peptide in HFIP as mentioned above and the peptide was diluted to final concentration of 1 mg/ml in phosphate-buffered saline (PBS) and incubated at 37 $^{\circ}$C for 24 h. This method of preparing $A\beta_{1-42}$ oligomers will be referred to as protocol 2 (Hu et al., 2013).

2.2.13 Immunoprecipitation

HSPB1 overexpressing PC12 cells were seeded at 200,000 cells/ml in a 25 cm^2 flask. The cells were then treated with 0.25 µM TG for 24 h. On the day of treatment, epoxy coated dynal beads (Novex) re-suspended in dimethylformamide was washed in the buffers supplied along with the kit. 1 mg beads were used per IP reaction and this was then conjugated with 2 µl of anti-HSPB1 or anti-phospho-ERK (p-ERK) or rabbit IgG (as a negative control) and the tubes were allowed to rotate for 16-24 h at 37°C. The total volume in the tube during this step is 100 µl/IP reaction. Immediately prior to use the

beads were collected on the magnetic rack and the supernatant was discarded. The beads were then washed with different buffers (HB, LB and SB) supplied in the kit. The supernatant is discarded at each step. The last wash with SB was done for 15 min at RT and the tubes were left rotating during this step. The supernatant was separated on magnet and the beads were stored in the same volume as coupling reaction and stored at 4°C until further use.

The cells were harvested by scraping into the medium and this was carried out on ice at all times. The cells were centrifuged at 800 rpm for 5 min. The pellet was then washed three times in 1 ml of ice cold 1X PBS. The cell pellets were lysed in lysis buffer adapted from cell signaling technology. The composition of lysis buffer is as follows: 20 mM Tris HCl (pH 7.5), 150 mM NaCl, 1 mM EGTA, and 1 mM EDTA, 1% Triton-X 100. The lysis buffer contained protease and phosphatase inhibitors ;1 mM β glycerophosphate, 1 mM sodium orthovanadate (Na_3VO_4), 10 µM Leupeptin, 1 mM PMSF and 5 mM NaF. The cells were lysed in 500 µl lysis buffer with inhibitors and allowed to rotate for 1 h at 4 °C. In the meantime, the beads were equilibrated with lysis buffer with inhibitors by washing the beads in lysis buffer and to the beads that were conjugated with either HSPB1 or phosho-ERK, 610 µl of lysis buffer with inhibitors were added and to the beads conjugated with IgG, 310 µl of lysis buffer with inhibitors were added. After the 1 h lysis of the cells, 40 µl of the sample was retained and this is called the Input. To the remaining lysate, 300 µl of beads conjugated with either anti- HSPB1 or anti-phospho-ERK or anti-rabbit IgG was added and allowed to rotate for 4 h at 4 °C. Next, the samples were placed on magnet and the beads were collected. 40 µl of the sample was retained (the Post-IP samples). The beads were then washed with 200 µl of lysis buffer with inhibitors and the supernatant was discarded. This step was repeated 4 times and the last wash was carried out by placing the tubes on a rotator for 5 min at RT. The beads were collected and to this 30 µl of EB supplied in the kit) was added and the samples were allowed to rotate for 5 min at RT. The tubes were placed on the magnetic rack and the supernatant was collected and transferred to a new Eppendorf tube. The beads were again eluted in 30 µl of EB and the resulting supernatant was combined to the supernatant collected from the previous step. This is the IP sample. 1 X Sample buffer was added to the samples and was boiled at 95 °C for 5 min. The samples were then resolved on 12% SDS-PAGE gel as described in section 2.2.3 and probed for BIM, HSPB1 and phospho-ERK.

2.2.14 Statistical analysis

Statistical analysis of the results was carried out using GraphPad Prism (for Chapters 3 and 5) or SPSS software (Chapter 4). Values are expressed as mean ± SEM of 3 independent experiments. The choice of statistical test used across this thesis in indicated in each chapter. Differences were considered statistically significant at $p<0.05$.

3 Chapter 3: Results

Nerve growth factor (NGF) mediated regulation of $p75^{NTR}$ expression contributes to chemotherapeutic resistance in triple negative breast cancer cells

3.1 Introduction

Breast cancer is the most common cause of cancer death followed by lung cancer in women (Ferlay et al., 2015). It can be subdivided into multiple types based on expression of estrogen (Er), progesterone (Pr) and Human epidermal growth factor receptor-2(Her2) receptors (Perou et al., 2000, Sorlie et al., 2001). Triple negative breast cancers (TNBCs), which lack expression of Er, Pr and Her2 (Perou et al., 2000), are the most difficult to treat because of the lack of targeted therapies (Foulkes et al., 2010).

Neurotrophins are a small family of polypeptides that are well characterized in their abilities to regulate the survival, development and functions of neurons (Reichardt, 2006, Hempstead, 2006). The neurotrophin family comprises nerve growth factor (NGF), brain derived-neurotrophic factor (BDNF), neurotrophin-3 (NT-3), neurotrophin- 4/5 (NT-4/5) (Hallbook et al., 2006). They bind to two distinct classes of receptor. The low affinity nerve growth factor receptor, also known as the p75 neurotrophin receptor ($p75^{NTR}$), belongs to the tumor necrosis factor receptor superfamily (TNFRSF) and can bind all neurotrophins with approximately equal affinity (Chao, 1994). In contrast, the tropomyosin related kinase (Trk) receptors exhibit specificity with TrkA binding NGF, TrkB binding BDNF and NT4/5 and TrkC binding NT3 (Vanhecke et al., 2011, Patani et al., 2011, Hondermarck, 2012, Descamps et al., 2001c).

Nerve growth factor (NGF) is produced by over 80% of primary breast tumors tested, giving it a potentially broader target range than ER or HER-2 (Adriaenssens et al., 2008). Pro-survival NGF signaling mediated by $p75^{NTR}$ may contribute to the resistance of breast tumors to chemotherapy (Adriaenssens et al., 2008). TNBCs are reported to secrete NGF and express its receptors, $p75^{NTR}$ and TrkA, leading to NGF-activated autocrine signaling (Dolle et al., 2003a). Normal breast cells do not secrete NGF, although they express both TrkA and $p75^{NTR}$ receptors. Hence, NGF-targeted treatment would be more specific to breast tumor cells (Adriaenssens et al., 2008). This provides a rationale for NGF as a potential therapeutic target for TNBC. Hence, NGF-targeted treatment would be specific to breast tumor cells (Dolle et al., 2003a). Anti-NGF therapy holds the possibility of increasing the effectiveness of cytotoxic/ genotoxic drugs used as adjuvant therapies in breast cancer treatment.

The $p75^{NTR}$/NGF signaling has been implicated in several cancers, including prostate (Sigala et al., 2008) and breast cancer (Descamps et al., 2001c). It has been reported that

NGF acts as an anti-apoptotic survival factor for breast cancer cells, and that this is mediated by $p75^{NTR}$-dependent activation of NF-kappaB (Descamps et al., 2001c). Interestingly, $p75^{NTR}$ expression is mainly in basal breast cancer cells (Reis-Filho et al., 2006). Therefore it may be a more relevant therapeutic target in the treatment of TNBCs.

Regulation of expression of $p75^{NTR}$ has been studied extensively over the last decade. Studies show that $p75^{NTR}$ expression is induced in apoptotic neurons after seizures (Roux et al., 1999), its expression is induced via nitric oxide in conditions like osmotic swelling following brain injuries (Peterson and Bogenmann, 2003). Basal levels of $p75^{NTR}$ are rapidly induced after focal cerebral ischemia (Irmady et al., 2014). There are reports of a few transcription factors that could potentially regulate expression of $p75^{NTR}$ under stress conditions. These include Sp1-dependent transcription in neurons (Ramos et al., 2007), direct activation of $p75^{NTR}$ gene expression by early growth response (Egr1 and Egr3) transcription regulators (Gao et al., 2007). Loss of $p75^{NTR}$ in prostate cancer is an indication of metastatic prostate cancer. NSAIDs (non-steroidal anti-inflammatory drugs) such as R-flurbiprofen or ibuprofen selectively induce the expression of $p75^{NTR}$. This results in reduced survival of human prostate tumor cells (Quann et al., 2007, Andrews et al., 2002). In prostate cancer cells exogenous NGF can upregulate $p75^{NTR}$ expression and thus reduce cell malignancy (Sigala et al., 2008).

In many cell types including PC12 cells or TNBC cells, it has been well documented that regulated intramembrane proteolysis of the $p75^{NTR}$ is a prerequisite for its signaling (Skeldal et al., 2011). $p75^{NTR}$ is cleaved by alpha-secretase to liberate its ectodomain, while the remaining C-terminal fragment is then cleaved by presenilin-dependent gamma-secretase, producing an intracellular domain (ICD) that is released into the cytosol (Skeldal et al., 2011) . It has been reported that NGF induces cleavage of $p75^{NTR}$ and that this requires TrkA activation in PC12 cells (Ceni et al., 2010). Proteolytic processing of $p75^{NTR}$ has also been recently reported in TNBC cells (Verbeke et al., 2013).

The aim of the current work is to investigate whether NGF is involved in the regulation of $p75^{NTR}$ in breast cancer cells. We show that NGF can regulate the levels of full length $p75^{NTR}$ ($FLp75^{NTR}$) in breast cancer cells and that this is linked to the increased resistance of TNBC cells to chemotherapeutic drug-induced cell death.

3.2 Results

3.2.1 Characterization of $p75^{NTR}$ in panel of breast cancers

Characterization of a panel of breast cancer cells across various subtypes including MCF-7, T47D (Luminal A) and MDA-MB-231 (TNBC) for expression of $p75^{NTR}$, was carried out using anti- $p75^{NTR}$ (ANT-007; Alamone labs) that was available in the lab. This antibody recognizes the extracellular epitope of human $p75^{NTR}$ (#ANT-007). From Fig. 3.1 A it is clear that this antibody picks up lot of other bands making the interpretation of the actual $p75^{NTR}$ band very difficult. Hence, anti-$p75^{NTR}$ antibody from Millipore (# 07-476) was obtained. This antibody recognizes the intracellular domain of $p75^{NTR}$. In order to characterize the breast cancer cell lines for expression of $p75^{NTR}$, optimization of anti-$p75^{NTR}$ was carried out. Various conditions were used to optimize the antibody.

Blots shown in Fig. 3.1 B (a) and (b) were blocked in 5% Milk-PBST for 2 h, but the difference between the two blots is that the blot shown in Fig. 3.1 B (a) was probed for anti-$p75^{NTR}$ at 1:5000 dilution made up in 5% BSA-PBST, while the blot shown in Fig. 3.1 B (b) was also probed for anti-$p75^{NTR}$ (1:5000 dilution) made up in 5% Milk-PBST. Similar conditions were used on the blots shown in Fig. 3.1 B (c) and (d), but these membranes were blocked in 5% Milk-PBST for 1 h. As seen in Fig. 3.1.B, anti-$p75^{NTR}$ obtained from Millipore gave a clear band for $p75^{NTR}$. This was confirmed by PC12 or HEKp75 cells (derived from HEK293 cells and stably expressed $p75^{NTR}$) which were used as a positive control for $p75^{NTR}$ (Landreth and Shooter, 1980). HEK293T cells were used as a negative control. Irrespective of the conditions used, the results show that MDA-MB-231 alone expresses a huge amount of $p75^{NTR}$ while MCF-7 or T47D do not. It has been well reported in the literature that MCF-7 cells express $p75^{NTR}$ (Descamps et al., 2001c). The data that shows MCF-7 not expressing $p75^{NTR}$ led to testing if milk solution was too harsh in blocking and that if it actually blocked the protein of interest. So, we tested if blocking with 5% BSA-PBST would make a difference to the expression pattern of $p75^{NTR}$. Using 5% BSA-PBST made no difference to the $p75^{NTR}$ expression pattern in MCF-7 or T47D cells. Fig. 3.1 C shows that on higher exposure, there is very faint band for $p75^{NTR}$ in MCF-7 and T47D. The cells were lysed in whole cell lysis buffer (WCLB In order to clarify if lysing cell pellet with WCLB was not efficient enough in these cells, a much harsher way of direct lysis with 2X Sample Buffer (2XSB) was taken. As shown in Fig. 3.1 D, the method of lysis also made no difference to the expression of $p75^{NTR}$ and on higher exposure; faint bands appear around 75 kDa. To be absolutely sure

that the band picked up on western blot around 75kDa was $p75^{NTR}$, the samples were subjected to digestion by PNGase F enzyme. It has been well documented in the literature that native $p75^{NTR}$ is a 55 kDa molecular weight protein that due to post translational modifications by addition of N and O- linked glycosylation acquired high molecular weight (Yeaman et al., 1997). PNGase F has been shown to remove N-linked glycosylation chains (Weskamp et al., 2004) which can be seen by down-shift in the band size of $p75^{NTR}$. From Fig. 3.1 E, it is obvious that PNGaseF removes the glycosylating residues both in Hekp75 and MDA-MB-231 cells and the size of $p75^{NTR}$ is reduced confirming that the band we obtain using anti-$p75^{NTR}$ is $p75^{NTR}$. For all the experiments requiring detection of $p75^{NTR}$, blocking for 2 h with 5% Milk-PBST followed by incubation of membrane with anti-$p75^{NTR}$ (1:5000 made up in 5% BSA-PBST) overnight was followed. To investigate the expression of $p75^{NTR}$ at mRNA level, RT-PCR with specifically designed primers for $p75^{NTR}$ was carried out and from Fig. 3.1 F and G, it is clear that the results from RT-PCR and western blot complement each other. Taking together the data from western blot and RT-PCR, it is not feasible to work with cell lines other than MDA-MB-231 cells expressing very low levels of $p75^{NTR}$ and so, MDA-MB-231 was used for further studies in this chapter.

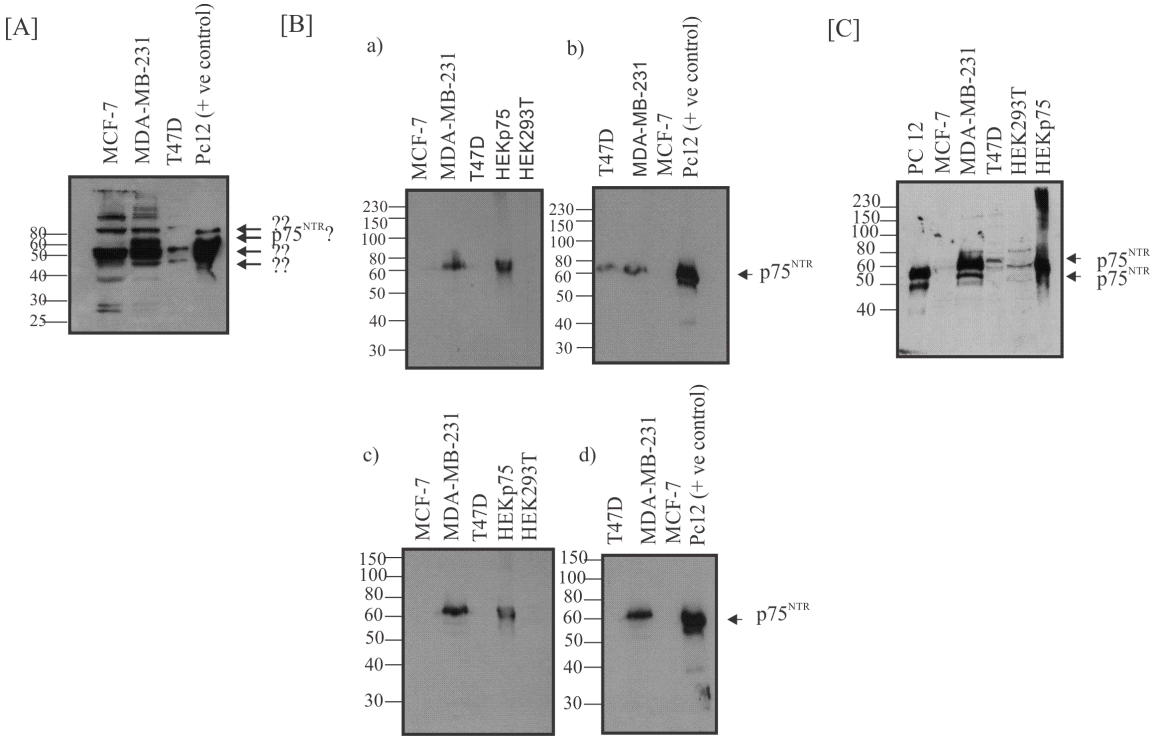

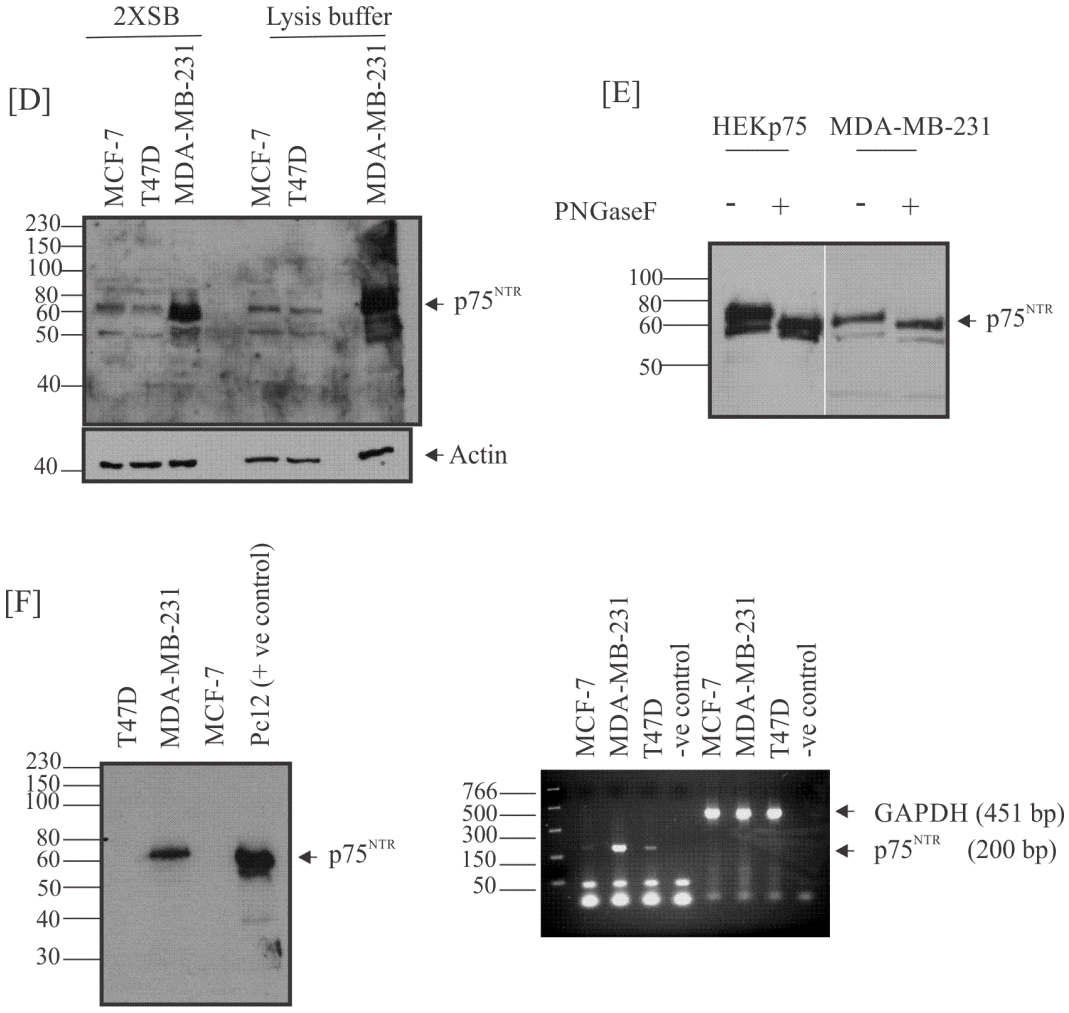

Fig. 3.1: Characterization of p75^{NTR} in a panel of breast cancer cell lines: Western Blot analysis on whole cell extracts to examine the expression of p75^{NTR} using ***[A]*** anti-p75^{NTR} (ANT-007) from Alamone labs. Optimization of anti-p75^{NTR} (07-476) obtained from Merck Millipore was carried out. ***[B]*** Membranes were blocked in 5% Milk-PBST for 2 h and incubated with anti-p75^{NTR} (1:5000) made up in (a) 5% BSA-PBST , (b) 5% Milk-PBST Membranes were blocked in 5% Milk-PBST for 1 h and incubated with anti-p75^{NTR} (1:5000) made up in (c) 5% BSA-PBST , (d) 5% Milk-PBST.***[C]*** Membrane was blocked in 5% BSA-PBST for 2 h and incubated with anti-p75^{NTR} (1:5000) made up in 5% BSA-PBST. ***[D]*** Cells were lysed in 2X SB or in WCLB and probed for anti-p75^{NTR} (07-476). ***[E]*** HEKp75 cells and MDA-MB-231 cells were subjected to de-glycosylation with PNGaseF and probed for anti-p75^{NTR}. This gel is assembled although the samples were all run in the same gel. ***[F]*** Expression of p75^{NTR} was determined henceforth with blocking membrane in 5% Milk-PBST for 2 h and incubating overnight with 1:5000 dilution of anti-p75^{NTR} (07-476) made up in 5% BSA-PBST. ***[G]*** Expression of p75^{NTR} was also confirmed at mRNA level using RT-PCR with specifically designed primers for p75^{NTR}. PC12 cells or HEKp75 cells were used as a positive control and HEK293T was used as a negative control.

3.2.2 Expression of p75^{NTR} increases during in vitro culture of TNBC cells

The expression of p75^{NTR} in culture in a panel of BC cells with addition of HCC1806, another cell line representative of TNBC was examined. Of the three cell lines, only MDA-MB-231 cells expressed p75^{NTR} at early (24 h) times in culture (Fig. 3.2 A). During culture of the cells for a further 2 days, the expression of p75^{NTR} increased in both of the TNBC cell lines, while in contrast, there was no increase in p75^{NTR} levels in MCF-7 cells (Fig. 3.2.A). The increase observed in both MDA-MB-231 and HCC1806 cells was blocked by inhibition of neurotrophin interaction with p75^{NTR} (Fig. 3.2 B), using Y1036, a small molecule inhibitor that can bind to NGF and BDNF and thus prevent their interaction with p75^{NTR} (Eibl et al., 2010), Ro 08-2750, a small molecule inhibitor that binds to NGF and induces a conformational change preventing its binding to p75^{NTR} (Niederhauser et al., 2000) and anti-NGF neutralizing antibody. These data indicate that neurotrophins may regulate the expression of p75^{NTR} in TNBC cells.

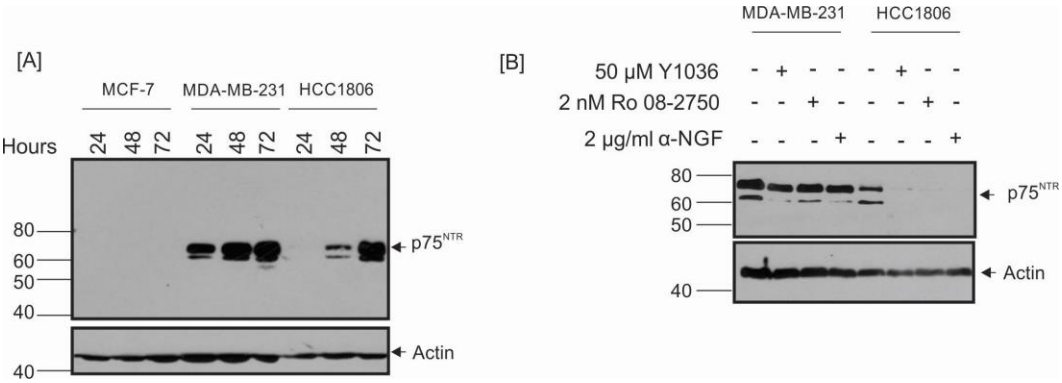

Fig. 3.2: Increase in expression of p75^{NTR} in culture: MCF-7, MDA-MB-231 and HCC1806 cell lines were seeded at 3x10^4 cells/cm^2. ***[A]*** Cells were harvested at 24 h, 48 h and 72 h. ***[B]*** MDA-MB-231 and HCC1806 cell lines were seeded and 24 h post-seeding, cells were treated with or without 50 µM Y1036, inhibitor of NGF/BDNF binding to p75^{NTR}, or 2 nM Ro 08-2750, inhibitor of NGF binding to p75^{NTR}, or 2 µg/ml α-NGF and harvested 24 h post-treatment. Western blot analysis on whole cell extracts was carried out to determine the expression of p75^{NTR}. Actin was used as a loading control. These data are representative of n=3.

3.2.3 Expression of neurotrophins and p75^{NTR} in TNBC cells

To confirm the involvement of neurotrophins in the regulation of its receptor, MDA-MB-231 and HCC 1806 cells was screened for expression of NGF, BDNF and p75^{NTR} using RT-PCR with GAPDH as a house-keeping control. Both cell lines were shown to express

NGF, BDNF and $p75^{NTR}$ as shown in Fig. 3.3 A. Using Western blotting, an increased level of proNGF was observed in the lysates from both of these cell lines during 3 days in culture (Fig. 3.3 B). This is indicative of increased production of NGF by the cells. To confirm this, an ELISA assay was used to quantify secretion of mature NGF into the culture medium at different days during culture of the cells (Fig. 3.3 C). There was a significant increase in NGF levels in the culture medium from both cell types, reaching almost 6 and 3 ng/ml for HCC1806 and MDA-MB-231 cells respectively, by 72 h (Fig. 3.3 C). We used an additional way to test if NGF was secreted into the medium of MDA-MB-231 cells. The medium from MDA-MB-231 cells which were 72 h in culture was collected and centrifuged to remove the cells. This media was then applied onto PC12 cells. These cells have been reported to differentiate and extend neurites upon NGF treatment (Drubin et al., 1985). If NGF is secreted into the media of MDA-MB-231 cells, by applying the conditioned media onto PC12 cells, they should extend neurites. Treatment of PC12 cells with 100 ng/ml of commercially available mNGF was used as a positive control. As indicated by arrows pointing towards neurites, in Fig. 3.3 D, when conditioned media from MDA-MB-231 cells was applied to PC12 cells and left for 4-5 days, PC12 cells started to extend neurites and this was not seen in PC12 cells treated with unconditioned media, indicating there could be possible secretion of NGF into the media of MDA-MB-231 cells. We used 2 µg/ml NGF-neutralizing antibody to antagonize the effect of mNGF in PC12 cells. However, use of NGF-neutralizing antibody could not completely prevent the neurite extensions in PC12 in the presence of MDA-MB-231 conditioned media. . But the secretion of NGF was detectable on ELISA as shown in Fig. 3.3 C.

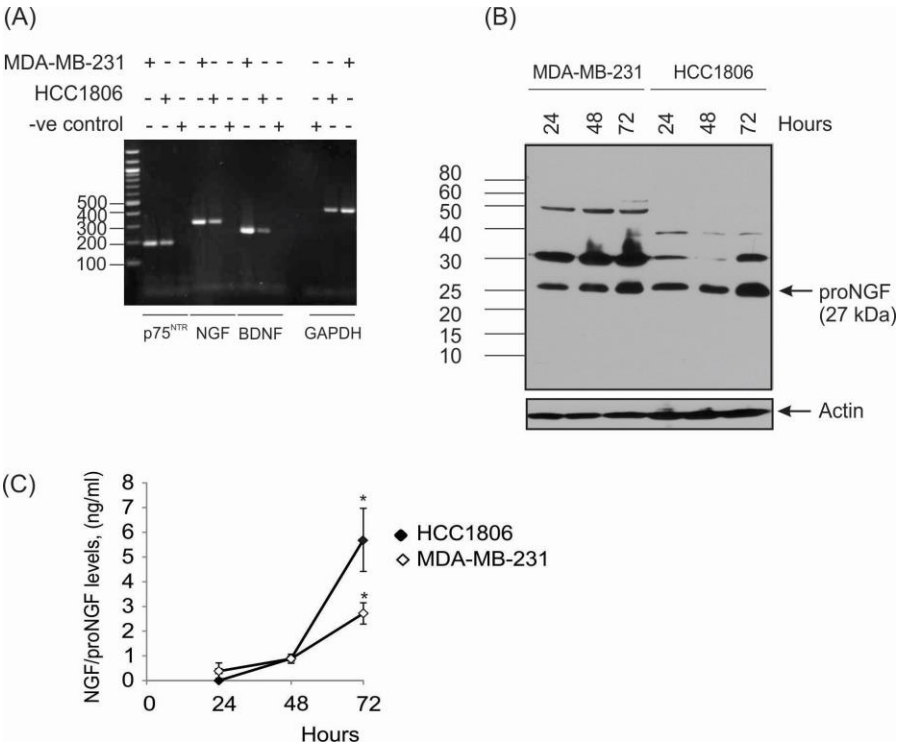

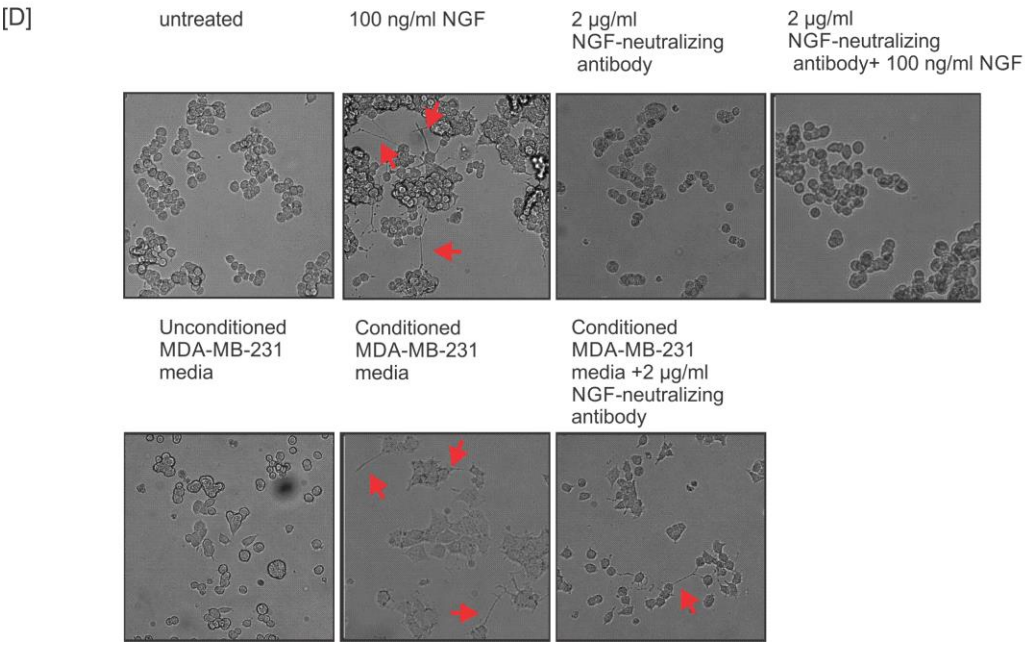

Fig. 3.3: Neurotrophins and neurotrophin receptor expression in TNBC cells: ***[A]*** MDA-MB-231 and HCC1806 cell lines were seeded at $3x10^4$ cells/cm^2. Total RNA was extracted using Trizol method and mRNA expression of $p75^{NTR}$ [201 bp], NGF [313 bp] and BDNF [266 bp] was carried out with specifically designed primers using RT-PCR. GAPDH [452 bp] was used as a

loading control. ***[B]*** Cells were harvested at 24 h, 48 h and 72 h and Western blot analysis was carried out on whole cell extracts to determine the expression of pro-NGF. Actin was used as a loading control. ***[C]*** NGF-ELISA was carried out on culture medium harvested at 24 h, 48 h and 72 h. The secretion of NGF was quantified with commercially available hβNGF as the standard. These data are representative of n=3. Statistical analysis using ANOVA with Tukey's post -hoc test was done between the different time points. In both the cell lines, amount of NGF secretion between 24 h vs 72 h and 48 h vs 72 h are statistically significant *p <0.05. ***[D]*** PC12 cells were seeded at $3x10^4$cells/cm^2 and treated with 100 ng/ml commercially available mNGF with/without 2 μg/ml α-NGF antibody or conditioned or unconditioned MDA-MB-231 media for 5 days. NGF was replenished alternate day to induce longer neurite outgrowth. The cells were imaged on day 5 under the microscope. The arrows in red indicate neurite outgrowth. Conditioned media from MDA-MB-231 cell were able to induce neurite in PC12 cells.

3.2.4 Expression of $p75^{NTR}$ correlates with the expression of neurotrophins in basal-like breast cancer subtype

The data shown so far suggests that increase in the expression of $p75^{NTR}$ or NGF corresponds to increase in the expression of the other in TNBC in culture. Therefore correlation between expression of NGFR ($p75^{NTR}$) and all neurotrophins primarily NGF and also (BDNF, NT3, NT4 was determined across patients with different subtypes of breast cancer. Gene correlation analysis was carried out using breast cancer gene-expression miner v3.1 (bc-GenExMiner v3.1). This permits one to compute correlation coefficients between gene expressions or to find lists of correlated genes in breast cancer across all subtypes (Jezequel et al., 2013). The gene expression correlation statistical analysis is applied on published annotated genomic datasets and the results are displayed as Pearson's pairwise correlation plot. On analyzing the correlation between $p75^{NTR}$ (NGFR) and neurotrophins, there was a weak yet highly significant ($p<0.0001$) positive correlation between $p75^{NTR}$ and NGF, NT3, NT4 but not with BDNF in all patients having breast cancer. A correlation between $p75^{NTR}$ and NGF in basal-like breast cancers was determined. A weak positive correlation between NGF and $p75^{NTR}$ yet with high significance was observed in basal-like breast cancers (Fig. 3.4 A and B). As mentioned before TNBCs are basal like breast cancer. The data shown in Fig. 3.1 A and Fig. 3.3 B agrees with the positive correlation between $p75^{NTR}$ and NGF in TNBC patients. Fig. 3.4 represents the Pearson's pairwise correlation plot between NGF vs $p75^{NTR}$ in [A] all patients, [B] in patients having basal-like subtype of breast cancer. Table 3.1 shows a summary of the significance of correlation between genes ($p75^{NTR}$ vs neurotrophins) with

indication of positive, negative or null correlation (r value) and of the sample size (n) across all subtypes of breast cancer.

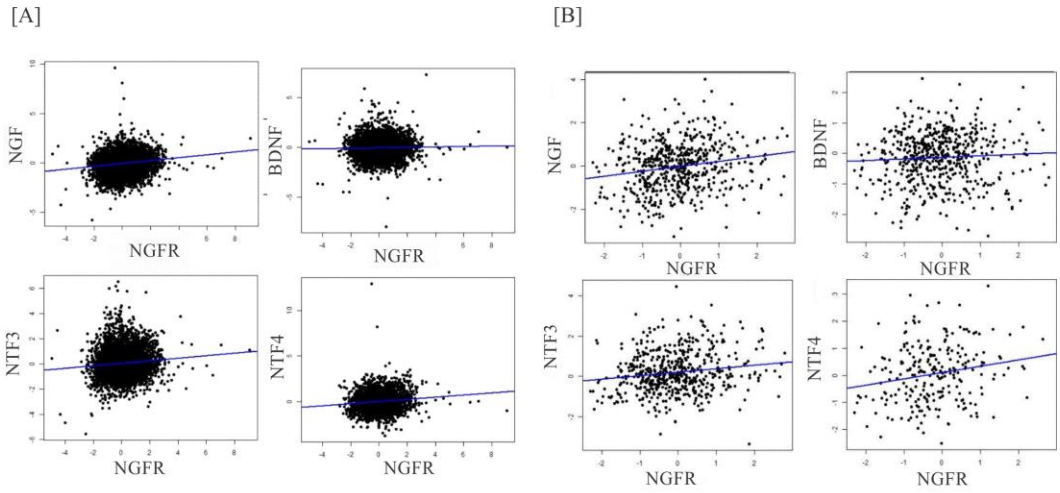

[C]

		NGFR						
		All patients	Basal like	ER positive	ER negative	Luminal A	Luminal B	HER2
NGF								
	r value	r=0.15	r=0.19	r=0.13	r=0.20	r=0.09	r=-0.06	r=-0.09
	p value	p<0.0001	p<0.0001	p<0.0001	p<0.0001	p=0.1117	p=0.6112	p=0.3358
	n	n=5543	n=554	n=3924	n=1557	n=314	n=80	n=110
BDNF								
	r value	r=0.02	r=0.06	r=0.02	r=0.05	r=0.00	r=0.14	r=0.05
	p value	p=0.0720	p=0.1483	p=0.2198	p=0.0669	p=0.9739	p=0.2256	p=0.6007
	n	n=5249	n=554	n=3758	n=1440	n=314	n=80	n=110
NT3								
	r value	r=0.10	r=0.16	r=0.08	r=0.15	r=-0.11	r=-0.02	r=0.10
	p value	p<0.0001	p=0.0002	p<0.0001	p<0.0001	p=0.0494	p=0.8942	p=0.3199
	n	n=5510	n=554	n=3923	n=1525	n=314	n=80	n=110
NT4								
	r value	r=0.12	r=0.20	r=0.11	r=0.14	r=0.20	r=-0.23	r=-0.01
	p value	p<0.0001	p=0.0018	p<0.0001	p=0.0001	p=0.0033	p=0.1055	p=0.9164
	n	n=2883	n=246	n=2039	n=803	n=219	n=50	n=62

Fig. 3.4: Expression of p75^{NTR} (NGFR) correlates with the expression of neurotrophins in basal-like breast cancer subtype: Pearson's pairwise correlation of NGFR vs neurotrophins; NGF, BDNF, NT3 and NT4 was carried out using breast cancer gene-expression miner v3.1 (bc-GenExMiner v3.1). ***[A]*** Correlation plot of NGFR vs neurotrophins (NGF, BDNF, NT3 and NT4) in all patients irrespective of the sub type of breast cancer. ***[B]*** Correlation plot of NGFR vs neurotrophins (NGF, BDNF, NT3 and NT4) in patients with basal-like breast cancer. ***[C]*** A summary of the correlation between NGFR vs NGF, BDNF, NT3 and NT4 across all subtypes of breast cancer. 'r' value represents the co-efficient of correlation that determines positive, negative

or null correlation between the two genes of interest, 'n' represents sample size and 'p' value indicates the statistical significance.

3.2.5 NGF induces an increase in expression of $p75^{NTR}$ in TNBC cells

NGF is reported to be secreted by many breast tumors, and is shown to activate its receptors through autocrine signaling (Dolle et al., 2003a). Given that TNBC cells express NGF, we hypothesized that the regulation of $p75^{NTR}$ could be due to secretion of NGF into the culture medium of the cells. This could increase $p75^{NTR}$ levels by stimulating transcription of $p75^{NTR}$ gene, or by inhibiting degradation of the full length protein which is known to undergo regulated intramembrane proteolysis (Verbeke et al., 2013, Skeldal et al., 2011). To test this hypothesis, we treated MDA-MB-231 cells with NGF for different times ranging from 0-12 h. Addition of exogenous NGF increased the expression of $p75^{NTR}$ protein and mRNA over time and addition of NGF inhibitors or neutralizing antibody inhibited this regulation (Fig. 3.5 A and B). To further investigate if this increase in expression of $p75^{NTR}$ was through NGF dependent transcriptional/translational regulation of $p75^{NTR}$, cells were treated with 10 μg/ml actinomycin D (an inhibitor of transcription) or 10 μg/ml cycloheximide (a global translational inhibitor), in the presence or absence of NGF. There was a decrease in the expression of $p75^{NTR}$ with actinomycin D and cycloheximide in the presence of NGF as opposed to NGF treated cells alone (Fig. 3.5 C). Taken together, these data indicate that NGF activates the transcription/translation of $p75^{NTR}$ in these cells. Next we investigated the role of TrkA and $p75^{NTR}$ in this effect. Inhibition of TrkA kinase activity by K252a (Tapley et al., 1992) or of $p75^{NTR}$ by TAT-Pep5 (which binds to the death domain of $p75^{NTR}$ to block downstream signaling) (Yamashita and Tohyama, 2003a) both caused a reduction in NGF-induced increase in $p75^{NTR}$ expression (Fig. 3.5 D).

Receptor intramembrane proteolysis of $p75^{NTR}$ is mediated by the action of α and γ secretases (Brown et al., 2000). Importantly, NGF has been shown to induce rapid and robust secretase-dependent proteolysis of $p75^{NTR}$ in PC12 cells (Ceni et al., 2010). To determine if the increase in expression of FL $p75^{NTR}$ in TNBC cells was due to inhibition of regulated intramembrane proteolysis of $p75^{NTR}$, cells were treated with NGF in the presence or absence of GM6001, an inhibitor of α secretase which cleaves $p75^{NTR}$ to produce the 25 kDa C-terminal fragment (CTF) or DAPT, an inhibitor of γ secretase whose action produces the 19 kDa intracellular domain (ICD) of $p75^{NTR}$ (Urra et al., 2007a). These treatments were performed in the presence of epoxomicin to inhibit

proteasomal degradation of the cleavage fragments (Wang et al., 2008). $p75^{NTR}$ was found to undergo constitutive cleavage in MDA-MB-231 cells, as seen by the presence of the ICD in samples treated with epoxomicin only (Fig. 3.5 E). Treatment of cells with NGF inhibits processing of $p75^{NTR}$, partially, at both the levels of cleavage, resulting in an increase in levels of $FLp75^{NTR}$ (Fig. 3.5 F).

In order to test the effect of inhibition of activity of secretases on cell survival, MDA-MB-231 cells were pre- treated with either 10 μM GM6001 or 10 μM DAPT for 2 h followed by treatment with 500 ng/ml TRAIL for 24 h and the cells were harvested for (a) SubG1 analysis or (b) TMRE assay. Fig. 3.5 G and H show that inhibition of α-secretase mediated cleavage results in sensitization of cells to TRAIL induced cell death, while inhibition of γ-secretase using DAPT did not have an effect than TRAIL alone. This suggests that inhibiting the processing of $FLp75^{NTR}$ has a negative effect on cell survival. However, NGF mediated inhibition of processing of $p75^{NTR}$ was not significant enough to induce cell death in our system.

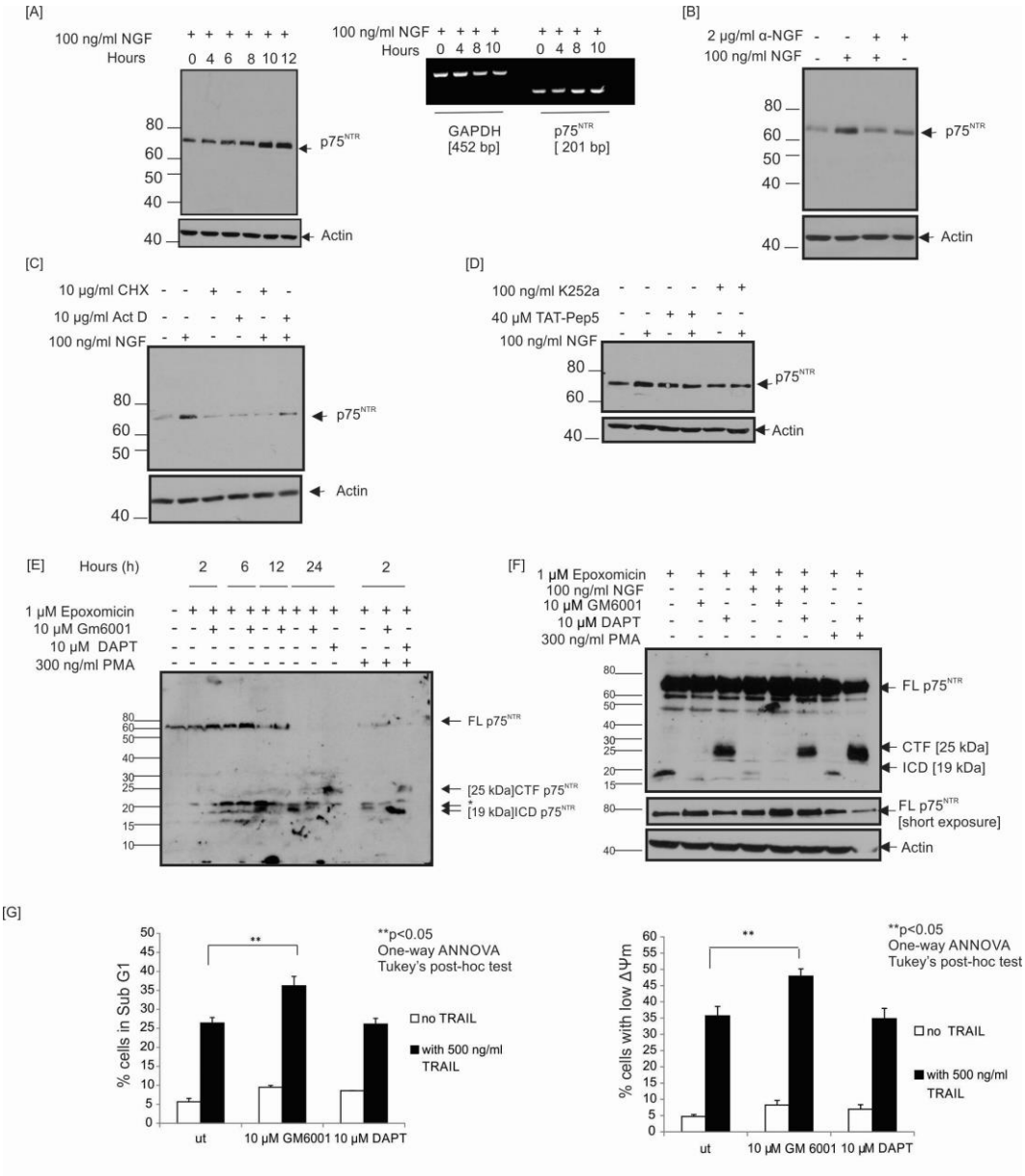

Fig. 3.5: NGF mediated increase in the expression of p75^{NTR}: MDA-MB-231 was seeded at 3x10^4 cells/cm^2. ***[A]*** MDA-MB-231 cells were treated with 100 ng/ml NGF for indicated time points and cells were harvested for WB and RT-PCR. ***[B]*** MDA-MB-231 cells were treated with 100 ng/ml NGF and/or 2 µG/ml NGF-neutralizing antibody (α- NGF). Cells were harvested 12 h post treatment and probed for anti-p75^{NTR}. Anti-actin was used as a loading control. ***[C]*** MDA-MB-231 cells were pre-treated with 10 µG/ml Actinomycin D or 10 µG/ml Cycloheximide for 1 hr prior to treatment with or without 100 ng/ml NGF for 12 h. Cells were harvested and western blotting was carried out to examine the expression of p75^{NTR}. ***[D]*** MDA-MB-231 cells were pre-treated with 100 nM K252a or 40 µM TAT-Pep5 for 1 h before addition of 100 ng/ml NGF for 12 h. Cells were harvested and western blotting was carried out on whole cell extracts and expression

of $p75^{NTR}$ was determined. ***[E]*** MDA-MB-231 cells were pre-treated with 1 μM Epoxomicin, a proteasomal degradation inhibitor and 10 μM GM6001, an α-secretase inhibitor or 10 μM DAPT, a γ-secretase inhibitor for 1 hr before treatment with 100 ng/ml NGF or 300 ng/ml Phorbol myristate acetate (PMA), an activator of secretases. Cells were harvested after 2, 6, 12 or 24 h. The positive control with PMA treatment was harvested after 2 h of treatment. ***[F]*** MDA-MB-231 cells were pre-treated with 1 μM Epoxomicin, a proteasomal degradation inhibitor and 10 μM GM6001,an α-secretase inhibitor or 10 μM DAPT, a γ-secretase inhibitor for 1 hr before treatment with 100 ng/ml NGF or 300 ng/ml Phorbol myristate acetate (PMA), an activator of secretases. Cells were harvested after 12 h. Western blot analysis was carried out on the whole cell extracts. The expression of $p75^{NTR}$ was examined. ***[G]*** MDA-MB-231 cells were treated with or without 10 μM GM6001, alpha-secretase inhibitor or 10 μM DAPT, 1 h prior to treatment with 500 ng/ml TRAIL for 24 h. The cells were then harvested for Sub G1 and TMRE assays. These data are the mean ± SEM of three independent experiments, *$p < 0.05$. One-way ANOVA followed by Tukey's post hoc-test was carried out. These data are representative of n=3.

3.2.6 Inhibition of interaction of NGF/$p75^{NTR}$ sensitizes cells to apoptosis in MDA-MB-231 cells

NGF/ $p75^{NTR}$ signaling is reported to promote resistance of breast cancer cells to apoptosis induction (Descamps et al., 2001b). To show that the NGF-induced increase in $p75^{NTR}$ is important for pro-survival signaling in TNBC cells, we initially tested the role of this receptor in the resistance of MDA-MB-231 cells to ceramide-induced cell death. Ro 08-2750 could sensitize MDA-MB-231 cells to C2-ceramide induced apoptosis indicated by the loss of mitochondrial transmembrane potential (Fig. 3.6 A). To test if inhibition of $p75^{NTR}$ also had similar effect to inhibition of NGF on the cells, $p75^{NTR}$ in MDA-MB-231 was (a) genetically knocked down or (b) chemically inhibited by TAT-Pep5. Fig. 3.6 B shows the transfection efficiency of $shp75^{NTR}$ with scrambled vector expressing eGFP as a control. The transfection was optimized using different concentrations of $shp75^{NTR}$ and with different lipid:DNA ratio over 24 h and 48 h using turbofect transfection reagent. The samples were analyzed using FACS to quantify the percentage of transfection efficiency. Knock down of $p75^{NTR}$ using shRNA directed against $p75^{NTR}$, also sensitized MDA-MB-231 cells to C2-ceramide induced apoptosis, as determined by an increase in the subG1 population (Fig. 3.6 C). Although, TAT-Pep5 did not sensitize MDA-MB-231 cells to C2-ceramide induced cell death, an additive effect was observed with the treatments as shown in Fig. 3.6 D. From these results, it is evident

that interfering with the interaction of NGF/p75^{NTR} sensitizes cells to drug induced cell death and that NGF and p75^{NTR} are pro-survival factors in our system.

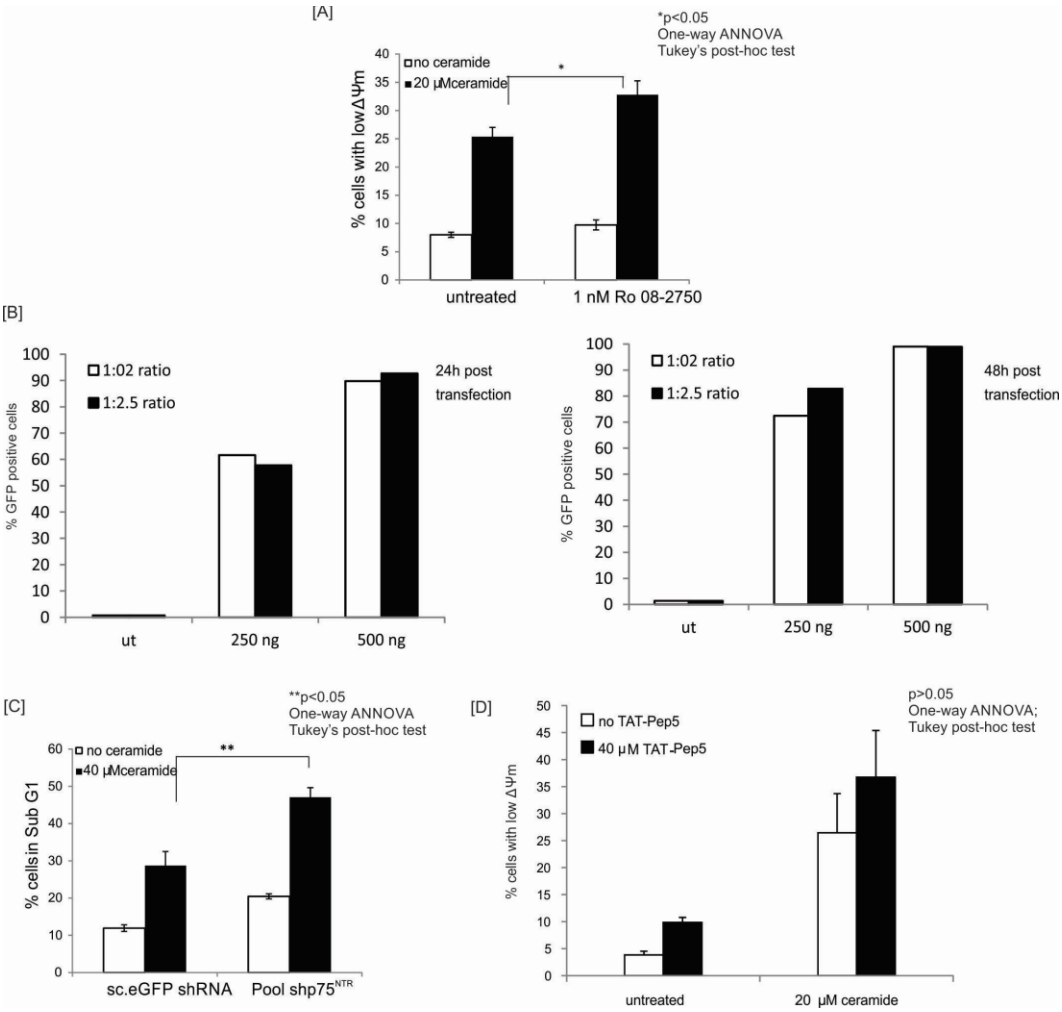

Fig. 3.6: Inhibition of p75^{NTR}/NGF interaction induces apoptosis in MDA-MB-231 cells: MDA-MB-231 cells were seeded at 3x10^4 cells/cm^2 and treated with ***[A]*** 1 nM Ro 08-2750 1 h prior to treatment with 20 µM ceramide for 24 h. Cells were harvested for TMRE assay. ***[B]*** MDA-MB-231 cells were transfected with different concentrations of sc.eGFP and shp75^{NTR} in different ratios and harvested at 24 h and 48 h. The samples were then harvested and % of GFP uptake was analyzed on the FACS. ***[C]*** MDA-MB-231 cells were transfected with 1 µg shp75^{NTR}and sc eGFP plasmid DNA. 24 h post transfection, cells were treated with or without 40 µM ceramide for another 24 h. Cells were harvested for Sub G1 analysis. ***[D]*** MDA-MB-231 cells were pre-treated with 40 µM TAT-Pep5 prior to treatment with 20 µM ceramide. Cells were harvested after 24 h for TMRE assay. These data are the mean ± SEM of three independent experiments, *p < 0.05, *8p<0.01.

3.2.7 Neurotrophin mediated increase in $p75^{NTR}$ promotes resistance of TNBC cells to apoptosis induction

Next the biological relevance of the increase in $p75^{NTR}$ by NGF was determined. The sensitivity of HCC1806 cells to Ro 08-2750 at 24 and 72 h was compared since these cells express almost no $p75^{NTR}$ at 24 h and exhibit a very large increase in $p75^{NTR}$ by 72 h (Fig. 3.2 A). This would allow us to distinguish the effect of $p75^{NTR}$ induction on these cells in response to C2-ceramide treatment clearly. HCC1806 cells exhibited a pronounced differential sensitivity to apoptosis induction at 24 and 72 h (Fig. 3.7 A, B and C). These findings were confirmed using DEVDase assay which showed sensitization of HCC1806 to C2-ceramide induced cell death in the presence of 2 nM Ro 08-2750 at the later time but not at the earlier time (Fig. 3.7 A). Analysis of loss of mitochondrial membrane permeability using TMRE showed that the cells were resistant to single or combination treatment at the earlier time, while at the later time the cells were sensitive to treatment with Ro 08-2750 alone, but were not further sensitized to C2-ceramide (Fig. 3.7 B).Analysis of nuclear morphology by DAPI staining showed more apoptotic bodies and nuclear condensation indicating apoptosis in response to NGF inhibition at the later time point (Fig. 3.7 C). Taken together, these data show that HCC1806 cells are sensitized to C2-ceramide induced death at later time points compared to earlier time points.

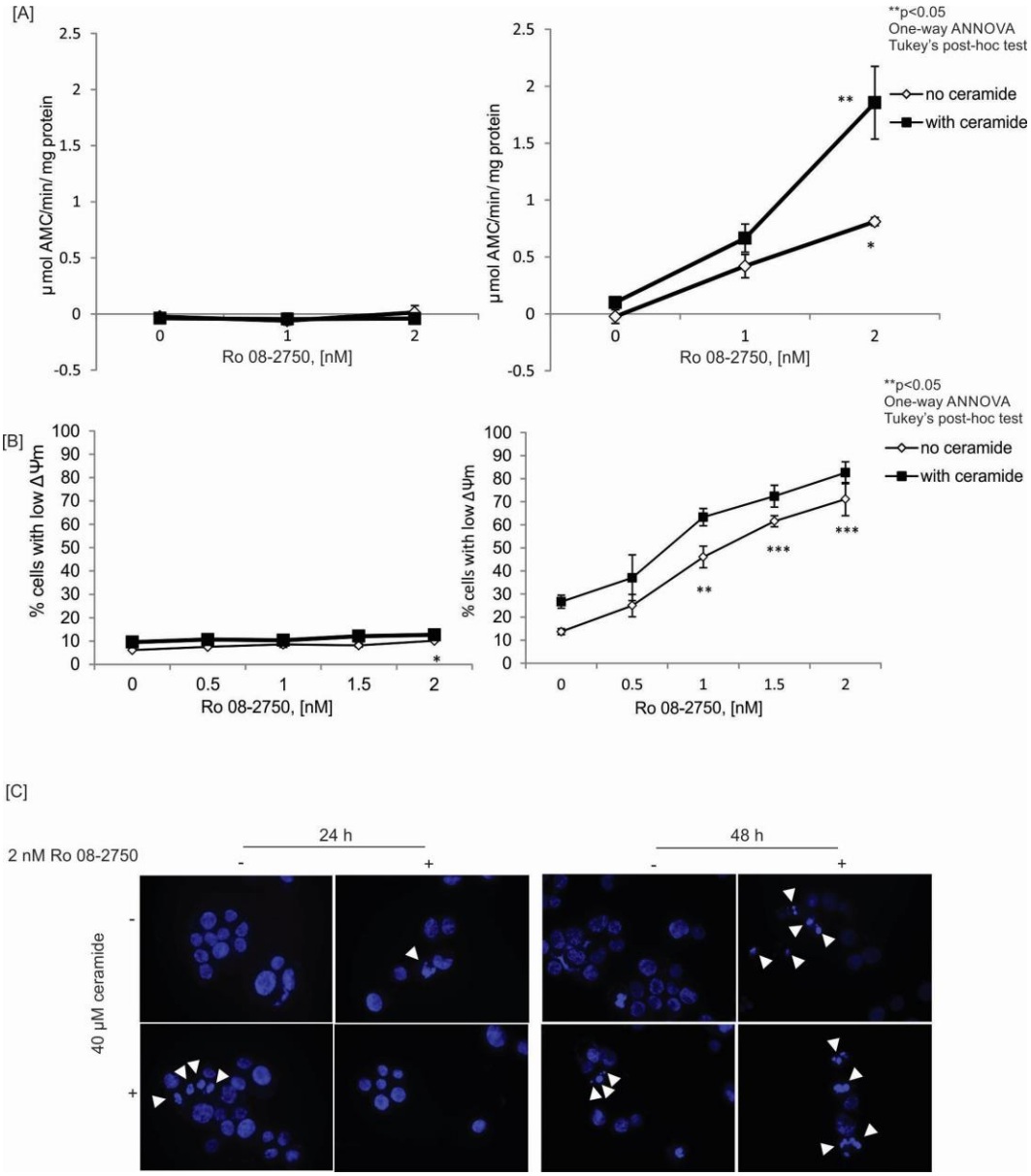

Fig. 3.7: p75^{NTR} promotes protection in TNBC cells: MDA-MB-231 cells were seeded at 3x10^4 cells/cm^2. For the early time point [on the left], HCC1806 cells were treated with 2 nM Ro 08-2750 4 h post seeding and 1 h after Ro 08-2750 treatment, cells were treated with 40 µM ceramide for 24 h. For the later time point [on the right], HCC1806 were treated 48 h post seeding with 2 nM Ro 08-2750 and after 1 h pre-treatment with Ro 08-2750, cells were treated with 40 µM ceramide for 24 h. Cells were harvested for ***[A]*** caspase-3 activity assay [DEVDase assay], ***[B]*** loss of mitochondrial membrane potential assay [TMRE assay] and ***[C]*** DAPI staining. Statistical analysis on DEVDase assay using One-way ANOVA followed by Tukey's post-hoc test showed

**p<0.05 and *p<0.05 on TMRE assay. These data are the mean ± SEM of three independent experiments.

3.2.8 Inhibition of $p75^{NTR}$ in culture induces basal cell death in TNBC cells

Similar to the approach taken to inhibit NGF secretion over time in culture and looking to sensitize the cells to apoptosis, HCC1806 cells which expressed massive $p75^{NTR}$ over time in culture were treated with 40 µM TAT-Pep5 at similar time points mentioned in the previous section. Although no significant sensitization was observed with combination treatments of TAT-Pep5 and C2-ceramide, TAT-Pep5 on its own was able to increase basal cell death in these cells as shown in Fig. 3.8 A and this basal cell death was increased at later time points where TAT-Pep5 would have more $p75^{NTR}$ to bind to and inhibit its signaling compared to earlier time point where there is less $p75^{NTR}$ expression. The last time point (72 h) mentioned in the previous section was omitted as the difference between 24 h and 48 h would be clearer where there little to no $p75^{NTR}$ at 24 h and huge induction at 48 h time point in HCC1806 cells (see Fig. 3.2 A) and the effect of TAT-Pep5 would be more obvious at these two time points. Similar effect was seen in MDA-MB-231 cells where TAT-Pep5 was able to increase basal cell death at 24 h and MDA-MB-231 cells have been shown to express $p75^{NTR}$ at this time point (see Fig. 3.2 A). The cells were harvested for TMRE assay as shown in Fig. 3.8 B. To further strengthen the data with TAT-Pep5, HCC1806 cells were transfected with $shp75^{NTR}$ using turbofect reagent. Knockdown of $p75^{NTR}$ in HCC1806 induces cell death which is shown by cleavage of PARP as seen is Fig. 3.8 C. Similar effects were observed in MDA-MB-231 cells., however, the assays used to determine cell death was determination of cells in the Sub G1 phase of cell cycle, and the knockdown of $p75^{NTR}$ was confirmed using Western blotting (Fig. 3.8 D).

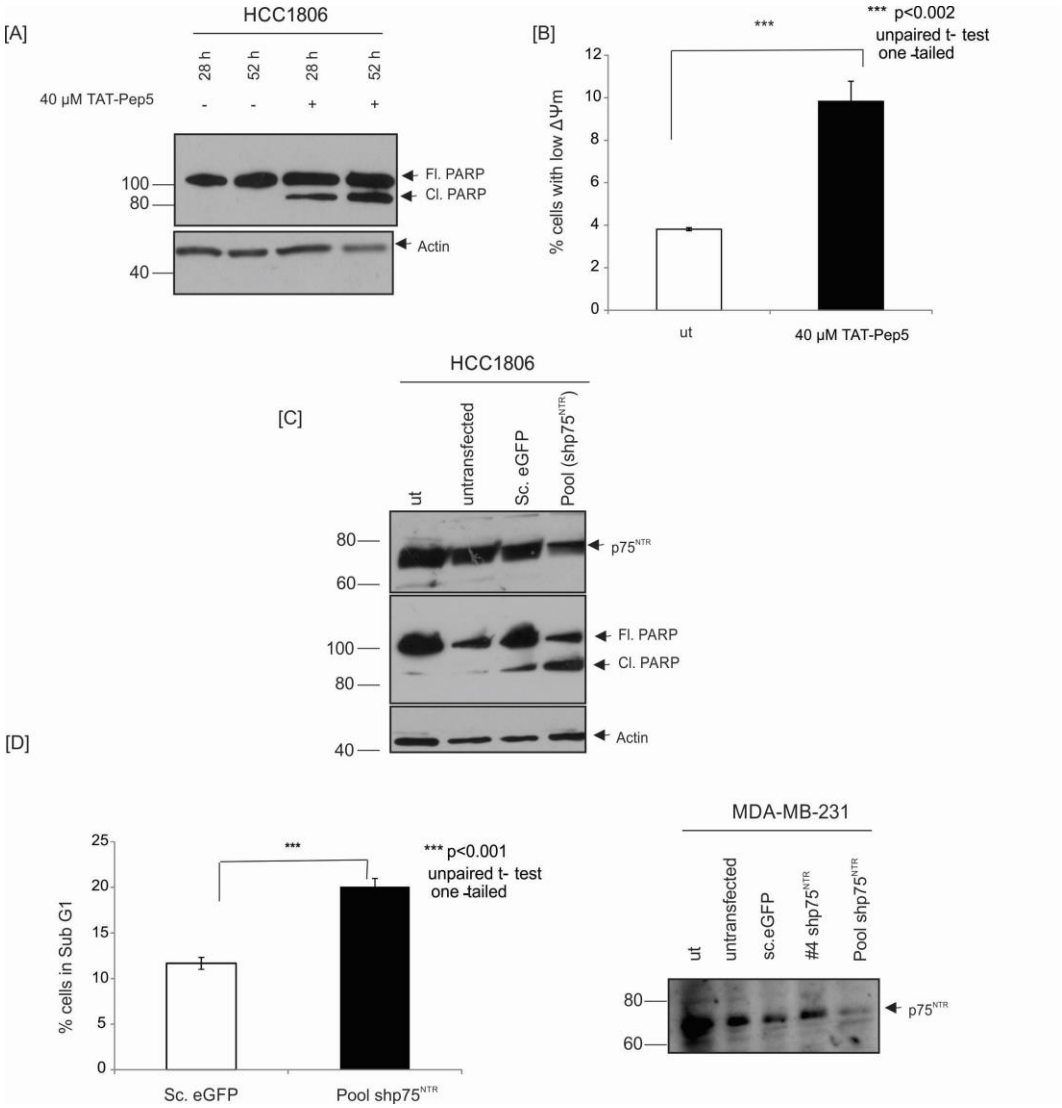

Fig. 3.8: Inhibiting p75^{NTR} expression in culture induces basal cell death in TNBC cells: MDA-MB-231 and HCC1806 cells were seeded at 3x10^4 cells/cm^2. ***[A]*** For the early time point, HCC1806 cells were treated with 40 μM TAT-Pep5 4 h post seeding and harvested 24 h post treatment and for the late time point to allow accumulation of p75^{NTR}, cells were treated with 40 μM TAT-Pep5 24 h before its harvest. Western blot analysis was carried out on whole cell extracts. The membrane was blotted for anti-PARP. ***[B]*** MDA-MB-231 cells were treated with 40 μM TAT-Pep5 and harvested after 24 h for TMRE assay. ***[C]*** HCC1806 cells were transfected with shp75^{NTR} along with its respective controls and knockdown of p75^{NTR} in itself was able to induce basal cell death. ***[D]*** Similar to HCC1806, MDA-MB-231cells were also transfected with shp75^{NTR} and the lysates were probed for expression of p75^{NTR}. To quantify the % of cell death, transfected MDA-MB-231 cells were harvested for Sub G1 analysis. These data are the mean± SEM of three independent experiments. Unpaired t-test was carried out to determine statistical significance.

3.3 Discussion

Dysregulation in the NGF signaling through its receptors and imbalance in the levels of expression of the receptors have been reported to contribute to the chemo-resistance in several cancers such as breast cancer (Descamps et al., 2001a, Verbeke et al., 2010, Zhang et al., 2015) or pancreatic cancers (Zhu et al., 2002). Therefore targeting NGF-mediated autocrine signaling or the expression of the NGF receptor has a high therapeutic potential. This study shows that NGF can regulate the expression of $p75^{NTR}$ in TNBC cells. NGF increased the expression of $p75^{NTR}$ by partially inhibiting the processing of $p75^{NTR}$ and by partially inhibiting the transcription of $p75^{NTR}$. This study also shows that inhibition of NGF/$p75^{NTR}$ interaction differentially sensitizes TNBC cells to apoptosis induction in the presence or absence of induction of $p75^{NTR}$ expression.

A panel of breast cancer cell lines across all subtypes was screened for the expression of $p75^{NTR.}$ Out of these, the basal-like breast cancer cells, also interchangeably called the TNBC cells expressed high levels of $p75^{NTR}$. An increase in expression of $p75^{NTR}$ over time in culture was observed in MDA-MB-231 and HCC1806 cells. High levels of expression of $p75^{NTR}$ in basal- like breast cancer subtype has been reported by (Reis-Filho et al., 2006). The increase in $p75^{NTR}$ expression diminished in the presence of NGF inhibitor Ro 08-2750, NGF /BDNF inhibitor Y1036 and also in the presence of NGF-neutralizing antibody (α-NGF). This suggested the involvement of neurotrophins in the regulation of $p75^{NTR}$.

It is well published that breast cancer cells express and secrete NGF that can activate the receptors through autocrine signaling (Descamps et al., 2001c). (Dolle et al., 2003b) has also shown that NGF is overexpressed in breast cancer cells maintained in culture. However, they did not show expression of proNGF in the culture. NGF is expressed in the cells in the pro-form, which then undergoes protein folding and maturation and is then secreted into the media as mature NGF (Kliemannel et al., 2007). The expression of proNGF corresponding to the increase in expression of $p75^{NTR}$ in culture was observed. However, to determine if secreted NGF was regulating the expression of $p75^{NTR}$, NGF-ELISA was carried out quantify the NGF secreted by TNBC cells. The amount of NGF secreted by these cells also increased over time in culture. This increase in secretion of NGF was not due to the increase in the number of cells in culture. This is because the approximate doubling time of these cell lines is 38 h (for MDA-MB-231) and 30 h (for

HCC1806). The increase in NGF over time was more than the number of cells at that time. The secretion of NGF into the TNBC cell media was also confirmed by applying the conditioned media on to PC12 cells, a model of rat pheochromocytoma, because these cells have been shown to extend neurites in the presence of NGF (Drubin et al., 1985). Commercially available NGF and conditioned media taken from MDA-MB-231 cells at day 3 in culture showed neurite outgrowth and anti-NGF inhibited the neurite outgrowth on PC12 cells treated with commercially available NGF. However, anti-NGF did not have an effect on neurite outgrowth on cells treated with conditioned media. Neurite extensions seen in the presence of MDA-MB-231 conditioned media could possibly also be due to stress resulting from the difference in the media composition of PC12 vs MDA-MB-231. Several other factors could also induce neurite formation in PC12 cells like; activation of stress- activated kinases (Giasson et al., 1999). The secretion of NGF was however confirmed by ELISA. The data from NGF ELISA confirmed the involvement of NGF in the regulation of $p75^{NTR}$.

To directly test the effect of NGF in the regulation of $p75^{NTR}$, MDA-MB-231 cells were treated with exogenous NGF for short time course up to 12 h. An increase in expression of $p75^{NTR}$ mRNA and protein was observed upon NGF treatment. This expression of $p75^{NTR}$ diminished in the presence of α-NGF. Expression of $p75^{NTR}$ has been shown to be induced in conditions of stress (Roux et al., 1999, Peterson and Bogenmann, 2003, Irmady et al., 2014). Transcriptional regulation of $p75^{NTR}$ has been previously reported under stressed conditions (Ramos et al., 2007, Gao et al., 2007). Therefore, the regulation of $p75^{NTR}$ by NGF at the transcriptional level was studied. This study also showed that the regulation of $p75^{NTR}$ expression was partially through NGF-dependent transcription of $p75^{NTR}$. To determine the mechanism of NGF-mediated regulation of $p75^{NTR}$, MDA-MB-231 cells were treated with Actinomycin D or Cycloheximide, in the presence or absence of NGF. NGF-mediated regulation of $p75^{NTR}$ expression diminished in the presence of the inhibitors suggesting that NGF could activate $p75^{NTR}$ transcription/translation. Next, the ability of NGF to regulate the expression of $p75^{NTR}$ by inhibiting the degradation of full length $p75^{NTR}$ was determined. $P75^{NTR}$ has been reported to undergo proteolytic processing in various cell types include breast cancer cells (Skeldal et al., 2011, Verbeke et al., 2013). A recent study by (Verbeke et al., 2013) show that $p75^{NTR}$ undergoes constitutive proteolytic cleavage in breast cancer cells and this regulated intramembrane proteolysis involves the activity of secretases. This mechanism is well established in cell

types including glioblastoma (Wang et al., 2008) or medulloblastoma (Wang et al., 2010). The effect of processing of $p75^{NTR}$ on the expression of $FLp75^{NTR}$ was determined. NGF partially inhibited the processing of $FLp75^{NTR}$ resulting in the increased expression of $FLp75^{NTR}$. Studies on PC12 cells show that activation of TrkA by NGF enhances the processing of $p75^{NTR}$ resulting in the generation of the ICD fragment (Urra et al., 2007b), which can activate various transcription factors (Kanning et al., 2003). TAT-Pep5, an inhibitor that binds to the death domain of $p75^{NTR}$ (Yamashita and Tohyama, 2003b) and K252a, a tyrosine kinase inhibitor that blocks the activation of Trk receptors (Tapley et al., 1992) increased basal FL $p75^{NTR}$ levels. However, these receptors are required in the active form for NGF to regulate expression of $p75^{NTR}$, i.e., inhibition of TrkA or $p75^{NTR}$ death domain diminishes NGF- mediated regulation of $p75^{NTR}$. In breast cancer cells, constitutive proteolytic processing of $p75^{NTR}$ is thought to be necessary for the turnover of $p75^{NTR}$ and for the NGF/$p75^{NTR}$ pro-survival signaling under normal conditions. It is possible that NGF regulates the expression of $p75^{NTR}$ by increasing the availability of full length $p75^{NTR}$ to interact with NGF, and mediate its pro-survival effect. In contrast to neuronal cells, where the ICD is essential to mediate survival effect, it has been shown that in breast cancer cells, the carboxy terminal fragment (CTF) is necessary for its survival (Verbeke et al., 2013).

It has been suggested that expression of $p75^{NTR}$ may be linked to a subgroup of basal-like breast carcinomas with good prognosis (Reis-Filho et al., 2006). As mentioned earlier, NGF is overexpressed across all the subtypes of breast cancer. Therefore, to target NGF-regulated induction of $p75^{NTR}$ might be of therapeutic relevance. TNBCs exhibited differential sensitivity to apoptosis with or without induction of $p75^{NTR}$. The cells with little to no $p75^{NTR}$ were very resistant to Ro 08-2750 because on ELISA, there was no detectable NGF after 24 h of cell culture; but when NGF and $p75^{NTR}$ were allowed to accumulate in the system, Ro 08-2750 was able to efficiently sensitize the cells to apoptosis. Overexpression of $p75^{NTR}$ has been reported to enhance breast cancer cell survival through $p21^{waf1}$ (Verbeke et al., 2010). Genetic knockdown of $p75^{NTR}$ by $p75^{NTR}$ shRNA was able to sensitize the cells to drug-induced apoptosis. Alternatively, peptide inhibitor, TAT-Pep5 was also used which increased basal cell death but failed to sensitize the cells to drug-induced apoptosis. However, it conferred an additive effect to drug induced cell death. A similar approach to using Ro 08-2750 at different time points was carried out using TAT-Pep5. There was an increase in PARP cleavage indicating an

increase in basal cell death where $p75^{NTR}$ expression was induced; however, there was no increased PARP cleavage in the presence of apoptosis inducer.

TNBC cells are difficult to treat subtype of breast cancer and are insensitive to current targeted therapies due to the lack of expression of Ee, Pr and Her-2 receptors (Perou et al., 2000, Foulkes et al., 2010). The fact that NGF signaling is specific to TNBC cells and not to NBEC indicates NGF as a potential therapeutic target. It has been reported that use of NGF-neutralizing antibody on MDA-MB-231 xenograft in SCID mice reduced the tumor growth, size and volume, thus highlighting the therapeutic potential of targeting NGF in breast cancers (Adriaenssens et al., 2008). A correlation between expression of NGF and $p75^{NTR}$ genes in patients with breast cancer was determined and this analysis showed a weak yet highly significant positive correlation between the expression of the two genes in all patients (irrespective of the subtypes), patients with basal-like breast cancer and Er+ or –ve breast cancers . However, this correlation was not significant in Luminal subtypes of breast cancer. This correlation was similar for NT3 or NT4 vs $p75^{NTR}$. This is consistent with the findings of this study where an increase in expression of $p75^{NTR}$ was observed in TNBC cells and not in Luminal subtypes. The increase in expression of $p75^{NTR}$ was accompanied by the increase in expression of proNGF and secretion of mature NGF into the media of TNBC cells. Therefore, targeting one of the two might have an effect on the other. Collectively, the data in this study show that NGF can regulate the levels of $FLp75^{NTR}$ in breast cancer cells and that this may be linked to the increased resistance of TNBC cells to chemotherapeutic drug-induced cell death. The findings from this study can be exploited therapeutically by targeting the activity of $p75^{NTR}$, thereby inducing more cell death.

Therefore, targeting NGF secretion and its interaction with $p75^{NTR}$ in combination with conventional chemotherapeutic drugs will be of high therapeutic value in TNBC patients where expression of $p75^{NTR}$ is a marker of good prognosis. This approach of targeting breast cancers is not restricted to basal like breast cancers but can also be applied across subtypes of breast cancer as they all overexpress NGF and express $p75^{NTR}$.

4 Chapter 4: Results

Biological activity of rationally designed NGF variants with predicted receptor specificity

4.1 Introduction

NGF is known to bind to two receptors; TrkA and $p75^{NTR}$ (Bradshaw et al., 1994). NGF-mediated TrkA signaling induces differentiation, neurite outgrowth, synaptic plasticity and pro-survival effect in neuronal cells (Bibel and Barde, 2000). It can induce proliferation through activation of MAPK pathway in various cancers such as breast cancer, pancreatic cancers and prostate cancers (Descamps et al., 2001c, Zhu et al., 2002, Djakiew, 2000). In contrast, NGF-mediated $p75^{NTR}$ signaling can induce pro-survival or pro-death signaling depending on the cellular context, and also on the form of NGF that binds, i.e., proNGF or mature NGF. For example, NGF signaling through $p75^{NTR}$ mediates pro-survival signaling through activation of NF-κB in breast cancer cells (Descamps et al., 2001c), whereas binding of proNGF and NGF to $p75^{NTR}$ mediates neuronal cell death through activation of JNK (Nykjaer et al., 2004, Gentry et al., 2000) . Thus, NGF signaling through its receptors mediates diverse biological effect depending on cellular context. Receptor imbalance and abnormality in the production of mature NGF are associated with pathogenicity of cancers and diseases like AD (Roux and Barker, 2002).

AD is a progressive neurodegenerative disorder characterized by extracellular deposition of amyloid- β (Aβ) peptides and the formation of intracellular neurofibrillary tangles, accompanied by synaptic dysfunction and cognitive decline (Selkoe, 2001). The number of predicted AD cases was estimated at 36 million in 2010, and is expected to triple by 2050 due to the aging population (Huang and Mucke, 2012). This increases the need for an effective treatment strategy for AD. Aβ has been implicated in the pathogenesis of AD by the discovery of mutations in the amyloid precursor protein (APP) in a small percentage of familial AD patients (Goate et al., 1991). It has been shown that the binding of Aβ to $p75^{NTR}$ induces neuronal apoptosis (Yaar et al., 1997) via activation of the c-Jun signaling pathway (Knowles et al., 2009). In contrast, $p75^{NTR}$ enhances neuronal survival when bound by NGF (Rabizadeh et al., 1994). The expression of $p75^{NTR}$ is abundant in basal forebrain cholinergic neurons (BCFN) (Rabizadeh et al., 1994) , while lower levels of NGF and TrkA have been reported in these cells (Scott et al., 1995). Together, this could explain the degeneration of BCFNs observed in AD (Rabizadeh et al., 1994). An early phase clinical trial of NGF gene therapy via implantation of autologous fibroblasts modified genetically to express human NGF in the forebrain showed a reduced rate of decline with cognitive testing (Tuszynski et al., 2005).

This method of using NGF as therapy has proved to be beneficial only on early stages of AD treatment and not in advanced stages due to enhanced amyloid toxicity (Olson et al., 1992).

Decreased NGF signaling through its receptors has been linked to insensitivity to pain (Minde et al., 2004, Einarsdottir et al., 2004) and high levels of NGF have been detected in several acute and chronic pain states (McKelvey et al., 2013). Anti-NGF therapies that inhibit NGF signaling through its receptors, thus causing insensitivity to pain, have been developed (Kumar and Mahal, 2012). One of the most successful therapies so far has been the administration of monoclonal anti-NGF antibody, Tanezumab, which is in Phase II and III of clinical trials for treatment of pain associated with osteoarthritis of the knee (Brown et al., 2012, Lane et al., 2010). The use of NGF neutralizing antibody has been reported on MDA-MB-231 xenograft in SCID mice that showed reduction in tumor size, volume and growth (Adriaenssens et al., 2008). This is an example of targeting altered NGF signaling in the context of cancers. However, development of patient tolerance and drug related immunogenicity is associated with use of biologics such as neutralizing antibodies; therefore an alternative therapeutic option is much sought after despite the success of Tanezumab (Pascual-Salcedo et al., 2011).

Rationally designed NGF variants were previously generated using the FoldX protein design algorithm in collaboration with van der Sloot and Serrano (Carleton, PhD thesis, 2013). This algorithm provides details of important interaction in the protein which contributes to the stability of protein and to the formation of protein complexes. This algorithm helps to generate mutations in proteins whose crystal structure has already been resolved. (Guerois et al., 2002). For each mutation generated in the NGF, the change in the free energy of unfolding of the ligand-receptor complex was calculated relative to that of the WT-NGF. The difference in the free energy of unfolding between the WT and the variant NGF was then determined ($\Delta\Delta G$). The variants that had increased binding affinity to the receptor were more difficult to unfold and had a higher free energy of unfolding giving a negative $\Delta\Delta G$. Conversely, if there was decreased binding affinity of ligand and the receptor, that was indicated with a positive $\Delta\Delta G$.

Based on this approach, several NGF variants with predicted altered binding affinity to TrkA or $p75^{NTR}$ receptors were generated, of which eight NGF variants were chosen for further study. A method of expressing WT-NGF and NGF variants in mammalian cells

was developed by Dr. Laura Carleton and the activity of the in-house recombinant human WT-NGF expressed was determined (Carleton, PhD thesis 2013). The actual binding affinity of the expressed NGF variants to TrkA or $p75^{NTR}$ was determined from the TrkA/$p75^{NTR}$ binding studies (Carleton, PhD thesis 2013) and is summarized in Table 4.1.

NGF variant	**TrkA**	**$P75^{NTR}$**
H4D	↑	↔
H4E	↑	↓
I31R	**0**	↔
K32R	↑	↑
G33M	↓	↔
R69D	**0**	**0**
H84Q	↓	↔
A98I	↑	↑

Table 4.1 Summary of NGF binding data: The table summarizes the actual binding affinity of each NGF variant to TrkA or $p75^{NTR}$ on the binding studies performed by Carleton (Carleton, PhD thesis, 2013). The symbols (↑) indicates increased binding to the receptor relative to WT-NGF, (↓) indicates decreased binding to the receptor, (0) indicates no binding to the receptor and (↔) indicates unchanged binding to the receptor.

The biological activity of NGF variants through TrkA or $p75^{NTR}$ was previously examined, revealing that some of the NGF variants were biologically active through their signaling via TrkA (H4D, H4E, K32R, G33M, H84Q and A98I), and this was confirmed by (a) their ability to activate ERK and AKT signaling pathways, (b) by their ability to induce neurite outgrowth in PC12 cells and (c) by their ability to protect PC12 cells against TG-induced cell death, an effect which was lost in the presence of pan-Trk inhibitor, K252a (Carleton, PhD thesis, 2013). In that study there did not appear to be any difference in the ability of the NGF variants tested to activate TrkA signaling. However, that may have been due to the use of NGF variants at saturating concentrations. Regarding $p75^{NTR}$, several approaches were taken to develop a biological assay to determine the activity of NGF through $p75^{NTR}$, with a view to testing the variants.

ProNGF/NGF-induced apoptosis through its signaling via $p75^{NTR}$ was investigated on several cell lines such as PC12, RN22, SK-N-MC, and NGF/$p75^{NTR}$-mediated pro-survival signaling through activation of NF-κB was tested on MDA-MB-231 cells or in HEK cells overexpressing $p75^{NTR}$. However, despite several approaches taken to test $p75^{NTR}$ biological activity, none of the assays was successful.

The aim of this chapter is to (a) distinguish the potency of individual NGF variants through TrkA signaling; (b) to develop a $p75^{NTR}$ biological assay; and (c) to test the biological activity of NGF variants through their signaling via $p75^{NTR}$.

4.2 Results

4.2.1 Expression of NGF variants

The protocol used for expressing in-house WT-NGF was followed to express the eight NGF variants chosen for this study. As the activity of in-house WT-NGF was comparable to that of commercially available hβNGF (referred to as hβNGFc from now on), WT-NGF was used as a positive control for comparison with the NGF variants. The NGF variants were expressed in HEK293T cells. ProNGF and mature NGF were expressed in the lysate while the secreted NGF was detected in the culture media of HEK293T cells as shown in Fig. 4.1.A. The secreted NGF was then quantified using NGF-ELISA as shown in Fig. 4.1.B. I31R, R69D and G33M NGF variants were secreted in lesser quantities, while the other NGF variants used in this study were secreted at levels comparable to the WT-NGF. The NGF variants were re-expressed as required whenever stocks of neat NGF variants ran low. Consistently, I31R and R69D NGF variants were secreted in lesser quantities.

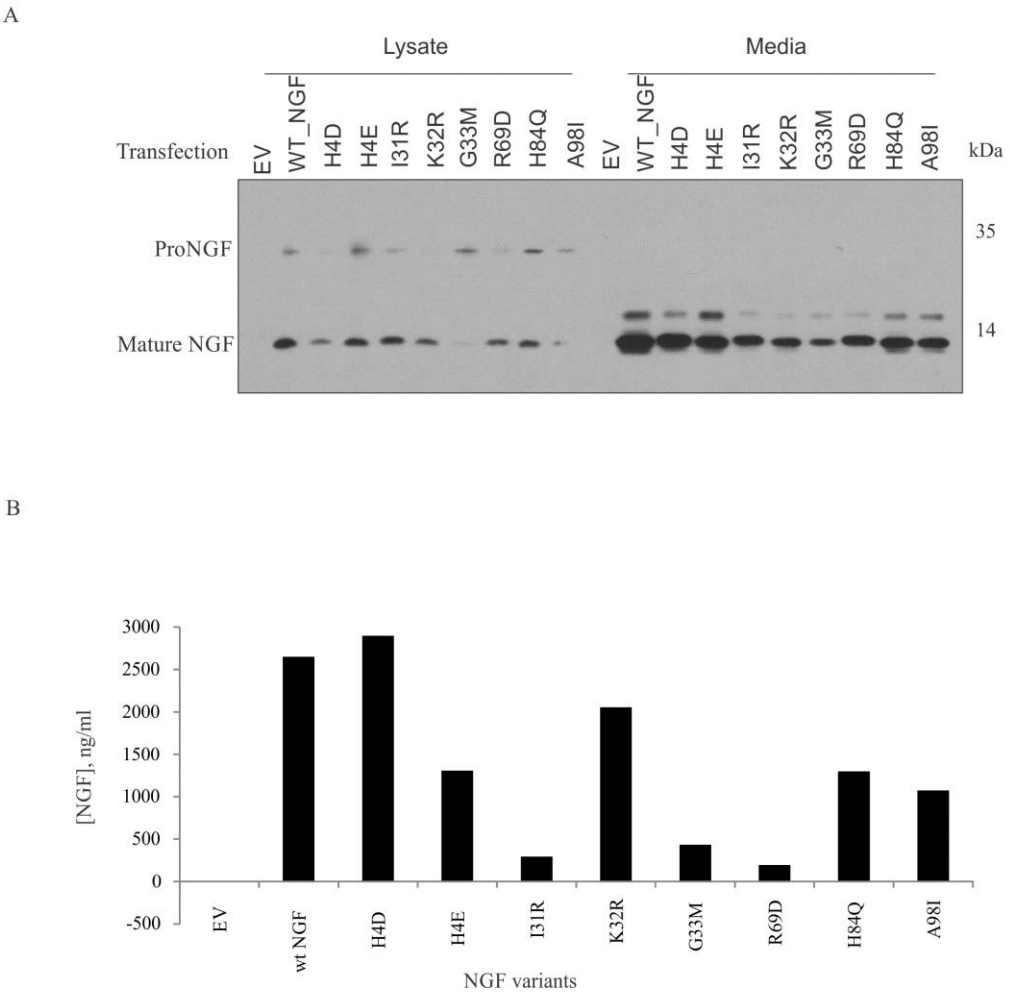

Fig. 4.1: Expression of the NGF variants

The NGF variant constructs were transfected into HEK293T cells using JetPEI transfection reagent. ***(A)*** 48 h after transfection the media were collected and the cells were lysed. Pro-NGF/NGF expression in the HEK293T cells and the secretion of the NGF into the media was analysed by Western blotting using an anti-NGF antibody. The data are representative of 3 independent experiments. ***(B)*** The concentrations of NGF secreted into the media were quantified using an ELISA. Commercially available hβNGF from R&D systems was used as standard for NGF concentration. These data are representative of n=1.

4.2.2 Biological activity of NGF variants through TrkA

4.2.2.1 Dose response of NGF variants to determine protection against TG-induced cell death

Previous studies in the lab have shown that NGF can protect PC12 cells from TG-induced cell death (Szegezdi et al., 2008) and that WT-NGF, H4D, H4E, K32R, G33M, H84Q

and A98I NGF variants could protect cells from TG-induced cell death in PC12 cells (Carleton, PhD thesis 2013). However, no distinguishable effect was observed in previous studies between NGF variants when they were used at 50 ng/ml. Therefore, a range of concentrations of WT-NGF or NGF variants (12.5-50 ng/ml) were tested to determine if any of the variants were more potent in mediating the pro-survival effect in response to TG-induced cell death. Consistent with the findings of Carleton (Carleton, PhD thesis, 2013), the WT-NGF or NGF variants except I31R and R69D mediated protection at a concentration of 50 ng/ml. From Fig. 4.2.A and B, NGF variants did not have significant effect at lower concentrations, and no NGF variant tested was more potent than WT-NGF in mediating protection.

A

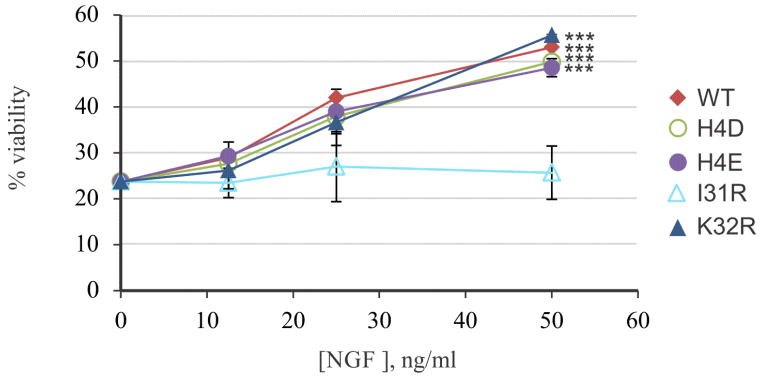

B

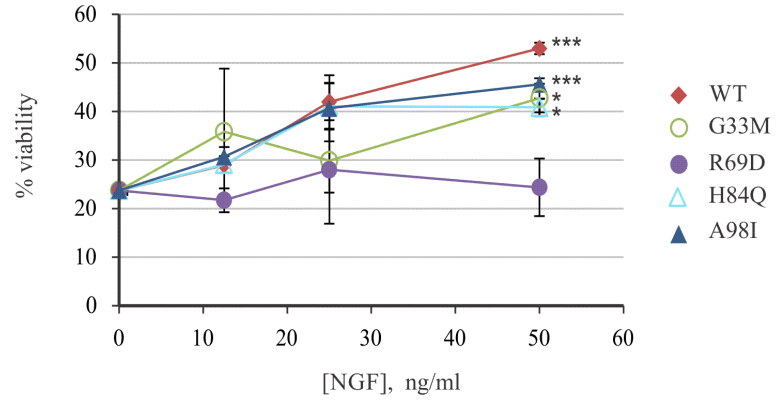

Fig. 4.2: NGF variant-mediated protection against TG-induced cell death: PC12 cells were treated with indicated concentrations of NGF-containing media followed by 0.25 µM TG treatments and cell viability was measured. In ***(A)*** the dose response of H4D, H4E, I31R and K32R variants and in ***(B)*** the dose response of G33M, R69D, H84Q and A98I variants are shown. The viability of cells treated with EV HEK293T conditioned media in the absence of TG was set

to 100%, all treatments were expressed as a percentage of that. The data are representative of 3 independent experiments +/- the Std. Dev *** $p<0.001$, ** $p<0.01$, * $p<0.05$.

4.2.3 Developing a $p75^{NTR}$ biological assay

Determination of the biological activity of NGF variants through $p75^{NTR}$ was a goal of the current study, for which a model showing NGF signaling through $p75^{NTR}$ was needed. Several approaches were previously taken to develop a NGF-$p75^{NTR}$ biological assay, using published approaches, but these were unsuccessful. Here, several other approaches were taken based on published literature involving NGF-$p75^{NTR}$ signaling.

4.2.3.1 NGF-mediated protection in breast cancer cells as a biological assay for $p75^{NTR}$ signaling

It is widely reported that NGF mediates pro-survival signaling in breast cancer cells through $p75^{NTR}$ by activating the NF-κB pathway (Descamps et al., 2001c). MDA-MB-231 cells, a model of TNBC, were used to determine the NGF-mediated protection in response to C2-ceramide induced cell death. C2-ceramide was chosen to induce cell death in an attempt to reproduce the results published by (Descamps et al., 2001c). In addition to C2-ceramide, etoposide, a genotoxic drug was also chosen. Etoposide has been used in treatment of metastatic breast cancers (Calvert et al., 1993). Cells were pre-treated with commercially available mouse NGF (mNGF) at 100 ng/ml for 24 h. Following this, the cells were treated with C2-ceramide or etoposide at the indicated concentrations. As shown in Fig. 4.3 A, loss of mitochondrial membrane potential was determined. NGF did not protect the cells from drug-induced apoptosis. A cell viability assay was performed where cells were treated with the indicated concentration of drugs in the presence or absence of two different concentrations of NGF. As 100 ng/ml NGF did not protect cells from drug induced cell death, shown in Fig. 4.3 A, a higher concentration of NGF was also included in this assay (Fig. 4.3 B). However, the higher concentration of NGF was also unable to protect cells from drug-induced cell death. As the outcome of both the assays showed no NGF-mediated protection in response to drug-induced cell death, the experiments were not performed multiple times; instead a different strategy was used to address our question.

The lack of protection with NGF may have been due to masking of any protective effect by the presence of growth factors present in the foetal bovine serum (FBS) since the experiments were performed in complete medium. In order to eliminate this possibility,

the cells were serum starved for 24 h prior to co-treatment with 100 ng/ml mNGF and 5 μM C2-ceramide for 24 h. The proportion of cells in SubG1 phase of cell cycle (Fig.4.3 C) and cells with low mitochondrial membrane potential ($\Delta\psi m$) were determined using FACS (Fig.4.3 D). In both assays NGF was seen to mediate a slight protection against C2-ceramide induced cell death; however, this was not statistically significant.

A

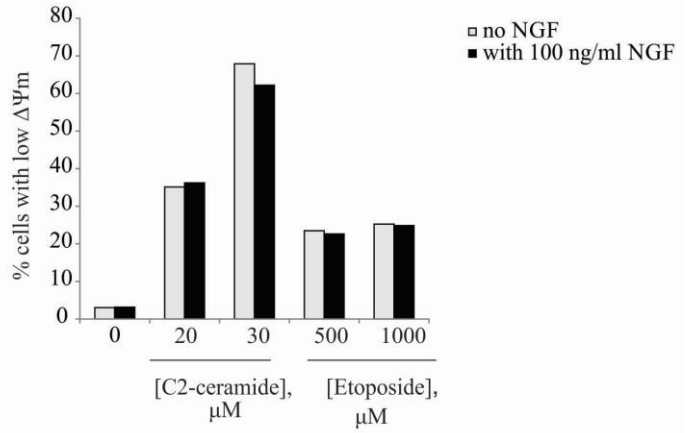
% cells with low ΔΨm
80
70
60
50
40
30
20
10
0
0
20
30
500
1000
[C2-ceramide], μM
[Etoposide], μM
no NGF
with 100 ng/ml NGF

B

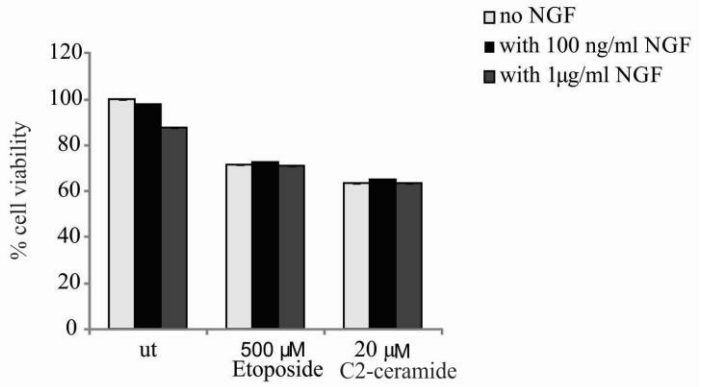
% cell viability
120
100
80
60
40
20
0
ut
500 μM Etoposide
20 μM C2-ceramide
no NGF
with 100 ng/ml NGF
with 1μg/ml NGF

C

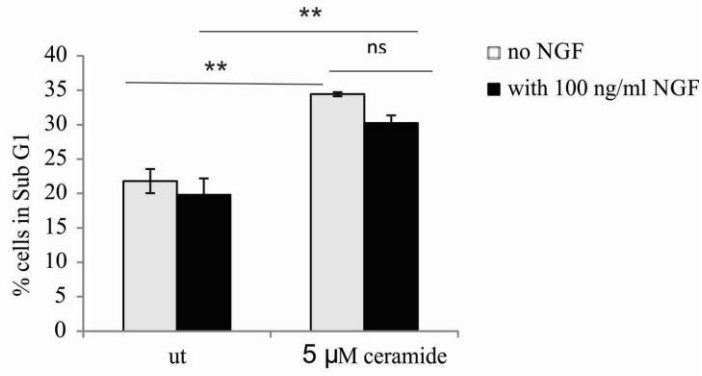
% cells in Sub G1
40
35
30
25
20
15
10
5
0
**
**
ns
ut
5 μM ceramide
no NGF
with 100 ng/ml NGF

D

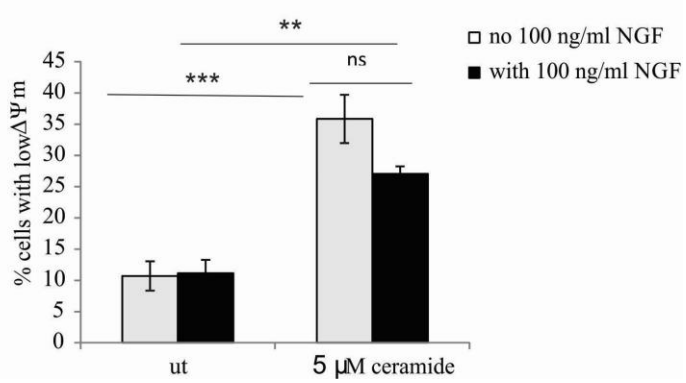
% cells with lowΔΨm
45
40
35
30
25
20
15
10
5
0
**
***
ns
ut
5 μM ceramide
no 100 ng/ml NGF
with 100 ng/ml NGF

Fig. 4.3: NGF-mediated protection in breast cancer cells: ***(A and B)*** MDA-MB-231 cells were pre-treated with 100 ng/ml or 1 µg/ml commercially available mouse NGF for 24 h followed by treatment with indicated doses of drugs for 24 h. ***(A)*** % cells with loss of mitochondrial membrane potential (Δψm) was measured ***(B)*** viability of cells was measured using MTT assay. The data are representative of n=1. ***(C and D)*** MDA-MB-231 cells were serum starved for 24 h, followed by co-treatment with 100 ng/ml NGF and/or 5 µM C2-ceramide for 24 h. ***(C)*** % of cells in sub-G1 population of cell cycle was measured ***(D)*** % cells with loss of mitochondrial membrane potential (Δψm) was measured. One way ANOVA was performed followed by Tukey's *post- hoc test* to determine statistical significance; *p<0.05.

4.2.3.2 $A\beta_{1-42}$ –induced cytotoxicity through $p75^{NTR}$ in PC12 cells

It is well documented that the binding of $A\beta_{1-42}$ mediates neuronal apoptosis through its binding to $p75^{NTR}$ (Rabizadeh et al., 1994). Recent studies have shown that in cortical neurons, in the presence of neurotrophins (NTs), $p75^{NTR}$ binds to NTs and Trk receptor to mediate pro-survival signaling through activation of AKT pathway, whereas in the absence of NTs, $p75^{NTR}$ forms a complex with death receptor 6 (DR6) and $A\beta_{1-42}$ and mediates activation of caspase-3 through oligomerization of the cytoplasmic death domain of $p75^{NTR}$ and DR6 receptors (Hu et al., 2013). The $A\beta_{1-42}$/$p75^{NTR}$- mediated pro-death signaling was determined in PC12 cells, which normally express $p75^{NTR}$ and in HEK293T engineered to overexpress $p75^{NTR}$.

Several reports in the literature suggest that AD is characterized by accumulation of several types of amyloid deposits containing the $A\beta_{1-42}$ peptides generated from the cleavage of APP (Glabe, 2008). These $A\beta_{1-42}$ form fibrillary aggregates, that are known to induce cytotoxicity in neurodegenerative diseases such as AD (Hu et al., 2013). However, there are also studies that show that the soluble $A\beta_{1-42}$ may form oligomers capable of causing about ten-fold inhibition in neuronal viability compared to the Aβ-fibrils (Stine et al., 2003). Two methods were used to re-suspend $A\beta_{1-42}$ peptide as described in Chapter 2. $A\beta_{1-42}$ peptide was re-suspended using protocol 1 to promote $A\beta_{1-42}$ oligomers and protocol 2 was used to promote $A\beta_{1-42}$ fibrils. The cytotoxicity mediated by oligomeric $A\beta_{1-42}$ (generated using Protocol 1) and fibrillary $A\beta_{1-42}$ (generated using Protocol 2) was tested on PC12 cells with the concentrations of $A\beta_{1-42}$ published in the respective protocols. As shown in Fig. 4.4.A and B, both forms of $A\beta_{1-42}$ induced a 40% reduction in PC12 cell viability, but oligomeric $A\beta_{1-42}$ was more potent than fibrillary $A\beta_{1-42}$, because the 40% reduction in cell viability was achieved at much lower concentration. This

finding was consistent with reports in the literature that oligomeric $A\beta_{1-42}$ was more potent in inhibiting neuronal cell viability. Therefore, oligomeric $A\beta_{1-42}$ was used in the subsequent experiments.

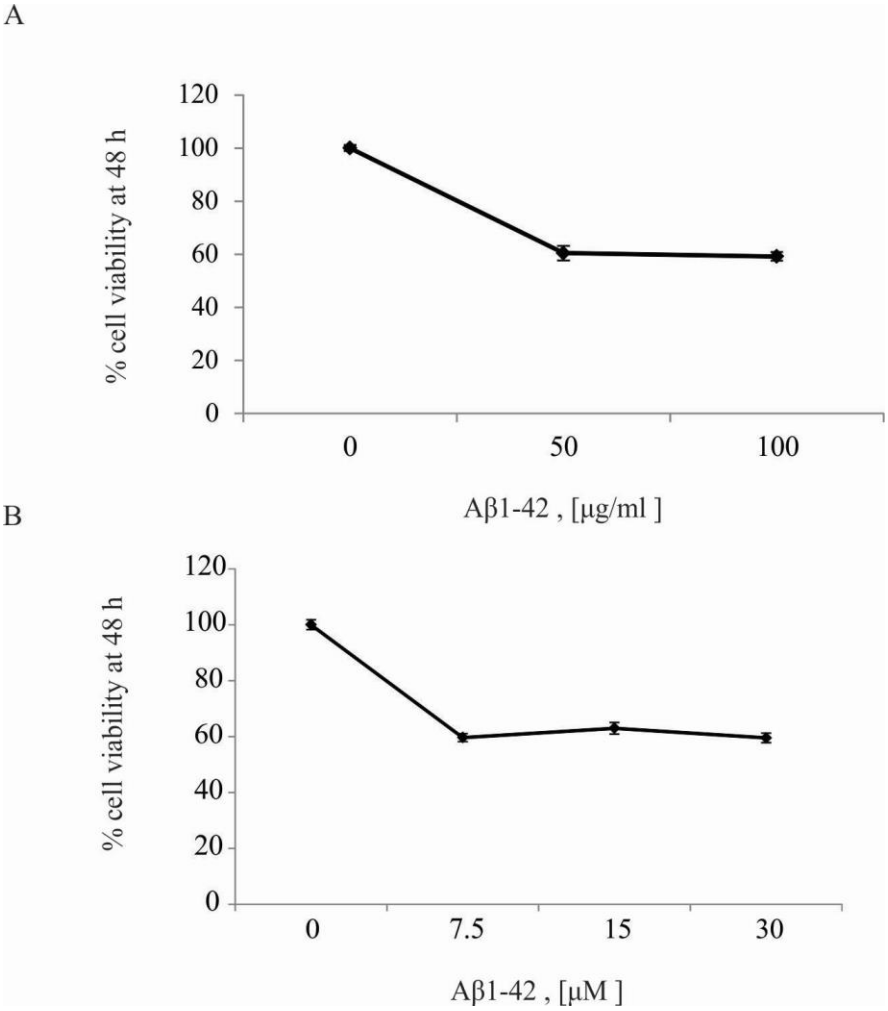

Fig. 4.4: $A\beta_{1-42}$ mediated cytotoxicity in $p75^{NTR}$ expressing cell lines: PC12 cells were treated with indicated concentrations of ***(A)*** fibrillar $A\beta_{1-42}$ or PBS (a vehicle control) ***(B)*** oligomeric $A\beta_{1-42}$ for 48 h. Cell viability was measured using MTT assay. The data are representative of n=2.

4.2.3.3 NGF-mediated protection against $A\beta_{1-42}$ -induced cytotoxicity in PC12 cells

Next, the ability of NGF to protect PC12 cells from $A\beta_{1-42}$ -induced cytotoxicity was determined. Cells were treated with $A\beta_{1-42}$ in the presence or absence of increasing concentrations of commercially available mNGF. No NGF-mediated protection was observed in response to $A\beta_{1-42}$–induced cytotoxicity in PC12 cells (Fig. 4.5 A and B B). PC12 cells have been reported to express both $p75^{NTR}$ and TrkA (Rabizadeh et al., 1994).

To confirm the the expression of $p75^{NTR}$ in PC12 cells Western blot analysis was performed (Fig.4.5.C).

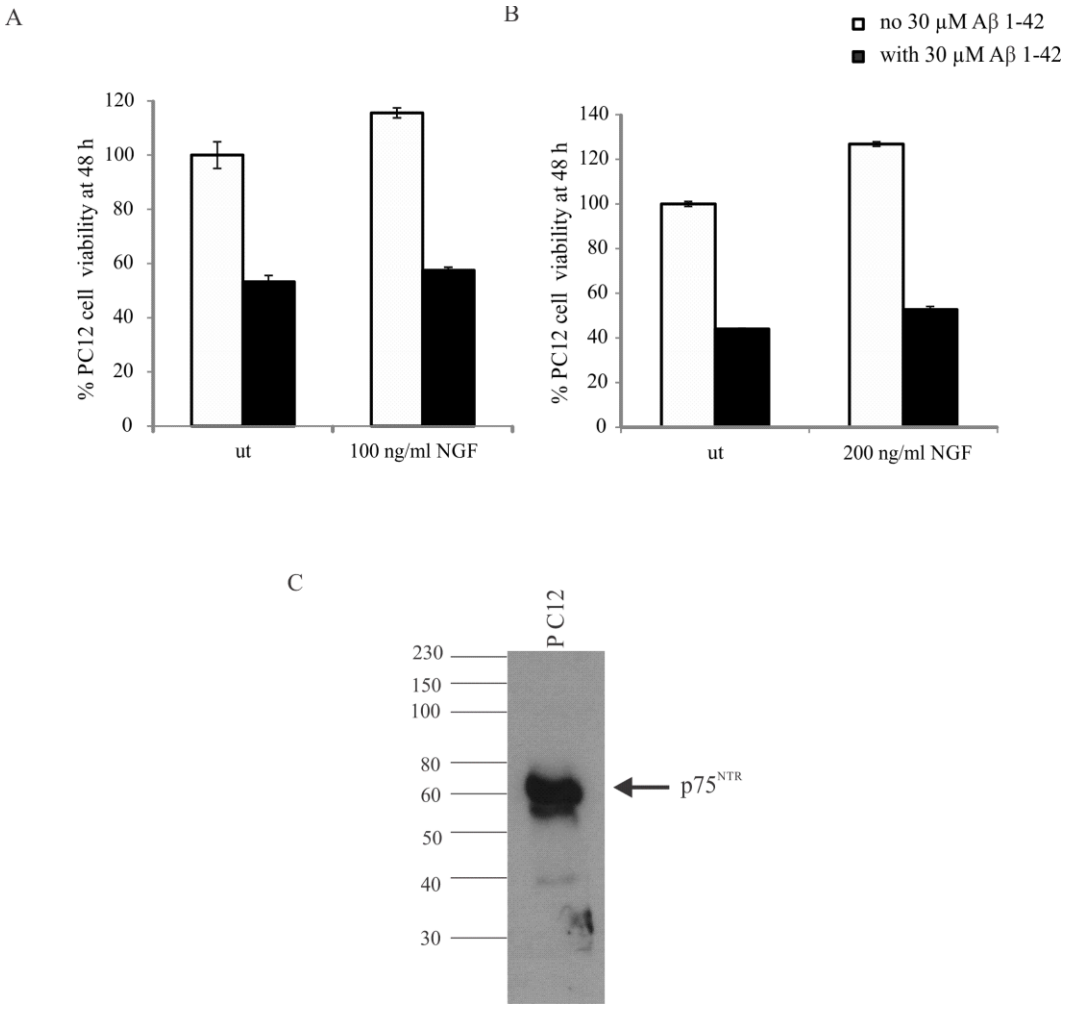

Fig. 4.5: $A\beta_{1-42}$ mediated cytotoxicity in $p75^{NTR}$ expressing cell lines: ***(A and B)*** PC12 cells were pre-treated with 100 ng/ml or 200 ng/ml mNGF in the presence or absence of 30 µM oligomeric $A\beta_{1-42}$ for 48 h and cell viability was measured by MTT assay. The data are representative of n=2. ***(C)*** A Western blot confirming the expression of $p75^{NTR}$ in PC12 cells.

4.2.3.4 $A\beta_{1-42}$ –induced cytotoxicity through $p75^{NTR}$ in HEK293T cells

It is known that the activity of NGF through $p75^{NTR}$ depends on the relative levels of the receptors (Masoudi et al., 2009, Fahnestock et al., 2004, Nykjaer et al., 2004). In approaches where cell lines expressing both $p75^{NTR}$ and TrkA were used, NGF/TrkA interactions could be obscuring any $p75^{NTR}$ response. Therefore, the use of cell lines that would express only $p75^{NTR}$ will allow studying NGF signaling through $p75^{NTR}$

independent of TrkA. HEK293T cells and HEK293T cells stably overexpressing $p75^{NTR}$ (HEKp75) were used to determine $A\beta_{1-42}$ -induced cytotoxicity. Firstly, the expression of $p75^{NTR}$ was confirmed using Western blot in HEKp75 cells and HEK293 cells did not express $p75^{NTR}$ as shown in Fig. 4.6 A. In order to test the effect of $A\beta_{1-42}$-induced cytotoxicity through $p75^{NTR}$, HEK293T and HEKp75 cells were treated with $A\beta_{1-42}$ and cell viability was assessed 48 h post-treatment using MTT assay. $A\beta_{1-42}$ induced cytotoxicity in both the cell lines, however, in contrast to the established reports, HEKp75 cells exhibited similar levels of $A\beta_{1-42}$ sensitivity to parental HEK293T cells as shown in Fig. 4.6 B.

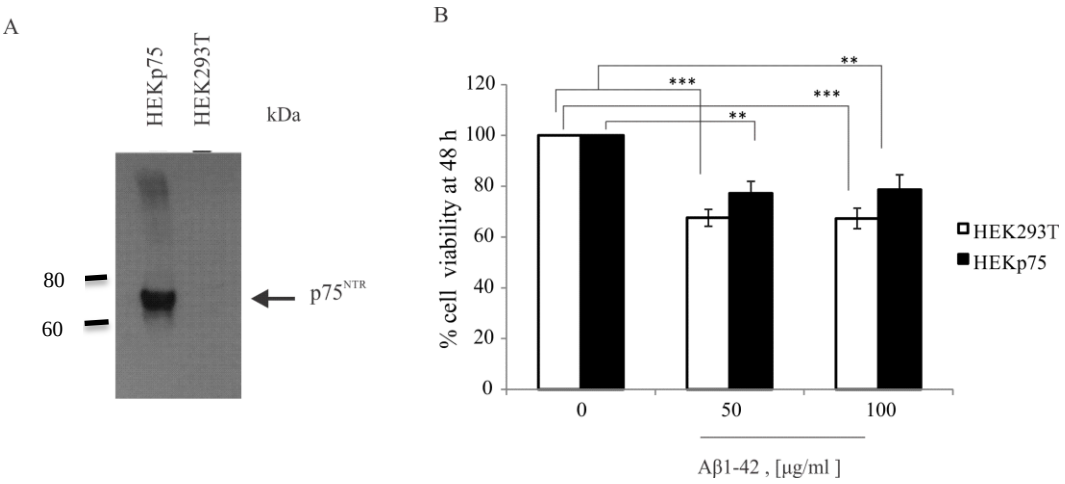

Fig. 4.6: $A\beta_{1-42}$ mediated cytotoxicity through $p75^{NTR}$ in HEK293T cells: ***(A)*** Western blotting was performed to determine the expression of $p75^{NTR}$ in HEK293 and HEKp75 cell lines. ***(B)*** HEK293T and HEKp75 cells were treated with the indicated concentrations of oligomeric $A\beta_{1-42}$ for 48 h and cell viability was measured using MTT assay. The data are representative of n=3. One way ANOVA was carried out followed by Tukey's *post-hoc* test. **p<0.01.

4.2.3.5 Effect of NGF on NF-κB activity in RN22 schwannoma cells

RN22 schwannoma cells have been reported to express only $p75^{NTR}$ and not TrkA (Gentry et al., 2000).

It has been shown that NGF activation of NF-κB through its signaling via $p75^{NTR}$ mediates an anti-apoptotic effect in RN22 schwannoma cells (Gentry et al., 2000). In RN22 schwannoma cells, NGF signaling through $p75^{NTR}$ can mediate pro-survival effects by activating NF-κB (Gentry et al., 2000). However, when NF-κB is inhibited, NGF can induce cell death through activation of JNK (Gentry et al., 2000). NGF has been shown to

cause a reduction in RN22 cell viability upon inhibition of NF-κB using peptide inhibitor, SN50 or non-degradable IκB mutants (Gentry et al., 2000). Therefore, the effect of NGF/$p75^{NTR}$ signaling upon NF-κB inhibition was determined. The protocol was adapted from Gentry *et al* because in my study, PS1145 was used as NF-κB inhibitor. RN22 cells in serum-free media were co-treated with commercially available mNGF and hβNGFc in the presence of PS1145, an inhibitor of the I-κK complex of the NF-κB (Yemelyanov et al., 2006). Cell viability was measured after 24 h. There was a 5-6% reduction in cell viability with hβNGFc. Co-treatment with PS1145 in the presence or absence of mNGF or hβNGFc reduced RN22 cell viability; however, there was only a modest reduction in cell viability (Fig. 4.7 A). A 30% reduction in cell viability was observed in the presence of NGF and inhibition of NF-κB with SN50 as shown by (Gentry et al., 2000).

Next, to determine the effect of NGF on NF-κB signaling, RN22 cells were washed in serum free media and the cells were treated with 100 ng/ml hβNGFc for 15 min. A decrease in total IκB was observed with NGF treatment compared to the untreated cells as shown in Fig. 4.7 B, indicating NGF-mediated activation of NF-κB through $p75^{NTR}$ signaling.

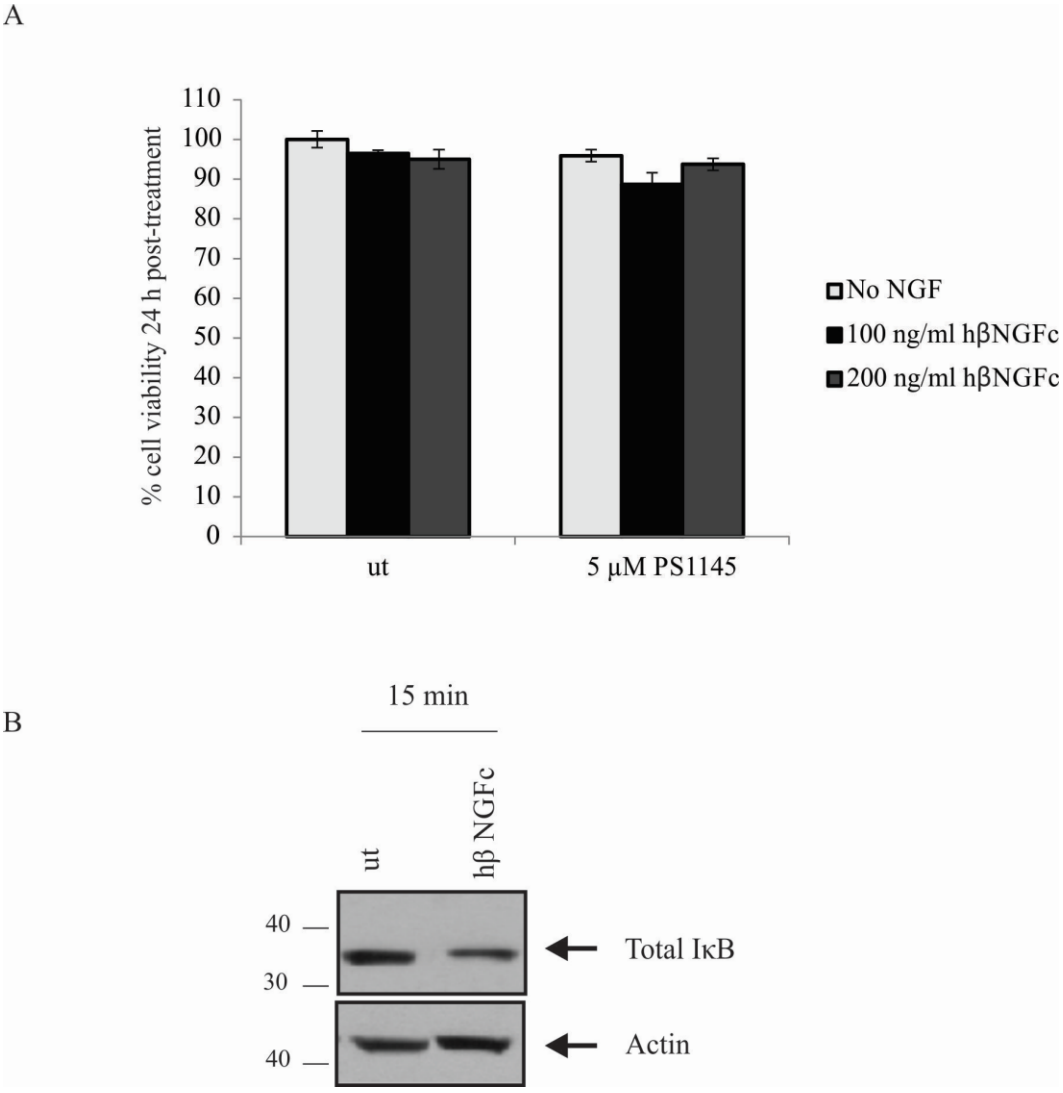

Fig. 4.7: NGF signaling through p75^{NTR} in RN22 cells: ***(A)*** RN22 cells were serum starved and co-treated with 5 µM PS1145 in the presence or absence of 100 or 200 ng/ml hβNGFc for 24 h and the cell viability was assessed using MTT assay. The data are representative of n=2 ***(B)*** RN22 cells were washed three times in serum free media and treated with or without 100 ng/ml hβNGFc for 15 min and cells were harvested. The expression of Total IκB was determined on Western blot using anti-Total IκB antibody. Actin was used as a loading control. The data are representative of n=3.

4.2.4 Biological activity of NGF variants through p75^{NTR} signaling

Out of all approaches used so far to examine NGF mediated signaling through p75^{NTR}, NGF signaling in RN22 showed the most promise. In the binding studies for NGF binding to p75^{NTR} or TrkA and in the biological activity of NGF variants through TrkA carried out previously (Carleton, PhD thesis, 2013), R69D showed no binding to either

TrkA or $p75^{NTR}$ and I31R showed no binding to TrkA but retained the binding to $p75^{NTR}$ (Table 4.1) and these data were reflected in the inability of these two variants to mediate a biological effect through TrkA signaling. Interestingly, I31R was the only one of the variants that retained binding affinity to $p75^{NTR}$ and not to TrkA. Therefore, the biological activity of I31R NGF variant through $p75^{NTR}$ signaling was tested in RN22 schwannoma cells. Two approaches were taken to determine the biological activity of the variants in RN22 cells. The effect of I31R, R69D and in-house WT-NGF on RN22 cell viability was tested at 24 h and 48 h. As the biological activity of WT-NGF and commercially available hβ NGFc were comparable from earlier studies WT-NGF was used as a positive control. As shown in Fig. 4.8 A, a reduction in cell viability was observed with WT-NGF at 48 h, however, EV, I31R and R69D showed much greater reduction in cell viability at 24 h and 48 h. This result was not able to discriminate between the NGF variants based on their activity through $p75^{NTR}$. In order to distinguish the effect of I31R from R69D and EV, RN22 cells were treated with these variants along with in-house WT-NGF as a positive control and their effect on the degradation of total IκB was determined at 15 min because at this time point hβNGFc caused degradation of total IκB (Fig. 4.8 B). The I31R NGF variant dramatically decreased the levels of total IκB. Intriguingly, there was also a drop in the level of total IκB with R69D; however the degradation of total IκB was greater in I31R treated cells. This suggested the ability of I31R to activate NF-κB through its binding to $p75^{NTR}$. These data is in agreement with the binding of I31R to $p75^{NTR}$ (Carleton, PhD thesis, 2013)

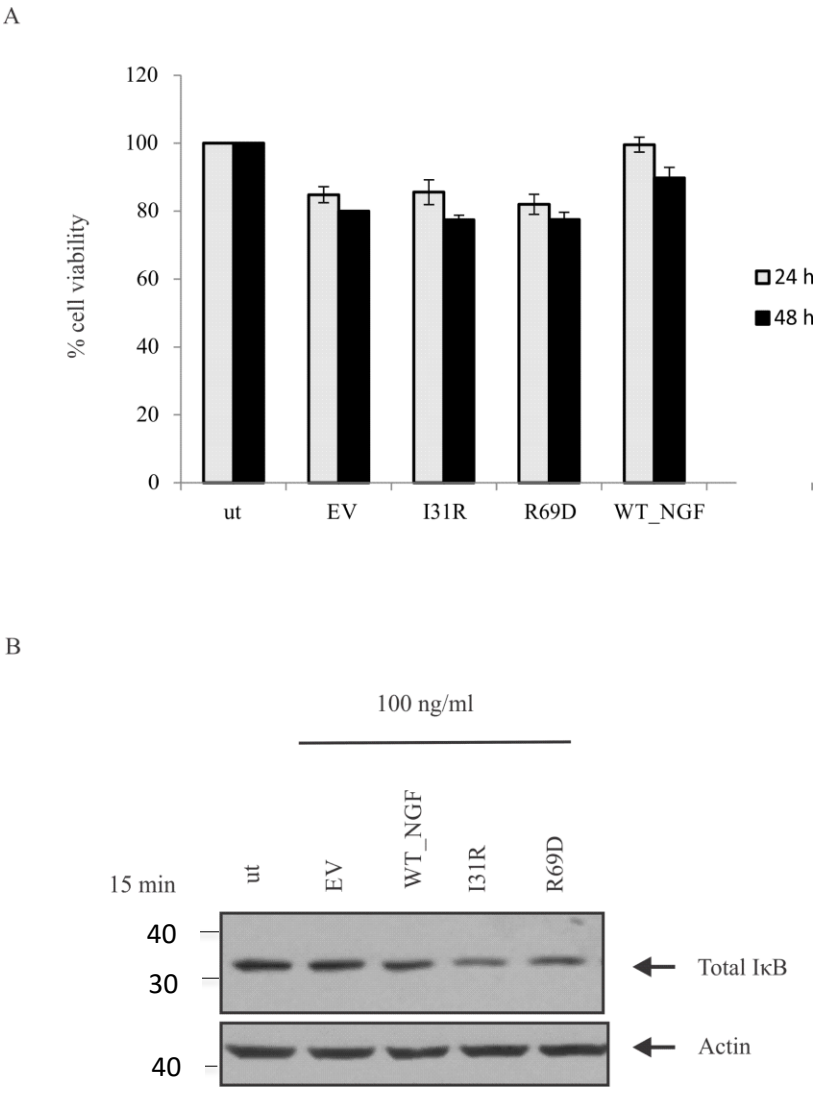

Fig. 4.8: NGF variants signaling through p75^{NTR} in RN22 cells: ***(A)*** RN22 cells were treated with 100 ng/ml NGF variants or WT-NGF for 24 h and 48 h. Cell viability was assessed using MTT assay. The data are representative of n=2. ***(B)*** RN22 cells were washed three times in serum free media and treated with or without 100 ng/ml NGF variants and WT-NGF for 15 min and cells were harvested. The levels of Total IκB was determined on Western blot using anti-Total IκB antibody. Actin was used as a loading control. The data are representative of n=3.

4.3 Discussion

An imbalance in the NGF signaling through its receptors has been shown to be involved in several diseases including Alzheimer's disease (Fahnestock et al., 2001), chronic pain (Indo et al., 1996, Minde et al., 2004), spinal cord injury (Beattie et al., 2002) and chemo-resistance of several cancers such as breast cancer (Descamps et al., 2001c), pancreatic cancer (Zhu et al., 2002). Therefore targeting NGF signaling has a high therapeutic potential. This study focused on determining the biological activity of the NGF variants designed using the FoldX protein design algorithm.

Previous studies in the lab in collaboration with van der Sloot and Serrano generated NGF variants using the FoldX protein design algorithm (Carleton, PhD thesis, 2013). This is an algorithm which determines the interactions of protein complexes and also determines the stability of the protein (Guerois et al., 2002). Based on this algorithm, single point mutations on NGF were generated that had predicted altered binding affinity to its receptors. This algorithm has been successfully used to generate mutations in TRAIL with high affinity to the death receptors (van der Sloot et al., 2006, Tur et al., 2008). The essential amino acids involved in the NGF/$p75^{NTR}$ or NGF/TrkA interaction have already been identified by introducing mutations in the NGF ligand and determining its effect on interaction with receptors (Bradshaw et al., 1994). Many of the NGF variants generated by FoldX algorithm were in the interaction sites of NGF and its receptor. It has been reported that NGF interacts with $p75^{NTR}$ through two sites, the site I interaction involves amino acid positions 23-35 (loop I) and at positions 92-100 (loop IV) of the NGF, and the site II interaction involves the amino acid positions 11-21 of NGF (He and Garcia, 2004, Wehrman et al., 2007). For example, the I31 residue on NGF has been shown to be located in loop I in the interaction site I and this has been shown to directly interact with $p75^{NTR}$ (He and Garcia, 2004) and TrkA (Wiesmann et al., 1999). The FoldX algorithm predicted this residue as an important site of NGF interaction and generated a mutation in that residue; I31R. The biological activity of I31R along with 7 other NGF variants was determined in this study.

A protocol to express in-house WT-NGF variants was developed in the lab (Carleton, PhD thesis, 2013). Based on this protocol, I expressed the eight variants chosen for the study in HEK293T cells and the secreted NGF was quantified using NGF ELISA. The expression of mature NGF was confirmed on Western blotting also. On the Western blot

for mature NGF in the media, the expression of I31R, K32R, R69D and A98I were comparable. However, when the secretion of NGF was quantified using NGF ELISA, the amounts of I31R NGF secreted was ~280 ng/ml and of R69D NGF was ~190 ng/ml and the levels of K32R and A98I was ~2000 ng/ml and ~1000 ng/ml. The discrepancies seen in the expression of I31R and R69D in Western blotting and ELISA may be attributed to the fact that the proteins detected on Western blotting are in the denatured form, whereas the ELISA detect proteins in their native form and cannot detect proteins in the denatured form.

The biological activity of these variants at TrkA confirmed the inability of these two variants to mediate signaling through TrkA. The remaining variants showed protection against TG-induced cell death in PC12 at a concentration of 50 ng/ml and at lower concentrations although some of them showed protection, this was not statistically significant. R69D was predicted to have no change in its binding to TrkA and it was predicted to have a decrease binding to $p75^{NTR}$. However, on the binding studies carried out previously in the lab, R69D showed no binding to either receptor (Carleton, PhD thesis, 2013). To determine if this was due to instability of the protein, the calculation of stability of protein was carried out using the FoldX algorithm (Guerois et al., 2002). R69D was predicted to be unstable on the FoldX algorithm (Carleton, PhD thesis, 2013). This is could be a possible reason for its inactivity and lack of binding to either receptor. Previously other variants of I31 have been generated, I31A, I31M and I31V (Bradshaw et al., 1994) and these variants exhibited altered binding affinity to TrkA. For instance, I31A and I31M exhibited a 30% TrkA binding relative to WT-NGF and I31V showed a 130% TrkA binding. This demonstrates the importance of this residue in its interaction with TrkA and the effect of substitution of amino acid on TrkA interaction (Ibanez et al., 1992). Consistent with altered binding affinity of mutated I31 residue of NGF, I31R mutant generated also showed no binding to TrkA. However, it did retain its binding to $p75^{NTR}$ (Carleton, PhD thesis, 2013). Of note is that the ability of the previously reported I31 mutations to mediate activity of $p75^{NTR}$ was not tested (Ibanez et al., 1992). The stability calculations of I31R indicated that this I31R NGF variant was stable and the lack of signaling through TrkA was indeed through its inability to bind to TrkA (Carleton, PhD thesis, 2013).

Out of the 8 variants tested, I31R was the only variant that was different from the other variants generated to have an altered receptor affinity (Carleton, PhD thesis, 2013). This

variant had no binding affinity to TrkA, yet retained its binding affinity to $p75^{NTR}$. With the intention of testing the biological activity of I31R NGF variant through $p75^{NTR}$, a $p75^{NTR}$ biological assay was aimed to be developed. Several approaches were taken in the lab previously to test pro/NGF mediated pro-death signaling and NGF mediated pro-survival signaling through $p75^{NTR}$ in various models. These experiments were unsuccessful (Carleton, PhD thesis, 2013). NGF-mediated signaling through $p75^{NTR}$ via the activation of NF-κB has been widely published in breast cancer (Descamps et al., 2001c). This model was used to test the effect of NGF signaling through $p75^{NTR}$. A breast cancer model where NGF has been shown to mediate pro-survival signaling in response to C2-ceramide induced death was used as first approach. Pre-treatment of MDA-MB-231 cells with NGF could not protect them from C2-ceramide induced cell death. It was considered that the failure of this assay may have been due to the interference of growth factors present in the FBS. FBS contains several growth promoting factors such as insulin, growth hormones and cortisol and it could be that these growth factors together mask any effect of NGF in the system. There are several reports that show the role of numerous other growth factors mediated pro-survival signaling in breast cancers such as insulin-like growth factor mediated (Nahta et al., 2003). In addition, cross-talk of growth factor signaling is at interplay in breast cancers (Lee et al., 2001a). Therefore, activation of several other growth factor- mediated receptor signaling could be taking place masking the effect of NGF. To eliminate these potential interfering factors the activity of NGF was tested under serum starved conditions. Although NGF could not significantly protect cells from C2-ceramide induced death, it did mediate a slight protection. It is shown in chapter 3 that the levels of expression of $p75^{NTR}$ are regulated in TNBC cells cultured *in vitro* and that they exhibit a differential sensitivity to apoptosis inducers depending on the levels of $p75^{NTR}$. The possible explanation for not observing significant protection could be due to low levels of expression of $p75^{NTR}$ in the cells at that time point. Whether serum starvation of cells has an effect on regulation of the expression of $p75^{NTR}$ in breast cancer cells is not known. However, NGF-mediated regulation of $p75^{NTR}$ has been reported in hippocampal astrocytes 48 h post-serum starvation (Cragnolini et al., 2009).

Next, $A\beta_{1-42}$-mediated cytotoxicity through signaling via $p75^{NTR}$ was examined. Although oligomeric $A\beta_{1-42}$ was able to induce cytotoxicity with higher potency than fibrillary $A\beta_{1-42}$, NGF was not able to protect PC12 cells from $A\beta_{1-42}$-induced cell death. The toxicity of

$A\beta_{1-42}$ is mediated through its binding to $p75^{NTR}$ in the absence of NGF, while in the presence of NGF, it potentiates neuronal survival (Rabizadeh et al., 1994). However, when NGF binds to TrkA, it enhances the toxicity of $A\beta_{1-42}$ peptide (Rabizadeh et al., 1994). Later studies in the field showed that $A\beta_{1-42}$ peptide does not bind to TrkA and it can only activate signaling pathways by binding to $p75^{NTR}$ (Yaar et al., 2002). It is possible that the presence of TrkA in PC12 cells obscures NGF signaling through $p75^{NTR}$, and this could be the reason for no observable NGF-mediated protection in PC12 cells in response to $A\beta_{1-42}$ peptide treatments.HEK293T cells engineered to overexpress $p75^{NTR}$ were used to study $p75^{NTR}$-mediated signaling. Based on the findings from the literature, one would expect increased $A\beta_{1-42}$–mediated cytotoxicity in $p75^{NTR}$ overexpressing cells (Yaar et al., 1997, Fombonne et al., 2009), but in contrast, HEKp75 cells exhibited similar levels of sensitivity to $A\beta_{1-42}$–mediated cytotoxicity when compared to parental cell lines. As HEK293T cells which lack $p75^{NTR}$ also seem to be sensitive to $A\beta_{1-42}$–treatments, the reduction in cell viability can be attributed to non- specific effect of the peptide. The experimental design can be improved by using a reverse $A\beta_{42-1}$ peptide which would serve as a negative control for the experiment and the effect of $A\beta_{1-42}$ can be determined on HEKp75 cells.

In contrast to NGF-mediated pro-survival signaling through TrkA in neuronal cells, NGF has also been shown to activate the c-Jun pathway in cultured oligodendrocytes, although that study did not show the induction of apoptosis in that system (Gentry et al., 2000). NGF has also been shown to activate NF-κB suggesting a possible role of NGF-mediated pro-survival mechanism in these cells. NGF has been shown to induce cell death through $p75^{NTR}$ signaling upon inhibition of NF-κB pathway in RN22 schwannoma cells (Gentry et al., 2000). First the effect of NGF and NGF variants on cell viability was determined. Although there was a slight reduction in the cell viability with WT-NGF and I31R, there was reduction in cell viability with R69D also which had no binding affinity to either receptor. This assay was not able to distinguish the activity of NGF variants. The same study showed NGF-induced degradation of total IκB in RN22 cells within 15 min of addition of NGF indicating the activation of NF-κB (Gentry et al., 2000). In order to distinguish the activity of I31R and R69D through $p75^{NTR}$, their effect on activation of NF-κB was determined. WT-NGF and I31R were able to activate NF-κB in RN22 cells at 15 min. This could suggest a possible activation of NF-κB through $p75^{NTR}$ in RN22 cells. This result is in agreement with the data obtained on $p75^{NTR}$ binding studies of variants,

where I31R variant retained its binding affinity to $p75^{NTR}$ (Carleton, PhD thesis, 2013). Interestingly, R69D which has been shown to have no binding affinity to either receptor has also been shown to activate NF-κB. This could suggest a $p75^{NTR}$-independent activation of NF-κB pathway. On the binding studies of $p75^{NTR}$, I31R did not show binding to $p75^{NTR}$ at an affinity greater than the WT-NGF (Carleton, PhD thesis, 2013). However, the fact that there is greater activation of NF-κB with I31R than WT-NGF on the Western blot may suggest a difference in binding kinetics of the NGF variants compared to WT-NGF and activation of NF-κB.

A previous study in the lab identified a key residue, I31, that plays an important role in NGF/TrkA interaction. This study focused mainly on determining the biological activity of the variants. However, the biological activity of I31R variant through $p75^{NTR}$ needs to be fully validated. The main limitation to the study is the lack of robust $p75^{NTR}$ biological assay to test the biological activity mediated through $p75^{NTR}$. Currently, of all approaches tested, the activation of NF-κB by NGF in RN22 cells showed the most promise. Although several reports show NGF-mediated activation of c-Jun can result in apoptosis (Yoon et al., 1998), this was observed not observed in RN22 cells where NGF was able to activate c-Jun. Reproducibility of the findings has been the major limitation in developing a p75 biological assay.

5 Chapter 5: Results

HSPB1 attenuates ER-stress induced apoptosis via degradation of the BH3-only protein, BIM

5.1 Introduction

Cellular stress can perturb the ER homeostasis resulting in ER stress. This results in the accumulation of misfolded proteins or unfolding of the newly synthesized proteins in the ER (Samali et al., 2001). HSPs are family of proteins that are induced in response to a wide range of stressors (Parsell et al., 1993). HSPB1 is one such member in the family that mediates cytoprotective effect in response to cytotoxic stimuli (Samali et al., 2001). They mediate their cytoprotective effects through various mechanisms such as acting as a molecular chaperone, by interacting with key components of the apoptotic pathway, by directly binding to caspases and inhibiting its activity, by modulating and maintaining the redox potential within cells, or by stabilizing F-actin microfilaments during stress (Concannon et al., 2003).

My work is based on a previous study in the lab which has shown that thermal preconditioning was able to protect Hela cells and PC12 cells from ER stress induced apoptosis through the regulation of BIM (Kennedy et al., 2014). The aim of my study is to delineate the role of overexpression of HSPB1 in protection against ER stress-induced apoptosis and to examine the mechanisms by which HSPB1 can regulate the expression of BIM in PC12 cells following ER stress. BIM is the BH3 only protein of the BCL-2 family that has been shown to be crucial in ER stress- mediated apoptosis across various cell types, and the depletion of which reduces ER stress-induced apoptosis (Szegezdi et al., 2008, Puthalakath et al., 2007).

It is well known that BIM can be regulated via transcriptional, post-transcriptional and post-translational mechanisms (See section 1.14.3.1.1), my contribution in this study was towards investigating the post-translational modification; i.e., phosphorylation of BIM regulated by HSPB1.

BIM gets phosphorylated by various stress kinases such as ERK1/2, JNK1/2. BIM is phosphorylated by ERK1/2 signaling at Ser-55, Ser-65 and Ser-73 (Hubner et al., 2008). Reports show that phosphorylation of BIM at Ser-65 (in rodents) and Ser-69 (in humans) by ERK1/2 was necessary and sufficient to bring about the degradation of BIM via the proteasome pathway resulting in the protection of K562 cells when compared to BIM phospho- mutant (S69G) which cannot be phosphorylated by ERK1/2 (Luciano et al., 2003). Interestingly, activated JNK1/2 can induce the expression of BIM and also phosphorylate BIM at Ser-65 resulting in the induction of apoptosis (Putcha et al., 2003).

Phosphorylation of BIM by JNK results in the expression and stabilization of the induced BIM resulting in apoptosis (Geissler et al., 2013). How phosphorylation of BIM at Ser-65 by ERK signaling can confer a pro-survival effect whereas phosphorylation at the same site by activated JNK can induce apoptosis is still not clear. It has been reported that one could phosphorylate in the absence of other but ERK has higher potential of phosphorylating BIM than JNK (Ley et al., 2005). Other sites on BIM that are phosphorylated by JNK 1/2 are Ser-100, Ser-112 and Ser-114 and the phosphorylation on these sites lead to stabilization of BIM (Geissler et al., 2013).

Interestingly, mutations in HSPB1 have been reported to be a cause of peripheral neuropathies such as Charcot-Marie-Tooth disease 2F (CMT2F) and distal hereditary motor neuropathy (dHMN) (Carra et al., 2012) . CMT is one of the most commonly inherited neurological disorders leading to a progressive degeneration of peripheral nerves (d'Ydewalle et al., 2012). HSPB1 mutants (S135F, R127W, R136W and T151L) have been reported to form intracellular aggregates, disrupting the neuro-filament network, inhibiting cell division and decreasing cell viability, ultimately leading to neuronal cell death (Evgrafov et al., 2004). No studies so far have shown the effect of mutations in HSPB1 on cellular responses to ER stress.

This study delineates the role of HSPB1 in ER stress-mediated cell death by (a) determining the effect of HSPB1 on the regulation of BIM, (b) identifying proteins interacting with HSPB1 to mediate the regulation of BIM expression and (c) determining the effect of mutations in the *HSPB1* gene on ER stress-induced cell death with focus on the regulation of BIM by HSPB1 mutants.

5.2 Results

5.2.1 HSPB1 overexpression protects cells from ER stress- induced cell death

To determine the role of HSPB1 in ER stress-induced apoptosis, stable clones of PC12 cells expressing human HSPB1 or empty vector (EV) pcDNA3.1 were generated. Overexpression of HSPB1 was confirmed by Western blot for anti-HSPB1 (Fig. 5.1 A). EV-transfected or HSPB1-overexpressing cells (EV or HSPB1 cells) were treated with the indicated doses of tunicamycin [TM], an inhibitor of N-linked glycosylation of luminal ER proteins (Zou et al., 2009) for 24 h and 48 h to induce ER stress. HSPB1 protected cells against ER stress compared to EV (Fig. 5.1 B) This was further confirmed by observing the cell morphology, where the cells were treated with 2 µg/ml TM for 48 h and stained with hematoxylin and eosin stain. EV cells treated with TM showed characteristics of apoptosis including cell shrinkage, while this was attenuated in HSPB1 cells (Fig. 5.1 C). Cell lysates were obtained from EV and HSPB1 cells treated with 2 µg/ml TM for 24 h and 48 h. Western blot for cleaved caspase-3 was carried out using anti-cleaved caspase-3 antibody. HSPB1 cells showed reduced cleavage of caspase -3 compared to the EV cells (Fig. 5.1 D). Similar experiments were carried out on parental PC12 cells transiently transfected with pcDNA3.1 or construct containing full length human HSPB1 (HSPB1). Following transfection, cells were treated with 2 µg/ml TM for 24 h. A mild reduction in the levels of cleaved caspase-3 was observed on Western blot in HSPB1 cells compared to EV cells (Fig. 5.1 E). The effect of overexpression of HSPB1 was tested in response to another ER stress inducer, thapsigargin (TG), an inhibitor of the ER Ca^{2+}-ATPase (Zou et al., 2009). HSPB1 protected PC12 cells from TG-induced cell death. As the level of protection conferred by HSPB1 in response to TG-induced cell death was more pronounced compared to the EV, the mechanism of HSPB1-mediated protection was investigated in response to TG-induced cell death (Fig. 5.1 F).

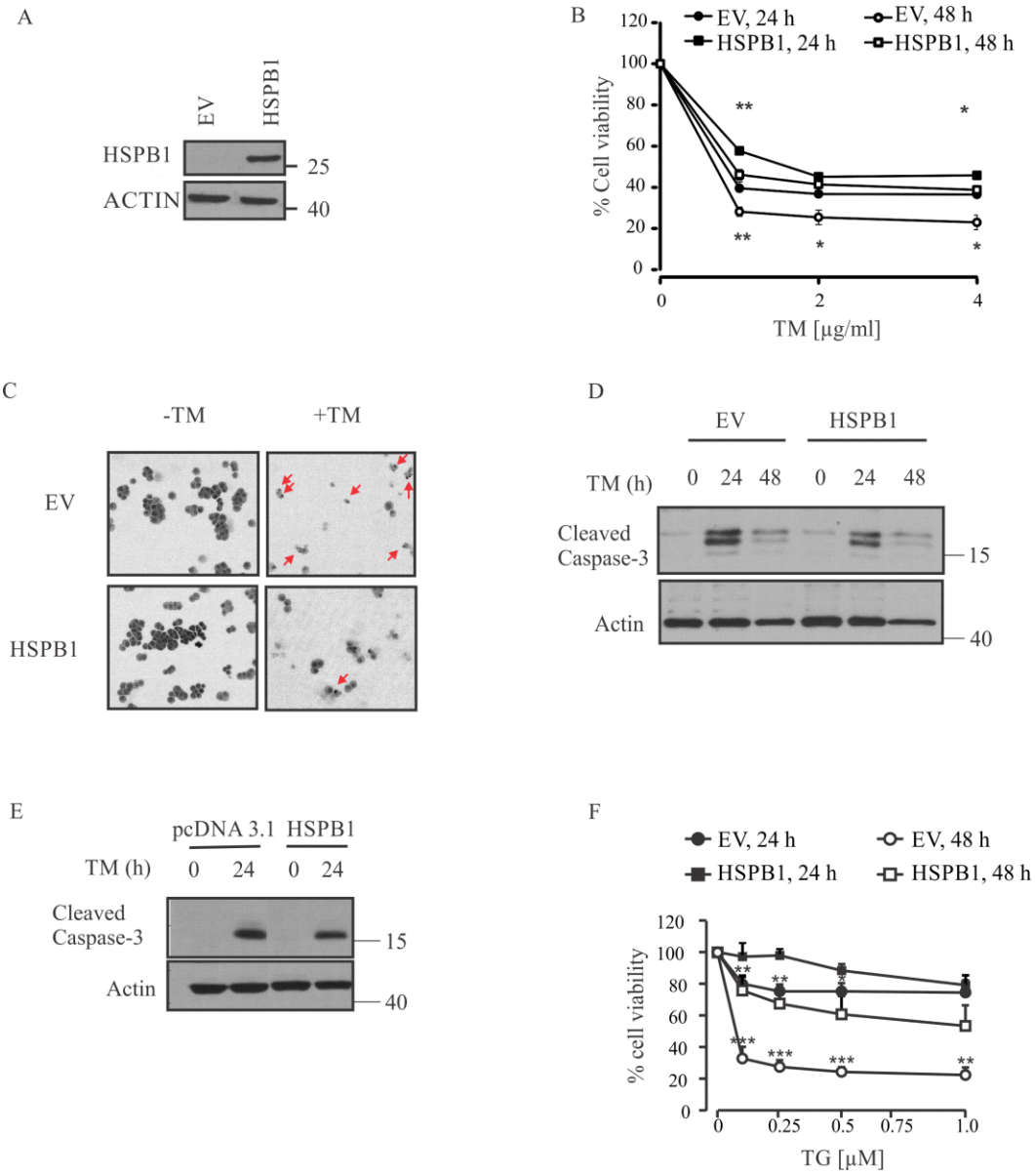

Fig. 5.1: HSPB1 overexpression protects cells from ER stress- induced apoptosis: ***(A)*** Protein extracts from empty vector (EV) and HSPB1 PC12 cells were analyzed by Western blotting using antibody against HSPB1. Actin was used as a loading control. ***(B)*** EV and HSPB1 PC12 cells were treated with 1, 2 and 4 µg/ml TM for 24 h or 48 h followed by MTT assessment of cell viability. ***(C)*** The morphology of the EV and HSPB1 cells untreated or treated with 2 µg/ml TM for 48 h was examined by haematoxylin and eosin staining. The arrows point to shrunken cells indicating apoptosis. ***(D)*** EV and HSPB1 cells were treated with 2 µg/ml TM for 24 h and 48 h. The lysates were immunoblotted for anti-cleaved caspase-3. Anti-actin was used as a loading control. ***(E)*** Parental wild type PC12 cells were transfected with pcDNA3.1 or human HSPB1 overexpressing construct and 24 h post-transfection, cells were treated with 2 µg/ml TM for 24 h.

Cell lysates were then immunoblotted for anti-cleaved caspase-3. Anti-actin was used as a loading control. ***(F)*** EV and HSPB1 PC12 cells were treated with 1, 2 and 4 µg/ml TM for 24 h or 48 h followed by MTT assessment of cell viability. Data are representative of at least three independent repeats. One-Way ANOVA followed by Tukey's post-hoc test was carried out, *p<0.05, **p<0.01.

5.2.2 HSPB1 overexpression- mediated protection is regulated through BIM_{EL}

A previous study in the lab has shown that thermal pre-conditioning was able to reduce the expression of BIM in response to ER stress (Kennedy et al., 2014). In order to address the question if HSPB1 overexpression mediated protection against ER stress induced - apoptosis through regulation of BIM, EV and HSPB1 cells were treated with 2 µg/ml TM for 24 h and 48 h. This showed a reduction in the levels of BIM in HSPB1 cells (Fig. 5.2 A). Similar results were obtained when PC12 cells were transiently transfected with pcDNA3.1 or HSPB1 and treated with 2 µg/ml TM for 24 h (Fig. 5.2 B). In order to determine if the HSPB1-mediated protection in response to ER stress was dependent on BIM, experiments with knockdown of *BIM* were designed. Fig. 5.2 C shows knockdown of *BIM* using siRNA at 24 h and 48 h in EV and HSPB1 cells. EV and HSPB1 cells were transfected with 20 nM BIM siRNA or non-coding siRNA (ctr) and treated with TG for 48 h. HSPB1 cells transfected with non-coding siRNA and treated with TG for 24 h showed reduced induction of BIM compared to the EV cells transfected and treated at that time point (Fig. 5.2 C). Assessment of caspase-3/7 activity showed that HSPB1 cells transfected with non-coding siRNA were more protected than EV cells transfected with non-coding siRNA. BIM siRNA treatment significantly reduced TG-induced caspase-3/7 activity demonstrating the functionality of the knockdown and underpinning the critical role of BIM in ER stress-induced apoptosis. No significant difference in caspase-3/7 activity was observed between TG-treated EV and HSPB1 cells in the presence of BIM siRNA, indicating that the mechanism of HSPB1-mediated protection in HSPB1 cells was indeed regulated through the downregulation of BIM (Fig. 5.2 D).

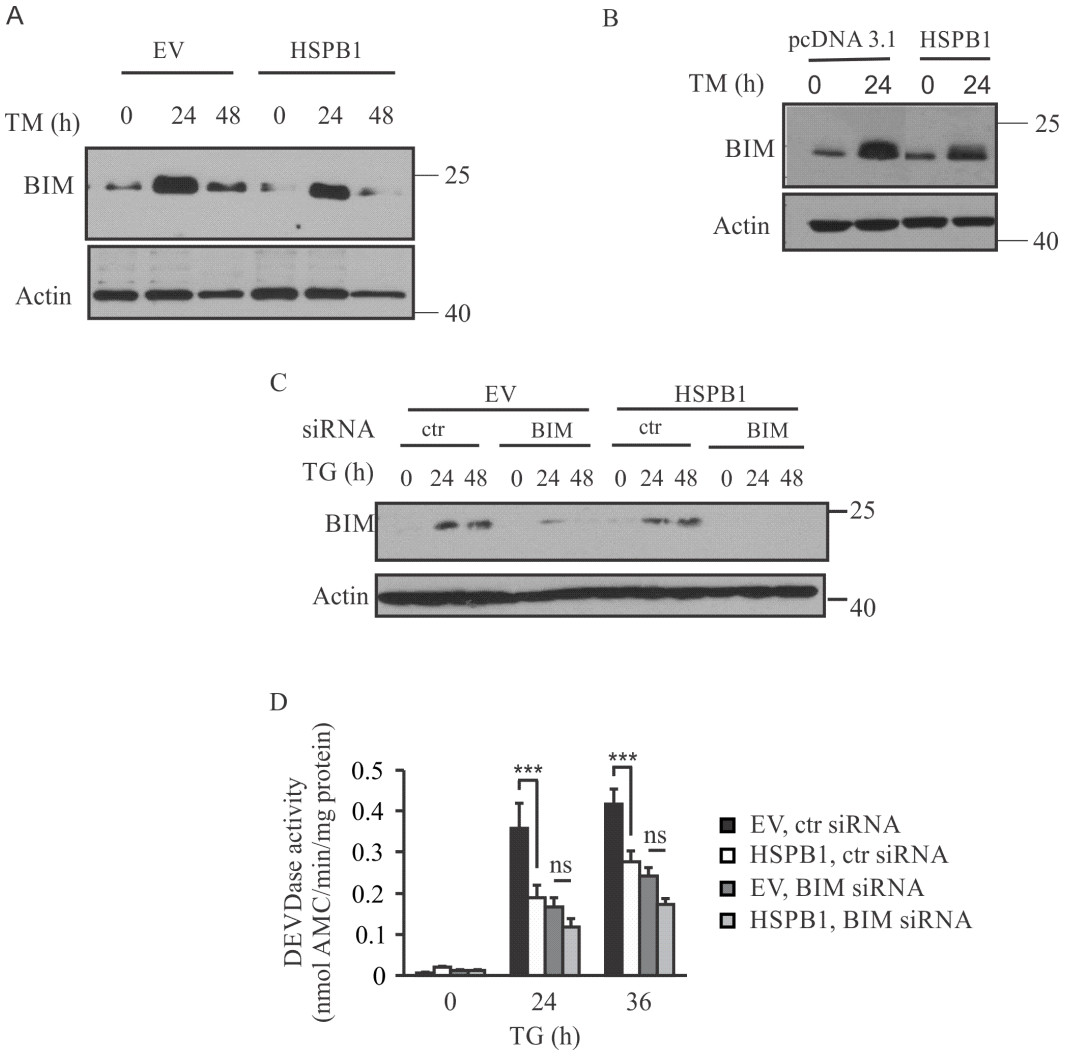

Fig. 5.2: HSPB1 overexpression- protection is dependent on BIM: ***(A)*** EV and HSPB1 cells were treated with 2 µg/ml TM for 24 h and 48 h. The lysates were immunoblotted for BIM. Anti-actin was used as a loading control. ***(B)*** Parental wild type PC12 cells were transfected with pcDNA3.1 or human HSPB1 overexpressing construct and 24 h post-transfection, cells were treated with 2 µg/ml TM for 24 h. Cell lysates were then immunoblotted for anti-BIM. Anti-actin was used as a loading control. ***(C)*** EV and HSPB1 cells were treated with 20 nM BIM siRNA or a non-targeting control siRNA (ctr). 24 h later cells were treated with a DMSO vehicle control or with 0.25 µM TG for 24 h or 48 h. To test for efficiency of BIM knockdown, cells were harvested and protein was analyzed by Western blotting using a specific anti-BIM antibody. Actin was used as a loading control. ***(D)*** EV and HSPB1 cells treated with either non-targeting control (ctr) siRNA or BIM siRNA following treatment with 0.25 µM TG for 24 or 36 h. Caspase activity was analyzed by DEVD-MCA hydrolysis. Data are representative of at least three independent repeats. Values shown are representative of at least three independent repeats. Two-Way ANOVA followed by Bonferroni's post-hoc test was carried out. * P <0.05, ** P<0.01, *** P< 0.001.

5.2.3 Post-translational regulation of BIM is dependent on MEK-ERK signaling in HSPB1 cells

Previous studies in the lab have ruled out the transcriptional and post-transcriptional regulation of BIM in HSPB1-mediated cytoprotection in response to ER stress-induced cell death. In addition to these findings, parallel studies in the lab also observed that the reduced induction of BIM in HSPB1 cells was due to the targeting of BIM for proteasomal degradation (Kennedy, PhD thesis 2013). Several reports in the literature show that BIM can be phosphorylated at Ser-65 by phospho-ERK 1/2, which then targets BIM for proteasomal degradation (Luciano et al., 2003). Hence, the levels of activated ERK 1/2 were investigated in HSPB1 cells. The basal levels of phospho-ERK 1/2 were higher in HSPB1 cell compared to EV cells as shown in Fig. 5.3 A. This could suggest that phospho-ERK 1/2 is stabilized in HSPB1 cells. The levels of BIM phosphorylated at Ser-65 after TG treatment was also determined; the levels of phosphorylated BIM at Ser-65 in HSPB1 cells were at comparable levels to EV cells, however, when taking into account the much reduced induction of total BIM in HSPB1 cells, the ratio of phosphorylated BIM (Ser-65) was much higher in HSPB1 cells (Fig. 5.3 A).

Next, the importance of MEK-ERK signaling in HSPB1-mediated protection in response to ER stress-induced cell death was determined. Upon chemical inhibition of MEK signaling using UO126, a highly selective inhibitor of both MEK1 and MEK2, or using genetic knockdown of MEK by MEK siRNA, the importance of MEK signaling was assessed. As shown in Fig. 5.3.A and C, UO126 or MEK siRNA were able to efficiently inhibit the activation of ERK 1/2, and this inhibition of MEK signaling was associated with an accumulation of total BIM in the HSPB1 cells upon TG treatments at 48 h, corresponding to reduced phosphorylation of BIM at Ser-65 at that time point. Interestingly, the levels of HSPB1 expression in HSPB1 cells were reduced under MEK inhibitory conditions (Fig. 5.3 C). Inhibition of MEK signaling was able to reverse the protection conferred by HSPB1 under active MEK-ERK signaling conditions in response to ER stress-induced apoptosis. As shown in Fig. 5.3 C and D, HSPB1 cells showed reduced caspase-3/7 activity compared to EV cells in response to TG-induced ER stress, whereas, under MEK inhibitory conditions, there was no difference in the caspase-3/7 activity between EV and HSPB1 cells treated with TG. Taking all these data together, it is evident that inhibiting MEK-ERK signaling was sufficient to reverse the protective

effect of HSPB1 in response to ER stress. The data confirm that HSPB1 mediated protection is highly dependent on ERK signaling.

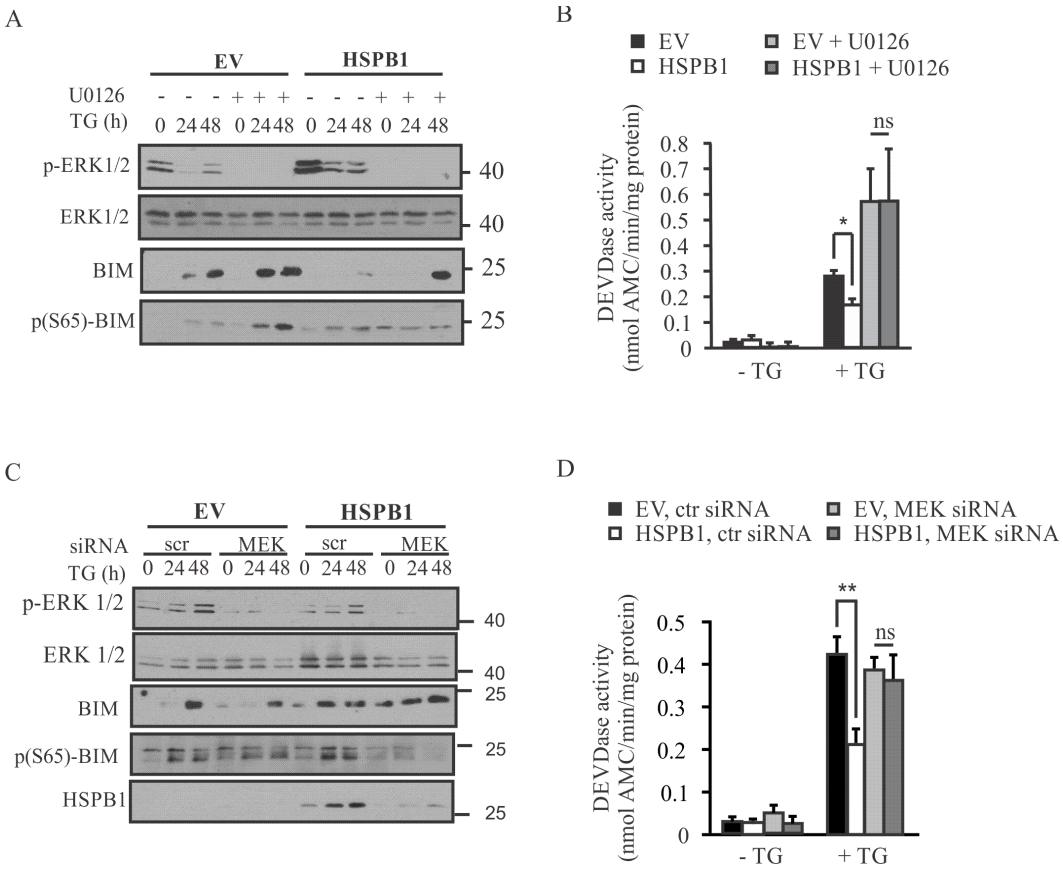

Fig. 5.3: Phosphorylation of BIM at Ser-65 is dependent on the MEK-ERK pathway: EV and HSPB1 PC12 cells were pre-treated with 10 µM UO126 or DMSO control for 2 h followed by treatment with TG for the indicated times. ***(A)*** Western blot analysis to determine the expression of phospho-ERK 1/2, total ERK 1/2 , total-BIM, phosphorylated BIM (Ser- 65). Actin was used as a loading control***.*** ***(B)*** DEVDase assay to determine the activity of caspase-3/7 following treatment with TG and/or UO126. ***(C)*** EV and HSPB1 cells were treated with 40 nM MEK siRNA or a non-targeting control siRNA (ctr). 24 h later cells were treated with a DMSO vehicle control or with TG for 24 h or 48 h. To test for efficiency of MEK knockdown cells were harvested and protein was analyzed by Western blotting using a specific anti- phospho- ERK 1/2 antibody. Expression of phospho-ERK 1/2, total ERK 1/2, total-BIM, phosphorylated BIM (Ser-65) and anti-HSPB1 were determined on Western blot analysis. Actin was used as a loading control***.*** ***(D)*** EV and HSPB1 cells treated with either non-targeting control (ctr) siRNA or MEK siRNA following treatment with TG for 36 h. Caspase activity was analyzed by DEVD-MCA hydrolysis. Data are representative of at least three independent repeats. Values shown are

representative of at least three independent repeats. Two-Way ANOVA followed by Bonferroni's post-hoc test was carried out, * P <0.05, ** P<0.01.

5.2.4 HSPB1 interacts with phospho-ERK 1/2 and BIM

HSPB1 has been described as a E4 factor, that acts as a scaffolding molecule which aids in the phosphorylation and subsequent ubiquitination of target proteins (Lanneau et al., 2010). It was hypothesized that HSPB1 acts as a scaffolding molecule that stabilizes phospho-ERK1/2 and brings it in close proximity to BIM and thus facilitates phosphorylation of BIM by active ERK 1/2 signaling. This phosphorylated BIM is then targeted for proteasomal degradation. To address the hypothesis, we immunoprecipitated HSPB1 from HSPB1 cells subjected to ER stress (TG) and probed for BIM and phospho-ERK 1/2. An interaction between HSPB1 and phospho-ERK 1/2 and BIM under both basal and TG-treated conditions was observed (Fig. 5.4 A). Similarly, a reciprocal immuno-precipitation (IP) with phospho-ERK 1/2 was also performed and was found that phospho-ERK 1/2 interacts with HSPB1 and BIM under both basal and treated conditions. However, the interaction of HSPB1 on reciprocal IP with phospho-ERK 1/2 was not as high under basal conditions as observed in immuno-precipitation of HSPB1.Together these data show an interaction between HSPB1, BIM and phospho-ERK 1/2 (Fig. 5.4 B).

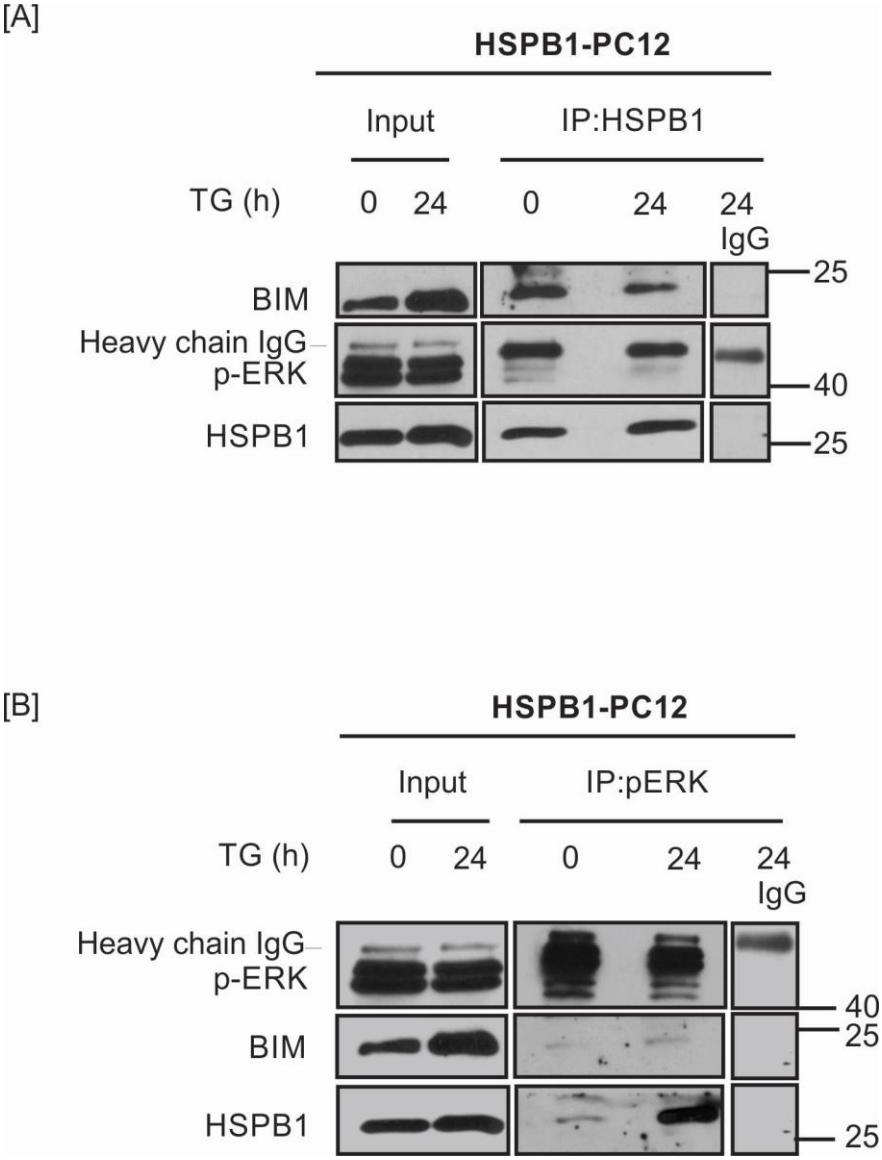

Fig. 5.4: HSPB1 interacts with phospho-ERK 1/2 and BIM: ***(A)*** HSPB1 PC12 cells were treated with 0.25 µM TG for the indicated time. Immuno-precipitation (IP) of HSPB1 with 2 µg/ml anti-HSPB1 antibody was carried out and immunoblotted for expression of BIM and phospho-ERK 1/2. ***(B)*** Immuno-precipitation was carried out with 2 µg/ml anti-phospho- ERK 1/2 antibody followed by immunoblotting for expression of BIM and HSPB1. The three lanes on (A) and (B) indicate, Input lanes which are cell lysates obtained before IP, the IP lanes and IgG was used as a negative control for the IP.

5.2.5 Inhibition of phosphorylation of HSPB1 decreased cell viability of HSPB1 cells in response to ER stress

HSPB1 is phosphorylated in response to ER stress (Ito et al., 2005). Phosphorylation of HSPB1 results in dissociation of large HSPB1 oligomers into smaller tetramers (Lavoie et al., 1995). Phosphorylation of HSPB1 mediates cytoprotection in response to stress such as oxidative stress (Huot et al., 1996). HSPB1 is phosphorylated by various stress kinases including MAPKAPK2/3 (Xu et al., 2006), PKC (Shin et al., 2005) , cGMP-dependent protein kinase (Butt et al., 2001). The effect of inhibiting the phosphorylation of HSPB1 in response to ER stress-induced cell death was investigated. To test this, KRIBB3, an inhibitor that directly binds to HSPB1 and inhibits its phosphorylation at Ser 78 was used (Shin et al., 2005). Cells were pre-treated for 2 h with 5 μM KRIBB3 followed by treatment with TG for 24 h. KRIBB3 did not have a significant effect on viability of EV cells undergoing ER stress which suggests a lack of off-target effects of the inhibitor. Inhibition of phosphorylation of HSPB1 in HSPB1 cells decreased protection significantly at 24 h (Fig. 5.5 A). The efficiency of inhibition by KRIBB3 of phosphorylation of HSPB1 at Ser-78 was confirmed as shown in Fig 5.5 B. As shown in Fig. 5.5 B, phospho-HSPB1 is induced in response to ER stress and in the presence of KRIBB3, a reduction in phospho-HSPB1 was observed at both 12 h and 24 h. The data so far suggest that HSPB1 could be protecting cells from ER stress-induced cell death through activation of ERK signaling. HSPB1 has been reported to undergo ERK-dependent phosphorylation (Robitaille et al., 2010). In addition, it was noted that HSPB1 cells have higher levels of ERK (Fig. 5.3 A) that could positively modulate HSPB1. Therefore, the effect of inhibition of phosphorylation of HSPB1 on phospho-ERK 1/2 levels was investigated. There was a reduction in phospho-ERK 1/2 levels in HSPB1 cells treated with KRIBB3 and TG at 0, 12 and 24 h. There was also a drop in phospho-ERK 1/2 levels in the presence of KRIBB3 alone in EV cells (Fig. 5.5 B). Together these data show that inhibition of HSPB1 phosphorylation can reverse the protective effect of phosphorylated HSPB1 in HSPB1 cells.

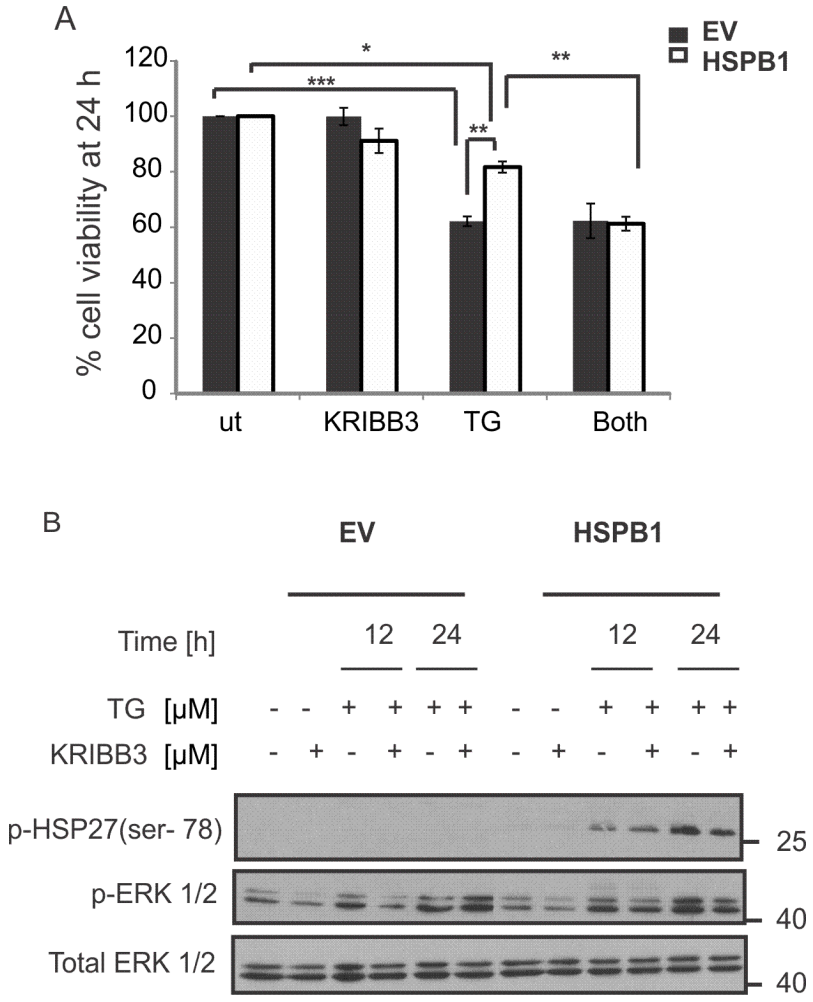

Fig. 5.5: Inhibition of phosphorylation of HSPB1 decreased cell viability of HSPB1 cells in response to ER stress: EV and HSPB1 PC12 cells were pre-treated with 5 μM KRIBB3 for 2 h followed by treatment with TG for 24 h and 48 h. ***(A)*** The cell viability was measured using MTT assay. Data are representative of three independent repeats. Values shown are representative of at least three independent repeats One-Way ANOVA was carried out with Tukey's multiple comparison post-hoc test *p<0.05, **p<0.01, ***p<0.001. ***(B)*** Western blotting was carried out to determine the levels of phospho-HSPB1 (Ser -78), phospho-ERK 1/2 and total ERK 1/2 using anti-phospho-HSPB1 (Ser -78), anti-phospho-ERK 1/2 and anti- total ERK 1/2 antibodies. These data are from a single experiment. This is an assembled gel with both parts of the blot arising from the same gel.

5.2.6 Cells expressing mutant variants of HSPB1 are not protected against ER stress (TG) induced apoptosis and express high levels of BIM

Mutations in the α-crystallin domain region of HSPB1 (S135F, R127W, R136W, T151L) has been reported to be associated with CMT and distal HMN (Evgrafov et al., 2004). Given the protection conferred by HSPB1 overexpression against ER stress-induced cell death, the effect of mutant HSPB1 overexpression involved in CMT and distal HMN phenotype on the cellular response to ER stress was investigated. To test this, stable cell lines overexpressing EV (pcDNA3.1) control plasmid, wild type HSPB1 (WT HSPB1), and HSPB1 mutants (S135F, R127W, R136W and T151L) in PC12 cell lines were generated. Cell lines were validated for expression of HSPB1 through immunoblot for human anti-HSPB1. EV showed no expression of HSPB1, while the levels of expression HSPB1 was similar in WT HSPB1 and in cell lines expressing HSPB1 mutants (Fig. 5.6 A).

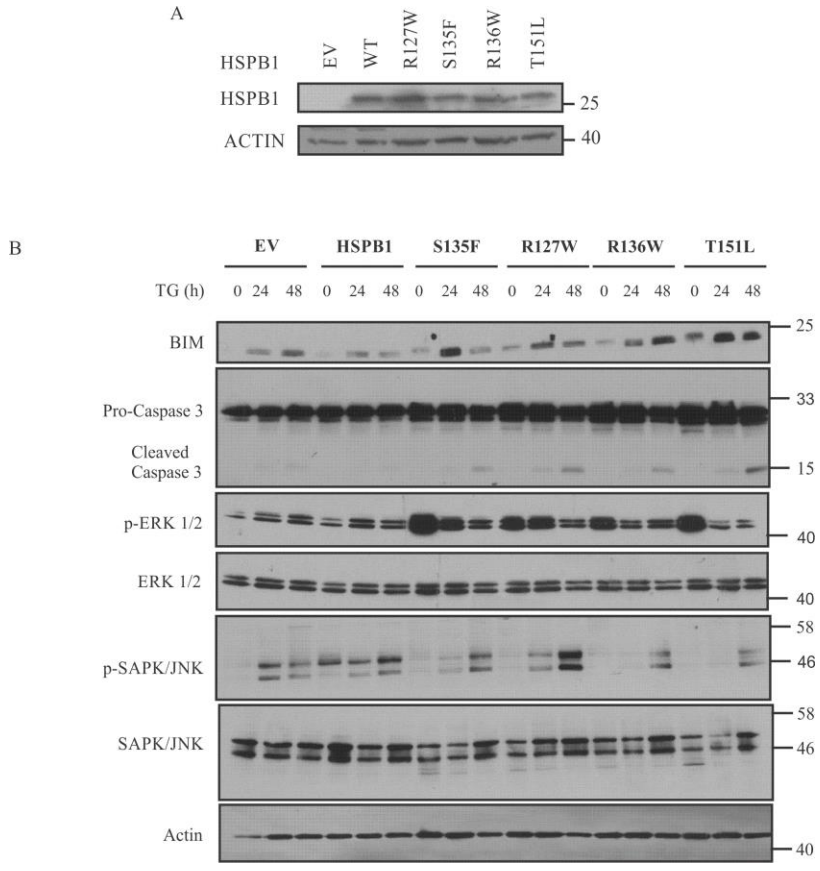

Fig. 5.6: Cells expressing mutant variants of HSPB1 fail to protect against ER stress induced apoptosis and express high levels of BIM: Parental PC12 cells were stably transfected with

pcDNA3.1 (EV) or WT HSPB1 or mutant HSPB1 constructs (R127W, S135F, R136W and T151L). ***(A)*** Western blotting was carried out to determine the expression of HSPB1 across stably transfected PC12 cell lines using anti-HSPB1 antibody. Actin was used as a loading control. EV, WT HSPB1 and HSPB1 mutants (S135F, R127W, R136W and T151L) were treated with TG for 24 h and 48 h and harvested for ***(B)*** Western blotting to determine the expression of BIM, cleaved caspase-3, phospho-ERK 1/2, total-ERK 1/2, phospho-JNK 1/2 and total JNK 1/2 using respective antibodies and actin was used as a loading control. The blots showing phospho-ERK 1/2 , total ERK 1/2, phospho-JNK 1/2 and total JNK 1/2 are representative of n=1.

Since HSPB1 overexpressing cells mediate a cytoprotective effect by regulating the expression of BIM, next, the expression levels of BIM in the HSPB1 mutant cell lines in response to ER stress was investigated. The induction of BIM in response to ER stress in all the four HSPB1 mutant cell lines was much higher compared to WT HSPB1 cell line (Fig. 5.6.B). This could suggest that BIM is not targeted for degradation in HSPB1 mutant cells. The levels of cleaved caspase-3 in the mutant HSPB1 cells were higher than the level of cleaved caspase-3 observed in WT HSPB1 cell line, indicating that the HSPB1 mutants cannot protect cells from ER stress-induced cell death (Fig. 5.6 B). From the data shown thus far on WT HSPB1 cells, activated ERK 1/2 regulates phosphorylation of BIM which gets targeted for proteasomal degradation. Therefore, the levels of phospho-ERK 1/2 across the HSPB1 mutant cell lines were investigated. The levels of expression of phospho-ERK 1/2 were very high in the untreated mutants followed by a large reduction in their levels upon treatment with TG. Intriguingly, the levels of phospho-ERK 1/2 were not high in WT HSPB1 cells compared to EV cells as shown previously in Fig. 5.3.A. Several factors such as age of cells in culture, or temperature changes in the incubator lead to fluctuation in the levels of phospho-ERK 1/2. The phospho-ERK 1/2 blot showed in Fig 5.6 is one such example. More repeats are needed to conclude the effect of ER stress on the expression and regulation of activated ERK 1/2 in HSPB1 mutant cell lines. We also investigated the levels of phospho-JNK 1/2 across these cell lines in response to ER stress. Only R127W showed increased phospho-JNK 1/2 in response to ER stress at 48 h while the levels of phospho-JNK 1/2 in all other HSPB1 mutant cell lines were comparable (Fig. 5.6 B). Taking together all the data on HSPB1 mutant cell lines, mutations in HSPB1 result in the inability of HSPB1 to protect cells in response to ER stress induced cell death.

5.2.7 Cells expressing mutant variants of HSPB1 are not protected against ER stress (TM) induced apoptosis and express high levels of BIM

The expression profile of BIM and cleaved capase-3 after TM–induced ER stress was determined across HSPB1 mutants. An increase in the expression of BIM was observed in S135F and R136W compared to the WT HSPB1, whereas R127W did not show an increase. Similarly, S135F and R136W expressed high levels of cleaved caspase-3 compared to WT HSPB1, whereas R127W did not show increase in cleaved caspase-3 activity. Although there is a difference in the protein expression pattern in R127W HSPB1 mutant, data on S135F and R136W suggest the inability of HSPB1 to protect cells in response to ER stress and their inability to target BIM for proteasomal degradation (Fig. 5.7 A).

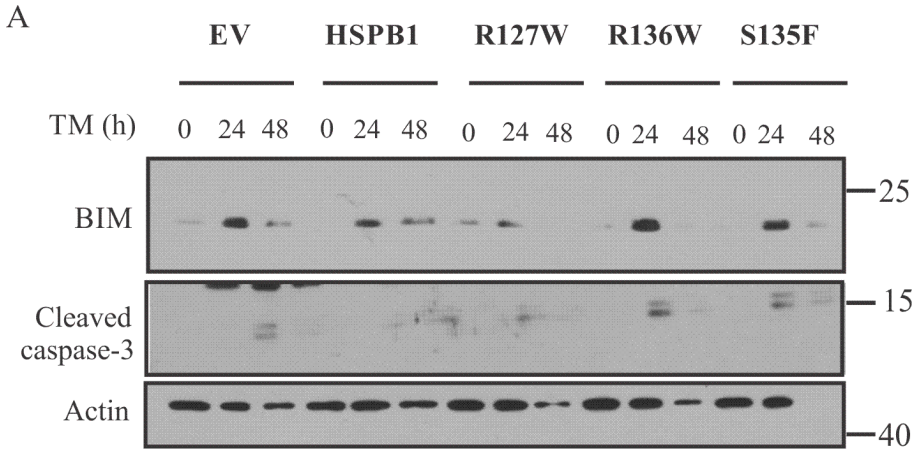

Fig. 5.7*:* Cells expressing mutant variants of HSPB1 fail to protect against TM-induced apoptosis and express high levels of BIM: EV, WT HSPB1 and HSPB1 mutants (S135F, R127W, R136W and T151L) were treated with 2 µg/ml TM for 24 h and 48 h. *(A)* Cells lysates were immunoblotted for BIM, and cleaved caspase-3 using anti-BIM and anti-cleaved caspase-3 antibodies. Actin was used as a loading control.

5.3 Discussion

This chapter highlights the importance and role of HSPB1 in mediating protection against ER stress-induced cell death through regulation of the BH3-only protein, BIM. This study demonstrates that ERK 1/2 was required for HSPB1-mediated cytoprotective effect in response to ER stress through phosphorylation of BIM, thereby targeting BIM for proteasomal degradation. This study also shows that cells expressing HSPB1 mutants do not protect against ER stress-induced cell death and fail to regulate BIM.

The functional relevance of HSPB1 and its role in ER-stress induced cell death has not yet been delineated. It is well known that ER stress-mediated cell death depends on the intrinsic apoptotic pathway, which is regulated by the BCL-2 family of proteins (Hetz, 2012). Out of all the BH3 only proteins, BIM has been reported to be a potent pro-apoptotic protein that is induced in response to ER stress (Puthalakath et al., 2007, Szegezdi et al., 2008). HSPB1 has been shown to mediate a cytoprotective effect through various mechanisms which include inhibition at several stages of the apoptotic pathway (Concannon et al., 2003). The cytoprotective effect has been shown to be downstream of mitochondria through direct binding of HSPB1 to cytochrome c (Bruey et al., 2000) or through its direct binding to the effector caspase-3 (Pandey et al., 2000). Parallel studies in the lab shows that HSPB1 can act upstream of MOMP by preventing the release of cytochrome c to protect cells against activation of caspase cascade in response to various ER stressors. Several studies have reported that HSPB1 could mediate cytoprotective effect upstream of MOMP. Reports have shown that HSPB1 in response to agents that damage the cytoskeleton of the mitochondria negatively regulates the re-distribution of BID to the mitochondria, thereby preventing the release of cytochrome c and subsequent activation of the intrinsic apoptotic pathway (Paul et al., 2002). The ability of HSPB1 to bind to F-actin and stabilize the cytoskeleton has been attributed to the cytoprotection. The stabilization of the cytoskeleton could only partially explain the protection conferred by HSPB1 upstream of mitochondria because in the presence of F-actin stabilizer, Phalloidin, HSPB1 was still able to enhance cell survival (Paul et al., 2002). This indicates a possibility for other mechanisms that might be involved in HSPB1- mediated protection upstream of mitochondria. As mentioned earlier that ER stress-induced cell death involves the intrinsic apoptotic pathway, the work focused on investigating the members of the BCL-2 family.

BIM, a pro-apoptotic member of the BCL-2 family has been reported to be induced in response to ER stress (Szegezdi et al., 2008, Puthalakath et al., 2007). Recently, it has been shown that thermal pre-conditioning of HeLa and PC12 cells protected them against ER stress-induced cell death by regulating the expression of BIM (Kennedy et al., 2014). It is well known that BIM can be regulated at multiple levels, i.e., transcriptional, post-transcriptional and post-translational regulation. Transcriptional regulation of BIM in response to ER stress (Kurata et al., 2011, Puthalakath et al., 2007), and growth factor withdrawal (Gilley et al., 2003) has been widely reported. A post-transcriptional regulation of BIM by HSPB1 has also been reported recently (Davila et al., 2014). Their study has shown that HSPB1 can directly bind to *BIM* 3'UTR and repress its translation under conditions of oxidative stress. My data showed that in the absence of BIM, the level of protection seen in EV and HSPB1 cells in response to ER stress were comparable. This confirms that HSPB1-mediated cytoprotection in response to ER stress was dependent on the regulation of BIM. This finding was supported by Annexin V staining of the cells to determine cell death (Kennedy, PhD thesis 2013). Previous findings in the lab ruled out the transcriptional and post-transcriptional regulation of BIM in HSPB1- mediated cytoprotection in response to ER stress (Kennedy, PhD thesis 2013). The findings from my study suggested possible HSPB1-mediated post-translational regulation of BIM. HSPB1 has been shown to enhance proteasome activity in response to cellular stress (Parcellier et al., 2003). Some of the proteins that are targeted for degradation by the activity of HSPB1 are $p27^{KIP1}$ and IκBα (Parcellier et al., 2003). It has been shown that HSPB1 overexpression mediated proteasomal degradation of BIM (Kennedy, PhD thesis 2013)

Protein regulation through post-translational modification is important in situations of stress when cells require rapid alteration in protein expression or function (Thomas and Lieberman, 2013). Activated ERK 1/2 has been reported to phosphorylate BIM_{EL} at Ser-65 (in rodents) which is then targeted rapidly for proteasomal degradation (Luciano et al., 2003) . HSPB1- overexpressing cells had a higher percentage of the total BIM phosphorylated at Ser-65. Furthermore, HSPB1 overexpressing cells have higher basal levels of phospho-ERK 1/2. This could suggest that in HSPB1 cells, sufficiently high levels of phospho-ERK 1/2 are stabilized to cause phosphorylation of BIM at Ser-65 targeting BIM for proteasomal degradation. Activated ERK 1/2 has been reported to phosphorylate and target BIM for ubiquitin mediated proteasomal degradation (Ley et al.,

2003). This can be confirmed with the use of inducible BIM phospho-mutants to determine the role of phosphorylation of BIM in the regulation of its stability by HSPB1. Whether HSPB1-mediated targeting of BIM for proteasomal degradation is due to ubiquitination-dependent or ubiquitin- independent 20S proteasome mediated degradation of BIM is not known. HSPB1 has been reported to be phosphorylated by phospho-ERK 1/2 (Robitaille et al., 2010). Therefore, a positive feedback loop may be operating where higher levels of phospho-ERK 1/2 can in turn modulate HSPB1. Together with these observations, it is suggested that in HSPB1 cells, HSPB1 acts as a scaffolding factor by bringing phospho-ERK 1/2 and BIM in close proximity such that phospho-ERK 1/2 can readily phosphorylate BIM which is then targeted for proteasomal degradation. This explanation is supported by the observation that HSPB1, phospho-ERK 1/2 and BIM interact with each other in a complex. To delineate the complex that mediates the degradation of BIM in HSPB1 cells, IP with HSPB1 and reciprocal IP with phospho-ERK 1/2 was carried out under untreated and TG treated conditions. Although an interaction between HSPB1, BIM and phospho-ERK 1/2 was observed, less HSPB1 was found to interact with phospho-ERK 1/2 under basal conditions on reciprocal IP with phospho-ERK 1/2 (Fig. 5. 5E). This could suggest that not all the HSPB1 available in the cells complexes with phospho-ERK 1/2, but more of phospho-ERK 1/2 in the pool interacts with HSPB1 in cells treated with TG. Or this could possibly be due to the phosphorylation status of HSPB1. HSPB1 is mostly un-phosphorylated in basal conditions and it has been shown to be phosphorylated in response to ER stress (Ito et al., 2005). The reason that less HSPB1 interacts with phospho-ERK 1/2 under untreated conditions in the reciprocal IP with phospho-ERK 1/2 could be that un-phosphorylated HSPB1 does not bind as efficiently to phospho-ERK 1/2. Whether the fraction of HSPB1 bound to phospho-ERK 1/2 and BIM under TG treated conditions was phosphorylated was not determined. Consistent with the findings in the literature that HSPB1 can be phosphorylated during ER stress; a slight shift in the HSPB1 band was observed in TG treated conditions suggesting the post-translational modification of HSPB1. A better way of confirming the data would be to inhibit the phosphorylation of HSPB1 and determine the pattern of complex formation. Alternatively, non-phosphorylatable HSPB1 mutants could also be used to determine their interaction with phospho-ERK 1/2 and BIM. The effect of inhibition of phosphorylation of HSPB1 (Ser-78) in response to ER stress was determined using KRIBB3. KRIBB3 directly binds to HSPB1 and prevents its phosphorylation through PKC (Shin et al., 2005). Inhibiting the phosphorylation of

HSPB1 reversed the protection conferred by HSPB1 in HSPB1 cells in response to ER stress. It is reported that HSPB1 phosphorylation at Ser-78/82 is critical to Src-Akt/ERK activation, and reduction in the phosphorylation of HSPB1 by KRIBB3 can attenuate TRAIL-induced activation of AKT and ERK survival signaling through suppressing the phosphorylation of Src (Qi et al., 2014). As HSPB1 cells had higher levels of phospho-ERK 1/2, the effect of inhibition of HSPB1 phosphorylation on the levels of activated ERK 1/2 was investigated. In HSPB1 cells, KRIBB3 was able to reduce the phosphorylation of HSPB1 (Ser-78) and also the levels of phospho-ERK 1/2 in response to ER stress. This could suggest a positive loop between the expressions of activated ERK 1/2 and phosphorylated HSPB1under conditions of ER stress. Why there was a reduction in phospho-ERK 1/2 in EV cells in the presence of KRIBB3 and TG at earlier time points (0 h and 12 h) is not clear, however KRIBB3 and TG did not have an effect on phospho-ERK 1/2 at 24 h, while there was a consistent reduction in the levels of phospho-ERK 1/2 across all time points in HSPB1 cells. Inhibition of phosphorylation of HSPB1 has been reported to sensitize cancer cells to death, where overexpression of HSPB1 is a common phenomenon (Shin et al., 2005).

The importance of ERK signaling in HSPB1-mediated regulation of BIM was demonstrated using chemical and genetic inhibition of MEK-ERK signaling pathway. Disruption of MEK-ERK signaling pathway led to a comparable level of BIM expression in EV and HSPB1 cells and reversed the HSPB1-mediated protection in response to ER stress. This was also confirmed upon staining cells for Annexin V to determine cell death (Kennedy, 2013). The functional relevance of ERK in the complex formed between HSPB1, BIM and phospho-ERK 1/2 can further be delineated by the use of MEK inhibitor, UO126. Its effect on the formation of the complex can be investigated.

Twenty different mutations in HSPB1 have been identified with diverse biochemical functions. R127W, R136W and S135F have increased monomerization and preferentially interact with tubulin to induce hyper-phosphorylation of neurofilaments (NFs) and reduce anterograde transport of NFs (Almeida-Souza et al., 2010). Increased monomerization of mutant HSPB1 has been reported to lead to protein hyperactivity in CMT (Almeida-Souza et al., 2010). In order to determine the effect of mutations in HSPB1 in response to ER stress stable clones of cell lines expressing mutations in HSPB1 (R127W, R136W, S135F and T151L) were generated. No studies so far have shown the effect of HSPB1 mutations under ER stressed conditions. This study shows that these mutant forms of

HSPB1 fail to regulate BIM and they no longer protect cells from ER stress- induced cell death. The levels of phospho-ERK 1/2 were also determined in the system. Although the clones expressing HSPB1 mutations show high expression of basal phospho-ERK 1/2, these levels drop rapidly in response to ER stress. It has been reported that when cells are heat shocked, ERK is activated through two mechanisms; by activation of MEK 1/2 signaling and by inhibition of ERK dephosphorylation. ERK dephosphorylation is brought about by ERK phosphatases such as MKP-3 (Yaglom et al., 2003). It is possible that the drop in the levels of phospho-ERK 1/2 could be due to the activation of ERK phosphatases resulting in the dephosphorylation of ERK 1/2. It is also possible that upon ER stress, HSPB1 cells can act as a scaffold protein stabilizing phospho-ERK 1/2 and bringing BIM into close interaction with phospho-ERK 1/2, whereas in contrast, in cells that express mutated forms of HSPB1, this scaffold activity of HSPB1 is lost, resulting in the inability of HSPB1 mutants to stabilize phospho-ERK 1/2 to form a complex with BIM. The rapid de-phosphorylation of phospho-ERK 1/2 results in its inability to phosphorylate BIM and to target it for proteasomal degradation in HSPB1 mutant cells. The effect of destabilized phospho-ERK 1/2 is the accumulation of total BIM that results in failure of HSPB1 to protect cells in response to ER stress. Alternatively, mutations in HSPB1 may alter its interaction with certain client proteins, leading to a consequent reduction in interaction with other clients required for survival of cells in response to ER stress. For example mutation in HSPB1 could alter the interaction of phospho-ERK 1/2 with HSPB1 and recruit other pro-apoptotic proteins that would stabilize BIM and mediate a pro-apoptotic effect. Future direction of the project could focus on delineating the differences in the regulation of BIM by investigating the proteins that would interact with wild type HSPB1 and HSPB1 mutants. It has been reported that activated-JNK 1/2 can phosphorylate BIM at Ser-65 and other sites such as Ser-100, Ser-112 and Ser-114 resulting in stabilization of BIM and thereby inducing apoptosis (Putcha et al., 2003, Geissler et al., 2013). The involvement of activated-JNK 1/2 in the stabilization of BIM in HSPB1 mutant cells can be determined by IP with phospho-JNK 1/2 and investigating any interaction between BIM and HSPB1.

Overall, the findings from this study can be extended towards various stressors involved in inducing cell death. This is of particular interest because HSPB1 undergoes dynamic structural changes in its phosphorylation and oligomerization in order to interact with client proteins to mount protective effect in response to different cellular stress (Gibert et

al., 2013). These modifications could result in activation of various other signaling pathways contributing to the cytoprotective mechanism. Also, the findings from our studies that contrast to (Davila et al., 2014) imply that the regulation of BIM by HSPB1 may depend on the type of cellular stress that induces BIM.

A cytoprotective effect mediated by overexpression of HSPB1 is advantageous for cancer cells and in this context; knockdown of *HSPB1* has been shown to sensitize cancer cells to drug- induced apoptosis (Shin et al., 2005). In contrast, cytoprotection conferred by overexpression of HSPB1 is beneficial in pathological conditions of cellular degeneration, where apoptosis can be inhibited (Gibert et al., 2011). A few examples have been reported in the literature describing peptide aptamers that can modulate interaction of HSPB1 with its client proteins (Gibert et al., 2013). Peptide aptamers PA11 (sequence: QLSGWVGRCL) and PA50 (YLLRRLCC) have been shown to interact with small oligomers of HSPB1 to counteract HSPB1 anti-apoptotic properties (Gibert et al., 2011). Importantly, these peptide aptamers were more potent in causing reduction of tumor growth in SQ20B cell xenografts than HSPB1 depletion using siRNA (Gibert et al., 2011). In contrast, PA23 (YILRRASR) has been shown to potentiate HSPB1-mediated cell resistance to staurosporine and oxidative stress. PA23 was able to attenuate stress-induced sensitivity of HeLa cells mediated by R120G mutant of HSPB5 (associated with myopathy) by disrupting mutant interaction with HSPB1(Gibert et al., 2013). By understanding how BIM and phospho-ERK 1/2 interact with HSPB1, a structure-based therapeutic approach could be used to potentiate or disturb complex formation.

Induction of BIM leads to apoptosis in Huntington's disease where overexpression of mutant Huntingtin protein leads to increased expression of BIM_{EL} (Leon et al., 2010). Similarly, phosphorylation of JNK due to overexpression of $p75^{NTR}$ results in the phosphorylation of BIM_{EL} at Ser-65 in primary cerebellar granule neurons resulting in neuronal apoptosis (Becker et al., 2004). In such conditions, HSPB1-mediated targeting of BIM for proteasomal degradation can be therapeutically relevant. Whereas for instance, in multiple myeloma cells, INFα- induced apoptosis was dependent on BIM (Gomez-Benito et al., 2007), in solid tumors BIM- mediated c-MYC induced apoptosis (Muthalagu et al., 2014), induction of apoptosis in lymphoma cells by BH3 mimetic, ABT-737 was due to the expression of BIM (Deng et al., 2007). In these conditions, BH3 mimetics have been shown to sensitize cancer cells to drug induced cell death and prove

to be of a high therapeutic relevance. The findings from this study can be extended to investigate whether solid tumors can survive ER stress through HSPB1-mediated regulation of BIM.

6 General discussion, future perspectives and conclusions

Dysregulated growth factor signaling is one of the hallmarks of cancer (Hanahan and Weinberg, 2011). Cancer cells make use of this aberrant extracellular growth factor signaling to sustain their proliferation, induce angiogenesis, and activate invasion and metastasis of primary tumors, and resist cell death (Hanahan and Weinberg, 2000). Altered signaling by neurotrophins such as NGF through its receptors has been implicated in the development and progression of several cancers and in the pathogenesis of other diseases like Alzheimer's disease (AD), spinal cord injury and chronic pain (Kruttgen et al., 2006, McKelvey et al., 2013, Beattie et al., 2002, Lad et al., 2003). The knowledge of NGF signaling in disease or cancer models highlights its therapeutic potential.

Current therapies available for the treatment of breast cancers are surgical intervention (mastectomy), radiation therapy, treatment with cytotoxic/genotoxic drugs and combination therapies (Lord et al., 2004). Most breast tumors become resistant to current therapies and the resistance has been attributed to pro-survival pathways mediated by the Er, Pr and Her-2 receptors expressed by breast cancer cells. In combination with conventional treatment strategies, adjuvants such as Tamoxifen (Er blocker), Herceptin (Her-2 antagonist) are being used in the clinic (Lord et al., 2004). However, there is basal-like subtype of breast cancer that do not express these markers (Perou et al., 2000). These are interchangeably called TNBCs. This subtype of breast cancers is therefore insensitive to conventional anti-hormone and anti-Her-2 treatments (Dolle et al., 2004). It is well documented that TNBCs express NGF and the NGF receptors, $p75^{NTR}$ and TrkA, in contrast to the NBEC that express only the receptors for NGF (Descamps et al., 1998). Moreover, it has also been reported that NGF mediates its signaling effect only on breast cancer cells and not on NBEC, thereby increasing the possibility of anti-NGF as a therapy for breast cancers (Descamps et al., 1998). NGF mediates pro-survival signaling through $p75^{NTR}$ (Descamps et al., 2001c). Targeting NGF/$p75^{NTR}$ mediated pro-survival signaling in breast cancers could increase the effectiveness of cytotoxic/genotoxic drugs used as adjuvant therapies. By this strategy, low doses of adjuvants can be administered which otherwise has been reported to be associated with unwanted side effects. For example, doxorubicin has been shown to cause myelosuppression and cardiomyopathies (Jones et al., 2007).

An imbalance in the expression of neurotrophins, neurotrophin receptors or in the maturation of NGF has been implicated in the pathogenesis of several diseases or cancers (Roux and Barker, 2002). Targeting NGF can be achieved by (a) targeting NGF itself, (b) targeting TrkA or NGF/TrkA signaling and (c) targeting $p75^{NTR}$ or NGF/$p75^{NTR}$ signaling.

Over expression of NGF has been shown to induce migration in metastatic melanoma cell lines (Truzzi et al., 2008), and increase perineural invasion associated with pancreatic cancers (Zhu et al., 2002). NGF can also in a paracrine or autocrine manner induce cancer cell invasion *in vivo* thereby contributing to the aggressiveness and poor prognosis of the disease (Zhu et al., 2002). NGF is overexpressed in all subtypes of breast cancer. By targeting NGF, its signaling through receptors can also be efficiently inhibited. In breast cancers, the use of anti-NGF has been shown to be of a high therapeutic potential. It has been shown that the use of NGF neutralizing antibodies led to significantly reduced tumor growth, tumor size and tumor volume in MDA-MB-231 xenografts in SCID mice (Adriaenssens et al., 2008). Anti-NGF antibodies have also been shown to reduce tumor cell migration by up to 40% in prostate cancer cell lines (Warrington and Lewis, 2011). High levels of NGF are associated with conditions of chronic pain (McKelvey et al., 2013). Disrupting NGF/TrkA signaling is a promising target for pain management. Tanezumab, a monoclonal antibody developed by Pfizer, is currently in Phase II and III clinical trials for treatment of pain associated with conditions like osteoarthritis of the knee and pain associated with cancers of the bone (Brown et al., 2012, Lane et al., 2010). Tanezumab mediates tolerance to pain by binding with high affinity to NGF and blocking the interaction of NGF with its receptors (Abdiche et al., 2008). With the use of anti-NGF antibodies, development of tolerance to the drug is often an issue. In addition to drug tolerance, immunogenicity to the drug is also an issue. How the development of drug immunogenicity can be counteracted is an area that needs to be investigated. Therefore, in addition to the currently available anti-NGF antibody, newer approaches to target NGF and its signaling are needed.

AD is caused by degeneration of basal BFCN expressing high levels of $p75^{NTR}$ and low levels of TrkA and NGF (Scott et al., 1995). In the treatment of AD, NGF was artificially secreted from implanted fibroblasts engineered to express human NGF (Wahlberg et al., 2012). The approach used in my study to express and investigate NGF/NGF variants signaling was similar and relevant to the therapeutically produced NGF in the treatment

of AD. Use of NGF in the clinic has been limited due to various factors such as low stability, negligible oral bio-availability (Saltzman et al., 1999) or minimal blood brain barrier penetration ability (Poduslo and Curran, 1996). However, small molecules to inhibit the ligand or its interaction with receptor have been developed to overcome this problem (Longo and Massa, 2013).

The second approach of targeting NGF is by targeting its receptors. In prostate cancer, $p75^{NTR}$ acts as a tumor suppressor gene, where its expression in lost in malignant stages. In such conditions, the main strategy of treatment is to inhibit TrkA-mediated proliferative signaling. NGF-mediated signaling through TrkA has been shown to be mediated through MAPK signaling in many cancers such as breast, pancreatic and prostate cancers (Descamps et al., 2001c, Zhu et al., 2002, Arrighi et al., 2010). Therefore, targeting the activity of TrkA will prove beneficial across these cancers. For example, pharmacological inhibitors of TrkA signaling, such as derivatives of pan-Trk inhibitor K252a, have shown promise. For instance, CEP-701, has been reported to block the invasive capability of prostate cancer cells *in vivo* (Festuccia et al., 2007), CEP-751 has been reported to induce apoptosis, decrease metastasis of malignant prostate cancer cells and enhance host survival in *in vivo* experimental models (Weeraratna et al., 2000). Recently, siRNA-mediated downregulation of TrkA has been shown to inhibit the proliferation of breast cancer cells, increase the chemosensitivity of breast cancer cells to paclitaxel and decreased the metastasis *in vivo* (Zhang et al., 2015). This finding indicates the potential use of TrkA inhibitors in breast cancer.

TNBCs have been reported to express high levels of $p75^{NTR}$ (Reis-Filho et al., 2006). A positive correlation has been shown to exist between the expression of NGF and $p75^{NTR}$ in patients with breast cancers (Jezequel et al., 2013). This part of my work shows that TNBCs can be sensitized to drug-induced cell death using small molecule inhibitors, particularly when they express high levels of $p75^{NTR}$ as occurs when there are increased levels of secreted NGF. The findings from this study can be related to other cancers where NGF/$p75^{NTR}$ mediates resistance to cell death. Small molecule inhibitors of $p75^{NTR}$ such as peptide inhibitors or non-peptide inhibitors have also been produced. A peptide inhibitor of $p75^{NTR}$ called Pep-5 has been synthesized and used in cell lines. Pep-5 is an 11-amino acid peptide that binds to the death domain of $p75^{NTR}$ and inhibits the downstream activation of $p75^{NTR}$ (Yamashita and Tohyama, 2003b). To make this peptide cell permeable, it is made available as a TAT-fusion peptide. In addition to these, small

molecule such as Ro 08-2750, Y1036 and PD90780 that interact with NGF or NGF/BDNF and change their conformation such that the neurotrophin can no longer bind to $p75^{NTR}$ are also available and these have proven useful in some experimental conditions tested (Niederhauser et al., 2000, Eibl et al., 2010, Colquhoun et al., 2004).

It has been reported that NGF interacts with $p75^{NTR}$ through two sites, the site I interaction involves amino acid positions 23-35 (loop I) and at positions 92-100 (loop IV) of the NGF, and the site II interaction involves the amino acid positions 11-21 of NGF (He and Garcia, 2004, Wiesmann et al., 1999). The interaction of NGF/$p75^{NTR}$ at the two sites mediates different biological function of $p75^{NTR}$. In addition to peptide inhibitors of $p75^{NTR}$ that are commercially available, non-peptide $p75^{NTR}$ ligands are also available. LM11A-24 (a non-peptide $p75^{NTR}$ ligand), is a neurotrophin loop I mimetic that has been shown to bind to $p75^{NTR}$ and block the proNGF and NGF-mediated cell death through $p75^{NTR}$ (Pehar et al., 2006). Similarly, LM11A-31 is also a small molecule, non-peptide $p75^{NTR}$ ligand that has structural and chemical features similar to NGF loop domain I (Simmons et al., 2014). In a model of Alzheimer's disease in which Aβ oligomers are added to cultured hippocampal neurons or slices, LM11A-31 and LM11A-24 inhibited Aβ-induced deleterious signaling (Yang et al., 2008). It has also been reported that in a transgenic mouse model of AD, LM11A-31, when administered orally inhibited degenerative signaling without toxic side-effects (Knowles et al., 2013). It was also shown to prevent deficits in novel object recognition and spatial working memory and reduced neuritic dystrophy with no effect on amyloid levels, proving to be a suitable *in vivo* target for AD (Knowles et al., 2013). In an in-silico screen, these compounds (LM11A-24 and LM11A-31) shown to interact with loop 1 of NGF, interrupted the interaction of NGF with $p75^{NTR}$. With a similar rationale to developing ligands that block activity of $p75^{NTR}$ by inhibiting its interaction with NGF, previous work in the lab generated NGF variants using FoldX algorithm where residues involving interaction of NGF with $p75^{NTR}$ and TrkA were identified and mutated. I31 is one such residue that was identified to be in the interaction site I, and this site has also been shown to interact directly with TrkA. The biological activity of NGF mutated at this residue (I31R) was tested. This I31R NGF variant did not bind to TrkA but it retained its binding affinity to p75NTR. Thus, this I31R NGF mutant also represents a feasible target for small molecule intervention for the treatment of pain and cancers.

So far, the role of growth factor (NGF), an extracellular ligand in mediating pro-survival signaling in the context of breast cancers and a neurodegenerative disease model; AD, has been discussed. The other part of my thesis showed the role of an intracellular small heat shock protein (HSPB1) in mediating pro-survival signaling in response to ER stress induced cell death. HSPB1-mediated cytoprotection has been observed in response to various stressors such as 6-hydroxydopamine, oxidative stress and heat shock (Gorman et al., 2005, Davila et al., 2014, Kennedy et al., 2014). The work from results chapter 5 shows that HSPB1 mediates cytoprotection in response to ER-stress induced cell death through post-translational regulation of BIM. This novel regulation by HSPB1 of BIM relies on MEK-ERK signaling.

Activation of ER stress pathway is a salient feature of neurodegenerative diseases (Doyle et al., 2011). BIM is one of the BH3-only proteins that is induced in response to ER stress (Szegezdi et al., 2008). Several reports highlight the role of BIM in neuronal cell death, for instance, in Amyotrophic Lateral Sclerosis (ALS) models (Soo et al., 2012). Reports have shown HSPB1-mediated protection in transgenic mouse models of mSOD ALS model, whether this is mediated through regulation of BIM is not known (Sharp et al., 2008). Recent studies have demonstrated the role of BIM in mediating neuronal cell death induced by Aβ. These reports show BIM induction by Aβ (Kudo et al., 2012, Sanphui and Biswas, 2013). It has been shown that Aβ caused a reduction in AKT and other survival kinases, which regulate the transcription factor FoxO3a. The transcriptional activation of FoxO3a resulted in the induction of BIM leading to activation of intrinsic apoptotic pathway (Sanphui and Biswas, 2013). From the findings in chapter 5, there could be a potential role of BIM in the pathogenesis of CMT. Investigation into the regulation of BIM in conditions where HSPB1 is mutated would be an avenue of research. This would reveal the role of other HSPB1-interacting client proteins. My work mainly focused on HSPB1-ERK-BIM signaling, but there are reports that suggest BIM can be phosphorylated at Ser-65 residue by JNK 1/2 also. Other residues on BIM can also be phosphorylated by JNK and these have been shown to result in stabilization of BIM (Geissler et al., 2013). In agreement with my studies where BIM accumulates in cell lines which express HSPB1 mutants, a potential role of JNK signaling might exist. This is yet another area to be explored.

HSPB1 has been shown to be phosphorylated in response to ER stress (Ito et al., 2005). This phosphorylation of HSPB1 has been attributed in part to its cytoprotective effect

(Shin et al., 2005). The findings from my study shows that HSPB1 can mediate protection against ER-stress induced cell death. Therefore, approaches by which HSPB1 can be induced and other mechanisms by which HSPB1 interacts with other client proteins could be an area that can be investigated. This might be of potential therapeutic relevance in neurodegenerative diseases where ER stress plays a pathophysiological role.

In addition to self-sufficient growth factor signaling as a hallmark of cancer, resistance to cell death is also another hallmark of cancer (Hanahan and Weinberg, 2000). Cancer cells can resist cell death by placing inhibitory effects on the cell death pathway at various levels. HSPB1 has been reported to be overexpressed in cancers including breast cancers (Shin et al., 2005). Inhibiting the expression of HSPB1 has been shown to sensitize cells to drug-induced cell death. As we know, HSPB1 mediates a cytoprotective effect in response to varied stimuli; it would be interesting to determine the link between HSPB1 overexpression and its regulation of BIM or other members of BH3-only family of proteins in conditions of ER stress in solid tumors.

In conclusion, this thesis highlighted the role of extracellular growth factor signaling-mediated and intracellular molecular chaperone- mediated pro-survival signaling in cancers, neurodegenerative diseases or in neuropathies. Although these pathways function at two different levels in the cells, they have a commonality in eliciting pro-survival signal. Drug tolerance is always a hindrance in the treatment of diseases. Therefore, targeting multiple factors that contribute to disease pathogenesis may help in better treatment of diseases. For instance, targeting NGF signaling and also finding a way to induce HSPB1 that would regulate expression of BIM could potentially help rescue neuronal cell death in AD.

7 Bibliography

ABDICHE, Y. N., MALASHOCK, D. S. & PONS, J. 2008. Probing the binding mechanism and affinity of tanezumab, a recombinant humanized anti-NGF monoclonal antibody, using a repertoire of biosensors. *Protein Sci,* 17**,** 1326-35.

ACEHAN, D., JIANG, X., MORGAN, D. G., HEUSER, J. E., WANG, X. & AKEY, C. W. 2002. Three-dimensional structure of the apoptosome: implications for assembly, procaspase-9 binding, and activation. *Mol Cell,* 9**,** 423-32.

ADAMS, J. 2003. The proteasome: structure, function, and role in the cell. *Cancer Treat Rev,* 29 Suppl 1**,** 3-9.

ADAMS, J. M. & CORY, S. 1998. The Bcl-2 protein family: arbiters of cell survival. *Science,* 281**,** 1322-6.

ADRIAENSSENS, E., VANHECKE, E., SAULE, P., MOUGEL, A., PAGE, A., ROMON, R., NURCOMBE, V., LE BOURHIS, X. & HONDERMARCK, H. 2008. Nerve growth factor is a potential therapeutic target in breast cancer. *Cancer Research,* 68**,** 346-351.

AKERFELT, M., MORIMOTO, R. I. & SISTONEN, L. 2010. Heat shock factors: integrators of cell stress, development and lifespan. *Nat Rev Mol Cell Biol,* 11**,** 545-55.

ALMEIDA-SOUZA, L., GOETHALS, S., DE WINTER, V., DIERICK, I., GALLARDO, R., VAN DURME, J., IROBI, J., GETTEMANS, J., ROUSSEAU, F., SCHYMKOWITZ, J., TIMMERMAN, V. & JANSSENS, S. 2010. Increased monomerization of mutant HSPB1 leads to protein hyperactivity in Charcot-Marie-Tooth neuropathy. *J Biol Chem,* 285**,** 12778-86.

ALNEMRI, E. S., LIVINGSTON, D. J., NICHOLSON, D. W., SALVESEN, G., THORNBERRY, N. A., WONG, W. W. & YUAN, J. 1996. Human ICE/CED-3 protease nomenclature. *Cell.*

AMBROS, V. 2004. The functions of animal microRNAs. *Nature,* 431**,** 350-5.

ANDREWS, J., DJAKIEW, D., KRYGIER, S. & ANDREWS, P. 2002. Superior effectiveness of ibuprofen compared with other NSAIDs for reducing the survival of human prostate cancer cells. *Cancer Chemother Pharmacol,* 50**,** 277-84.

ANDRIEU, C., TAIEB, D., BAYLOT, V., ETTINGER, S., SOUBEYRAN, P., DE-THONEL, A., NELSON, C., GARRIDO, C., SO, A., FAZLI, L., BLADOU, F.,

GLEAVE, M., IOVANNA, J. L. & ROCCHI, P. 2010. Heat shock protein 27 confers resistance to androgen ablation and chemotherapy in prostate cancer cells through eIF4E. *Oncogene,* 29**,** 1883-96.

AREVALO, J. C., CONDE, B., HEMPSTEAD, B. L., CHAO, M. V., MARTIN-ZANCA, D. & PEREZ, P. 2000. TrkA immunoglobulin-like ligand binding domains inhibit spontaneous activation of the receptor. *Mol Cell Biol,* 20**,** 5908-16.

ARRIGHI, N., BODEI, S., ZANI, D., SIMEONE, C., CUNICO, S. C., MISSALE, C., SPANO, P. & SIGALA, S. 2010. Nerve growth factor signaling in prostate health and disease. *Growth Factors,* 28**,** 191-201.

ARRIGO, A. P. 2013. Human small heat shock proteins: protein interactomes of homo- and hetero-oligomeric complexes: an update. *FEBS Lett,* 587**,** 1959-69.

ARRIGO, A. P., SIMON, S., GIBERT, B., KRETZ-REMY, C., NIVON, M., CZEKALLA, A., GUILLET, D., MOULIN, M., DIAZ-LATOUD, C. & VICART, P. 2007. Hsp27 (HspB1) and alphaB-crystallin (HspB5) as therapeutic targets. *FEBS Lett,* 581**,** 3665-74.

ASHKENAZI, A. & DIXIT, V. M. 1998. Death receptors: signaling and modulation. *Science,* 281**,** 1305-8.

ASTHANA, A., BOLLAPALLI, M., TANGIRALA, R., BAKTHISARAN, R. & MOHAN RAO, C. 2014. Hsp27 suppresses the Cu(2+)-induced amyloidogenicity, redox activity, and cytotoxicity of alpha-synuclein by metal ion stripping. *Free Radic Biol Med,* 72**,** 176-90.

BAEHRECKE, E. H. 2002. How death shapes life during development. *Nat Rev Mol Cell Biol,* 3**,** 779-87.

BAKTHISARAN, R., TANGIRALA, R. & RAO CH, M. 2015. Small heat shock proteins: Role in cellular functions and pathology. *Biochim Biophys Acta,* 1854**,** 291-319.

BALDWIN, A. N. & SHOOTER, E. M. 1995. Zone mapping of the binding domain of the rat low affinity nerve growth factor receptor by the introduction of novel N-glycosylation sites. *J Biol Chem,* 270**,** 4594-602.

BARANOVA, E. V., WEEKS, S. D., BEELEN, S., BUKACH, O. V., GUSEV, N. B. & STRELKOV, S. V. 2011. Three-dimensional structure of alpha-crystallin domain dimers of human small heat shock proteins HSPB1 and HSPB6. *J Mol Biol,* 411**,** 110-22.

BARDE, Y. A., EDGAR, D. & THOENEN, H. 1982. Purification of a new neurotrophic factor from mammalian brain. *Embo j,* 1**,** 549-53.

BARRY, M. & BLEACKLEY, R. C. 2002. Cytotoxic T lymphocytes: all roads lead to death. *Nat Rev Immunol,* 2**,** 401-9.

BEATTIE, M. S., HARRINGTON, A. W., LEE, R., KIM, J. Y., BOYCE, S. L., LONGO, F. M., BRESNAHAN, J. C., HEMPSTEAD, B. L. & YOON, S. O. 2002. ProNGF induces p75-mediated death of oligodendrocytes following spinal cord injury. *Neuron,* 36**,** 375-86.

BECKER, E. B., HOWELL, J., KODAMA, Y., BARKER, P. A. & BONNI, A. 2004. Characterization of the c-Jun N-terminal kinase-BimEL signaling pathway in neuronal apoptosis. *J Neurosci,* 24**,** 8762-70.

BERKEMEIER, L. R., WINSLOW, J. W., KAPLAN, D. R., NIKOLICS, K., GOEDDEL, D. V. & ROSENTHAL, A. 1991. Neurotrophin-5: a novel neurotrophic factor that activates trk and trkB. *Neuron,* 7**,** 857-66.

BIBEL, M. & BARDE, Y. A. 2000. Neurotrophins: key regulators of cell fate and cell shape in the vertebrate nervous system. *Genes Dev,* 14**,** 2919-37.

BOUILLET, P. & STRASSER, A. 2002. BH3-only proteins - evolutionarily conserved proapoptotic Bcl-2 family members essential for initiating programmed cell death. *J Cell Sci,* 115**,** 1567-74.

BRADSHAW, R. A., MURRAY-RUST, J., IBANEZ, C. F., MCDONALD, N. Q., LAPATTO, R. & BLUNDELL, T. L. 1994. Nerve growth factor: structure/function relationships. *Protein Sci,* 3**,** 1901-13.

BROWN, M. S., YE, J., RAWSON, R. B. & GOLDSTEIN, J. L. 2000. Regulated intramembrane proteolysis: a control mechanism conserved from bacteria to humans. *Cell,* 100**,** 391-8.

BROWN, M. T., MURPHY, F. T., RADIN, D. M., DAVIGNON, I., SMITH, M. D. & WEST, C. R. 2012. Tanezumab reduces osteoarthritic knee pain: results of a randomized, double-blind, placebo-controlled phase III trial. *J Pain,* 13**,** 790-8.

BRUEY, J. M., DUCASSE, C., BONNIAUD, P., RAVAGNAN, L., SUSIN, S. A., DIAZ-LATOUD, C., GURBUXANI, S., ARRIGO, A. P., KROEMER, G., SOLARY, E. & GARRIDO, C. 2000. Hsp27 negatively regulates cell death by interacting with cytochrome c. *Nat Cell Biol,* 2**,** 645-52.

BRUNELLE, J. K. & LETAI, A. 2009. Control of mitochondrial apoptosis by the Bcl-2 family. *J Cell Sci,* 122**,** 437-41.

BUDIHARDJO, I., OLIVER, H., LUTTER, M., LUO, X. & WANG, X. 1999. Biochemical pathways of caspase activation during apoptosis. *Annu Rev Cell Dev Biol,* 15**,** 269-90.

BUSH, K. T., GOLDBERG, A. L. & NIGAM, S. K. 1997. Proteasome inhibition leads to a heat-shock response, induction of endoplasmic reticulum chaperones, and thermotolerance. *J Biol Chem,* 272**,** 9086-92.

BUTT, E., IMMLER, D., MEYER, H. E., KOTLYAROV, A., LAASS, K. & GAESTEL, M. 2001. Heat shock protein 27 is a substrate of cGMP-dependent protein kinase in intact human platelets: phosphorylation-induced actin polymerization caused by HSP27 mutants. *J Biol Chem,* 276**,** 7108-13.

CAIN, K., BRATTON, S. B. & COHEN, G. M. 2002. The Apaf-1 apoptosome: a large caspase-activating complex. *Biochimie,* 84**,** 203-14.

CALVERT, A. H., LIND, M. J., MILLWARD, M. M., CANTWELL, B. M., GUMBRELL, L., PROCTOR, M., SIMMONS, D., CHAPMAN, F., ROBINSON, A., CHARLTON, C. & ET AL. 1993. Long-term oral etoposide in metastatic breast cancer: clinical and pharmacokinetic results. *Cancer Treat Rev,* 19 Suppl C**,** 27-33.

CARRA, S., CRIPPA, V., RUSMINI, P., BONCORAGLIO, A., MINOIA, M., GIORGETTI, E., KAMPINGA, H. H. & POLETTI, A. 2012. Alteration of protein folding and degradation in motor neuron diseases: Implications and protective functions of small heat shock proteins. *Prog Neurobiol,* 97**,** 83-100.

CARTER, B. D. & LEWIN, G. R. 1997. Neurotrophins live or let die: does p75NTR decide? *Neuron,* 18**,** 187-90.

CENI, C., KOMMADDI, R. P., THOMAS, R., VEREKER, E., LIU, X. Y., MCPHERSON, P. S., RITTER, B. & BARKER, P. A. 2010. The p75NTR intracellular domain generated by neurotrophin-induced receptor cleavage potentiates Trk signaling. *Journal of Cell Science,* 123**,** 2299-2307.

CHANG, H. Y. & YANG, X. 2000. Proteases for cell suicide: functions and regulation of caspases. *Microbiol Mol Biol Rev,* 64**,** 821-46.

CHAO, M. V. 1994. The p75 neurotrophin receptor. *J Neurobiol,* 25**,** 1373-85.

CHAPMAN, B. S. 1995. A region of the 75 kDa neurotrophin receptor homologous to the death domains of TNFR-I and Fas. *FEBS Lett,* 374**,** 216-20.

CHARETTE, S. J., LAVOIE, J. N., LAMBERT, H. & LANDRY, J. 2000. Inhibition of Daxx-mediated apoptosis by heat shock protein 27. *Mol Cell Biol,* 20**,** 7602-12.

CHITTKA, A., AREVALO, J. C., RODRIGUEZ-GUZMAN, M., PEREZ, P., CHAO, M. V. & SENDTNER, M. 2004. The p75NTR-interacting protein SC1 inhibits cell cycle progression by transcriptional repression of cyclin E. *J Cell Biol,* 164**,** 985-96.

COHEN, G. M. 1997. Caspases: the executioners of apoptosis. *Biochem J,* 326 (Pt 1)**,** 1-16.

COLQUHOUN, A., LAWRANCE, G. M., SHAMOVSKY, I. L., RIOPELLE, R. J. & ROSS, G. M. 2004. Differential activity of the nerve growth factor (NGF) antagonist PD90780 [7-(benzolylamino)-4,9-dihydro-4-methyl-9-oxo-pyrazolo[5,1-b]quinazoline-2-carbox ylic acid] suggests altered NGF-p75NTR interactions in the presence of TrkA. *J Pharmacol Exp Ther,* 310**,** 505-11.

CONCANNON, C. G., GORMAN, A. M. & SAMALI, A. 2003. On the role of Hsp27 in regulating apoptosis. *Apoptosis,* 8**,** 61-70.

CONCANNON, C. G., ORRENIUS, S. & SAMALI, A. 2001. Hsp27 inhibits cytochrome c-mediated caspase activation by sequestering both pro-caspase-3 and cytochrome c. *Gene Expr,* 9**,** 195-201.

CORBIT, K. C., FOSTER, D. A. & ROSNER, M. R. 1999. Protein kinase Cdelta mediates neurogenic but not mitogenic activation of mitogen-activated protein kinase in neuronal cells. *Mol Cell Biol,* 19**,** 4209-18.

CRAGNOLINI, A. B., HUANG, Y., GOKINA, P. & FRIEDMAN, W. J. 2009. Nerve growth factor attenuates proliferation of astrocytes via the p75 neurotrophin receptor. *Glia,* 57**,** 1386-92.

CUNNINGHAM, M. E. & GREENE, L. A. 1998. A function-structure model for NGF-activated TRK. *Embo j,* 17**,** 7282-93.

D'YDEWALLE, C., BENOY, V. & VAN DEN BOSCH, L. 2012. Charcot-Marie-Tooth disease: emerging mechanisms and therapies. *Int J Biochem Cell Biol,* 44**,** 1299-304.

DAVILA, D., JIMENEZ-MATEOS, E. M., MOONEY, C. M., VELASCO, G., HENSHALL, D. C. & PREHN, J. H. 2014. Hsp27 binding to the 3'UTR of bim mRNA prevents neuronal death during oxidative stress-induced injury: a novel cytoprotective mechanism. *Mol Biol Cell,* 25**,** 3413-23.

DEGTEREV, A., BOYCE, M. & YUAN, J. 2003. A decade of caspases. *Oncogene,* 22**,** 8543-67.

DENG, J., CARLSON, N., TAKEYAMA, K., DAL CIN, P., SHIPP, M. & LETAI, A. 2007. BH3 profiling identifies three distinct classes of apoptotic blocks to predict response to ABT-737 and conventional chemotherapeutic agents. *Cancer Cell,* 12**,** 171-85.

DESCAMPS, S., LEBOURHIS, X., DELEHEDDE, M., BOILLY, B. & HONDERMARCK, H. 1998. Nerve growth factor is mitogenic for cancerous but not normal human breast epithelial cells. *Journal of Biological Chemistry,* 273**,** 16659-16662.

DESCAMPS, S., PAWLOWSKI, V., REVILLION, F., HORNEZ, L., HEBBAR, M., BOILLY, B., HONDERMARCK, H. & PEYRAT, J. P. 2001a. Expression of nerve growth factor receptors and their prognostic value in human breast cancer. *Cancer Research,* 61**,** 4337-4340.

DESCAMPS, S., TOILLON, R., ADRIAENSSENS, E., PAWLOWSKI, V., COOL, S., NURCOMBE, V., LE BOURHIS, X., BOILLY, B., PEYRAT, J. & HONDERMARCK, H. 2001b. Nerve growth factor stimulates proliferation and survival of human breast cancer cells through two distinct signaling pathways. *Journal of Biological Chemistry,* 276**,** 17864-17870.

DESCAMPS, S., TOILLON, R. A., ADRIAENSSENS, E., PAWLOWSKI, V., COOL, S. M., NURCOMBE, V., LE BOURHIS, X. F., BOILLY, B., PEYRAT, J. P. & HONDERMARCK, H. 2001c. Nerve growth factor stimulates proliferation and survival of human breast cancer cells through two distinct signaling pathways. *Journal of Biological Chemistry,* 276**,** 17864-17870.

DIARRA, A., GEETHA, T., POTTER, P. & BABU, J. R. 2009. Signaling of the neurotrophin receptor p75 in relation to Alzheimer's disease. *Biochem Biophys Res Commun,* 390**,** 352-6.

DING, K., SU, Y., PANG, L., LU, Q., WANG, Z., ZHANG, S., ZHENG, S., MAO, J. & ZHU, Y. 2009. Inhibition of apoptosis by downregulation of hBex1, a novel mechanism, contributes to the chemoresistance of Bcr/Abl+ leukemic cells. *Carcinogenesis.* England.

DIXON, S. J., LEMBERG, K. M., LAMPRECHT, M. R., SKOUTA, R., ZAITSEV, E. M., GLEASON, C. E., PATEL, D. N., BAUER, A. J., CANTLEY, A. M., YANG, W. S., MORRISON, B., 3RD & STOCKWELL, B. R. 2012. Ferroptosis: an iron-dependent form of nonapoptotic cell death. *Cell,* 149**,** 1060-72.

DJAKIEW, D. 2000. Dysregulated expression of growth factors and their receptors in the development of prostate cancer. *Prostate.* United States.

DOLLE, L., ADRIAENSSENS, E., EL YAZIDI-BELKOURA, I., LE BOURHIS, X., NURCOMBE, V. & HONDERMARCK, H. 2004. Nerve growth factor receptors and signaling in breast cancer. *Curr Cancer Drug Targets,* 4**,** 463-70.

DOLLE, L., EL YAZIDI-BELKOURA, I., ADRIAENSSENS, E., NURCOMBE, V. & HONDERMARCK, H. 2003a. Nerve growth factor overexpression and autocrine loop in breast cancer cells. *Oncogene,* 22**,** 5592-601.

DOLLE, L., EL YAZIDI-BELKOURA, I., ADRIAENSSENS, E., NURCOMBE, V. & HONDERMARCK, H. 2003b. Nerve growth factor overexpression and autocrine loop in breast cancer cells. *Oncogene,* 22**,** 5592-5601.

DOLLE, L., OLIVEIRA, M. J., BRUYNEEL, E., HONDERMARCK, H. & BRACKE, M. 2005. Nerve growth factor mediates its pro-invasive effect in parallel with the release of a soluble E-cadherin fragment from breast cancer MCF-7/AZ cells. *J Dairy Res,* 72 Spec No**,** 20-6.

DOYLE, K. M., KENNEDY, D., GORMAN, A. M., GUPTA, S., HEALY, S. J. & SAMALI, A. 2011. Unfolded proteins and endoplasmic reticulum stress in neurodegenerative disorders. *J Cell Mol Med,* 15**,** 2025-39.

DRUBIN, D. G., FEINSTEIN, S. C., SHOOTER, E. M. & KIRSCHNER, M. W. 1985. Nerve growth factor-induced neurite outgrowth in PC12 cells involves the coordinate induction of microtubule assembly and assembly-promoting factors. *J Cell Biol,* 101**,** 1799-807.

EIBL, J. K., CHAPELSKY, S. A. & ROSS, G. M. 2010. Multipotent neurotrophin antagonist targets brain-derived neurotrophic factor and nerve growth factor. *J Pharmacol Exp Ther,* 332**,** 446-54.

EINARSDOTTIR, E., CARLSSON, A., MINDE, J., TOOLANEN, G., SVENSSON, O., SOLDERS, G., HOLMGREN, G., HOLMBERG, D. & HOLMBERG, M. 2004. A mutation in the nerve growth factor beta gene (NGFB) causes loss of pain perception. *Hum Mol Genet,* 13**,** 799-805.

EL YAZIDI-BELKOURA, I., ADRIAENSSENS, E., DOLLE, L., DESCAMPS, S. & HONDERMARCK, H. 2003. Tumor necrosis factor receptor-associated death domain protein is involved in the neurotrophin receptor-mediated antiapoptotic activity of nerve growth factor in breast cancer cells. *Journal of Biological Chemistry,* 278**,** 16952-16956.

ELLIS, H. M. & HORVITZ, H. R. 1986. Genetic control of programmed cell death in the nematode C. elegans. *Cell,* 44**,** 817-29.

ELLIS, R. E., YUAN, J. Y. & HORVITZ, H. R. 1991. Mechanisms and functions of cell death. *Annu Rev Cell Biol,* 7**,** 663-98.

ELLIS, R. J. 1993. The general concept of molecular chaperones. *Philos Trans R Soc Lond B Biol Sci,* 339**,** 257-61.

ELMORE, S. 2007. Apoptosis: a review of programmed cell death. *Toxicol Pathol,* 35**,** 495-516.

EVGRAFOV, O. V., MERSIYANOVA, I., IROBI, J., VAN DEN BOSCH, L., DIERICK, I., LEUNG, C. L., SCHAGINA, O., VERPOORTEN, N., VAN IMPE, K., FEDOTOV, V., DADALI, E., AUER-GRUMBACH, M., WINDPASSINGER, C., WAGNER, K., MITROVIC, Z., HILTON-JONES, D., TALBOT, K., MARTIN, J. J., VASSERMAN, N., TVERSKAYA, S., POLYAKOV, A., LIEM, R. K., GETTEMANS, J., ROBBERECHT, W., DE JONGHE, P. & TIMMERMAN, V. 2004. Mutant small heat-shock protein 27 causes axonal Charcot-Marie-Tooth disease and distal hereditary motor neuropathy. *Nat Genet,* 36**,** 602-6.

FAHNESTOCK, M., MICHALSKI, B., XU, B. & COUGHLIN, M. D. 2001. The precursor pro-nerve growth factor is the predominant form of nerve growth factor in brain and is increased in Alzheimer's disease. *Mol Cell Neurosci.* United States: 2001 Academic Press.

FAHNESTOCK, M., YU, G., MICHALSKI, B., MATHEW, S., COLQUHOUN, A., ROSS, G. M. & COUGHLIN, M. D. 2004. The nerve growth factor precursor proNGF exhibits neurotrophic activity but is less active than mature nerve growth factor. *J Neurochem,* 89**,** 581-92.

FERLAY, J., SOERJOMATARAM, I., DIKSHIT, R., ESER, S., MATHERS, C., REBELO, M., PARKIN, D. M., FORMAN, D. & BRAY, F. 2015. Cancer incidence and mortality worldwide: Sources, methods and major patterns in GLOBOCAN 2012. *Int J Cancer,* 136**,** E359-86.

FESTUCCIA, C., MUZI, P., GRAVINA, G. L., MILLIMAGGI, D., SPECA, S., DOLO, V., RICEVUTO, E., VICENTINI, C. & BOLOGNA, M. 2007. Tyrosine kinase inhibitor CEP-701 blocks the NTRK1/NGF receptor and limits the invasive capability of prostate cancer cells in vitro. *Int J Oncol,* 30**,** 193-200.

FOMBONNE, J., RABIZADEH, S., BANWAIT, S., MEHLEN, P. & BREDESEN, D. E. 2009. Selective vulnerability in Alzheimer's disease: amyloid precursor protein and p75(NTR) interaction. *Ann Neurol,* 65**,** 294-303.

FOULKES, W. D., SMITH, I. E. & REIS-FILHO, J. S. 2010. Triple-negative breast cancer. *N Engl J Med,* 363**,** 1938-48.

FRANKE, T. F., KAPLAN, D. R. & CANTLEY, L. C. 1997. PI3K: downstream AKTion blocks apoptosis. *Cell,* 88**,** 435-7.

FRIANT, S., MEIER, K. D. & RIEZMAN, H. 2003. Increased ubiquitin-dependent degradation can replace the essential requirement for heat shock protein induction. *Embo j,* 22**,** 3783-91.

FRIEDMAN, W. J. & GREENE, L. A. 1999. Neurotrophin signaling via Trks and p75. *Exp Cell Res,* 253**,** 131-42.

FULDA, S., GORMAN, A. M., HORI, O. & SAMALI, A. 2010. Cellular stress responses: cell survival and cell death. *Int J Cell Biol,* 2010**,** 214074.

GALLUZZI, L., VITALE, I., ABRAMS, J. M., ALNEMRI, E. S., BAEHRECKE, E. H., BLAGOSKLONNY, M. V., DAWSON, T. M., DAWSON, V. L., EL-DEIRY, W. S., FULDA, S., GOTTLIEB, E., GREEN, D. R., HENGARTNER, M. O., KEPP, O., KNIGHT, R. A., KUMAR, S., LIPTON, S. A., LU, X., MADEO, F., MALORNI, W., MEHLEN, P., NUNEZ, G., PETER, M. E., PIACENTINI, M., RUBINSZTEIN, D. C., SHI, Y., SIMON, H. U., VANDENABEELE, P., WHITE, E., YUAN, J., ZHIVOTOVSKY, B., MELINO, G. & KROEMER, G. 2012. Molecular definitions of cell death subroutines: recommendations of the Nomenclature Committee on Cell Death 2012. *Cell Death Differ,* 19**,** 107-20.

GAO, X., DAUGHERTY, R. L. & TOURTELLOTTE, W. G. 2007. Regulation of low affinity neurotrophin receptor (p75(NTR)) by early growth response (Egr) transcriptional regulators. *Mol Cell Neurosci,* 36**,** 501-14.

GARRIDO, C., BRUEY, J. M., FROMENTIN, A., HAMMANN, A., ARRIGO, A. P. & SOLARY, E. 1999. HSP27 inhibits cytochrome c-dependent activation of procaspase-9. *Faseb j,* 13**,** 2061-70.

GEISSLER, A., HAUN, F., FRANK, D. O., WIELAND, K., SIMON, M. M., IDZKO, M., DAVIS, R. J., MAURER, U. & BORNER, C. 2013. Apoptosis induced by the fungal pathogen gliotoxin requires a triple phosphorylation of Bim by JNK. *Cell Death Differ,* 20**,** 1317-29.

GENTRY, J. J., CASACCIA-BONNEFIL, P. & CARTER, B. D. 2000. Nerve growth factor activation of nuclear factor kappaB through its p75 receptor is an anti-apoptotic signal in RN22 schwannoma cells. *J Biol Chem,* 275**,** 7558-65.

GEORGOPOULOS, C. & WELCH, W. J. 1993. Role of the major heat shock proteins as molecular chaperones. *Annu Rev Cell Biol,* 9**,** 601-34.

GIASSON, B. I., BRUENING, W., DURHAM, H. D. & MUSHYNSKI, W. E. 1999. Activation of stress-activated protein kinases correlates with neurite outgrowth induced by protease inhibition in PC12 cells. *J Neurochem,* 72**,** 1081-7.

GIBERT, B., HADCHITY, E., CZEKALLA, A., ALOY, M. T., COLAS, P., RODRIGUEZ-LAFRASSE, C., ARRIGO, A. P. & DIAZ-LATOUD, C. 2011. Inhibition of heat shock protein 27 (HspB1) tumorigenic functions by peptide aptamers. *Oncogene,* 30**,** 3672-81.

GIBERT, B., SIMON, S., DIMITROVA, V., DIAZ-LATOUD, C. & ARRIGO, A. P. 2013. Peptide aptamers: tools to negatively or positively modulate HSPB1(27) function. *Philos Trans R Soc Lond B Biol Sci,* 368**,** 20120075.

GILLEY, J., COFFER, P. J. & HAM, J. 2003. FOXO transcription factors directly activate bim gene expression and promote apoptosis in sympathetic neurons. *J Cell Biol,* 162**,** 613-22.

GLABE, C. G. 2008. Structural classification of toxic amyloid oligomers. *J Biol Chem,* 283**,** 29639-43.

GOATE, A., CHARTIER-HARLIN, M. C., MULLAN, M., BROWN, J., CRAWFORD, F., FIDANI, L., GIUFFRA, L., HAYNES, A., IRVING, N., JAMES, L. & ET AL. 1991. Segregation of a missense mutation in the amyloid precursor protein gene with familial Alzheimer's disease. *Nature,* 349**,** 704-6.

GOMEZ-BENITO, M., BALSAS, P., CARVAJAL-VERGARA, X., PANDIELLA, A., ANEL, A., MARZO, I. & NAVAL, J. 2007. Mechanism of apoptosis induced by IFN-alpha in human myeloma cells: role of Jak1 and Bim and potentiation by rapamycin. *Cell Signal,* 19**,** 844-54.

GORMAN, A. M., SZEGEZDI, E., QUIGNEY, D. J. & SAMALI, A. 2005. Hsp27 inhibits 6-hydroxydopamine-induced cytochrome c release and apoptosis in PC12 cells. *Biochem Biophys Res Commun,* 327**,** 801-10.

GROB, P. M., ROSS, A. H., KOPROWSKI, H. & BOTHWELL, M. 1985. Characterization of the human melanoma nerve growth factor receptor. *J Biol Chem,* 260**,** 8044-9.

GROSS, A., MCDONNELL, J. M. & KORSMEYER, S. J. 1999. BCL-2 family members and the mitochondria in apoptosis. *Genes Dev,* 13**,** 1899-911.

GUEROIS, R., NIELSEN, J. E. & SERRANO, L. 2002. Predicting changes in the stability of proteins and protein complexes: a study of more than 1000 mutations. *J Mol Biol,* 320**,** 369-87.

GUPTA, S., READ, D. E., DEEPTI, A., CAWLEY, K., GUPTA, A., OOMMEN, D., VERFAILLIE, T., MATUS, S., SMITH, M. A., MOTT, J. L., AGOSTINIS, P., HETZ, C. & SAMALI, A. 2012. Perk-dependent repression of miR-106b-25 cluster is required for ER stress-induced apoptosis. *Cell Death Dis,* 3**,** e333.

GUSEV, N. B., BOGATCHEVA, N. V. & MARSTON, S. B. 2002. Structure and properties of small heat shock proteins (sHsp) and their interaction with cytoskeleton proteins. *Biochemistry (Mosc),* 67**,** 511-9.

HALLBOOK, F., IBANEZ, C. F. & PERSSON, H. 1991. Evolutionary studies of the nerve growth factor family reveal a novel member abundantly expressed in Xenopus ovary. *Neuron,* 6**,** 845-58.

HALLBOOK, F., WILSON, K., THORNDYKE, M. & OLINSKI, R. P. 2006. Formation and evolution of the chordate neurotrophin and Trk receptor genes. *Brain Behav Evol.*

HANAHAN, D. & WEINBERG, R. A. 2000. The hallmarks of cancer. *Cell,* 100**,** 57-70.

HANAHAN, D. & WEINBERG, R. A. 2011. Hallmarks of cancer: the next generation. *Cell,* 144**,** 646-74.

HARRINGTON, A. W., KIM, J. Y. & YOON, S. O. 2002. Activation of Rac GTPase by p75 is necessary for c-jun N-terminal kinase-mediated apoptosis. *J Neurosci.*

HASLBECK, M., FRANZMANN, T., WEINFURTNER, D. & BUCHNER, J. 2005. Some like it hot: the structure and function of small heat-shock proteins. *Nat Struct Mol Biol,* 12**,** 842-6.

HAVASI, A., LI, Z., WANG, Z., MARTIN, J. L., BOTLA, V., RUCHALSKI, K., SCHWARTZ, J. H. & BORKAN, S. C. 2008. Hsp27 inhibits Bax activation and apoptosis via a phosphatidylinositol 3-kinase-dependent mechanism. *J Biol Chem,* 283**,** 12305-13.

HE, X. L. & GARCIA, K. C. 2004. Structure of nerve growth factor complexed with the shared neurotrophin receptor p75. *Science,* 304**,** 870-5.

HEMPSTEAD, B. L. 2006. Dissecting the diverse actions of pro- and mature neurotrophins. *Curr Alzheimer Res,* 3**,** 19-24.

HEMPSTEAD, B. L., MARTIN-ZANCA, D., KAPLAN, D. R., PARADA, L. F. & CHAO, M. V. 1991. High-affinity NGF binding requires coexpression of the trk proto-oncogene and the low-affinity NGF receptor. *Nature,* 350**,** 678-83.

HENGARTNER, M. O. 2000. The biochemistry of apoptosis. *Nature,* 407**,** 770-6.

HETZ, C. 2012. The unfolded protein response: controlling cell fate decisions under ER stress and beyond. *Nat Rev Mol Cell Biol,* 13**,** 89-102.

HONDERMARCK, H. 2012. Neurotrophins and their receptors in breast cancer. *Cytokine & Growth Factor Reviews,* 23**,** 357-365.

HORWITZ, J. 1992. Alpha-crystallin can function as a molecular chaperone. *Proc Natl Acad Sci U S A,* 89**,** 10449-53.

HOTCHKISS, R. S., STRASSER, A., MCDUNN, J. E. & SWANSON, P. E. 2009. Cell death. *N Engl J Med,* 361**,** 1570-83.

HOULDEN, H., LAURA, M., WAVRANT-DE VRIEZE, F., BLAKE, J., WOOD, N. & REILLY, M. M. 2008. Mutations in the HSP27 (HSPB1) gene cause dominant, recessive, and sporadic distal HMN/CMT type 2. *Neurology,* 71**,** 1660-8.

HSU, H., XIONG, J. & GOEDDEL, D. V. 1995. The TNF receptor 1-associated protein TRADD signals cell death and NF-kappa B activation. *Cell,* 81**,** 495-504.

HU, Y., LEE, X., SHAO, Z., APICCO, D., HUANG, G., GONG, B. J., PEPINSKY, R. B. & MI, S. 2013. A DR6/p75(NTR) complex is responsible for β-amyloid-induced cortical neuron death. *Cell Death Dis,* 4**,** e579.

HUANG, D. C. & STRASSER, A. 2000. BH3-Only proteins-essential initiators of apoptotic cell death. *Cell,* 103**,** 839-42.

HUANG, E. J. & REICHARDT, L. F. 2003. Trk receptors: roles in neuronal signal transduction. *Annu Rev Biochem,* 72**,** 609-42.

HUANG, Y. & MUCKE, L. 2012. Alzheimer mechanisms and therapeutic strategies. *Cell,* 148**,** 1204-22.

HUBNER, A., BARRETT, T., FLAVELL, R. A. & DAVIS, R. J. 2008. Multisite phosphorylation regulates Bim stability and apoptotic activity. *Mol Cell,* 30**,** 415-25.

HUOT, J., HOULE, F., SPITZ, D. R. & LANDRY, J. 1996. HSP27 phosphorylation-mediated resistance against actin fragmentation and cell death induced by oxidative stress. *Cancer Res,* 56**,** 273-9.

IBANEZ, C. F., EBENDAL, T., BARBANY, G., MURRAY-RUST, J., BLUNDELL, T. L. & PERSSON, H. 1992. Disruption of the low affinity receptor-binding site in

NGF allows neuronal survival and differentiation by binding to the trk gene product. *Cell,* 69**,** 329-41.

IGNEY, F. H. & KRAMMER, P. H. 2002. Death and anti-death: tumour resistance to apoptosis. *Nat Rev Cancer,* 2**,** 277-88.

INDO, Y., TSURUTA, M., HAYASHIDA, Y., KARIM, M. A., OHTA, K., KAWANO, T., MITSUBUCHI, H., TONOKI, H., AWAYA, Y. & MATSUDA, I. 1996. Mutations in the TRKA/NGF receptor gene in patients with congenital insensitivity to pain with anhidrosis. *Nat Genet,* 13**,** 485-8.

IRMADY, K., JACKMAN, K. A., PADOW, V. A., SHAHANI, N., MARTIN, L. A., CERCHIETTI, L., UNSICKER, K., IADECOLA, C. & HEMPSTEAD, B. L. 2014. Mir-592 regulates the induction and cell death-promoting activity of p75NTR in neuronal ischemic injury. *J Neurosci,* 34**,** 3419-28.

ITO, H., IWAMOTO, I., INAGUMA, Y., TAKIZAWA, T., NAGATA, K., ASANO, T. & KATO, K. 2005. Endoplasmic reticulum stress induces the phosphorylation of small heat shock protein, Hsp27. *J Cell Biochem,* 95**,** 932-41.

JARIEL-ENCONTRE, I., BOSSIS, G. & PIECHACZYK, M. 2008. Ubiquitin-independent degradation of proteins by the proteasome. *Biochim Biophys Acta,* 1786**,** 153-77.

JEZEQUEL, P., FRENEL, J. S., CAMPION, L., GUERIN-CHARBONNEL, C., GOURAUD, W., RICOLLEAU, G. & CAMPONE, M. 2013. bc-GenExMiner 3.0: new mining module computes breast cancer gene expression correlation analyses. *Database (Oxford),* 2013.

JOHNSON, D., LANAHAN, A., BUCK, C. R., SEHGAL, A., MORGAN, C., MERCER, E., BOTHWELL, M. & CHAO, M. 1986. Expression and structure of the human NGF receptor. *Cell,* 47**,** 545-54.

JOLLY, C. & MORIMOTO, R. I. 2000. Role of the heat shock response and molecular chaperones in oncogenesis and cell death. *J Natl Cancer Inst,* 92**,** 1564-72.

JONES, L. W., HAYKOWSKY, M., PEDDLE, C. J., JOY, A. A., PITUSKIN, E. N., TKACHUK, L. M., COURNEYA, K. S., SLAMON, D. J. & MACKEY, J. R. 2007. Cardiovascular risk profile of patients with HER2/neu-positive breast cancer treated with anthracycline-taxane-containing adjuvant chemotherapy and/or trastuzumab. *Cancer Epidemiol Biomarkers Prev,* 16**,** 1026-31.

KAMPINGA, H. H., HAGEMAN, J., VOS, M. J., KUBOTA, H., TANGUAY, R. M., BRUFORD, E. A., CHEETHAM, M. E., CHEN, B. & HIGHTOWER, L. E.

2009. Guidelines for the nomenclature of the human heat shock proteins. *Cell Stress Chaperones,* 14**,** 105-11.

KANNING, K. C., HUDSON, M., AMIEUX, P. S., WILEY, J. C., BOTHWELL, M. & SCHECTERSON, L. C. 2003. Proteolytic processing of the p75 neurotrophin receptor and two homologs generates C-terminal fragments with signaling capability. *Journal of Neuroscience,* 23**,** 5425-5436.

KAPLAN, D. R., HEMPSTEAD, B. L., MARTIN-ZANCA, D., CHAO, M. V. & PARADA, L. F. 1991. The trk proto-oncogene product: a signal transducing receptor for nerve growth factor. *Science,* 252**,** 554-8.

KASE, H., IWAHASHI, K. & MATSUDA, Y. 1986. K-252a, a potent inhibitor of protein kinase C from microbial origin. *J Antibiot (Tokyo),* 39**,** 1059-65.

KATAOKA, T., SCHROTER, M., HAHNE, M., SCHNEIDER, P., IRMLER, M., THOME, M., FROELICH, C. J. & TSCHOPP, J. 1998. FLIP prevents apoptosis induced by death receptors but not by perforin/granzyme B, chemotherapeutic drugs, and gamma irradiation. *J Immunol,* 161**,** 3936-42.

KATO, K., HASEGAWA, K., GOTO, S. & INAGUMA, Y. 1994. Dissociation as a result of phosphorylation of an aggregated form of the small stress protein, hsp27. *J Biol Chem,* 269**,** 11274-8.

KENNEDY, D., MNICH, K. & SAMALI, A. 2014. Heat shock preconditioning protects against ER stress-induced apoptosis through the regulation of the BH3-only protein BIM. *FEBS Open Bio,* 4**,** 813-21.

KERR, J. F., WYLLIE, A. H. & CURRIE, A. R. 1972. Apoptosis: a basic biological phenomenon with wide-ranging implications in tissue kinetics. *Br J Cancer,* 26**,** 239-57.

KHURSIGARA, G., BERTIN, J., YANO, H., MOFFETT, H., DISTEFANO, P. S. & CHAO, M. V. 2001. A prosurvival function for the p75 receptor death domain mediated via the caspase recruitment domain receptor-interacting protein 2. *J Neurosci.*

KHURSIGARA, G., ORLINICK, J. R. & CHAO, M. V. 1999. Association of the p75 neurotrophin receptor with TRAF6. *J Biol Chem,* 274**,** 2597-600.

KIM, K. K., KIM, R. & KIM, S. H. 1998. Crystal structure of a small heat-shock protein. *Nature,* 394**,** 595-9.

KISCHKEL, F. C., HELLBARDT, S., BEHRMANN, I., GERMER, M., PAWLITA, M., KRAMMER, P. H. & PETER, M. E. 1995. Cytotoxicity-dependent APO-1

(Fas/CD95)-associated proteins form a death-inducing signaling complex (DISC) with the receptor. *Embo j,* 14**,** 5579-88.

KLEIN, R., CONWAY, D., PARADA, L. F. & BARBACID, M. 1990. The trkB tyrosine protein kinase gene codes for a second neurogenic receptor that lacks the catalytic kinase domain. *Cell,* 61**,** 647-56.

KLEIN, R., JING, S. Q., NANDURI, V., O'ROURKE, E. & BARBACID, M. 1991. The trk proto-oncogene encodes a receptor for nerve growth factor. *Cell,* 65**,** 189-97.

KLIEMANNEL, M., GOLBIK, R., RUDOLPH, R., SCHWARZ, E. & LILIE, H. 2007. The pro-peptide of proNGF: structure formation and intramolecular association with NGF. *Protein Sci,* 16**,** 411-9.

KLIEMANNEL, M., RATTENHOLL, A., GOLBIK, R., BALBACH, J., LILIE, H., RUDOLPH, R. & SCHWARZ, E. 2004. The mature part of proNGF induces the structure of its pro-peptide. *FEBS Lett,* 566**,** 207-12.

KNOWLES, J. K., RAJADAS, J., NGUYEN, T. V., YANG, T., LEMIEUX, M. C., VANDER GRIEND, L., ISHIKAWA, C., MASSA, S. M., WYSS-CORAY, T. & LONGO, F. M. 2009. The p75 neurotrophin receptor promotes amyloid-beta(1-42)-induced neuritic dystrophy in vitro and in vivo. *J Neurosci,* 29**,** 10627-37.

KNOWLES, J. K., SIMMONS, D. A., NGUYEN, T. V., VANDER GRIEND, L., XIE, Y., ZHANG, H., YANG, T., POLLAK, J., CHANG, T., ARANCIO, O., BUCKWALTER, M. S., WYSS-CORAY, T., MASSA, S. M. & LONGO, F. M. 2013. Small molecule p75NTR ligand prevents cognitive deficits and neurite degeneration in an Alzheimer's mouse model. *Neurobiol Aging,* 34**,** 2052-63.

KOENIG, U., ECKHART, L. & TSCHACHLER, E. 2001. Evidence that caspase-13 is not a human but a bovine gene. *Biochem Biophys Res Commun,* 285**,** 1150-4.

KONISHI, H., MATSUZAKI, H., TANAKA, M., TAKEMURA, Y., KURODA, S., ONO, Y. & KIKKAWA, U. 1997. Activation of protein kinase B (Akt/RAC-protein kinase) by cellular stress and its association with heat shock protein Hsp27. *FEBS Lett,* 410**,** 493-8.

KROEMER, G., GALLUZZI, L., VANDENABEELE, P., ABRAMS, J., ALNEMRI, E. S., BAEHRECKE, E. H., BLAGOSKLONNY, M. V., EL-DEIRY, W. S., GOLSTEIN, P., GREEN, D. R., HENGARTNER, M., KNIGHT, R. A., KUMAR, S., LIPTON, S. A., MALORNI, W., NUNEZ, G., PETER, M. E., TSCHOPP, J., YUAN, J., PIACENTINI, M., ZHIVOTOVSKY, B. & MELINO,

G. 2009. Classification of cell death: recommendations of the Nomenclature Committee on Cell Death 2009. *Cell Death Differ,* 16**,** 3-11.

KRUTTGEN, A., SCHNEIDER, I. & WEIS, J. 2006. The dark side of the NGF family: Neurotrophins in neoplasias. *Brain Pathology,* 16**,** 304-310.

KRYGIER, S. & DJAKIEW, D. 2001. Molecular characterization of the loss of p75(NTR) expression in human prostate tumor cells. *Mol Carcinog.* United States: 2001 Wiley-Liss, Inc.

KRYGIER, S. & DJAKIEW, D. 2002. Neurotrophin receptor p75(NTR) suppresses growth and nerve growth factor-mediated metastasis of human prostate cancer cells. *Int J Cancer.* United States: 2001 Wiley-Liss, Inc.

KUDO, W., LEE, H. P., SMITH, M. A., ZHU, X., MATSUYAMA, S. & LEE, H. G. 2012. Inhibition of Bax protects neuronal cells from oligomeric Abeta neurotoxicity. *Cell Death Dis,* 3**,** e309.

KULTZ, D. 2003. Evolution of the cellular stress proteome: from monophyletic origin to ubiquitous function. *J Exp Biol,* 206**,** 3119-24.

KUMAR, V. & MAHAL, B. A. 2012. NGF - the TrkA to successful pain treatment. *J Pain Res,* 5**,** 279-87.

KURATA, M., YAMAZAKI, Y., KANNO, Y., ISHIBASHI, S., TAKAHARA, T., KITAGAWA, M. & NAKAMURA, T. 2011. Anti-apoptotic function of Xbp1 as an IL-3 signaling molecule in hematopoietic cells. *Cell Death Dis,* 2**,** e118.

LAD, S. P., NEET, K. E. & MUFSON, E. J. 2003. Nerve growth factor: structure, function and therapeutic implications for Alzheimer's disease. *Curr Drug Targets CNS Neurol Disord,* 2**,** 315-34.

LAGADEC, C., MEIGNAN, S., ADRIAENSSENS, E., FOVEAU, B., VANHECKE, E., ROMON, R., TOILLON, R. A., OXOMBRE, B., HONDERMARCK, H. & LE BOURHIS, X. 2009. TrkA overexpression enhances growth and metastasis of breast cancer cells. *Oncogene.*

LAMBERT, H., CHARETTE, S. J., BERNIER, A. F., GUIMOND, A. & LANDRY, J. 1999. HSP27 multimerization mediated by phosphorylation-sensitive intermolecular interactions at the amino terminus. *J Biol Chem,* 274**,** 9378-85.

LANDRETH, G. E. & SHOOTER, E. M. 1980. Nerve growth factor receptors on PC12 cells: ligand-induced conversion from low- to high-affinity states. *Proc Natl Acad Sci U S A,* 77**,** 4751-5.

LANDRY, J., CHRETIEN, P., LAMBERT, H., HICKEY, E. & WEBER, L. A. 1989. Heat shock resistance conferred by expression of the human HSP27 gene in rodent cells. *J Cell Biol,* 109**,** 7-15.

LANE, N. E., SCHNITZER, T. J., BIRBARA, C. A., MOKHTARANI, M., SHELTON, D. L., SMITH, M. D. & BROWN, M. T. 2010. Tanezumab for the treatment of pain from osteoarthritis of the knee. *N Engl J Med,* 363**,** 1521-31.

LANNEAU, D., WETTSTEIN, G., BONNIAUD, P. & GARRIDO, C. 2010. Heat shock proteins: cell protection through protein triage. *ScientificWorldJournal,* 10**,** 1543-52.

LAVOIE, J. N., LAMBERT, H., HICKEY, E., WEBER, L. A. & LANDRY, J. 1995. Modulation of cellular thermoresistance and actin filament stability accompanies phosphorylation-induced changes in the oligomeric structure of heat shock protein 27. *Mol Cell Biol,* 15**,** 505-16.

LEE, A. V., CUI, X. & OESTERREICH, S. 2001a. Cross-talk among estrogen receptor, epidermal growth factor, and insulin-like growth factor signaling in breast cancer. *Clin Cancer Res,* 7**,** 4429s-4435s; discussion 4411s-4412s.

LEE, R., KERMANI, P., TENG, K. K. & HEMPSTEAD, B. L. 2001b. Regulation of cell survival by secreted proneurotrophins. *Science,* 294**,** 1945-8.

LEI, K. & DAVIS, R. J. 2003. JNK phosphorylation of Bim-related members of the Bcl2 family induces Bax-dependent apoptosis. *Proc Natl Acad Sci U S A,* 100**,** 2432-7.

LEON, R., BHAGAVATULA, N., ULUKPO, O., MCCOLLUM, M. & WEI, J. 2010. BimEL as a possible molecular link between proteasome dysfunction and cell death induced by mutant huntingtin. *Eur J Neurosci,* 31**,** 1915-25.

LESSMANN, V., GOTTMANN, K. & MALCANGIO, M. 2003. Neurotrophin secretion: current facts and future prospects. *Prog Neurobiol,* 69**,** 341-74.

LETTRE, G. & HENGARTNER, M. O. 2006. Developmental apoptosis in C. elegans: a complex CEDnario. *Nat Rev Mol Cell Biol,* 7**,** 97-108.

LEVI-MONTALCINI, R. & ANGELETTI, P. U. 1968. Nerve growth factor. *Physiol Rev,* 48**,** 534-69.

LEY, R., BALMANNO, K., HADFIELD, K., WESTON, C. & COOK, S. J. 2003. Activation of the ERK1/2 signaling pathway promotes phosphorylation and proteasome-dependent degradation of the BH3-only protein, Bim. *J Biol Chem,* 278**,** 18811-6.

LEY, R., EWINGS, K. E., HADFIELD, K. & COOK, S. J. 2005. Regulatory phosphorylation of Bim: sorting out the ERK from the JNK. *Cell Death Differ.*

LI, H., ZHU, H., XU, C. J. & YUAN, J. 1998. Cleavage of BID by caspase 8 mediates the mitochondrial damage in the Fas pathway of apoptosis. *Cell,* 94**,** 491-501.

LINDQUIST, S. 1986. The heat-shock response. *Annu Rev Biochem,* 55**,** 1151-91.

LONGO, F. M. & MASSA, S. M. 2013. Small-molecule modulation of neurotrophin receptors: a strategy for the treatment of neurological disease. *Nat Rev Drug Discov,* 12**,** 507-25.

LORD, S., GHERSI, D., GATTELLARI, M., WORTLEY, S., WILCKEN, N. & SIMES, J. 2004. Antitumour antibiotic containing regimens for metastatic breast cancer. *Cochrane Database Syst Rev***,** Cd003367.

LUCIANO, F., JACQUEL, A., COLOSETTI, P., HERRANT, M., CAGNOL, S., PAGES, G. & AUBERGER, P. 2003. Phosphorylation of Bim-EL by Erk1/2 on serine 69 promotes its degradation via the proteasome pathway and regulates its proapoptotic function. *Oncogene,* 22**,** 6785-93.

MACRAE, T. H. 2000. Structure and function of small heat shock/alpha-crystallin proteins: established concepts and emerging ideas. *Cell Mol Life Sci,* 57**,** 899-913.

MAISONPIERRE, P. C., BELLUSCIO, L., SQUINTO, S., IP, N. Y., FURTH, M. E., LINDSAY, R. M. & YANCOPOULOS, G. D. 1990. Neurotrophin-3: a neurotrophic factor related to NGF and BDNF. *Science,* 247**,** 1446-51.

MARTINON, F., BURNS, K. & TSCHOPP, J. 2002. The inflammasome: a molecular platform triggering activation of inflammatory caspases and processing of proIL-beta. *Mol Cell,* 10**,** 417-26.

MARTINOU, J. C. & GREEN, D. R. 2001. Breaking the mitochondrial barrier. *Nat Rev Mol Cell Biol,* 2**,** 63-7.

MARTINVALET, D., ZHU, P. & LIEBERMAN, J. 2005. Granzyme A induces caspase-independent mitochondrial damage, a required first step for apoptosis. *Immunity,* 22**,** 355-70.

MASOUDI, R., IOANNOU, M. S., COUGHLIN, M. D., PAGADALA, P., NEET, K. E., CLEWES, O., ALLEN, S. J., DAWBARN, D. & FAHNESTOCK, M. 2009. Biological activity of nerve growth factor precursor is dependent upon relative levels of its receptors. *J Biol Chem,* 284**,** 18424-33.

MATTSON, M. P. 2000. Apoptosis in neurodegenerative disorders. *Nat Rev Mol Cell Biol,* 1**,** 120-130.

MCDONALD, N. Q., LAPATTO, R., MURRAY-RUST, J., GUNNING, J., WLODAWER, A. & BLUNDELL, T. L. 1991. New protein fold revealed by a 2.3-A resolution crystal structure of nerve growth factor. *Nature,* 354**,** 411-4.

MCILWAIN, D. R., BERGER, T. & MAK, T. W. 2013. Caspase functions in cell death and disease. *Cold Spring Harb Perspect Biol,* 5**,** a008656.

MCKELVEY, L., SHORTEN, G. D. & O'KEEFFE, G. W. 2013. Nerve growth factor-mediated regulation of pain signalling and proposed new intervention strategies in clinical pain management. *J Neurochem,* 124**,** 276-89.

MEHLEN, P., SCHULZE-OSTHOFF, K. & ARRIGO, A. P. 1996. Small stress proteins as novel regulators of apoptosis. Heat shock protein 27 blocks Fas/APO-1- and staurosporine-induced cell death. *J Biol Chem,* 271**,** 16510-4.

MINDE, J., TOOLANEN, G., ANDERSSON, T., NENNESMO, I., REMAHL, I. N., SVENSSON, O. & SOLDERS, G. 2004. Familial insensitivity to pain (HSAN V) and a mutation in the NGFB gene. A neurophysiological and pathological study. *Muscle Nerve,* 30**,** 752-60.

MIRON, T., VANCOMPERNOLLE, K., VANDEKERCKHOVE, J., WILCHEK, M. & GEIGER, B. 1991. A 25-kD inhibitor of actin polymerization is a low molecular mass heat shock protein. *J Cell Biol,* 114**,** 255-61.

MOLITORIS, J. K., MCCOLL, K. S. & DISTELHORST, C. W. 2011. Glucocorticoid-mediated repression of the oncogenic microRNA cluster miR-17~92 contributes to the induction of Bim and initiation of apoptosis. *Mol Endocrinol,* 25**,** 409-20.

MORIMOTO, R. I. 1993. Cells in stress: transcriptional activation of heat shock genes. *Science,* 259**,** 1409-10.

MORIMOTO, R. I. 1998. Regulation of the heat shock transcriptional response: cross talk between a family of heat shock factors, molecular chaperones, and negative regulators. *Genes Dev,* 12**,** 3788-96.

MOVASSAGH, M. & FOO, R. S. 2008. Simplified apoptotic cascades. *Heart Fail Rev,* 13**,** 111-9.

MUPPIDI, J. R., TSCHOPP, J. & SIEGEL, R. M. 2004. Life and death decisions: secondary complexes and lipid rafts in TNF receptor family signal transduction. *Immunity.*

MUTHALAGU, N., JUNTTILA, M. R., WIESE, K. E., WOLF, E., MORTON, J., BAUER, B., EVAN, G. I., EILERS, M. & MURPHY, D. J. 2014. BIM is the primary mediator of MYC-induced apoptosis in multiple solid tissues. *Cell Rep,* 8**,** 1347-53.

NADERI, A., LIU, J. & BENNETT, I. C. 2010a. BEX2 regulates mitochondrial apoptosis and G1 cell cycle in breast cancer. *Int J Cancer,* 126**,** 1596-610.

NADERI, A., LIU, J. & HUGHES-DAVIES, L. 2010b. BEX2 has a functional interplay with c-Jun/JNK and p65/RelA in breast cancer. *Mol Cancer.*

NADERI, A., TESCHENDORFF, A. E., BEIGEL, J., CARIATI, M., ELLIS, I. O., BRENTON, J. D. & CALDAS, C. 2007. BEX2 is overexpressed in a subset of primary breast cancers and mediates nerve growth factor/nuclear factor-kappaB inhibition of apoptosis in breast cancer cell lines. *Cancer Res.*

NAHTA, R., HORTOBAGYI, G. N. & ESTEVA, F. J. 2003. Growth factor receptors in breast cancer: potential for therapeutic intervention. *Oncologist,* 8**,** 5-17.

NAKADA, M., NAKADA, S., DEMUTH, T., TRAN, N. L., HOELZINGER, D. B. & BERENS, M. E. 2007. Molecular targets of glioma invasion. *Cell Mol Life Sci,* 64**,** 458-78.

NGUYEN, M., MILLAR, D. G., YONG, V. W., KORSMEYER, S. J. & SHORE, G. C. 1993. Targeting of Bcl-2 to the mitochondrial outer membrane by a COOH-terminal signal anchor sequence. *J Biol Chem,* 268**,** 25265-8.

NIEDERHAUSER, O., MANGOLD, M., SCHUBENEL, R., KUSZNIR, E. A., SCHMIDT, D. & HERTEL, C. 2000. NGF ligand alters NGF signaling via p75(NTR) and trkA. *J Neurosci Res.* United States: 2000 Wiley-Liss, Inc.

NOVER, L., BHARTI, K., DORING, P., MISHRA, S. K., GANGULI, A. & SCHARF, K. D. 2001. Arabidopsis and the heat stress transcription factor world: how many heat stress transcription factors do we need? *Cell Stress Chaperones,* 6**,** 177-89.

NYKJAER, A., LEE, R., TENG, K. K., JANSEN, P., MADSEN, P., NIELSEN, M. S., JACOBSEN, C., KLIEMANNEL, M., SCHWARZ, E., WILLNOW, T. E., HEMPSTEAD, B. L. & PETERSEN, C. M. 2004. Sortilin is essential for proNGF-induced neuronal cell death. *Nature,* 427**,** 843-8.

O'REILLY, L. A., CULLEN, L., VISVADER, J., LINDEMAN, G. J., PRINT, C., BATH, M. L., HUANG, D. C. & STRASSER, A. 2000. The proapoptotic BH3-only protein bim is expressed in hematopoietic, epithelial, neuronal, and germ cells. *Am J Pathol,* 157**,** 449-61.

OLSON, L., NORDBERG, A., VON HOLST, H., BÄCKMAN, L., EBENDAL, T., ALAFUZOFF, I., AMBERLA, K., HARTVIG, P., HERLITZ, A. & LILJA, A. 1992. Nerve growth factor affects 11C-nicotine binding, blood flow, EEG, and verbal episodic memory in an Alzheimer patient (case report). *J Neural Transm Park Dis Dement Sect,* 4**,** 79-95.

OLTERSDORF, T., ELMORE, S. W., SHOEMAKER, A. R., ARMSTRONG, R. C., AUGERI, D. J., BELLI, B. A., BRUNCKO, M., DECKWERTH, T. L., DINGES, J., HAJDUK, P. J., JOSEPH, M. K., KITADA, S., KORSMEYER, S. J., KUNZER, A. R., LETAI, A., LI, C., MITTEN, M. J., NETTESHEIM, D. G., NG, S., NIMMER, P. M., O'CONNOR, J. M., OLEKSIJEW, A., PETROS, A. M., REED, J. C., SHEN, W., TAHIR, S. K., THOMPSON, C. B., TOMASELLI, K. J., WANG, B., WENDT, M. D., ZHANG, H., FESIK, S. W. & ROSENBERG, S. H. 2005. An inhibitor of Bcl-2 family proteins induces regression of solid tumours. *Nature,* 435**,** 677-81.

OLTVAI, Z. N., MILLIMAN, C. L. & KORSMEYER, S. J. 1993. Bcl-2 heterodimerizes in vivo with a conserved homolog, Bax, that accelerates programmed cell death. *Cell,* 74**,** 609-19.

PANDEY, P., FARBER, R., NAKAZAWA, A., KUMAR, S., BHARTI, A., NALIN, C., WEICHSELBAUM, R., KUFE, D. & KHARBANDA, S. 2000. Hsp27 functions as a negative regulator of cytochrome c-dependent activation of procaspase-3. *Oncogene,* 19**,** 1975-81.

PARCELLIER, A., SCHMITT, E., GURBUXANI, S., SEIGNEURIN-BERNY, D., PANCE, A., CHANTOME, A., PLENCHETTE, S., KHOCHBIN, S., SOLARY, E. & GARRIDO, C. 2003. HSP27 is a ubiquitin-binding protein involved in I-kappaBalpha proteasomal degradation. *Mol Cell Biol,* 23**,** 5790-802.

PARSELL, D. A., TAULIEN, J. & LINDQUIST, S. 1993. The role of heat-shock proteins in thermotolerance. *Philos Trans R Soc Lond B Biol Sci,* 339**,** 279-85; discussion 285-6.

PASCUAL-SALCEDO, D., PLASENCIA, C., RAMIRO, S., NUNO, L., BONILLA, G., NAGORE, D., RUIZ DEL AGUA, A., MARTINEZ, A., AARDEN, L., MARTIN-MOLA, E. & BALSA, A. 2011. Influence of immunogenicity on the efficacy of long-term treatment with infliximab in rheumatoid arthritis. *Rheumatology (Oxford),* 50**,** 1445-52.

PATANI, N., JIANG, W. G. & MOKBEL, K. 2011. Brain-derived neurotrophic factor expression predicts adverse pathological & clinical outcomes in human breast cancer. *Cancer Cell Int.*

PATAPOUTIAN, A. & REICHARDT, L. F. 2001. Trk receptors: mediators of neurotrophin action. *Curr Opin Neurobiol,* 11**,** 272-80.

PAUL, C., MANERO, F., GONIN, S., KRETZ-REMY, C., VIROT, S. & ARRIGO, A. P. 2002. Hsp27 as a negative regulator of cytochrome C release. *Mol Cell Biol,* 22**,** 816-34.

PEHAR, M., CASSINA, P., VARGAS, M. R., XIE, Y., BECKMAN, J. S., MASSA, S. M., LONGO, F. M. & BARBEITO, L. 2006. Modulation of p75-dependent motor neuron death by a small non-peptidyl mimetic of the neurotrophin loop 1 domain. *Eur J Neurosci,* 24**,** 1575-80.

PEROU, C. M., SORLIE, T., EISEN, M. B., VAN DE RIJN, M., JEFFREY, S. S., REES, C. A., POLLACK, J. R., ROSS, D. T., JOHNSEN, H., AKSLEN, L. A., FLUGE, O., PERGAMENSCHIKOV, A., WILLIAMS, C., ZHU, S. X., LONNING, P. E., BORRESEN-DALE, A. L., BROWN, P. O. & BOTSTEIN, D. 2000. Molecular portraits of human breast tumours. *Nature,* 406**,** 747-52.

PETERSON, S. & BOGENMANN, E. 2003. Osmotic swelling induces p75 neurotrophin receptor (p75NTR) expression via nitric oxide. *J Biol Chem,* 278**,** 33943-50.

PISTRITTO, G., JOST, M., SRINIVASULA, S. M., BAFFA, R., POYET, J. L., KARI, C., LAZEBNIK, Y., RODECK, U. & ALNEMRI, E. S. 2002. Expression and transcriptional regulation of caspase-14 in simple and complex epithelia. *Cell Death Differ,* 9**,** 995-1006.

PODUSLO, J. F. & CURRAN, G. L. 1996. Permeability at the blood-brain and blood-nerve barriers of the neurotrophic factors: NGF, CNTF, NT-3, BDNF. *Brain Res Mol Brain Res,* 36**,** 280-6.

POP, C. & SALVESEN, G. S. 2009. Human caspases: activation, specificity, and regulation. *J Biol Chem,* 284**,** 21777-81.

PREVILLE, X., SCHULTZ, H., KNAUF, U., GAESTEL, M. & ARRIGO, A. P. 1998. Analysis of the role of Hsp25 phosphorylation reveals the importance of the oligomerization state of this small heat shock protein in its protective function against TNFalpha- and hydrogen peroxide-induced cell death. *J Cell Biochem,* 69**,** 436-52.

PUTCHA, G. V., LE, S., FRANK, S., BESIRLI, C. G., CLARK, K., CHU, B., ALIX, S., YOULE, R. J., LAMARCHE, A., MARONEY, A. C. & JOHNSON, E. M., JR. 2003. JNK-mediated BIM phosphorylation potentiates BAX-dependent apoptosis. *Neuron,* 38**,** 899-914.

PUTHALAKATH, H., HUANG, D. C., O'REILLY, L. A., KING, S. M. & STRASSER, A. 1999. The proapoptotic activity of the Bcl-2 family member Bim is regulated by interaction with the dynein motor complex. *Mol Cell,* 3**,** 287-96.

PUTHALAKATH, H., O'REILLY, L. A., GUNN, P., LEE, L., KELLY, P. N., HUNTINGTON, N. D., HUGHES, P. D., MICHALAK, E. M., MCKIMM-BRESCHKIN, J., MOTOYAMA, N., GOTOH, T., AKIRA, S., BOUILLET, P. & STRASSER, A. 2007. ER stress triggers apoptosis by activating BH3-only protein Bim. *Cell,* 129**,** 1337-49.

QI, S., XIN, Y., QI, Z., XU, Y., DIAO, Y., LAN, L., LUO, L. & YIN, Z. 2014. HSP27 phosphorylation modulates TRAIL-induced activation of Src-Akt/ERK signaling through interaction with beta-arrestin2. *Cell Signal,* 26**,** 594-602.

QI, X. J., WILDEY, G. M. & HOWE, P. H. 2006. Evidence that Ser87 of BimEL is phosphorylated by Akt and regulates BimEL apoptotic function. *J Biol Chem,* 281**,** 813-23.

QIAN, L., VAN LAAKE, L. W., HUANG, Y., LIU, S., WENDLAND, M. F. & SRIVASTAVA, D. 2011. miR-24 inhibits apoptosis and represses Bim in mouse cardiomyocytes. *J Exp Med,* 208**,** 549-60.

QUANN, E. J., KHWAJA, F., ZAVITZ, K. H. & DJAKIEW, D. 2007. The aryl propionic acid R-flurbiprofen selectively induces p75NTR-dependent decreased survival of prostate tumor cells. *Cancer Res,* 67**,** 3254-62.

RABIZADEH, S., BITLER, C. M., BUTCHER, L. L. & BREDESEN, D. E. 1994. Expression of the low-affinity nerve growth factor receptor enhances beta-amyloid peptide toxicity. *Proc Natl Acad Sci U S A,* 91**,** 10703-6.

RAMAGE, P., CHENEVAL, D., CHVEI, M., GRAFF, P., HEMMIG, R., HENG, R., KOCHER, H. P., MACKENZIE, A., MEMMERT, K., REVESZ, L. & ET AL. 1995. Expression, refolding, and autocatalytic proteolytic processing of the interleukin-1 beta-converting enzyme precursor. *J Biol Chem,* 270**,** 9378-83.

RAMOS, A., HO, W. C., FORTE, S., DICKSON, K., BOUTILIER, J., FAVELL, K. & BARKER, P. A. 2007. Hypo-osmolar stress induces p75NTR expression by activating Sp1-dependent transcription. *J Neurosci,* 27**,** 1498-506.

RANE, M. J., PAN, Y., SINGH, S., POWELL, D. W., WU, R., CUMMINS, T., CHEN, Q., MCLEISH, K. R. & KLEIN, J. B. 2003. Heat shock protein 27 controls apoptosis by regulating Akt activation. *J Biol Chem,* 278**,** 27828-35.

RATTENHOLL, A., RUOPPOLO, M., FLAGIELLO, A., MONTI, M., VINCI, F., MARINO, G., LILIE, H., SCHWARZ, E. & RUDOLPH, R. 2001. Pro-sequence assisted folding and disulfide bond formation of human nerve growth factor. *J Mol Biol,* 305**,** 523-33.

REICHARDT, L. F. 2006. Neurotrophin-regulated signalling pathways. *Philos Trans R Soc Lond B Biol Sci,* 361**,** 1545-64.

REIS-FILHO, J. S., STEELE, D., DI PALMA, S., JONES, R. L., SAVAGE, K., JAMES, M., MILANEZI, F., SCHMITT, F. C. & ASHWORTH, A. 2006. Distribution and significance of nerve growth factor receptor (NGFR/p75NTR) in normal, benign and malignant breast tissue. *Mod Pathol,* 19**,** 307-19.

RICHTER, K., HASLBECK, M. & BUCHNER, J. 2010. The heat shock response: life on the verge of death. *Mol Cell,* 40**,** 253-66.

RITOSSA, F. 1996. Discovery of the heat shock response. *Cell Stress Chaperones,* 1**,** 97-8.

ROBITAILLE, H., SIMARD-BISSON, C., LAROUCHE, D., TANGUAY, R. M., BLOUIN, R. & GERMAIN, L. 2010. The small heat-shock protein Hsp27 undergoes ERK-dependent phosphorylation and redistribution to the cytoskeleton in response to dual leucine zipper-bearing kinase expression. *J Invest Dermatol,* 130**,** 74-85.

ROMON, R., ADRIAENSSENS, E., LAGADEC, C., GERMAIN, E., HONDERMARCK, H. & LE BOURHIS, X. 2010. Nerve growth factor promotes breast cancer angiogenesis by activating multiple pathways. *Mol Cancer.*

ROUSE, J., COHEN, P., TRIGON, S., MORANGE, M., ALONSO-LLAMAZARES, A., ZAMANILLO, D., HUNT, T. & NEBREDA, A. R. 1994. A novel kinase cascade triggered by stress and heat shock that stimulates MAPKAP kinase-2 and phosphorylation of the small heat shock proteins. *Cell,* 78**,** 1027-37.

ROUX, P. P. & BARKER, P. A. 2002. Neurotrophin signaling through the p75 neurotrophin receptor. *Progress in Neurobiology,* 67**,** 203-233.

ROUX, P. P., COLICOS, M. A., BARKER, P. A. & KENNEDY, T. E. 1999. p75 neurotrophin receptor expression is induced in apoptotic neurons after seizure. *J Neurosci,* 19**,** 6887-96.

SALARI, S., SEIBERT, T., CHEN, Y. X., HU, T., SHI, C., ZHAO, X., CUERRIER, C. M., RAIZMAN, J. E. & O'BRIEN, E. R. 2013. Extracellular HSP27 acts as a signaling molecule to activate NF-kappaB in macrophages. *Cell Stress Chaperones,* 18**,** 53-63.

SALTZMAN, W. M., MAK, M. W., MAHONEY, M. J., DUENAS, E. T. & CLELAND, J. L. 1999. Intracranial delivery of recombinant nerve growth factor: release kinetics and protein distribution for three delivery systems. *Pharm Res,* 16**,** 232-40.

SAMALI, A., FULDA, S., GORMAN, A. M., HORI, O. & SRINIVASULA, S. M. 2010. Cell stress and cell death. *Int J Cell Biol,* 2010**,** 245803.

SAMALI, A., ROBERTSON, J. D., PETERSON, E., MANERO, F., VAN ZEIJL, L., PAUL, C., COTGREAVE, I. A., ARRIGO, A. P. & ORRENIUS, S. 2001. Hsp27 protects mitochondria of thermotolerant cells against apoptotic stimuli. *Cell Stress Chaperones,* 6**,** 49-58.

SANPHUI, P. & BISWAS, S. C. 2013. FoxO3a is activated and executes neuron death via Bim in response to beta-amyloid. *Cell Death Dis,* 4**,** e625.

SCHNEIDER, R. & SCHWEIGER, M. 1991. A novel modular mosaic of cell adhesion motifs in the extracellular domains of the neurogenic trk and trkB tyrosine kinase receptors. *Oncogene,* 6**,** 1807-11.

SCOTT, S. A., MUFSON, E. J., WEINGARTNER, J. A., SKAU, K. A. & CRUTCHER, K. A. 1995. Nerve growth factor in Alzheimer's disease: increased levels throughout the brain coupled with declines in nucleus basalis. *J Neurosci,* 15**,** 6213-21.

SEIDAH, N. G., BENJANNET, S., PAREEK, S., SAVARIA, D., HAMELIN, J., GOULET, B., LALIBERTE, J., LAZURE, C., CHRETIEN, M. & MURPHY, R. A. 1996. Cellular processing of the nerve growth factor precursor by the mammalian pro-protein convertases. *Biochem J,* 314 (Pt 3)**,** 951-60.

SELKOE, D. J. 2001. Presenilin, Notch, and the genesis and treatment of Alzheimer's disease. *Proc Natl Acad Sci U S A,* 98**,** 11039-41.

SESSLER, T., HEALY, S., SAMALI, A. & SZEGEZDI, E. 2013. Structural determinants of DISC function: new insights into death receptor-mediated apoptosis signalling. *Pharmacol Ther,* 140**,** 186-99.

SHARP, P. S., AKBAR, M. T., BOURI, S., SENDA, A., JOSHI, K., CHEN, H. J., LATCHMAN, D. S., WELLS, D. J. & DE BELLEROCHE, J. 2008. Protective effects of heat shock protein 27 in a model of ALS occur in the early stages of disease progression. *Neurobiol Dis,* 30**,** 42-55.

SHI, Y. 2004. Caspase activation: revisiting the induced proximity model. *Cell,* 117**,** 855-8.

SHIN, K. D., LEE, M. Y., SHIN, D. S., LEE, S., SON, K. H., KOH, S., PAIK, Y. K., KWON, B. M. & HAN, D. C. 2005. Blocking tumor cell migration and invasion with biphenyl isoxazole derivative KRIBB3, a synthetic molecule that inhibits Hsp27 phosphorylation. *J Biol Chem,* 280**,** 41439-48.

SHOOTER, E. M. 2001. Early days of the nerve growth factor proteins. *Annu Rev Neurosci,* 24**,** 601-29.

SIGALA, S., BODEI, S., MISSALE, C., ZANI, D., SIMEONE, C., CUNICO, S. C. & SPANO, P. F. 2008. Gene expression profile of prostate cancer cell lines: effect of nerve growth factor treatment. *Mol Cell Endocrinol,* 284**,** 11-20.

SIMMONS, D. A., KNOWLES, J. K., BELICHENKO, N. P., BANERJEE, G., FINKLE, C., MASSA, S. M. & LONGO, F. M. 2014. A small molecule p75NTR ligand, LM11A-31, reverses cholinergic neurite dystrophy in Alzheimer's disease mouse models with mid- to late-stage disease progression. *PLoS One,* 9**,** e102136.

SKELDAL, S., MATUSICA, D., NYKJAER, A. & COULSON, E. J. 2011. Proteolytic processing of the p75 neurotrophin receptor: A prerequisite for signalling?: Neuronal life, growth and death signalling are crucially regulated by intra-membrane proteolysis and trafficking of p75(NTR). *Bioessays,* 33**,** 614-25.

SONG, X. Y., HU, J. F., SUN, M. N., LI, Z. P., WU, D. H., JI, H. J., YUAN, Y. H., ZHU, Z. X., HAN, N., LIU, G. & CHEN, N. H. 2013. IMM-H004, a novel coumarin derivative compound, protects against amyloid beta-induced neurotoxicity through a mitochondrial-dependent pathway. *Neuroscience,* 242**,** 28-38.

SOO, K. Y., ATKIN, J. D., FARG, M., WALKER, A. K., HORNE, M. K. & NAGLEY, P. 2012. Bim links ER stress and apoptosis in cells expressing mutant SOD1 associated with amyotrophic lateral sclerosis. *PLoS One,* 7**,** e35413.

SORLIE, T., PEROU, C. M., TIBSHIRANI, R., AAS, T., GEISLER, S., JOHNSEN, H., HASTIE, T., EISEN, M. B., VAN DE RIJN, M., JEFFREY, S. S., THORSEN, T., QUIST, H., MATESE, J. C., BROWN, P. O., BOTSTEIN, D., LONNING, P. E. & BORRESEN-DALE, A. L. 2001. Gene expression patterns of breast carcinomas distinguish tumor subclasses with clinical implications. *Proc Natl Acad Sci U S A,* 98**,** 10869-74.

STINE, W. B., JR., DAHLGREN, K. N., KRAFFT, G. A. & LADU, M. J. 2003. In vitro characterization of conditions for amyloid-beta peptide oligomerization and fibrillogenesis. *J Biol Chem,* 278**,** 11612-22.

STOKOE, D., ENGEL, K., CAMPBELL, D. G., COHEN, P. & GAESTEL, M. 1992. Identification of MAPKAP kinase 2 as a major enzyme responsible for the phosphorylation of the small mammalian heat shock proteins. *FEBS Lett,* 313**,** 307-13.

SUN, X., FONTAINE, J. M., REST, J. S., SHELDEN, E. A., WELSH, M. J. & BENNDORF, R. 2004. Interaction of human HSP22 (HSPB8) with other small heat shock proteins. *J Biol Chem,* 279**,** 2394-402.

SUN, X., OU, Z., XIE, M., KANG, R., FAN, Y., NIU, X., WANG, H., CAO, L. & TANG, D. 2015. HSPB1 as a novel regulator of ferroptotic cancer cell death. *Oncogene*.

SUN, Y. & MACRAE, T. H. 2005. Small heat shock proteins: molecular structure and chaperone function. *Cell Mol Life Sci,* 62**,** 2460-76.

SUTER, U., HEYMACH, J. V., JR. & SHOOTER, E. M. 1991. Two conserved domains in the NGF propeptide are necessary and sufficient for the biosynthesis of correctly processed and biologically active NGF. *Embo j,* 10**,** 2395-400.

SZEGEZDI, E., HERBERT, K. R., KAVANAGH, E. T., SAMALI, A. & GORMAN, A. M. 2008. Nerve growth factor blocks thapsigargin-induced apoptosis at the level of the mitochondrion via regulation of Bim. *J Cell Mol Med,* 12**,** 2482-96.

TAIT, S. W. & GREEN, D. R. 2010. Mitochondria and cell death: outer membrane permeabilization and beyond. *Nat Rev Mol Cell Biol,* 11**,** 621-32.

TAPLEY, P., LAMBALLE, F. & BARBACID, M. 1992. K252a is a selective inhibitor of the tyrosine protein kinase activity of the trk family of oncogenes and neurotrophin receptors. *Oncogene,* 7**,** 371-81.

TAYLOR, R. C., CULLEN, S. P. & MARTIN, S. J. 2008. Apoptosis: controlled demolition at the cellular level. *Nat Rev Mol Cell Biol,* 9**,** 231-41.

TAYLOR, R. P. & BENJAMIN, I. J. 2005. Small heat shock proteins: a new classification scheme in mammals. *J Mol Cell Cardiol,* 38**,** 433-44.

TENG, H. K., TENG, K. K., LEE, R., WRIGHT, S., TEVAR, S., ALMEIDA, R. D., KERMANI, P., TORKIN, R., CHEN, Z. Y., LEE, F. S., KRAEMER, R. T., NYKJAER, A. & HEMPSTEAD, B. L. 2005. ProBDNF induces neuronal apoptosis via activation of a receptor complex of p75NTR and sortilin. *J Neurosci.*

THERIAULT, J. R., LAMBERT, H., CHAVEZ-ZOBEL, A. T., CHAREST, G., LAVIGNE, P. & LANDRY, J. 2004. Essential role of the NH2-terminal WD/EPF motif in the phosphorylation-activated protective function of mammalian Hsp27. *J Biol Chem,* 279**,** 23463-71.

THOMAS, M. P. & LIEBERMAN, J. 2013. Live or let die: posttranscriptional gene regulation in cell stress and cell death. *Immunol Rev,* 253**,** 237-52.

THORNBERRY, N. A., RANO, T. A., PETERSON, E. P., RASPER, D. M., TIMKEY, T., GARCIA-CALVO, M., HOUTZAGER, V. M., NORDSTROM, P. A., ROY, S., VAILLANCOURT, J. P., CHAPMAN, K. T. & NICHOLSON, D. W. 1997. A combinatorial approach defines specificities of members of the caspase family and granzyme B. Functional relationships established for key mediators of apoptosis. *J Biol Chem,* 272**,** 17907-11.

TINEL, A. & TSCHOPP, J. 2004. The PIDDosome, a protein complex implicated in activation of caspase-2 in response to genotoxic stress. *Science,* 304**,** 843-6.

TRUZZI, F., MARCONI, A., LOTTI, R., DALLAGLIO, K., FRENCH, L. E., HEMPSTEAD, B. L. & PINCELLI, C. 2008. Neurotrophins and their receptors stimulate melanoma cell proliferation and migration. *J Invest Dermatol.*

TUR, V., VAN DER SLOOT, A. M., REIS, C. R., SZEGEZDI, E., COOL, R. H., SAMALI, A., SERRANO, L. & QUAX, W. J. 2008. DR4-selective tumor necrosis factor-related apoptosis-inducing ligand (TRAIL) variants obtained by structure-based design. *J Biol Chem,* 283**,** 20560-8.

TUSZYNSKI, M. H., THAL, L., PAY, M., SALMON, D. P., U, H. S., BAKAY, R., PATEL, P., BLESCH, A., VAHLSING, H. L., HO, G., TONG, G., POTKIN, S. G., FALLON, J., HANSEN, L., MUFSON, E. J., KORDOWER, J. H., GALL, C. & CONNER, J. 2005. A phase 1 clinical trial of nerve growth factor gene therapy for Alzheimer disease. *Nat Med,* 11**,** 551-5.

U, M., MIYASHITA, T., SHIKAMA, Y., TADOKORO, K. & YAMADA, M. 2001. Molecular cloning and characterization of six novel isoforms of human Bim, a member of the proapoptotic Bcl-2 family. *FEBS Lett,* 509**,** 135-41.

URRA, S., ESCUDERO, C. A., RAMOS, P., LISBONA, F., ALLENDE, E., COVARRUBIAS, P., PARRAGUEZ, J. I., ZAMPIERI, N., CHAO, M. V., ANNAERT, W. & BRONFMAN, F. C. 2007a. TrkA receptor activation by nerve growth factor induces shedding of the p75 neurotrophin receptor followed by endosomal gamma-secretase-mediated release of the p75 intracellular domain. *J Biol Chem,* 282**,** 7606-15.

URRA, S., ESCUDERO, C. A., RAMOS, P., LISBONA, F., ALLENDE, E., COVARRUBIAS, P., PARRAGUEZ, J. I., ZAMPIERI, N., CHAO, M. V., ANNAERT, W. & BRONFMAN, F. C. 2007b. TrkA receptor activation by nerve growth factor induces shedding of the p75 neurotrophin receptor followed by endosomal gamma-secretase-mediated release of the p75 intracellular domain. *J Biol Chem.*.

VAN DELFT, M. F. & HUANG, D. C. 2006. How the Bcl-2 family of proteins interact to regulate apoptosis. *Cell Res,* 16**,** 203-13.

VAN DER SLOOT, A. M., TUR, V., SZEGEZDI, E., MULLALLY, M. M., COOL, R. H., SAMALI, A., SERRANO, L. & QUAX, W. J. 2006. Designed tumor necrosis factor-related apoptosis-inducing ligand variants initiating apoptosis exclusively via the DR5 receptor. *Proc Natl Acad Sci U S A,* 103**,** 8634-9.

VANHECKE, E., ADRIAENSSENS, E., VERBEKE, S., MEIGNAN, S., GERMAIN, E., BERTEAUX, N., NURCOMBE, V., LE BOURHIS, X. & HONDERMARCK, H. 2011. Brain-derived neurotrophic factor and neurotrophin-4/5 are expressed in breast cancer and can be targeted to inhibit tumor cell survival. *Clin Cancer Res.*

VERBEKE, S., MEIGNAN, S., LAGADEC, C., GERMAIN, E., HONDERMARCK, H., ADRIAENSSENS, E. & LE BOURHIS, X. 2010. Overexpression of p75(NTR) increases survival of breast cancer cells through p21(waf1). *Cellular Signalling,* 22**,** 1864-1873.

VERBEKE, S., TOMELLINI, E., DHAMANI, F., MEIGNAN, S., ADRIAENSSENS, E. & XUEFEN, L. B. 2013. Extracellular cleavage of the p75 neurotrophin receptor is implicated in its pro-survival effect in breast cancer cells. *FEBS Lett,* 587**,** 2591-6.

VILAR, M., CHARALAMPOPOULOS, I., KENCHAPPA, R. S., SIMI, A., KARACA, E., REVERSI, A., CHOI, S., BOTHWELL, M., MINGARRO, I., FRIEDMAN, W. J., SCHIAVO, G., BASTIAENS, P. I., VERVEER, P. J., CARTER, B. D. & IBANEZ, C. F. 2009. Activation of the p75 neurotrophin receptor through conformational rearrangement of disulphide-linked receptor dimers. *Neuron,* 62**,** 72-83.

VILAR, M., MURILLO-CARRETERO, M., MIRA, H., MAGNUSSON, K., BESSET, V. & IBANEZ, C. F. 2006. Bex1, a novel interactor of the p75 neurotrophin receptor, links neurotrophin signaling to the cell cycle. *EMBO J.*

VOS, M. J., HAGEMAN, J., CARRA, S. & KAMPINGA, H. H. 2008. Structural and functional diversities between members of the human HSPB, HSPH, HSPA, and DNAJ chaperone families. *Biochemistry,* 47**,** 7001-11.

VROEGOP, S., DECKER, D., HINZMANN, J., POORMAN, R. & BUXSER, S. 1992. Probing the structure-function relationship of nerve growth factor. *J Protein Chem,* 11**,** 71-82.

WAHLBERG, L. U., LIND, G., ALMQVIST, P. M., KUSK, P., TORNOE, J., JULIUSSON, B., SODERMAN, M., SELLDEN, E., SEIGER, A., ERIKSDOTTER-JONHAGEN, M. & LINDEROTH, B. 2012. Targeted delivery of nerve growth factor via encapsulated cell biodelivery in Alzheimer disease: a technology platform for restorative neurosurgery. *J Neurosurg,* 117**,** 340-7.

WAJANT, H. 2002. The Fas signaling pathway: more than a paradigm. *Science,* 296**,** 1635-6.

WANG, J. & LENARDO, M. J. 2000. Roles of caspases in apoptosis, development, and cytokine maturation revealed by homozygous gene deficiencies. *J Cell Sci,* 113 (Pt 5)**,** 753-7.

WANG, L., RAHN, J. J., LUN, X., SUN, B., KELLY, J. J., WEISS, S., ROBBINS, S. M., FORSYTH, P. A. & SENGER, D. L. 2008. Gamma-secretase represents a therapeutic target for the treatment of invasive glioma mediated by the p75 neurotrophin receptor. *PLoS Biol,* 6**,** e289.

WANG, X., CUI, M., WANG, L., CHEN, X. & XIN, P. 2010. Inhibition of neurotrophin receptor p75 intramembran proteolysis by gamma-secretase inhibitor reduces medulloblastoma spinal metastasis. *Biochem Biophys Res Commun.* United States: 2010 Elsevier Inc.

WARRINGTON, R. J. & LEWIS, K. E. 2011. Natural antibodies against nerve growth factor inhibit in vitro prostate cancer cell metastasis. *Cancer Immunol Immunother,* 60**,** 187-95.

WEERARATNA, A. T., ARNOLD, J. T., GEORGE, D. J., DEMARZO, A. & ISAACS, J. T. 2000. Rational basis for Trk inhibition therapy for prostate cancer. *Prostate.* United States: 2000 Wiley-Liss, Inc.

WEHRMAN, T., HE, X., RAAB, B., DUKIPATTI, A., BLAU, H. & GARCIA, K. C. 2007. Structural and mechanistic insights into nerve growth factor interactions with the TrkA and p75 receptors. *Neuron,* 53**,** 25-38.

WELCH, W. J. 1993. Heat shock proteins functioning as molecular chaperones: their roles in normal and stressed cells. *Philos Trans R Soc Lond B Biol Sci,* 339**,** 327-33.

WESKAMP, G., SCHLONDORFF, J., LUM, L., BECHERER, J. D., KIM, T. W., SAFTIG, P., HARTMANN, D., MURPHY, G. & BLOBEL, C. P. 2004. Evidence for a critical role of the tumor necrosis factor alpha convertase (TACE) in ectodomain shedding of the p75 neurotrophin receptor (p75NTR). *J Biol Chem,* 279**,** 4241-9.

WESTERHEIDE, S. D. & MORIMOTO, R. I. 2005. Heat shock response modulators as therapeutic tools for diseases of protein conformation. *J Biol Chem,* 280**,** 33097-100.

WIESMANN, C. & DE VOS, A. M. 2001. Nerve growth factor: structure and function. *Cell Mol Life Sci,* 58**,** 748-59.

WIESMANN, C., ULTSCH, M. H., BASS, S. H. & DE VOS, A. M. 1999. Crystal structure of nerve growth factor in complex with the ligand-binding domain of the TrkA receptor. *Nature,* 401**,** 184-8.

XU, L., CHEN, S. & BERGAN, R. C. 2006. MAPKAPK2 and HSP27 are downstream effectors of p38 MAP kinase-mediated matrix metalloproteinase type 2 activation and cell invasion in human prostate cancer. *Oncogene,* 25**,** 2987-98.

YAAR, M., ZHAI, S., FINE, R. E., EISENHAUER, P. B., ARBLE, B. L., STEWART, K. B. & GILCHREST, B. A. 2002. Amyloid beta binds trimers as well as monomers of the 75-kDa neurotrophin receptor and activates receptor signaling. *J Biol Chem,* 277**,** 7720-5.

YAAR, M., ZHAI, S., PILCH, P. F., DOYLE, S. M., EISENHAUER, P. B., FINE, R. E. & GILCHREST, B. A. 1997. Binding of beta-amyloid to the p75 neurotrophin

receptor induces apoptosis. A possible mechanism for Alzheimer's disease. *J Clin Invest,* 100**,** 2333-40.

YAGLOM, J., O'CALLAGHAN-SUNOL, C., GABAI, V. & SHERMAN, M. Y. 2003. Inactivation of dual-specificity phosphatases is involved in the regulation of extracellular signal-regulated kinases by heat shock and hsp72. *Mol Cell Biol,* 23**,** 3813-24.

YAMASHITA, T. & TOHYAMA, M. 2003a. The p75 receptor acts as a displacement factor that releases Rho from Rho-GDI. *Nat Neurosci,* 6**,** 461-7.

YAMASHITA, T. & TOHYAMA, M. 2003b. The p75 receptor acts as a displacement factor that releases Rho from Rho-GDI. *Nat Neurosci.*

YAMIN, T. T., AYALA, J. M. & MILLER, D. K. 1996. Activation of the native 45-kDa precursor form of interleukin-1-converting enzyme. *J Biol Chem,* 271**,** 13273-82.

YANG, T., KNOWLES, J. K., LU, Q., ZHANG, H., ARANCIO, O., MOORE, L. A., CHANG, T., WANG, Q., ANDREASSON, K., RAJADAS, J., FULLER, G. G., XIE, Y., MASSA, S. M. & LONGO, F. M. 2008. Small molecule, non-peptide p75 ligands inhibit Abeta-induced neurodegeneration and synaptic impairment. *PLoS One,* 3**,** e3604.

YE, X., MEHLEN, P., RABIZADEH, S., VANARSDALE, T., ZHANG, H., SHIN, H., WANG, J. J., LEO, E., ZAPATA, J., HAUSER, C. A., REED, J. C. & BREDESEN, D. E. 1999. TRAF family proteins interact with the common neurotrophin receptor and modulate apoptosis induction. *J Biol Chem,* 274**,** 30202-8.

YEAMAN, C., LE GALL, A. H., BALDWIN, A. N., MONLAUZEUR, L., LE BIVIC, A. & RODRIGUEZ-BOULAN, E. 1997. The O-glycosylated stalk domain is required for apical sorting of neurotrophin receptors in polarized MDCK cells. *J Cell Biol,* 139**,** 929-40.

YEMELYANOV, A., GASPARIAN, A., LINDHOLM, P., DANG, L., PIERCE, J. W., KISSELJOV, F., KARSELADZE, A. & BUDUNOVA, I. 2006. Effects of IKK inhibitor PS1145 on NF-kappaB function, proliferation, apoptosis and invasion activity in prostate carcinoma cells. *Oncogene,* 25**,** 387-98.

YOON, S. O., CASACCIA-BONNEFIL, P., CARTER, B. & CHAO, M. V. 1998. Competitive signaling between TrkA and p75 nerve growth factor receptors determines cell survival. *J Neurosci,* 18**,** 3273-81.

ZAMPIERI, N. & CHAO, M. V. 2006. Mechanisms of neurotrophin receptor signalling. *Biochem Soc Trans.*

ZHANG, J., WANG, L. S., YE, S. L., LUO, P. & WANG, B. L. 2015. Blockage of tropomyosin receptor kinase a (TrkA) enhances chemo-sensitivity in breast cancer cells and inhibits metastasis in vivo. *Int J Clin Exp Med,* 8**,** 634-41.

ZHU, Z., KLEEFF, J., KAYED, H., WANG, L., KORC, M., BUCHLER, M. W. & FRIESS, H. 2002. Nerve growth factor and enhancement of proliferation, invasion, and tumorigenicity of pancreatic cancer cells. *Mol Carcinog,* 35**,** 138-47.

ZOU, C. G., CAO, X. Z., ZHAO, Y. S., GAO, S. Y., LI, S. D., LIU, X. Y., ZHANG, Y. & ZHANG, K. Q. 2009. The molecular mechanism of endoplasmic reticulum stress-induced apoptosis in PC-12 neuronal cells: the protective effect of insulin-like growth factor I. *Endocrinology,* 150**,** 277-85.